



# **Guidelines for Fatigue Assessment of Ships and Offshore Units**

**November 2020**

**Rule Note  
NI 611 DT R01 E**



## GENERAL CONDITIONS

### 1. INDEPENDENCE OF THE SOCIETY AND APPLICABLE TERMS

- 1.1 The Society shall remain at all times an independent contractor and neither the Society nor any of its officers, employees, servants, agents or subcontractors shall be or act as an employee, servant or agent of any other party hereto in the performance of the Services.
- 1.2 The operations of the Society in providing its Services are exclusively conducted by way of random inspections and do not, in any circumstances, involve monitoring or exhaustive verification.
- 1.3 The Society acts as a services provider. This cannot be construed as an obligation bearing on the Society to obtain a result or as a warranty. The Society is not and may not be considered as an underwriter, broker in Unit's sale or chartering, expert in Unit's valuation, consulting engineer, controller, naval architect, designer, manufacturer, shipbuilder, repair or conversion yard, charterer or shipowner; none of them above listed being relieved of any of their expressed or implied obligations as a result of the interventions of the Society.
- 1.4 The Society only is qualified to apply and interpret its Rules.
- 1.5 The Client acknowledges the latest versions of the Conditions and of the applicable Rules applying to the Services' performance.
- 1.6 Unless an express written agreement is made between the Parties on the applicable Rules, the applicable Rules shall be the Rules applicable at the time of entering into the relevant contract for the performance of the Services.
- 1.7 The Services' performance is solely based on the Conditions. No other terms shall apply whether express or implied.

### 2. DEFINITIONS

- 2.1 "Certificate(s)" means classification or statutory certificates, attestations and reports following the Society's intervention.
- 2.2 "Certification" means the activity of certification in application of national and international regulations or standards, in particular by delegation from different governments that can result in the issuance of a Certificate.
- 2.3 "Classification" means the classification of a Unit that can result or not in the issuance of a classification Certificate with reference to the Rules. Classification is an appraisalment given by the Society to the Client, at a certain date, following surveys by its surveyors on the level of compliance of the Unit to the Society's Rules or to the documents of reference for the Services provided. They cannot be construed as an implied or express warranty of safety, fitness for the purpose, seaworthiness of the Unit or of its value for sale, insurance or chartering.
- 2.4 "Client" means the Party and/or its representative requesting the Services.
- 2.5 "Conditions" means the terms and conditions set out in the present document.
- 2.6 "Industry Practice" means international maritime and/or offshore industry practices.
- 2.7 "Intellectual Property" means all patents, rights to inventions, utility models, copyright and related rights, trade marks, logos, service marks, trade dress, business and domain names, rights in trade dress or get-up, rights in goodwill or to sue for passing off, unfair competition rights, rights in designs, rights in computer software, database rights, topography rights, moral rights, rights in confidential information (including know-how and trade secrets), methods and protocols for Services, and any other intellectual property rights, in each case whether capable of registration, registered or unregistered and including all applications for and renewals, reversions or extensions of such rights, and all similar or equivalent rights or forms of protection in any part of the world.
- 2.8 "Parties" means the Society and Client together.
- 2.9 "Party" means the Society or the Client.
- 2.10 "Register" means the public electronic register of ships updated regularly by the Society.
- 2.11 "Rules" means the Society's classification rules and other documents. The Society's Rules take into account at the date of their preparation the state of currently available and proven technical minimum requirements but are not a standard or a code of construction neither a guide for maintenance, a safety handbook or a guide of professional practices, all of which are assumed to be known in detail and carefully followed at all times by the Client.
- 2.12 "Services" means the services set out in clauses 2.2 and 2.3 but also other services related to Classification and Certification such as, but not limited to: ship and company safety management certification, ship and port security certification, maritime labour certification, training activities, all activities and duties incidental thereto such as documentation on any supporting means, software, instrumentation, measurements, tests and trials on board. The Services are carried out by the Society according to the applicable referential and to the Bureau Veritas' Code of Ethics. The Society shall perform the Services according to the applicable national and international standards and Industry Practice and always on the assumption that the Client is aware of such standards and Industry Practice.
- 2.13 "Society" means the classification society 'Bureau Veritas Marine & Offshore SAS', a company organized and existing under the laws of France, registered in Nanterre under number 821 131 844, or any other legal entity of Bureau Veritas Group as may be specified in the relevant contract, and whose main activities are Classification and Certification of ships or offshore units.
- 2.14 "Unit" means any ship or vessel or offshore unit or structure of any type or part of it or system whether linked to shore, river bed or sea bed or not, whether operated or located at sea or in inland waters or partly on land, including submarines, hovercrafts, drilling rigs, offshore installations of any type and of any purpose, their related and ancillary equipment, subsea or not, such as well head and pipelines, mooring legs and mooring points or otherwise as decided by the Society.

### 3. SCOPE AND PERFORMANCE

- 3.1 Subject to the Services requested and always by reference to the Rules, the Society shall:
  - review the construction arrangements of the Unit as shown on the documents provided by the Client;
  - conduct the Unit surveys at the place of the Unit construction;
  - class the Unit and enter the Unit's class in the Society's Register;
  - survey the Unit periodically in service to note whether the requirements for the maintenance of class are met.The Client shall inform the Society without delay of any circumstances which may cause any changes on the conducted surveys or Services.
- 3.2 The Society will not:
  - declare the acceptance or commissioning of a Unit, nor its construction in conformity with its design, such activities remaining under the exclusive responsibility of the Unit's owner or builder;
  - engage in any work relating to the design, construction, production or repair checks, neither in the operation of the Unit or the Unit's trade, neither in any advisory services, and cannot be held liable on those accounts.

### 4. RESERVATION CLAUSE

- 4.1 The Client shall always: (i) maintain the Unit in good condition after surveys; (ii) present the Unit for surveys; and (iii) inform the Society in due time of any circumstances that may affect the given appraisalment of the Unit or cause to modify the scope of the Services.
- 4.2 Certificates are only valid if issued by the Society.
- 4.3 The Society has entire control over the Certificates issued and may at any time withdraw a Certificate at its entire discretion including, but not limited to, in the following situations: where the Client fails to comply in due time with instructions of the Society or where the Client fails to pay in accordance with clause 6.2 hereunder.
- 4.4 The Society may at times and at its sole discretion give an opinion on a design or any technical element that would 'in principle' be acceptable to the Society. This opinion shall not presume on the final issuance of any Certificate or on its content in the event of the actual issuance of a Certificate. This opinion shall only be an appraisal made by the Society which shall not be held liable for it.

### 5. ACCESS AND SAFETY

- 5.1 The Client shall give to the Society all access and information necessary for the efficient performance of the requested Services. The Client shall be the sole responsible for the conditions of presentation of the Unit for tests, trials and surveys and the conditions under which tests and trials are carried out. Any information, drawing, etc. required for the performance of the Services must be made available in due time.
- 5.2 The Client shall notify the Society of any relevant safety issue and shall take all necessary safety-related measures to ensure a safe work environment for the Society or any of its officers, employees, servants, agents or subcontractors and shall comply with all applicable safety regulations.

### 6. PAYMENT OF INVOICES

- 6.1 The provision of the Services by the Society, whether complete or not, involve, for the part carried out, the payment of fees thirty (30) days upon issuance of the invoice.

6.2 Without prejudice to any other rights hereunder, in case of Client's payment default, the Society shall be entitled to charge, in addition to the amount not properly paid, interests equal to twelve (12) months LIBOR plus two (2) per cent as of due date calculated on the number of days such payment is delinquent. The Society shall also have the right to withhold Certificates and other documents and/or to suspend or revoke the validity of Certificates.

- 6.3 In case of dispute on the invoice amount, the undisputed portion of the invoice shall be paid and an explanation on the dispute shall accompany payment so that action can be taken to solve the dispute.

### 7. LIABILITY

- 7.1 The Society bears no liability for consequential loss. For the purpose of this clause consequential loss shall include, without limitation:
  - Indirect or consequential loss;
  - Any loss and/or deferral of production, loss of product, loss of use, loss of bargain, loss of revenue, loss of profit or anticipated profit, loss of business and business interruption, in each case whether direct or indirect.The Client shall defend, release, save, indemnify, defend and hold harmless the Society from the Client's own consequential loss regardless of cause.
- 7.2 Except in case of wilful misconduct of the Society, death or bodily injury caused by the Society's negligence and any other liability that could not be, by law, limited, the Society's maximum liability towards the Client is limited to one hundred and fifty per-cents (150%) of the price paid by the Client to the Society for the Services having caused the damage. This limit applies to any liability of whatsoever nature and howsoever arising, including fault by the Society, breach of contract, breach of warranty, tort, strict liability, breach of statute.
- 7.3 All claims shall be presented to the Society in writing within three (3) months of the completion of Services' performance or (if later) the date when the events which are relied on were first discovered by the Client. Any claim not so presented as defined above shall be deemed waived and absolutely time barred.

### 8. INDEMNITY CLAUSE

- 8.1 The Client shall defend, release, save, indemnify and hold harmless the Society from and against any and all claims, demands, lawsuits or actions for damages, including legal fees, for harm or loss to persons and/or property tangible, intangible or otherwise which may be brought against the Society, incidental to, arising out of or in connection with the performance of the Services (including for damages arising out of or in connection with opinions delivered according to clause 4.4 above) except for those claims caused solely and completely by the gross negligence of the Society, its officers, employees, servants, agents or subcontractors.

### 9. TERMINATION

- 9.1 The Parties shall have the right to terminate the Services (and the relevant contract) for convenience after giving the other Party thirty (30) days' written notice, and without prejudice to clause 6 above.
- 9.2 In such a case, the Classification granted to the concerned Unit and the previously issued Certificates shall remain valid until the date of effect of the termination notice issued, subject to compliance with clause 4.1 and 6 above.
- 9.3 In the event where, in the reasonable opinion of the Society, the Client is in breach, or is suspected to be in breach of clause 16 of the Conditions, the Society shall have the right to terminate the Services (and the relevant contracts associated) with immediate effect.

### 10. FORCE MAJEURE

- 10.1 Neither Party shall be responsible or liable for any failure to fulfil any term or provision of the Conditions if and to the extent that fulfilment has been delayed or temporarily prevented by a force majeure occurrence without the fault or negligence of the Party affected and which, by the exercise of reasonable diligence, the said Party is unable to provide against.
- 10.2 For the purpose of this clause, force majeure shall mean any circumstance not being within a Party's reasonable control including, but not limited to: acts of God, natural disasters, epidemics or pandemics, wars, terrorist attacks, riots, sabotages, impositions of sanctions, embargoes, nuclear, chemical or biological contaminations, laws or action taken by a government or public authority, quotas or prohibition, expropriations, destructions of the worksite, explosions, fires, accidents, any labour or trade disputes, strikes or lockouts.

### 11. CONFIDENTIALITY

- 11.1 The documents and data provided to or prepared by the Society in performing the Services, and the information made available to the Society, are treated as confidential except where the information:
  - is properly and lawfully in the possession of the Society;
  - is already in possession of the public or has entered the public domain, otherwise than through a breach of this obligation;
  - is acquired or received independently from a third party that has the right to disseminate such information;
  - is required to be disclosed under applicable law or by a governmental order, decree, regulation or rule or by a stock exchange authority (provided that the receiving Party shall make all reasonable efforts to give prompt written notice to the disclosing Party prior to such disclosure).
- 11.2 The Parties shall use the confidential information exclusively within the framework of their activity underlying these Conditions.
- 11.3 Confidential information shall only be provided to third parties with the prior written consent of the other Party. However, such prior consent shall not be required when the Society provides the confidential information to a subsidiary.
- 11.4 Without prejudice to sub-clause 11.1, the Society shall have the right to disclose the confidential information if required to do so under regulations of the International Association of Classifications Societies (IACS) or any statutory obligations.

### 12. INTELLECTUAL PROPERTY

- 12.1 Each Party exclusively owns all rights to its Intellectual Property created before or after the commencement date of the Conditions and whether or not associated with any contract between the Parties.
- 12.2 The Intellectual Property developed by the Society for the performance of the Services including, but not limited to drawings, calculations, and reports shall remain the exclusive property of the Society.

### 13. ASSIGNMENT

- 13.1 The contract resulting from to these Conditions cannot be assigned or transferred by any means by a Party to any third party without the prior written consent of the other Party.
- 13.2 The Society shall however have the right to assign or transfer by any means the said contract to a subsidiary of the Bureau Veritas Group.

### 14. SEVERABILITY

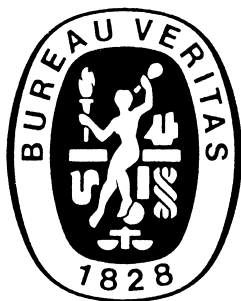
- 14.1 Invalidity of one or more provisions does not affect the remaining provisions.
- 14.2 Definitions herein take precedence over other definitions which may appear in other documents issued by the Society.
- 14.3 In case of doubt as to the interpretation of the Conditions, the English text shall prevail.

### 15. GOVERNING LAW AND DISPUTE RESOLUTION

- 15.1 These Conditions shall be construed and governed by the laws of England and Wales.
- 15.2 The Parties shall make every effort to settle any dispute amicably and in good faith by way of negotiation within thirty (30) days from the date of receipt by either one of the Parties of a written notice of such a dispute.
- 15.3 Failing that, the dispute shall finally be settled under the Rules of Arbitration of the Maritime Arbitration Chamber of Paris ("CAMP"), which rules are deemed to be incorporated by reference into this clause. The number of arbitrators shall be three (3). The place of arbitration shall be Paris (France). The Parties agree to keep the arbitration proceedings confidential.

### 16. PROFESSIONAL ETHICS

- 16.1 Each Party shall conduct all activities in compliance with all laws, statutes, rules, economic and trade sanctions (including but not limited to UN sanctions and EU sanctions) and regulations applicable to such Party including but not limited to: child labour, forced labour, collective bargaining, discrimination, abuse, working hours and minimum wages, anti-bribery, anti-corruption, copyright and trademark protection, personal data protection (<https://personal.dataprotection.bureauveritas.com/privacypolicy>).
- Each of the Parties warrants that neither it, nor its affiliates, has made or will make, with respect to the matters provided for hereunder, any offer, payment, gift or authorization of the payment of any money directly or indirectly, to or for the use or benefit of any official or employee of the government, political party, official, or candidate.
- 16.2 In addition, the Client shall act consistently with the Bureau Veritas' Code of Ethics.  
<https://group.bureauveritas.com/group/corporate-social-responsibility>



## GUIDANCE NOTE NI 611

# Guidelines for Fatigue Assessment of Ships and Offshore Units

---

<b>SECTION</b>	<b>1</b>	<b>GENERAL CONSIDERATIONS</b>
<b>SECTION</b>	<b>2</b>	<b>LOADS TO BE CONSIDERED FOR FATIGUE ANALYSIS</b>
<b>SECTION</b>	<b>3</b>	<b>HOT SPOT STRESS BASED ON ANALYTICAL APPROACH FOR LONGITUDINAL STIFFENERS</b>
<b>SECTION</b>	<b>4</b>	<b>HOT SPOT STRESS BASED ON ANALYTICAL APPROACH FOR TUBULAR JOINTS</b>
<b>SECTION</b>	<b>5</b>	<b>FEA HOT SPOT STRESS FOR PLATED WELDED JOINTS AND FEA LOCAL NOMINAL STRESS FOR NON-WELDED DETAILS</b>
<b>SECTION</b>	<b>6</b>	<b>HOT SPOT STRESS BASED ON FEA FOR TUBULAR JOINTS</b>
<b>SECTION</b>	<b>7</b>	<b>WELD STRESS FOR ROOT CRACKING ANALYSIS</b>
<b>SECTION</b>	<b>8</b>	<b>STRESS ANALYSIS OF BOLTED CONNECTIONS</b>
<b>SECTION</b>	<b>9</b>	<b>BASIC DESIGN S-N CURVES FOR STEEL DETAILS</b>
<b>SECTION</b>	<b>10</b>	<b>FACTORS AFFECTING FATIGUE STRENGTH OF STEEL DETAILS</b>
<b>SECTION</b>	<b>11</b>	<b>FATIGUE DAMAGE CALCULATION AND ACCEPTANCE CRITERIA</b>
<b>SECTION</b>	<b>12</b>	<b>FATIGUE ASSESSMENT BASED ON CRACK PROPAGATION</b>

**APPENDIX 1      METHODOLOGY FOR DIRECT  
HYDRO-STRUCTURE CALCULATION**

**APPENDIX 2      FATIGUE STRENGTH OF ALUMINIUM ALLOYS PLATED WELDED  
DETAILS**

## **Section 1 General Considerations**

<b>1</b>	<b>Scope of application</b>	<b>11</b>
1.1	Purpose	
1.2	Application	
<b>2</b>	<b>Definitions</b>	<b>12</b>
2.1	Main definitions	
<b>3</b>	<b>Assumptions</b>	<b>14</b>
3.1	Material	
3.2	Temperature	
3.3	Corrosion	
<b>4</b>	<b>Fatigue process in ship and offshore unit structures</b>	<b>15</b>
4.1	Fatigue failure and phenomenom	
<b>5</b>	<b>Methodology</b>	<b>16</b>
5.1	General	
5.2	Approaches for fatigue assessment	
5.3	Design stage fatigue assessment	
5.4	In service fatigue assessment	

## **Section 2 Loads to be Considered for Fatigue Analysis**

<b>1</b>	<b>Ships and floating offshore units</b>	<b>19</b>
1.1	Loads	
1.2	Loading conditions	
1.3	Rule calculations	
1.4	Spectral and time-domain calculations	
<b>2</b>	<b>Fixed offshore structures</b>	<b>20</b>
2.1	Loads types	
2.2	Determination of loads	

## **Section 3 Hot Spot Stress Based on Analytical Approach for Longitudinal Stiffeners**

<b>1</b>	<b>General</b>	<b>21</b>
1.1	Application	
1.2	Axial and bending stress fatigue	
1.3	Shear stress fatigue	
<b>2</b>	<b>Axial and bending hot spot stress</b>	<b>23</b>
2.1	General	
2.2	Global axial stress	
2.3	Local bending stress	
2.4	Stress due to relative displacements of primary supporting members	
<b>3</b>	<b>Stress concentration factors (SCF)</b>	<b>28</b>
3.1	Stress concentration factors for longitudinal stiffener end connections	
3.2	SCF for unsymmetrical stiffeners	
3.3	SCF for longitudinal stiffener end connections - Calculation by FEM	

4	Hot spot stress	38
4.1	Hot spot stress range and mean value for rule based approach	
4.2	Hot spot stress for direct calculation approach	

## **Section 4 Hot Spot Stress Based on Analytical Approach for Tubular Joints**

1	General	40
1.1	Principles	
2	Tubular node welded joints	40
2.1	General	
2.2	Joint modelling	
2.3	Simple tubular joints	
2.4	Other tubular joints	
3	Tubular butt welded joints	44
3.1	General	
3.2	Classification of tubular butt welded joints	
3.3	Applicable S-N curves	

## **Section 5 FEA Hot Spot Stress for Plated Welded Joints and FEA Local Nominal Stress for Non-Welded Details**

1	General	46
1.1	Application	
1.2	Type of details	
1.3	Types of hot spots for ordinary welded joints	
2	Finite element models	47
2.1	General	
2.2	Global FEM model	
2.3	Finite element modelling for hot spot stress calculation	
3	Hot spot stress for ordinary welded details	50
3.1	General	
3.2	Hot spot stress calculation	
3.3	Type 'a' stress readout for element with the prescribed size	
3.4	Type 'a' stress readout for elements smaller than the prescribed size	
3.5	Type 'a' stress readout for elements larger than the prescribed size	
4	Hot spot stress for web-stiffened cruciform joints	57
4.1	Application	
4.2	Hot spot stress calculation at the flange	
4.3	Hot spot stress calculation in the web	
5	Hot spot stress for bent hopper knuckle details	60
5.1	Bent hopper knuckle details	
6	Local nominal stress for non-welded details	61
6.1	Plate cut edge details	

7	Stress range and mean stress for rule based approach	61
7.1	General	
7.2	Principal hot spot stress	
7.3	Ordinary welded details	
7.4	Web-stiffened cruciform joint	
7.5	Plate cut edge details	

## Section 6 Hot Spot Stress Based on FEA for Tubular Joints

1	Global model	65
1.1	Modelling recommendations	
2	Hot spot stress for tubular joints	65
2.1	General	
2.2	Finite element modelling	
2.3	Stress extrapolation	
2.4	Applicable S-N curve	

## Section 7 Weld Stress for Root Cracking Analysis

1	Scope of application	68
1.1	General	
2	Weld stress calculation procedures	68
2.1	Definitions	
2.2	Plated joints, weld root stress computed by FEA	
2.3	Plate butt-welded joints welded from one side	
2.4	Tubular butt-welded joints	
2.5	Tubular joints welded from one side	

## Section 8 Stress Analysis of Bolted Connections

1	General	75
1.1	Bolt layout	
2	Bolted connection stress analysis procedures	75
2.1	Bolted plate fatigue checking	
2.2	Bolt fatigue checking	

## Section 9 Basic Design S-N Curves For Steel Details

1	General	77
1.1	Basic design S-N curves	
1.2	Scope of application	
1.3	Basic design S-N curves formulae	

<b>2</b>	<b>As-welded joints, toe cracking</b>	<b>79</b>
2.1	Plated joints, hot spot stress	
2.2	Plated butt-welded joints, local nominal stress	
2.3	Tubular welded joints, hot spot stress	
2.4	Tubular butt-welded joints, local nominal stress	
2.5	Tubular cast joints, hot spot stress	
<b>3</b>	<b>Welded joints, root cracking</b>	<b>82</b>
3.1	Plated joints, weld root stress computed by FEA	
3.2	Plated butt-welded joints, local nominal stress	
3.3	Single-sided tubular joints, weld root stress based on analytical approach	
3.4	Tubular butt-welded joints, local nominal stress	
<b>4</b>	<b>Tables of S-N curves</b>	<b>83</b>
4.1	Tables of S-N curves for steel plated welded joints	
4.2	Tables of S-N curves from ISO 19902 for tubular welded joints, tubular butt-welded joints and tubular cast joints	
<b>5</b>	<b>Post welding improved welded joints, toe cracking</b>	<b>86</b>
5.1	Application	
5.2	S-N curves for post-weld improved plated joints	
5.3	Fatigue life improvement for post weld treated tubular joints	
<b>6</b>	<b>Cut edges</b>	<b>87</b>
6.1	General	
6.2	S-N curves for cut edge details	
<b>7</b>	<b>Bolted connections</b>	<b>89</b>
7.1	General	
7.2	S-N curves for bolted connections	
<b>8</b>	<b>Design S-N curves obtained from fatigue testing</b>	<b>90</b>
8.1	General	
8.2	Fatigue testing procedure	
8.3	Structural hot spot stress measurement for plated joints	
8.4	Measurement of structural hot spot stress for tubular joints	
8.5	Data statistical treatment	

## **Section 10 Factors Affecting Fatigue Strength Of Steel Details**

<b>1</b>	<b>General</b>	<b>94</b>
1.1	General	
<b>2</b>	<b>Effect of yield strength</b>	<b>95</b>
2.1	Correction factor	
<b>3</b>	<b>Thickness effect</b>	<b>95</b>
3.1	General	
3.2	Plated welded joints	
3.3	Bolted connections	
<b>4</b>	<b>Mean stress and residual stress relaxation</b>	<b>99</b>
4.1	As-welded joints	
4.2	Post weld treated joints	
4.3	Cut edges	
4.4	Preloaded bolts	



<b>5</b>	<b>Stress concentration factors due to misalignment</b>	<b>102</b>
5.1	General	
5.2	Plate butt weld - Axial misalignment	
5.3	Plate butt weld - Angular misalignment	
5.4	Plate cruciform joint misalignment	
5.5	Stress concentration factors due to eccentricities for tubular butt-welded joints	
<b>6</b>	<b>Corrosive environment</b>	<b>108</b>
6.1	General	
<b>7</b>	<b>Workmanship</b>	<b>108</b>
7.1	General	
7.2	Building misalignment	
7.3	Welding procedures	
7.4	Post weld treatments for welded joints	

## **Section 11 Fatigue Damage Calculation and Acceptance Criteria**

<b>1</b>	<b>General</b>	<b>112</b>
1.1	Principles	
1.2	Design fatigue life patterns	
1.3	Fatigue damage	
1.4	Fatigue life	
1.5	Acceptance criteria	
<b>2</b>	<b>Simplified rule based approach</b>	<b>114</b>
2.1	General	
2.2	Reference fatigue stress range for wave loads	
2.3	Design S-N curve	
2.4	Fatigue damage calculation	
<b>3</b>	<b>Spectral analysis</b>	<b>119</b>
3.1	General	
3.2	Hydrodynamic and structural models	
3.3	Stress to be used for spectral analysis	
3.4	Short-term statistics	
3.5	Short-term fatigue damage	
3.6	Long-term fatigue damage	
3.7	Combination of low frequency and high frequency cycles	
3.8	Fatigue due to loading and unloading	
3.9	Intermittent wetting	
<b>4</b>	<b>Time-domain fatigue analysis</b>	<b>131</b>
4.1	Non-linear simulations	
4.2	Stress to be used for time-domain analysis	
4.3	Analysis of long duration time-domain simulations	
4.4	Short-term fatigue damage	
4.5	Long-term fatigue damage	

**Section 12    Fatigue Assessment Based on Crack Propagation**

<b>1</b>	<b>General</b>	<b>137</b>
1.1	Scope	
1.2	General considerations	
<b>2</b>	<b>Crack propagation analysis</b>	<b>139</b>
2.1	Procedure	
2.2	Crack models	
2.3	Fatigue cracks modeling	
2.4	Initial crack size	
2.5	Determination of the stresses and stress intensity factors	
2.6	Crack propagation	
2.7	Crack propagation termination	
<b>3</b>	<b>Failure criteria</b>	<b>145</b>
3.1	Failure modes	
3.2	Failure assessment diagram (FAD)	
<b>4</b>	<b>Determination of the stress intensity factors</b>	<b>148</b>
4.1	General	
4.2	Stress intensity factors by closed-form expression	
4.3	Stress intensity factors by the finite element method (FEM)	
<b>5</b>	<b>Wave loads modelling</b>	<b>149</b>
5.1	General	
5.2	Short-term analysis	
5.3	Long-term analysis based on sea state sequences	
5.4	Long-term analysis based on stress histogram	
<b>6</b>	<b>Material characteristics</b>	<b>154</b>
6.1	General	
6.2	Young modulus	
6.3	Yield stress and tensile strength	
6.4	Toughness	
6.5	Crack propagation law parameters	
<b>7</b>	<b>Initial crack size</b>	<b>158</b>
7.1	General	
7.2	Visual inspection	
7.3	Ultrasonic inspection	
7.4	Other inspection techniques	

**Appendix 1    Methodology for Direct Hydro-Structure Calculation**

<b>1</b>	<b>General</b>	<b>160</b>
1.1	Introduction	
<b>2</b>	<b>Wave environment description</b>	<b>160</b>
2.1	Wave scatter diagram	
2.2	Wave spectrum	

<b>3</b>	<b>Hydro-structural model</b>	<b>167</b>
3.1	General	
3.2	Hydrodynamic loads	
3.3	Internal liquid loads	
3.4	Structural ship response	
3.5	General modelling considerations	
3.6	Types of hydro-structural simulations	
<b>4</b>	<b>Statistical analysis of the response in an irregular sea state</b>	<b>172</b>
4.1	Spectral analysis of frequency domain simulations	
4.2	Analysis of time-domain simulations	
<b>5</b>	<b>Long-term analysis</b>	<b>173</b>
5.1	General	
5.2	Complete long-term analysis	
5.3	Multiple Design Sea States approach	
5.4	Single Design Sea State approach	
5.5	Equivalent Design Wave approach	

## **Appendix 2 Fatigue strength of aluminium alloys plated welded details**

<b>1</b>	<b>Basic design S-N curves for plated welded details in aluminium alloys</b>	<b>179</b>
1.1	General	
1.2	Scope of application	
1.3	Basic design S-N curve formulae	
<b>2</b>	<b>As-welded aluminium joints, toe cracking</b>	<b>180</b>
2.1	Plated joints, hot spot stress	
2.2	Plated butt-welded joints, local nominal stress	
<b>3</b>	<b>Welded aluminium joints, root cracking</b>	<b>180</b>
3.1	Plated joints, weld root stress computed by FEA	
3.2	Plated butt-welded joints, local nominal stress	
<b>4</b>	<b>Table of S-N curves for aluminium alloys plated welded details</b>	<b>181</b>
4.1	General	
<b>5</b>	<b>Factors affecting fatigue strength of aluminium plated welded details</b>	<b>181</b>
5.1	General	
5.2	Thickness effect	
5.3	Mean stress and residual stress relaxation	
<b>6</b>	<b>Stress concentration factors due to misalignment</b>	<b>182</b>
6.1	General	
6.2	Plate butt weld - Axial misalignment	
6.3	Plate butt weld - Angular misalignment	
6.4	Plate cruciform joint misalignment	
<b>7</b>	<b>Workmanship</b>	<b>183</b>
7.1	General	
7.2	Building misalignment	
7.3	Welding procedures	



# SECTION 1

# GENERAL CONSIDERATIONS

## Symbols

The following is a summary of the main symbols used throughout the Guidance Note:

$E$	: Young's Modulus, in N/mm <sup>2</sup>
$D$	: Fatigue damage ratio
$K_g$	: Geometric stress concentration factor
$L$	: Floating unit rule length, in m
$R_{eH}$	: Specified minimum yield stress, in N/mm <sup>2</sup>
$R_{p0,2}$	: 0,2% proof stress (yield strength), in N/mm <sup>2</sup>
$R_m$	: Specified minimum ultimate tensile strength, in N/mm <sup>2</sup>
$T_{DF}$	: Design fatigue life, in years
$T_{Prot}$	: Time during which the fatigue detail is considered as protected against corrosion, in years
$\Delta\sigma$	: Stress range, in N/mm <sup>2</sup> .

Other symbols are locally defined in Section where they are used.

## 1 Scope of application

### 1.1 Purpose

**1.1.1** This Guidance Note provides guidelines for the assessment of fatigue capacity of marine and offshore structures throughout their entire life i.e. at design stage and during their service life.

Guidance for fatigue assessment is given for welded details and non-welded details (cut edge details, bolted connections) of marine and offshore structures as detailed in [1.2.1].

This Guidance Note presents recommendations in relation to fatigue analysis based on S-N curves approach or fracture mechanics approach including safety margin.

**1.1.2** At design stage, the aim is to ensure that critical details are adequately designed to reach the required fatigue life. The associated fatigue assessment methodology is based on S-N curve/cumulative damage approach and several stress assessment methods are proposed according to the fatigue failure modes.

**1.1.3** During service life, fatigue assessment may be necessary in the following cases:

- prior to a survey in view to optimize the inspection program
- for life extension study
- for repair when a fatigue failure is detected during an inspection.

Fatigue assessment may be performed either by means of S-N curve/cumulative damage approach for life extension for example or by means of fracture mechanics analysis for repair decision when cracks are detected.

### 1.2 Application

#### 1.2.1 Types of structures

This Guidance Note is applicable for evaluation of fatigue strength of the following marine structures:

- sea-going steel and aluminium alloys ships
- floating steel offshore units
- fixed steel offshore structures such as jacket structures made of a frame of welded tubular steel members which is piled into the seabed (towers mentioned in API and ISO are not addressed).

### 1.2.2 Types of environment

Four types of fatigue detail conditions are considered:

- in air
- in corrosive environment without protection
- in corrosive environment with cathodic protection
- in corrosive environment with protective coating.

## 2 Definitions

### 2.1 Main definitions

#### 2.1.1 Applicable rules

This means the rules or standards applicable for the design of the ship or offshore unit for which fatigue calculations are performed.

#### 2.1.2 Constant amplitude loading

A type of loading causing a regular stress fluctuation with constant magnitudes of maximum and minimum stresses.

#### 2.1.3 Crack propagation rate

Increase of crack size per stress cycle.

#### 2.1.4 Crack propagation threshold

Limiting value of stress intensity factor range below which the crack propagation can be considered as negligible, i.e. stress cycles are not damaging.

#### 2.1.5 Cycle counting method

A procedure for stress range counting from a stress time history. The “Rainflow” counting method is a standardized cycle counting method.

#### 2.1.6 Direct calculation

A calculation in which the response of the structure to waves is computed using fluid mechanics and solid mechanics models, as opposed to responses given by formulas or tabulated data. Direct calculations are carried out either in frequency domain (corresponding to spectral calculation) or in time domain.

#### 2.1.7 Eccentricity

Misalignment of plates at welded connections.

#### 2.1.8 Equivalent stress range

For practical reasons, an equivalent stress range is defined in this Guidance Note to take into account the factors influencing the fatigue strength. It corresponds to the reference fatigue stress range affected by the correction that should have theoretically been applied to the S-N curve.

#### 2.1.9 Fatigue

Process of deterioration of a structure subjected to fluctuating stresses, going through several stages from the initial “crack-free” state to a “failure” state.

#### 2.1.10 Fatigue damage ratio

Ratio of the number of applied stress cycles and the corresponding number of stress cycles to failure at constant stress range (by use of S-N curve).

#### 2.1.11 Fatigue life

Total time corresponding to the number of stress cycles required to cause fatigue failure of the component. The fatigue life is generally expressed in terms of number of years.

#### 2.1.12 Fatigue limit

Stress range for which the fatigue strength under constant amplitude loading corresponds to a number of cycles large enough to be considered as infinite by a design code.

#### 2.1.13 Fracture mechanics

A branch of mechanics dealing with the behavior and strength of components containing cracks. Fracture mechanics cover the domains of brittle fracture and crack propagation.

#### 2.1.14 Geometric stress

The value of structural stress on the surface at the structural discontinuity.

#### 2.1.15 Hot spot

A location in a structure where a fatigue crack may initiate, due to the combined effect of the structural stress fluctuation and of a stress concentration effect induced by a structural discontinuity such as a weld. It corresponds to the point where the geometric stress range is maximum.

#### 2.1.16 Hot spot stress

The value of structural stress on the surface at the hot spot. Hot spot stress is defined as the maximum geometric stress relative to the structural discontinuity.

#### 2.1.17 Local nominal stress

Nominal stress including macro-geometric effects, concentrated load effects and misalignments, but disregarding the stress raising effects due to structural discontinuities and due to the welded joint itself.

#### 2.1.18 Loading condition

A loading condition is a distribution of weights carried in the ship or offshore unit spaces.

#### 2.1.19 Load case

A load case is a state of the ship or offshore unit structure subjected to a combination of loads.

#### 2.1.20 Local notch

A local notch is a localized geometric feature, such as the toe of a weld, which causes stress concentration. The local notch does not modify the structural stress but generates a non-linear stress peak.

#### 2.1.21 Macro-geometric discontinuity

A global discontinuity such as a large opening, a curved part in a beam, a bend in a flange not supported by diaphragms or stiffeners, discontinuities in pressure containing shells, eccentricity in a lap joint.

#### 2.1.22 Macro-geometric effect

A stress raising effect due to macro-geometric discontinuity in the vicinity of the welded joint, but not due to the welded joint itself.

#### 2.1.23 Membrane stress

Average normal stress across the thickness of a plate or shell.

#### 2.1.24 Miner sum

Summation of individual fatigue damage ratios caused by each stress cycle or stress range block according to the Palmgren-Miner rule.

#### 2.1.25 Misalignment

Axial and angular misalignments caused either by detail design or by poor fabrication or welding distortion.

#### 2.1.26 Nominal stress

A stress in a structural component, disregarding the stress raising effects due to structural discontinuities and due to the welded joint itself, calculated using general theories, e.g. beam theory.

#### 2.1.27 Non-linear stress peak

The stress component of a notch stress which exceeds the linearly distributed structural stress at a local notch.

#### 2.1.28 Paris's law

An experimentally determined relation between fatigue crack growth rate and stress intensity factor range (fracture mechanics).

#### 2.1.29 Palmgren-Miner rule

Method for estimating fatigue life under variable amplitude loading from the constant amplitude S-N curve. Often referred to as Miner's rule.

#### 2.1.30 Reference fatigue stress range

Stress range calculated for a dynamic load case at a given probability level and used as a reference to build a long-term stress range distribution when using rule based approach.

#### 2.1.31 Shell bending stress

Bending stress in a shell or plate-like part of a component, linearly distributed across the thickness as assumed in the theory of shells.

### 2.1.32 S-N curve

Graphical presentation of the dependence of the number of stress cycles to failure (N) on the applied constant stress range  $\Delta S$ , also known as Wöhler curve.

### 2.1.33 Stress cycle

A part of a stress history containing a stress maximum and a stress minimum.

### 2.1.34 Stress history

A time-based presentation of a fluctuating stress for either the total life or a certain period of time.

### 2.1.35 Stress intensity factor

Factor used in fracture mechanics to characterize the stress field at the vicinity of a crack tip.

### 2.1.36 Stress range

The difference between the maximum and minimum stresses in a stress cycle.

### 2.1.37 Stress range exceedance

A tabular or graphical presentation of the cumulative number of occurrences of stress range exceedance, i.e. the number of stress ranges exceeding a particular magnitude of stress range in stress history.

### 2.1.38 Stress ratio

Ratio of minimum to maximum stress values in a stress cycle.

### 2.1.39 Structural discontinuity

A geometric discontinuity due to the structural detail of the welded joint, but excluding the discontinuity due to the weld itself.

### 2.1.40 Structural stress

A stress in a component, calculated to take into account the effects of a structural discontinuity, and consisting of membrane and shell bending stress components.

### 2.1.41 Structural (or geometric) stress concentration factor

The ratio of the geometric stress to the local nominal stress.

### 2.1.42 Variable amplitude loading

A type of loading causing irregular stress fluctuation with stress ranges (and amplitudes) of variable magnitude.

### 2.1.43 Weld root structural stress

The stress corresponding to the maximum value of structural stress at the weld root.

## 3 Assumptions

### 3.1 Material

#### 3.1.1 Yield stress

This Guidance Note is valid for:

- ferritic/pearlitic or bainitic steel materials with specified minimum yield stress  $R_{eH}$  not greater than 960 MPa for details in air and not greater than 500 MPa for details in corrosive environment under free corrosion or with cathodic protection
- austenitic stainless steel materials with minimum yield strength  $R_{p0.2}$  not greater than 300 Mpa for details in air and corrosive environment (NR216, Sec1, [9.6])
- welded aluminium alloys of series 5000 (aluminium-magnesium alloy) and series 6000 (aluminium-magnesium-silicon alloy) except the alloys grade 6005A and 6061 as defined in (NR216, Ch3, Sec2, [2.3]). The minimum yield strength  $R_{p0.2}$  of aluminium products are given in NR216, Ch3, Sec2, Tab 2 and Tab 3.



## 3.2 Temperature

### 3.2.1 Domain of application for steel

For design temperatures up to 100°C, the fatigue strength at room temperature may be considered.

For design temperatures greater than 100°C, the decrease of fatigue strength with the temperature increase is to be considered. IIW Fatigue Recommendations (IIW-XIII-1823-07, 2008) propose fatigue strength reduction factor for steel at temperatures greater than 100°C and less than 600°C.

Special attention should be paid to the validity of S-N curves and of fracture mechanics material characteristics for low temperature applications. For austenitic stainless steel, the S-N curve may be improved for cryogenic temperatures provided that fatigue tests results are approved by the Society.

### 3.2.2 Domain of application for aluminium alloys

The S-N curves for aluminium alloys are valid for temperatures up to 70°. This value may be raised if fatigue test results are approved by the Society.

For low and cryogenic temperatures, the S-N curves for some 5000 alloys grades may be improved. Fatigue tests are to be carried out and fatigue tests results have to be approved by the Society.

## 3.3 Corrosion

### 3.3.1 General

The effects of corrosive environment on fatigue life are taken into account by means of:

- Increase of stress in the considered detail due to thickness decrease induced by corrosion phenomenon  
Net scantling concept is to be used as described in [3.3.2].
- Decrease of fatigue strength  
The corrosive environment, such as sea water, decreases the fatigue resistance and modifies the S-N curves for steel details (see Sec 10, [6]).

For aluminium alloys, no corrosion effect has to be taken into account for the fatigue strength.

### 3.3.2 Corrosion allowances

Appropriate corrosion allowances are to be considered (gross thickness reduction or net thickness increment) taking into account possible thickness reductions during the expected life of the structure, according to corrosion exposure for each type of structural components. Recommendations for minimum corrosion allowance recommendations are provided in the applicable rules.

Net scantlings are to be considered throughout the Guidance Note, as specified in the applicable rules.

### 3.3.3 Local stress and global stress corrosion allowances

The applicable rules may prescribe two different corrosion allowances, to be applied separately for the computation of global stress on one hand, and of local stress on the other hand. The corrosion allowances are typically higher for local stress calculation than for global stress calculation.

In such a case, two different approaches are proposed in this Guidance Note:

- A single structural model is used, for simplification reasons or in case where the global and local stress cannot be evaluated separately  
In this case, some stress correction factors need to be applied in order to take into account, in a simplified way, the difference between the prescribed corrosion allowances and those in the structural model. These correction factors are introduced in Sec 3 and in Sec 11. The correction factors values to be used are given in the applicable rules.
- Two different structural models with the associated appropriate corrosion allowances are used for determining separately the local and global stress, using analytical models for example  
In this case no stress correction is needed and correction factors are taken equal to 1,0.

## 4 Fatigue process in ship and offshore unit structures

### 4.1 Fatigue failure and phenomenon

#### 4.1.1 Fatigue failure process

For steel and aluminium structures, the fatigue process includes three main phases:

- initiation of crack at a hot spot location
- crack propagation or crack growth, and
- final failure by ductile tearing or brittle fracture, when the crack has reached a critical size.

### 4.1.2 Fatigue failure modes

For welded or cut edge details, fatigue crack growth to failure may occur according to several failure modes, as follows:

- weld toe failure: fatigue crack initiates from the weld toe and grows into the base material
- weld root failure: fatigue crack initiates from the weld root and grows through the weld throat or into the plate section under the weld
- cut edge failure: fatigue crack initiates from surface irregularity or notch at cut edge details and grows into the base material
- bolted connections failure.

The fatigue strength in each of these modes is substantially different, and every failure mode should be checked.

### 4.1.3 High-cycle / low-cycle fatigue

The fatigue phenomenon is normally divided in two different domains:

- high stress, low-cycle fatigue occurring for a low number of cycles, less than  $10^4$ , in the range of plastic deformations
- low stress, high-cycle fatigue occurring for a large number of cycles more than  $10^4$ , in the range of elastic deformations.

High-cycle fatigue is due to wave load cycles: it is the most common cause for fatigue cracking. During a service life of 20 to 25 years, sea-going ships will normally encounter between  $6 \cdot 10^7$  to  $10^8$  wave load cycles.

Low cycles events may correspond to loading/unloading operations. Changing of loading condition from ballast to loaded condition generates fluctuating stress cycles, typically on primary supporting members connections. A typical examples of low-cycle fatigue are units frequently subjected to loading and discharge operations like FPSO and FSO or ships with specific operational profile such as shuttle tankers.

## 5 Methodology

### 5.1 General

5.1.1 Fatigue assessment of structural details may be based on either one of the following approaches:

- S-N curves approach, which is appropriate for the initiation phase. It is used when no crack is considered. This approach is detailed in [5.2.1]
- Fracture mechanics approach, which is appropriate for the propagation phase. It is used when a crack is considered. This approach is detailed in [5.2.2].

### 5.2 Approaches for fatigue assessment

#### 5.2.1 S-N curves approach

This approach is based on fatigue tests (S-N curves) combined with linear cumulative damage (Miner's law). Fatigue damage calculation procedure as detailed in Sec 11 is based on S-N curves approach. The calculated fatigue life is derived from the fatigue damage. The design S-N curves for steel details are given in Sec 9. The S-N curves for aluminium plated welded details are given in App 2.

The achieved fatigue life is to be compared with the specified design fatigue life.

The following fatigue damage calculation procedures may be used:

- a) Simplified approach based on equivalent design wave

Typically, it may be used for ship hull and offshore unit hull structures for which rule loads are defined. Stresses are based on analytical rule loads given at an appropriate probability level. They may be calculated by structural analysis (analytical analysis or finite element method). In this approach, a Weibull distribution is assumed for the long-term stress range distribution allowing a closed form approach fatigue damage.

- b) Spectral calculation, where the environment is described by series of short-term spectra

This method may be used for ships, offshore floating or fixed units. It is a practical method allowing to represent the random nature of the wave environment. This approach assumes the linear load effect and linear stress response. Thus, suitable linearization of non-linear elements in the problem formulations is to be done.

- c) Time-domain calculation, where the short-term spectra are used to generate time series of wave elevation

Time-domain simulations are used for the non-linear response of the structure when dynamic effects are large. Full time-domain simulation is the most accurate method to capture the combined high frequency (dynamic), wave frequency and low frequency responses but it is computer time consuming. In addition, resulting stress time series shall be post-processed using a cycle counting procedure to derive stress ranges to be considered for fatigue analysis. This method may be used for estimation of non-linear fatigue including whipping contribution to fatigue damage.

### 5.2.2 Fracture mechanics approach

This approach may be used to evaluate the residual life of in-service structure which involves existing cracks. It allows estimating the time of propagation of a crack with a specified initial size up to the final crack size corresponding to the failure criteria.

The failure criteria may correspond to a through thickness crack or a specific size of the crack leading to a brittle or ductile rupture.

Two levels of analysis may be used, depending on the complexity of the structure:

a) A simplified analytical method, which involves the following assumptions:

- stress determination in the intact structure
- calculation of the stress intensity factors with an analytical solution
- no explicit stress redistribution while the crack is growing

b) An advanced approach, which involves the following assumptions:

- crack included in the FEM model
- calculation of the stress intensity factors by FEM
- explicit stress redistribution while the crack is growing.

## 5.3 Design stage fatigue assessment

### 5.3.1 Fatigue approach

The fatigue assessment of structural details at design stage is to be performed according to S-N curves approach.

Fatigue assessment is to be performed for structural details in order to prevent the following fatigue failure modes occurring:

- weld toe failure
- weld root failure
- cut edge failure
- bolted connections failure.

The stress assessment methods for each of these fatigue failure modes are detailed in [5.3.2] to [5.3.5].

### 5.3.2 Weld toe failure assessment

Weld toe failure assessment requires to determine the stress at the weld toe according to the hot spot stress approach as detailed in Sec 3 to Sec 6 according to the type of structural analysis.

In this case, two stress assessment methods may be used, as required by the applicable rules:

- Hot spot stress calculation based on geometric stress concentration factor according to Sec 3 and Sec 4

The hot spot stress is based on analytical approach: it is obtained by multiplying the nominal stress by a geometric stress concentration factor ( $K_g$ ).

- Hot spot stress calculation by FEM

Hot spot stress is calculated directly by a very fine mesh FE analysis according to Sec 5 for plated joints and Sec 6 for tubular joints.

### 5.3.3 Weld root failure assessment

Weld root failure assessment requires to determine the weld stress by FEM analysis or by an analytical approach according to Sec 7.

### 5.3.4 Cut edge failure assessment

Cut edge failure assessment requires to determine the local nominal stress at the hot spot according to Sec 5.

### 5.3.5 Bolted connections failure assessment

Bolted Connections failure assessment requires to determine the nominal stress, according to Sec 8.

## **5.4 In service fatigue assessment**

### **5.4.1 Survey, inspection program**

To help the definition of an inspection program, a fatigue assessment based on cumulative damage may be performed following the same procedure as for design, but using the estimated actual past load history.

The results allow to determine the most loaded areas and details with respect to cumulative fatigue.

### **5.4.2 Life extension**

For life extension study, a fatigue assessment of the unit is to be performed following the same procedure as for design, including:

- a) calculation of the cumulative fatigue damage using the estimated actual past load history
- b) calculation of the cumulative damage for the expected following life time using the design load history limited to this time
- c) verification of the cumulative fatigue acceptance according to applicable rules.

### **5.4.3 In service failure**

When a fatigue crack is detected during inspection, a fatigue analysis may be performed to evaluate possible repair solutions.

Fatigue crack propagation analysis (see Sec 12) may also be applied in order to plan repairs, taking into account the constraints due to operating conditions.

## SECTION 2                      LOADS TO BE CONSIDERED FOR FATIGUE ANALYSIS

### 1 Ships and floating offshore units

#### 1.1 Loads

**1.1.1** The common loads to be considered for fatigue analysis of hull details are as follows:

- hydrostatic internal liquid and external sea pressures
- inertial internal liquid pressure and wave sea pressures
- static loads resulting from fixed weights subjected to gravity
- inertial loads resulting from fixed weights subjected to accelerations induced by ship motions.

**1.1.2** The hull girder loads to be considered for ships and ship-shaped offshore units are:

- hull girder still water loads such as bending moment and shear force resulting from internal weights (lightship, containers, bulks, liquids...) and external hydrostatic sea pressure
- hull girder wave induced loads such as wave bending moments, wave torque (only for ships with large deck openings such as bulk carriers and container ships) and shear forces resulting from inertial loads and external wave sea pressure.

**1.1.3** When relevant, the following additional loads may be considered:

- loads due to cargo loading and unloading
- dynamic loads due to impact loads such as slamming, sloshing
- dynamic loads due to natural hull girder vibration (springing response)
- operational loads.

#### 1.1.4 Additional loads for offshore units

Mooring loads are to be taken into account for hull foundations of permanent mooring equipment, and for turret/hull interface in case of turret moored offshore unit.

For units fitted with risers, the riser loads cycles are to be taken into account for fatigue assessment of riser supports and their foundations.

**1.1.5** The following loads are not considered for fatigue analysis in this Guidance Note:

- dynamic loads resulting from main engine or propeller induced vibratory forces
- transient loads such as thermal stresses.

#### 1.2 Loading conditions

**1.2.1** The loading conditions, as well as the fraction of time for each loading condition over the life of the ship, to be considered for fatigue analysis are to be selected according to the applicable rules.

In this Guidance Note, quantities related to a particular loading condition are denoted with a (j) subscript.

#### 1.2.2 Loading/unloading

For the analysis of fatigue due to loading/unloading process, a sequence of still water loads (loading conditions) representative of an entire loading and unloading sequence is to be used to derive the maximum stress ranges.

## 1.3 Rule calculations

### 1.3.1 Load cases

Load cases for fatigue assessment are to be selected according to the applicable rules. The load cases are associated to a reference level of probability  $p_R$  (meaning that the long-term probability for the wave loads to exceed the wave loads in the load case is equal to  $p_R$ ) defined in the applicable rules.  $p_R = 10^{-2}$  is the recommended value for fatigue load cases.

Load cases to be considered for fatigue assessment are to be selected according to the applicable rules.

For each loading condition defined above, all fatigue load cases are to be considered to determine the fatigue damage as per Sec 11.

## 1.4 Spectral and time-domain calculations

### 1.4.1 Operational conditions

The operational conditions to be considered are as follows:

- Environmental conditions (scatter diagram, wave spectrum)

The wave scatter diagram is to be representative of the operational route or area. Wave spectrum (e.g. Pierson-Moskowitz, Jonswap) modelling the sea state energy is to be used:

- for sea-going ships, Pierson-Moskowitz spectrum is generally used as corresponding to navigation in open seas
- for offshore units, the wave Scatter diagram to be used is the one associated to the site under consideration, each sea-state being described by a wave spectrum of appropriate shape (e.g. Pierson-Moskowitz, Jonswap, Ochi-Hubble).

Selection of the applicable environmental conditions is to be performed according to the applicable rules.

- Loading conditions

Fatigue analysis is to be carried out for all the selected loading conditions, considering their corresponding occurrence probability.

The loading conditions, as well as the fraction of time for each loading condition over the life of the unit, to be considered for fatigue analysis are to be selected according to the applicable rules.

- Speed profile

Unless otherwise specified by the applicable rules, the ship speed is to be taken as 75% of the design speed. It is assumed that this above speed corresponds to the actual forward speed in moderate wave heights, which are responsible for most of the fatigue damage.

## 2 Fixed offshore structures

### 2.1 Loads types

**2.1.1** For fixed offshore structures, the fluctuating loads resulting in fatigue damage are mainly due to wave induced loads during the in-service conditions.

The following sources of fatigue damage are also to be considered, when relevant:

- vortex induced vibrations (VIV) due to wave and/or wind
- wind cyclic loads
- transportation
- installation, in particular during pile driving.

### 2.2 Determination of loads

**2.2.1** The determination of the fatigue loads depends on the calculation procedure. The ocean environment description considered for the local wave actions calculations can be addressed with the following methods:

- deterministic method: the ocean environment is described by series of individual periodic waves with a particular height, period and direction and an associated number of occurrences (see ISO 19902, 16.8)
- spectral calculation: the ocean environment is described by series of short-term sea spectra (see ISO 19902, 16.7)
- time-domain: the short-term seastates are represented by time-domain simulations on irregular waves (see Sec 11, [4]).

## SECTION 3

## HOT SPOT STRESS BASED ON ANALYTICAL APPROACH FOR LONGITUDINAL STIFFENERS

### 1 General

#### 1.1 Application

##### 1.1.1 Scope

This Section defines the procedure for the analytical calculation of the hot spot stress in longitudinal stiffener connections.

##### 1.1.2 Fatigue modes

Two main types of fatigue cracks are encountered at longitudinal stiffeners connection with primary supporting members:

- axial and bending stress induced fatigue (see [1.2]), and
- shear stress induced fatigue (see [1.3]).

##### 1.1.3 Net scantling

For the stress calculation, the net scantling approach as defined in Sec 1, [3.3] is to be applied, except otherwise prescribed by the applicable rules.

#### 1.2 Axial and bending stress fatigue

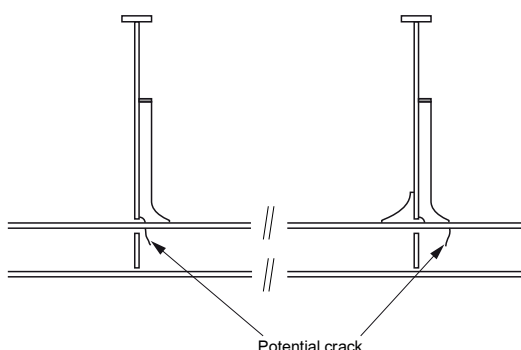
##### 1.2.1 General

This sub-article deals with the assessment of fatigue induced by the axial and bending modes (see Fig 1) in way of longitudinal stiffener connections to primary members.

The analytical stress analysis aims at evaluating the hot spot stress at the flange of longitudinal stiffener connections with primary supporting members. The longitudinal stiffener is considered as a beam subjected to:

- axial loads induced by hull girder bending, and
- local bending induced by lateral pressure.

**Figure 1 : Cracks in longitudinal stiffener web due to bending mode**



##### 1.2.2 Hot spots

The hot spot stress ranges and hot spot mean stresses, in way of both end connections of longitudinal stiffeners, are to be evaluated at the flange of the longitudinal stiffener, at the hot spots located at point 'A' and point 'B' (see Fig 2).

##### 1.2.3 Effect of primary structure distortion

For web frames or floors that are part of a transverse bulkhead or are in way of a transverse stool, the additional hot spot stress due to the relative displacement of the primary structure is to be considered.

For other web frames or floors, additional hot spot stress due to the relative displacement does not need to be considered.

Figure 2 : Hot spots at connection of longitudinal stiffeners with transverse members



1.2.4 Applicable S-N curve

The applicable S-N curve to be used for the assessment of longitudinal stiffener welded connections is the  $P_{\perp}$  curve, since the calculated hot spot stress is taken perpendicular to the weld.

The basic  $P_{\perp}$  S-N curve to be used is given in Sec 9, [2]. This basic S-N curve is to be corrected for factors affecting the fatigue strength as described in Sec 10.

If the weld toe angle is lower than or equal to  $30^{\circ}$ , the S-N curve to be used is  $P_{//}$ .

1.3 Shear stress fatigue

1.3.1 General

In addition to the fatigue cracks in the stiffener flange, some fatigue crack may occur in the web of the primary supporting members or in the collar plate, due to shear (see Fig 3).

The typical hot spots at the collar plate and in the slot are shown in Fig 4.

Figure 3 : Cracks in web of primary supporting members due to shear mode

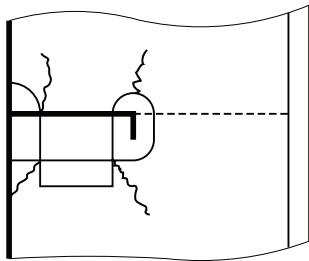
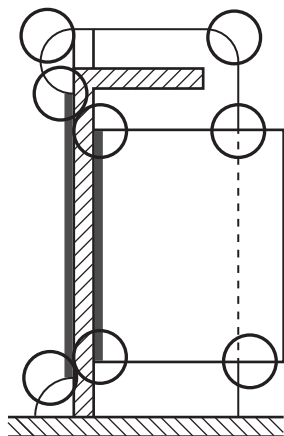


Figure 4 : Typical hot spots at collar plate and slot





### 1.3.2 Driving loads

Cracks under shear mode are mainly due to the combination of global and local phenomena (see Fig 5).

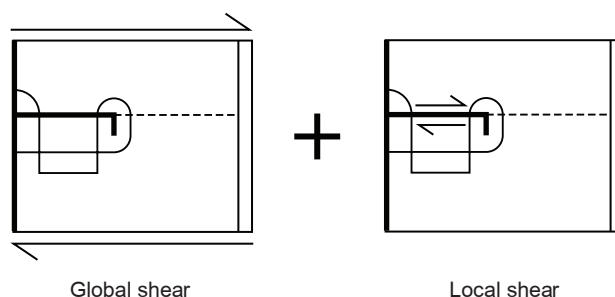
The global phenomenon corresponds to the bending of primary supporting members. The maximum shear stress induced by this bending occurs at the neutral fibre which is usually close to the cut out.

The local phenomenon corresponds to the shear stress induced in the longitudinal stiffener under lateral pressure.

### 1.3.3 Fatigue assessment

Prescriptions for the verification of the fatigue strength with regard to the shear mode fatigue can be found in the applicable rules.

**Figure 5 : Fatigue phenomenon under shear mode**



## 2 Axial and bending hot spot stress

### 2.1 General

#### 2.1.1 Principle

The determination of the longitudinal stiffener end connections hot spot stress is based on nominal stresses and stress concentration factors.

The hot spot stress is to be calculated at both stiffener end connections (point 'A' and point 'B') of the stiffener flange (see Fig 2).

#### 2.1.2 Nominal stress

The nominal stress includes:

- axial stress due to global hull girder bending moments
- local bending stress due to local pressures applied to the stiffener attached plate
- additional local bending stress due to the relative displacement of the primary structure for some locations (i.e. transverse webs or floors located at transverse bulkhead, including swash bulkhead, or in way of stool)
- warping stress when relevant.

Net thickness approach is used (see Sec 1, [3.3]).

#### 2.1.3 Stress concentration factors

For each hot spot of each connection, two geometric stress concentration factors ( $K_{ga}$  and  $K_{gb}$ ) are defined, for both the axial stress and the bending stress respectively.

Some geometric stress concentration factors are given in [3.1] for typical stiffener end connection geometries.

If a structural detail is different from those given in [3.1], the geometric stress concentration factors are to be calculated by a very fine mesh FE analysis according to the procedure given in [3.3].

#### 2.1.4 Additional stress concentration factors

The following additional stress concentration factors are to be applied, as relevant:

- stress concentration for unsymmetrical stiffener on laterally loaded panels, as given in [3.2]
- stress concentration due to workmanship issues (axial and angular misalignments), as given in Sec 10, [5].

#### 2.1.5 Hot spot stress range and mean stress for the rule based fatigue procedure

For the rule based fatigue procedure described in Sec 11, [2], the hot spot stress range calculation is described in [4.1.2]. The associated mean hot spot stress calculation is described in [4.1.3].

### 2.1.6 Hot spot stress for the direct calculation procedures

For the direct calculation fatigue procedures described in Sec 11, [3] and Sec 11, [4], the hot spot stress calculation is described in [4.2].

## 2.2 Global axial stress

### 2.2.1 Hull girder bending stress

The hull girder hot spot stress  $\sigma_G$ , in N/mm<sup>2</sup> is obtained from the following formula:

$$\sigma_G = f_{c-a} \cdot K_{ga} \cdot \left[ \frac{M_V}{I_{yy}} \cdot (z - z_{NA}) - \left( \frac{M_H}{I_{zz}} \cdot y \right) \right] \cdot 10^{-3}$$

where:

- $M_V$  : Vertical bending moment, in kN.m, taken positive when the upper part is in tension (hogging)
- $M_H$  : Horizontal bending moment, in kN.m, taken positive when starboard side is in tension
- $I_{yy}$  : Vertical hull girder moment of inertia at the longitudinal position being considered, in m<sup>4</sup>, in the net scantling as prescribed in [1.1.3]
- $I_{zz}$  : Horizontal hull girder moment of inertia at the longitudinal position being considered, in m<sup>4</sup>, in the net scantling as prescribed in [1.1.3]
- $y$  : Transverse coordinate of the stress calculation point under consideration, in m, taken positive toward portside
- $z$  : Vertical coordinate of the stress calculation point under consideration, in m, taken positive upwards
- $z_{NA}$  : Distance from the baseline to the horizontal neutral axis, in m
- $K_{ga}$  : Geometric stress concentration factor due to axial load
- $f_{c-a}$  : Correction factor for the effect of corrosion, applied on the axial stress:
  - in case the single structural model approach described in Sec 1, [3.3.3] has been selected: the value of  $f_{c-a}$  is given in the applicable rules
  - otherwise:  $f_{c-a} = 1,0$

### 2.2.2 Hull girder warping stress

For ships with large deck openings, or if required by the applicable rules, the longitudinal stress induced by the restrained hull girder section warping is to be calculated in way of the fatigue details.

The hot spot warping stress  $\sigma_\Omega$ , in N/mm<sup>2</sup>, is obtained from the following formula:

$$\sigma_\Omega = f_{c-a} \cdot K_{ga} \cdot \sigma_{warp}$$

where:

- $K_{ga}$  : Geometric stress concentration factor due to axial load
- $\sigma_{warp}$  : Warping nominal stress due to the torsion, in N/mm<sup>2</sup>
- $f_{c-a}$  : Correction factor for the effect of corrosion, applied on the axial stress, as defined in [2.2.1].

The nominal warping stress is determined according to the prescriptions of the applicable rules.

## 2.3 Local bending stress

### 2.3.1 Stress due to stiffener bending

The hot spot stress  $\sigma_L$ , in N/mm<sup>2</sup>, due to the local pressure is obtained from the following formula, or from the formula prescribed by the applicable rules:

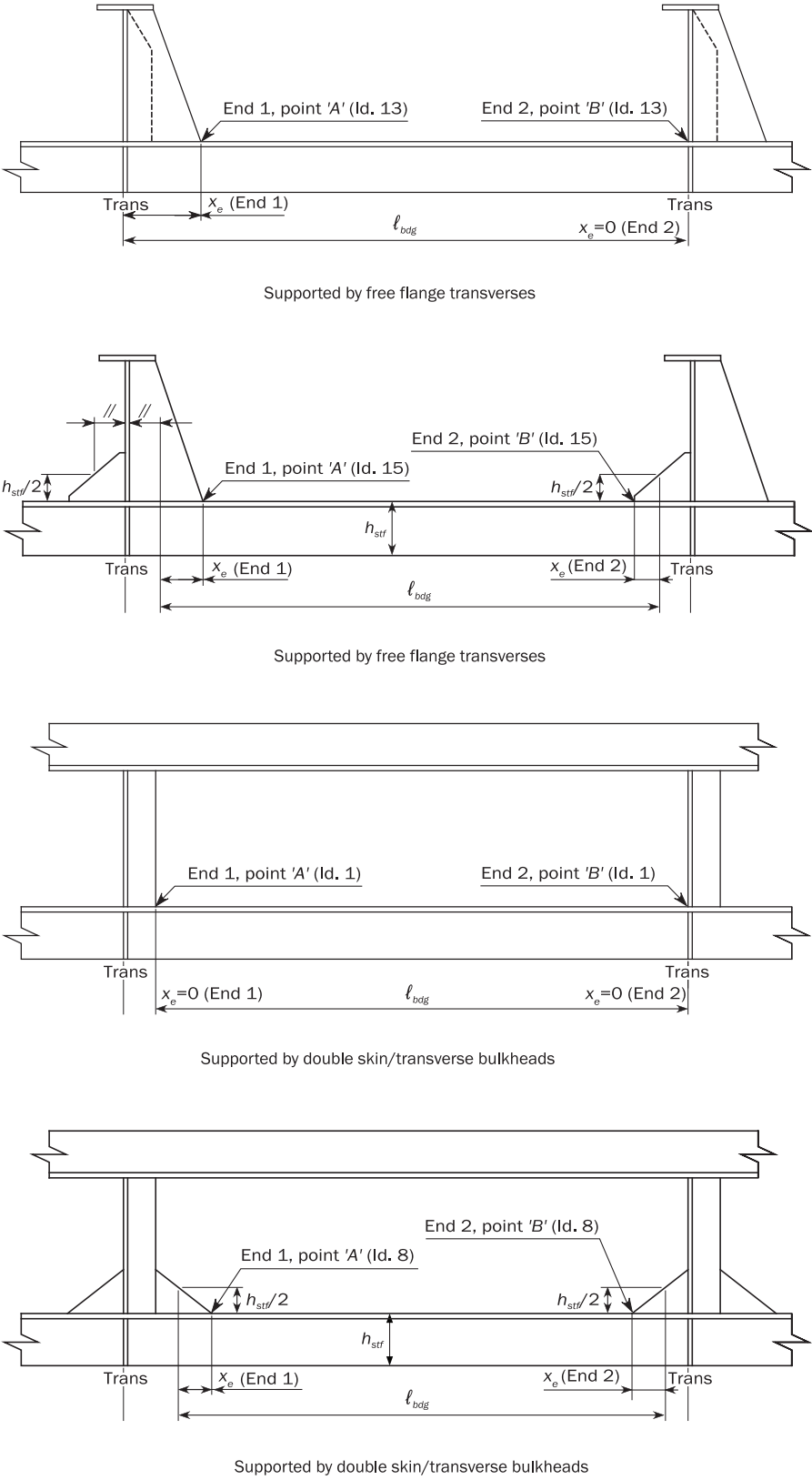
$$\sigma_L = f_{c-b} \cdot K_{gb} \cdot \left[ K_n \cdot s \cdot \ell_{bdg}^2 \cdot P_{LT} \cdot \left( 1 - \frac{6x_e}{\ell_{bdg}} + \frac{6x_e^2}{\ell_{bdg}^2} \right) \right] / (12 \cdot Z_{eff})$$

where:

- $\ell_{bdg}$  : Effective bending span of stiffener, in m, as defined in Fig 6, unless otherwise specified in the applicable rules
- $s$  : Stiffener spacing, in mm
- $K_n$  : Additional stress concentration factor due to unsymmetrical stiffener geometry, as defined in [3.2]
- $P_{LT}$  : Local pressure at mid span, in kN/m<sup>2</sup>, as defined in [2.3.2]
- $x_e$  : Distance, in m, to the hot spot from the closest end of the bending span, as defined in Fig 6
- $Z_{eff}$  : Section modulus, in cm<sup>3</sup>, of the considered stiffener calculated, considering an effective breadth  $b_{eff}$  of the attached plating
- $K_{gb}$  : Geometric stress concentration factor due to lateral pressure given in [3.1] or determined as per [3.3]

- $f_{c,b}$  : Correction factor for the effect of corrosion, applied on the local bending stress:
- in case the single structural model approach described in Sec 1, [3.3.3] has been selected: the value of  $f_{c,b}$  is given in the applicable rules
  - otherwise:  $f_{c,b} = 1,0$

**Figure 6 : Definition of effective span ( $\ell_{bdg}$ ) and distance ( $x_e$ ) to the hot spot**



### 2.3.2 Total local pressure

The total pressure acting on the stiffener attached plate is given by:

$$P_{LT} = P_{L\_Stif} - P_{L\_Opp}$$

where:

$P_{L\_Stif}$  : Pressure at mid span, in kN/m<sup>2</sup>, applied on the stiffener side of the attached plating

$P_{L\_Opp}$  : Pressure at mid span, in kN/m<sup>2</sup>, applied on the plating side opposite to the stiffener side.

### 2.3.3 Effective breadth

The effective breadth  $b_{eff}$ , in mm, of the attached plating to be used for the computation of the effective stiffener modulus is given by:

- for  $\frac{\ell_{bdg}}{s} \left(1 - \frac{1}{\sqrt{3}}\right) \cdot 10^3 \geq 1$ :

$$b_{eff} = s \cdot \text{Min} \left\{ 1, 04 / \left[ 1 + 3 \left( \frac{\ell_{bdg}}{s} \left(1 - \frac{1}{\sqrt{3}}\right) \cdot 10^3 \right)^{-1,35} \right] ; 1, 0 \right\}$$

- for  $\frac{\ell_{bdg}}{s} \left(1 - \frac{1}{\sqrt{3}}\right) \cdot 10^3 < 1$ :

$$b_{eff} = 0, 26 \cdot \ell_{bdg} \cdot \left(1 - \frac{1}{\sqrt{3}}\right) \cdot 10^3$$

where:

$\ell_{bdg}$  : Effective bending span of stiffener, as defined in [2.3.1]

$s$  : Stiffener spacing, in mm.

## 2.4 Stress due to relative displacements of primary supporting members

### 2.4.1 General

The additional hot spot stress due to the relative displacement of primary supporting members is to be considered for longitudinal stiffener end connections fitted on transverse web frames or floors located:

- in way of plane transverse bulkheads (including swash bulkheads in cargo holds), or
- in way of transverse stools and cofferdam bulkheads.

### 2.4.2 Displacement of primary supporting members

The displacement of primary supporting members is to be evaluated using a finite element model that satisfies the prescriptions given in the applicable rules.

The displacement of a primary supporting member is the displacement of the point located at the intersection of the stiffener flange, the stiffener web and the supporting member web. This displacement is measured along the line defined by the intersection between the stiffener web and the primary supporting member web in the non-deformed state of the finite element model.

The displacement is counted positive in the direction from the stiffener flange towards the attached plating.

### 2.4.3 Relative displacements of primary supporting members

For the primary supporting members where the longitudinal stiffener fatigue details are located, two values of relative displacement are computed (see Fig 7):

- the relative displacement  $\delta_{Fwd}$  for the stiffener span in the forward direction, corresponding to the displacement of the first primary supporting member forward minus the displacement of the considered primary supporting member, and
- the relative displacement  $\delta_{Aft}$  for the stiffener span in the aft direction, corresponding to the displacement of the first primary supporting member aftward minus the displacement of the considered primary supporting member.

### 2.4.4 Relative displacements in way of transverse stools, cofferdam bulkheads and container carrier transverse bulkheads

For longitudinal stiffener connection details located in way of a transverse stool, a cofferdam bulkhead, or a container carrier transverse bulkhead, four different primary supporting members come into play: the two web frames in way of the transverse stool or bulkhead, and the two adjacent web frames in the forward and aft directions.

The longitudinal stiffener connection details located on the two web frames in way of the transverse stool are to be considered:

- for the details located on the foremost web frame in way of the stool:
  - the relative displacement  $\delta_{Fwd}$  is the displacement of the first adjacent web frame forward of the stool minus the displacement of the foremost stool web frame
  - the relative displacement  $\delta_{Aft}$  is the displacement of the aftmost stool web frame minus the displacement of the foremost stool web frame
- for the details located on the aftmost web frame in way of the stool:
  - the relative displacement  $\delta_{Aft}$  is the displacement of the first adjacent web frame aft of the stool minus the displacement of the aftmost stool web frame
  - the relative displacement  $\delta_{Fwd}$  is the displacement of the foremost stool web frame minus the displacement of the aftmost stool web frame.

#### 2.4.5 Stress due to relative displacement

The stress due to relative displacements, in N/mm<sup>2</sup>, for both locations 'a' and 'f' shown on Fig 7, is to be obtained directly from the following formulae:

- for location 'a':

$$\sigma_D = f_{c,b} \cdot K_{gb} \cdot (\sigma_{d_{Fwd,a}} + \sigma_{d_{Aft,a}})$$

- for location 'f':

$$\sigma_D = f_{c,b} \cdot K_{gb} \cdot (\sigma_{d_{Fwd,f}} + \sigma_{d_{Aft,f}})$$

where:

$K_{gb}$  : Geometric stress concentration factor for stiffener bending stress for the location 'a' or 'f'. Each location 'a' or 'f' may correspond to point 'A' or 'B' as defined in Tab 1 depending on the stiffener end connection design

$f_{c,b}$  : Correction factor for the effect of corrosion, applied on the local bending stress, as defined in [2.3.1]

$\sigma_{d_{Fwd,a}}, \sigma_{d_{Aft,a}}$  : Additional stresses at location 'a', in N/mm<sup>2</sup>, due to the relative displacements of the primary supporting members, obtained from the following formulae:

$$\sigma_{d_{Fwd,a}} = \frac{3,9\delta_{Fwd} \cdot E \cdot I_{Aft} \cdot I_{Fwd}}{Z_{Aft} \cdot \ell_{Fwd} \cdot (\ell_{Aft} \cdot I_{Fwd} + \ell_{Fwd} \cdot I_{Aft})} \left(1 - 1,15 \frac{|x_{e,Aft}|}{\ell_{Aft}}\right) 10^{-5}$$

$$\sigma_{d_{Aft,a}} = \left[ \frac{3,9\delta_{Aft} \cdot E \cdot I_{Aft} \cdot I_{Fwd}}{Z_{Aft} \cdot \ell_{Aft} \cdot (\ell_{Aft} \cdot I_{Fwd} + \ell_{Fwd} \cdot I_{Aft})} \left(1 - 1,15 \frac{|x_{e,Aft}|}{\ell_{Aft}}\right) - \frac{0,9\delta_{Aft} \cdot E \cdot I_{Aft} \cdot |x_{e,Aft}|}{Z_{Aft} \cdot \ell_{Aft}^3} \right] 10^{-5}$$

$\sigma_{d_{Fwd,f}}, \sigma_{d_{Aft,f}}$  : Additional stresses at location 'f', in N/mm<sup>2</sup>, due to the relative displacements of the primary supporting members, obtained from the following formulae:

$$\sigma_{d_{Fwd,f}} = \left[ \frac{3,9\delta_{Fwd} \cdot E \cdot I_{Aft} \cdot I_{Fwd}}{Z_{Fwd} \cdot \ell_{Fwd} \cdot (\ell_{Aft} \cdot I_{Fwd} + \ell_{Fwd} \cdot I_{Aft})} \left(1 - 1,15 \frac{|x_{e,Fwd}|}{\ell_{Fwd}}\right) - \frac{0,9\delta_{Fwd} \cdot E \cdot I_{Fwd} \cdot |x_{e,Fwd}|}{Z_{Fwd} \cdot \ell_{Fwd}^3} \right] 10^{-5}$$

$$\sigma_{d_{Aft,f}} = \frac{3,9\delta_{Aft} \cdot E \cdot I_{Aft} \cdot I_{Fwd}}{Z_{Fwd} \cdot \ell_{Aft} \cdot (\ell_{Aft} \cdot I_{Fwd} + \ell_{Fwd} \cdot I_{Aft})} \left(1 - 1,15 \frac{|x_{e,Fwd}|}{\ell_{Fwd}}\right) 10^{-5}$$

where:

$I_{Fwd}, I_{Aft}$  : Moments of inertia, in net scantlings, of the forward and aftward longitudinals, in cm<sup>4</sup>

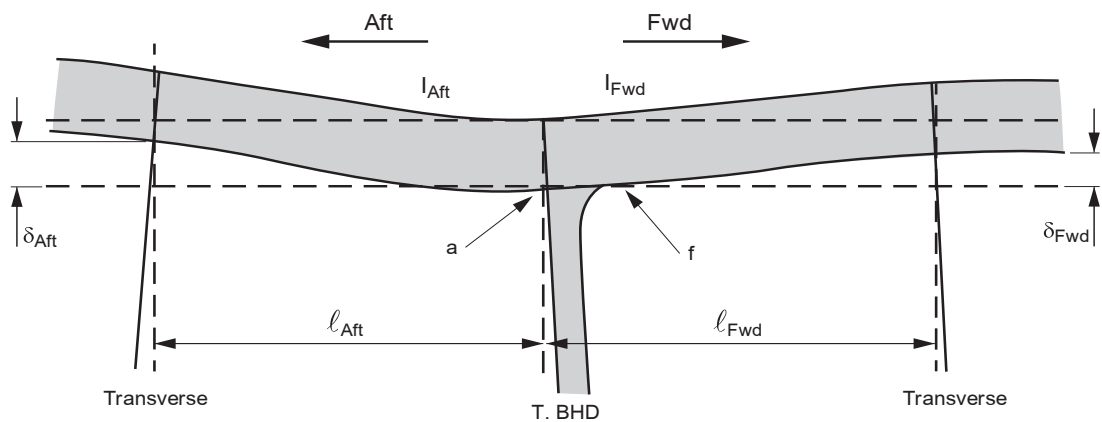
$Z_{Fwd}, Z_{Aft}$  : Section moduli, in net scantlings, of the forward and aftward stiffeners, in cm<sup>3</sup>

$\ell_{Fwd}, \ell_{Aft}$  : Spans, in m, of the forward and aftward longitudinals, as shown in Fig 7

$x_{e,Fwd}, x_{e,Aft}$  : Distances, in m, to the hot spot in location 'a' or 'f', from the closest end of the forward and aftward longitudinal spans, respectively, as shown in Fig 6

$\delta_{Fwd}, \delta_{Aft}$  : Relative displacements, in mm, between the transverse bulkhead (or floor) and the forward or aftward web frame (or floor) determined according to [2.4.3] or [2.4.4].

Figure 7 : Definition of the relative displacement (ordinary transverse bulkhead)



3 Stress concentration factors (SCF)

3.1 Stress concentration factors for longitudinal stiffener end connections

3.1.1 Standard connection types

Stress concentration factors  $K_{ga}$  and  $K_{gb}$  are given in Tab 1 for end connection of stiffeners subjected to axial and lateral loads. The values for soft toe given in Tab 1 are valid provided that the toe geometry of web stiffener and backing bracket complies with the following requirements:

$\theta \leq 20$

$h_{toe} \leq \text{Max} (t_{bkt\_gr} ; 15)$

where:

$\theta$  : Angle of the bracket toe, in deg, as shown in Fig 8 and Fig 9

$h_{toe}$  : Height of the bracket toe, in mm

$t_{bkt\_gr}$  : Gross thickness of the bracket, in mm.

3.1.2 Other connection types

When the connection types are different from those given in Tab 1, the stress concentration factors should be determined using FEM analysis according to the requirements in [3.3].

Otherwise, the hot spot stress can be directly obtained as described in Sec 5.

Figure 8 : Detail design for soft toes and backing brackets

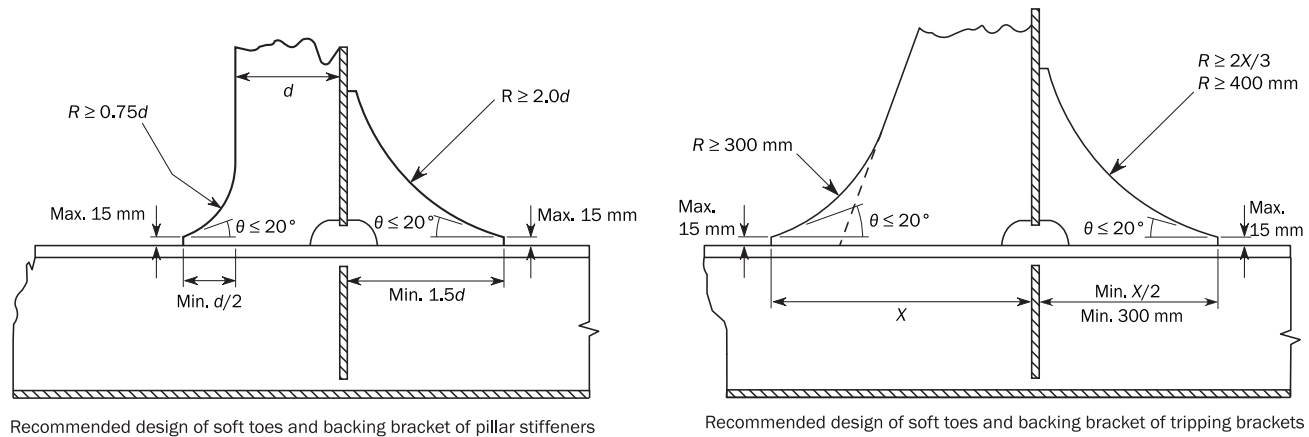


Figure 9 : Recommended alternative design of soft toes of tripping brackets

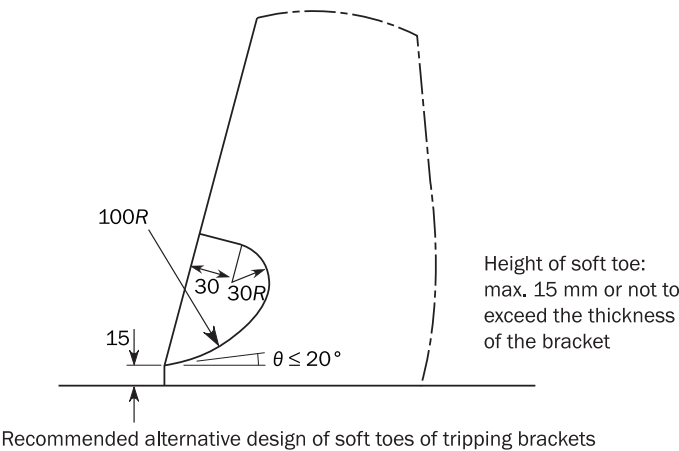
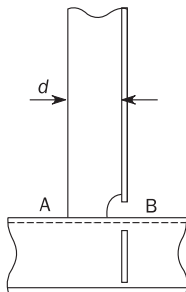
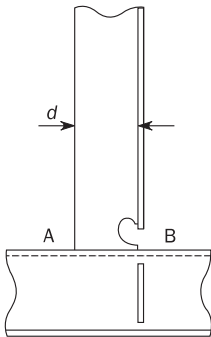
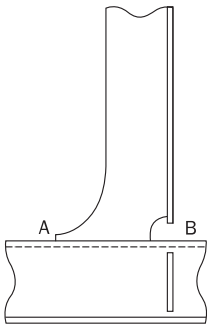
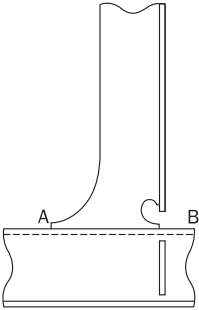
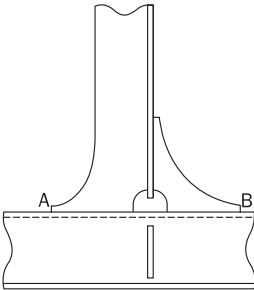
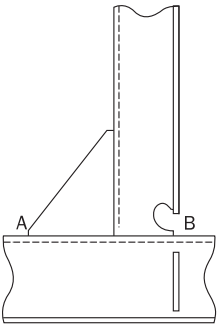
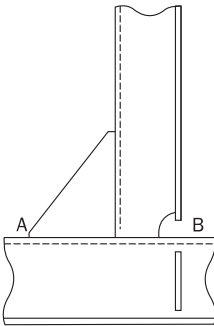
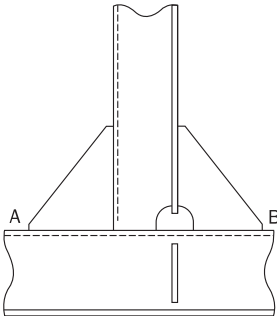
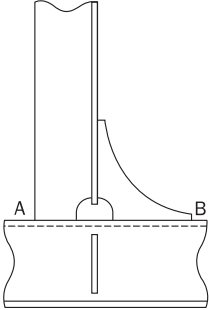
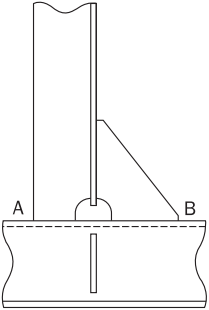
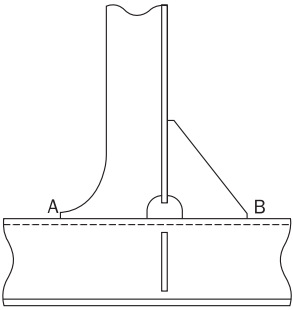
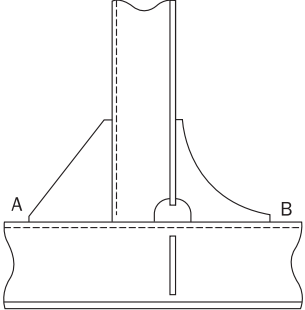
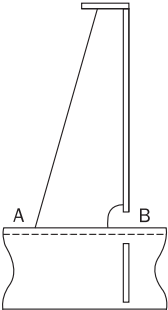


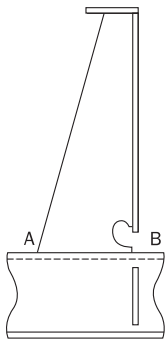
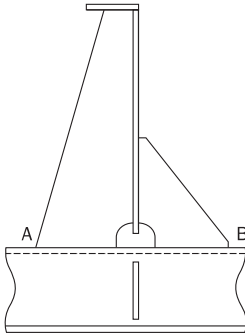
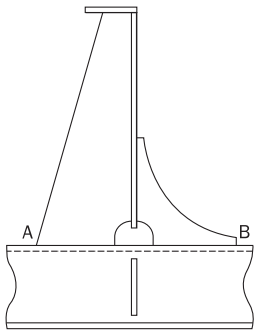
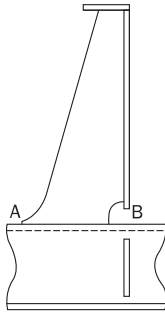
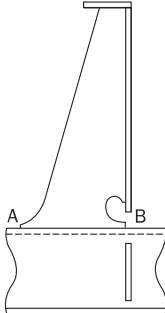
Table 1 : Geometric stress concentration factors  $K_{ga}$  and  $K_{gb}$

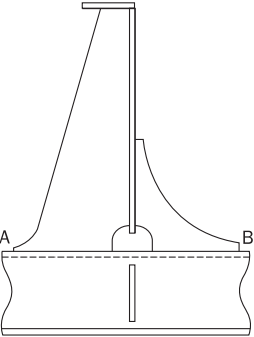
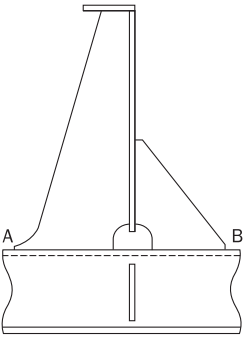
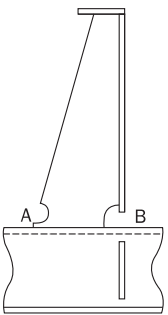
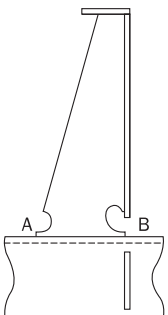
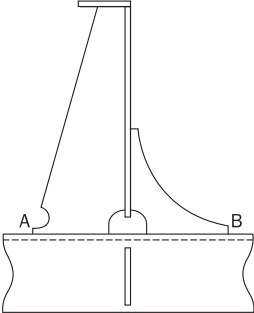
ID	Connection type (1)	Point 'A'		Point 'B'	
		$K_{ga}$	$K_{gb}$	$K_{ga}$	$K_{gb}$
1 (2)		<ul style="list-style-type: none"><li>for <math>d \leq 150</math>: <math>K_{ga} = 1,28</math></li><li>for <math>150 &lt; d \leq 250</math>: <math>K_{ga} = 1,36</math></li><li>for <math>d &gt; 250</math>: <math>K_{ga} = 1,45</math></li></ul>	<ul style="list-style-type: none"><li>for <math>d \leq 150</math>: <math>K_{gb} = 1,40</math></li><li>for <math>150 &lt; d \leq 250</math>: <math>K_{gb} = 1,50</math></li><li>for <math>d &gt; 250</math>: <math>K_{gb} = 1,60</math></li></ul>	<ul style="list-style-type: none"><li>for <math>d \leq 150</math>: <math>K_{ga} = 1,28</math></li><li>for <math>150 &lt; d \leq 250</math>: <math>K_{ga} = 1,36</math></li><li>for <math>d &gt; 250</math>: <math>K_{ga} = 1,45</math></li></ul>	$K_{gb} = 1,60$
2 (2)		<ul style="list-style-type: none"><li>for <math>d \leq 150</math>: <math>K_{ga} = 1,28</math></li><li>for <math>150 &lt; d \leq 250</math>: <math>K_{ga} = 1,36</math></li><li>for <math>d &gt; 250</math>: <math>K_{ga} = 1,45</math></li></ul>	<ul style="list-style-type: none"><li>for <math>d \leq 150</math>: <math>K_{gb} = 1,40</math></li><li>for <math>150 &lt; d \leq 250</math>: <math>K_{gb} = 1,50</math></li><li>for <math>d &gt; 250</math>: <math>K_{gb} = 1,60</math></li></ul>	<ul style="list-style-type: none"><li>for <math>d \leq 150</math>: <math>K_{ga} = 1,14</math></li><li>for <math>150 &lt; d \leq 250</math>: <math>K_{ga} = 1,24</math></li><li>for <math>d &gt; 250</math>: <math>K_{ga} = 1,34</math></li></ul>	$K_{gb} = 1,27$
3		$K_{ga} = 1,28$	$K_{gb} = 1,34$	$K_{ga} = 1,52$	$K_{gb} = 1,67$

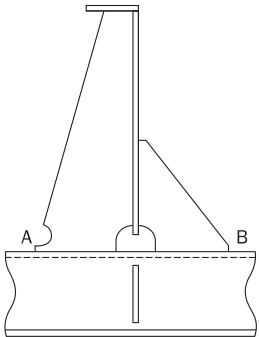
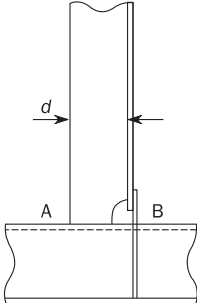
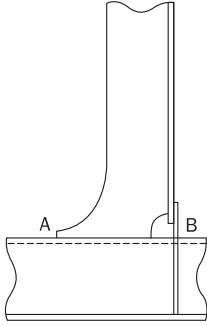
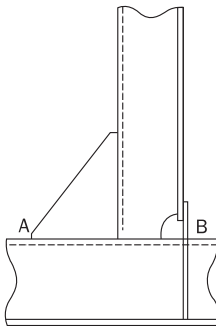
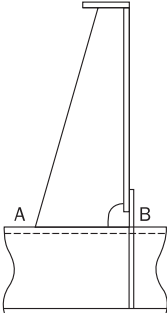
ID	Connection type (1)	Point 'A'		Point 'B'	
		$K_{ga}$	$K_{gb}$	$K_{ga}$	$K_{gb}$
4		$K_{ga} = 1,28$	$K_{gb} = 1,34$	$K_{ga} = 1,34$	$K_{gb} = 1,34$
5		$K_{ga} = 1,28$	$K_{gb} = 1,34$	$K_{ga} = 1,28$	$K_{gb} = 1,34$
6		$K_{ga} = 1,52$	$K_{gb} = 1,67$	$K_{ga} = 1,34$	$K_{gb} = 1,34$
7		$K_{ga} = 1,52$	$K_{gb} = 1,67$	$K_{ga} = 1,52$	$K_{gb} = 1,67$
8		$K_{ga} = 1,52$	$K_{gb} = 1,67$	$K_{ga} = 1,52$	$K_{gb} = 1,67$

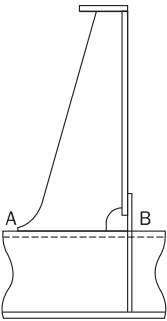
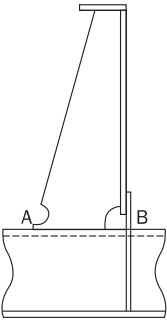
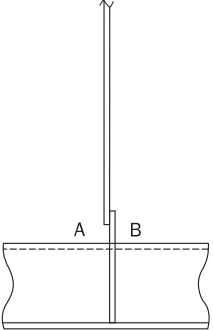
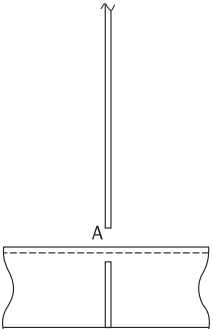


ID	Connection type (1)	Point 'A'		Point 'B'	
		$K_{ga}$	$K_{gb}$	$K_{ga}$	$K_{gb}$
9		$K_{ga} = 1,52$	$K_{gb} = 1,67$	$K_{ga} = 1,28$	$K_{gb} = 1,34$
10		$K_{ga} = 1,52$	$K_{gb} = 1,67$	$K_{ga} = 1,52$	$K_{gb} = 1,67$
11		$K_{ga} = 1,28$	$K_{gb} = 1,34$	$K_{ga} = 1,52$	$K_{gb} = 1,67$
12		$K_{ga} = 1,52$	$K_{gb} = 1,67$	$K_{ga} = 1,28$	$K_{gb} = 1,34$
13		$K_{ga} = 1,52$	$K_{gb} = 1,67$	$K_{ga} = 1,52$	$K_{gb} = 1,67$

ID	Connection type (1)	Point 'A'		Point 'B'	
		$K_{ga}$	$K_{gb}$	$K_{ga}$	$K_{gb}$
14		$K_{ga} = 1,52$	$K_{gb} = 1,67$	$K_{ga} = 1,34$	$K_{gb} = 1,34$
15		$K_{ga} = 1,52$	$K_{gb} = 1,67$	$K_{ga} = 1,52$	$K_{gb} = 1,67$
16		$K_{ga} = 1,52$	$K_{gb} = 1,67$	$K_{ga} = 1,28$	$K_{gb} = 1,34$
17		$K_{ga} = 1,28$	$K_{gb} = 1,34$	$K_{ga} = 1,52$	$K_{gb} = 1,67$
18		$K_{ga} = 1,28$	$K_{gb} = 1,34$	$K_{ga} = 1,34$	$K_{gb} = 1,34$

ID	Connection type (1)	Point 'A'		Point 'B'	
		$K_{ga}$	$K_{gb}$	$K_{ga}$	$K_{gb}$
19		$K_{ga} = 1,28$	$K_{gb} = 1,34$	$K_{ga} = 1,28$	$K_{gb} = 1,34$
20		$K_{ga} = 1,28$	$K_{gb} = 1,34$	$K_{ga} = 1,52$	$K_{gb} = 1,67$
21		$K_{ga} = 1,28$	$K_{gb} = 1,34$	$K_{ga} = 1,52$	$K_{gb} = 1,67$
22		$K_{ga} = 1,28$	$K_{gb} = 1,34$	$K_{ga} = 1,34$	$K_{gb} = 1,34$
23		$K_{ga} = 1,28$	$K_{gb} = 1,34$	$K_{ga} = 1,28$	$K_{gb} = 1,34$

ID	Connection type (1)	Point 'A'		Point 'B'	
		$K_{ga}$	$K_{gb}$	$K_{ga}$	$K_{gb}$
24		$K_{ga} = 1,28$	$K_{gb} = 1,34$	$K_{ga} = 1,52$	$K_{gb} = 1,67$
25 (2)		<ul style="list-style-type: none"><li>• for <math>d \leq 150</math>: <math>K_{ga} = 1,28</math></li><li>• for <math>150 &lt; d \leq 250</math>: <math>K_{ga} = 1,36</math></li><li>• for <math>d &gt; 250</math>: <math>K_{ga} = 1,45</math></li></ul>	<ul style="list-style-type: none"><li>• for <math>d \leq 150</math>: <math>K_{gb} = 1,40</math></li><li>• for <math>150 &lt; d \leq 250</math>: <math>K_{gb} = 1,50</math></li><li>• for <math>d &gt; 250</math>: <math>K_{gb} = 1,60</math></li></ul>	<ul style="list-style-type: none"><li>• for <math>d \leq 150</math>: <math>K_{ga} = 1,14</math></li><li>• for <math>150 &lt; d \leq 250</math>: <math>K_{ga} = 1,24</math></li><li>• for <math>d &gt; 250</math>: <math>K_{ga} = 1,34</math></li></ul>	<ul style="list-style-type: none"><li>• for <math>d \leq 150</math>: <math>K_{gb} = 1,25</math></li><li>• for <math>150 &lt; d \leq 250</math>: <math>K_{gb} = 1,36</math></li><li>• for <math>d &gt; 250</math>: <math>K_{gb} = 1,47</math></li></ul>
26		$K_{ga} = 1,28$	$K_{gb} = 1,34$	$K_{ga} = 1,34$	$K_{gb} = 1,47$
27		$K_{ga} = 1,52$	$K_{gb} = 1,67$	$K_{ga} = 1,34$	$K_{gb} = 1,47$
28		$K_{ga} = 1,52$	$K_{gb} = 1,67$	$K_{ga} = 1,34$	$K_{gb} = 1,47$

ID	Connection type (1)	Point 'A'		Point 'B'	
		$K_{ga}$	$K_{gb}$	$K_{ga}$	$K_{gb}$
29		$K_{ga} = 1,28$	$K_{gb} = 1,34$	$K_{ga} = 1,34$	$K_{gb} = 1,47$
30		$K_{ga} = 1,28$	$K_{gb} = 1,34$	$K_{ga} = 1,34$	$K_{gb} = 1,47$
31		$K_{ga} = 1,13$	$K_{gb} = 1,20$	$K_{ga} = 1,13$	$K_{gb} = 1,20$
32 (3) (4)		$K_{ga} = 1,13$	$K_{gb} = 1,14$	—	—

- (1) Where the longitudinal stiffener is a flat bar and there is a web stiffener/bracket welded to the flat bar stiffener, the stress concentration factor listed in the Table is to be multiplied by a factor of 1,12 when the thickness of attachment is thicker than the 0,7 times thickness of flat bar stiffener. This also applies to unsymmetrical profiles where there is less than 8 mm clearance between the edge of the stiffener flange and the attachment, e.g. bulb or angle profiles where the clearance of 8 mm cannot be achieved.
- (2) The attachment length  $d$ , in mm, is defined as the length of the welded attachment on the longitudinal stiffener flange without deduction of scallop.
- (3) For connection type ID 32 with no collar and/or web plate welded to the flange, the stress concentration factors provided in this Table are to be used irrespective of slot configuration.
- (4) The fatigue assessment point 'A' is located at the connection between the stiffener web and the transverse web frame or lug plate.

3.2 SCF for unsymmetrical stiffeners

3.2.1 Angle profiles

The stress concentration factor  $K_n$  for unsymmetrical flange of built-up and rolled angle stiffeners under lateral load, calculated at the web mid-thickness position, as shown in Fig 10, is given by:

$$K_n = \frac{1 + \lambda \cdot \beta^2}{1 + \lambda \cdot \beta^2 \cdot \Psi_z}$$

where:

$$\lambda = \frac{3 \left( 1 + \frac{\eta}{280} \right)}{1 + \frac{\eta}{40}}$$

$$\beta = 1 - \frac{2 \cdot b_g}{b_f} \quad \text{for built-up profiles}$$

$$\beta = 1 - \frac{t_w}{b_f} \quad \text{for rolled angle profiles}$$

$$\Psi_z = \frac{h_w^2 \cdot t_w}{4 \cdot Z} \cdot 10^{-3}$$

with:

$$\eta = \frac{\ell_{bdg}^4 \cdot 10^{12}}{b_f^3 \cdot t_f \cdot h_{stf}^2 \cdot \left( \frac{4 \cdot h_{stf}}{t_w^3} + \frac{s}{t_p^3} \right)}$$

- $b_g$  : Eccentricity of the stiffener, equal to the distance from the flange edge to the web centreline, in mm, as shown in Fig 11
- $b_f$  : Flange breadth, in mm, as shown in Fig 11
- $t_w$  : Web thickness, in mm, as shown in Fig 11
- $t_f$  : Flange thickness, in mm, as shown in Fig 11
- $h_{stf}$  : Stiffener height, including the face plate, in mm, as shown in Fig 11
- $t_p$  : Thickness of the attached plating, in mm, as shown in Fig 11
- $h_w$  : Web height, in mm, as shown in Fig 11
- $Z$  : Section modulus, in  $\text{cm}^3$ , of the stiffener with an attached plating breadth equal to the stiffener spacing.

Figure 10 : Bending stress in stiffener with symmetrical or unsymmetrical flange

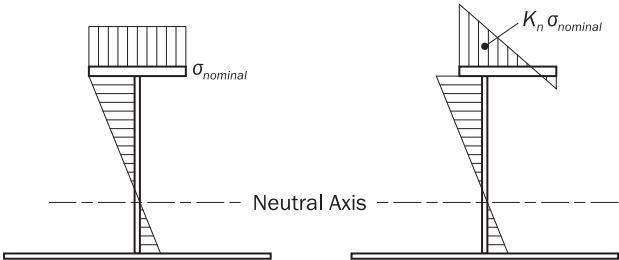
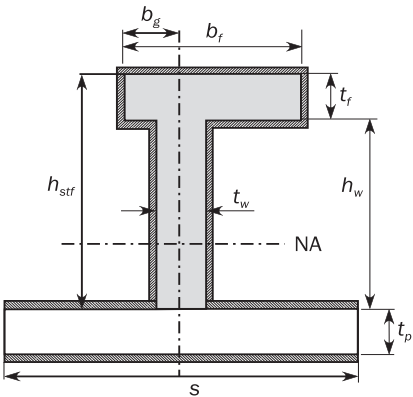


Figure 11 : Stiffener - Net scantling



### 3.2.2 Bulb profiles

For bulb profiles, factor  $K_n$  may be calculated using an equivalent built-up profile.

The equivalent built-up profile is to have the same properties as the bulb profile, i.e. the same:

- cross-sectional area
- moment of inertia of the profile about the horizontal neutral axis position, and
- moment of inertia of the profile about the vertical neutral axis position.

In addition, torsional constant and shear centre position of the equivalent built-up profile are to be checked.

Attention should be paid to the accuracy of this calculation. More accurate results can be obtained by determining the stress concentration factors by means of a FEM model as described in [3.3].

## 3.3 SCF for longitudinal stiffener end connections - Calculation by FEM

### 3.3.1 General

Upon agreement by the Society, the stress concentration factors for alternative designs are to be calculated by a very fine mesh FE analysis according to the requirements given in Sec 5.

Additional requirements for the derivation of stress concentration factors for stiffener end connections using very fine mesh FE analysis are given in this sub-article.

### 3.3.2 FE model extent

The FE model (see Fig 12) is to cover at least four web frame spacings in the longitudinal stiffener direction. The considered detail is to be located at the middle frame. The same type of end connection is to be modelled at all web frames. In the transverse direction, the model may be limited to one stiffener spacing.

### 3.3.3 Load application

In general, two loading cases are to be considered:

- axial loading, by enforced displacement applied to the model ends, and
- lateral loading, by unit pressure load applied to the shell plating.

### 3.3.4 Boundary conditions

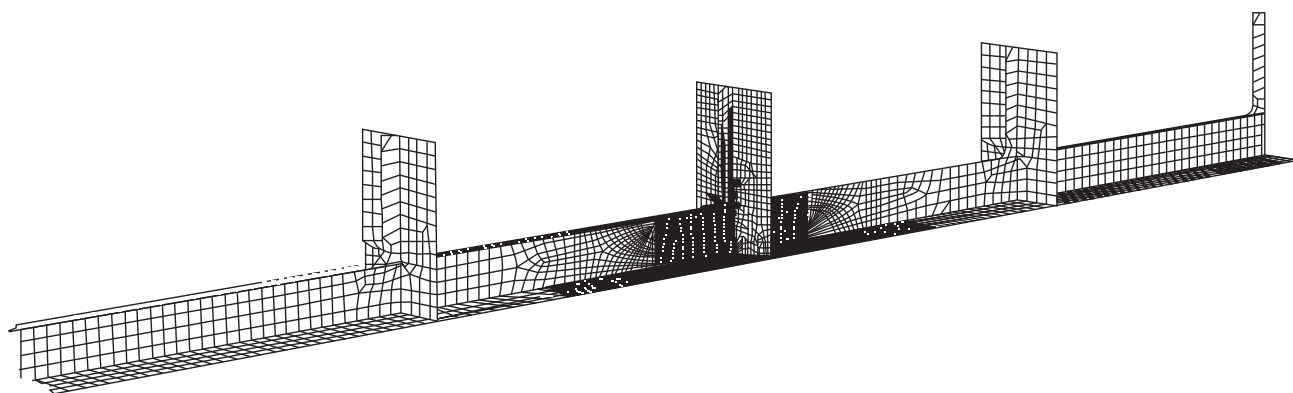
The following boundary conditions are to be applied on the FEM model:

- Symmetry conditions are applied along the longitudinal cut of the plate flange, along transverse and vertical cuts on web frames and on top of the web stiffener
- The model is to be fixed:
  - for lateral pressure loading: at both forward and aft ends in all degrees of freedom
  - for axial loading: at the aft end of the model for displacement in the longitudinal direction while enforced axial displacement is applied at the forward end, or vice versa.

### 3.3.5 FE mesh density

At the location of the hot spots under consideration, the element size shall be in the range of the thickness of the stiffener flange. In the remaining part of the model, the element size shall be in the range of  $s/10$ , where  $s$  is the stiffener spacing.

**Figure 12 : Example of fine mesh finite element model for the derivation of geometrical stress concentration factor**



### 3.3.6 Bulb profiles

When computing the stress concentration factors for a bulb profile, a solid elements FE model is recommended to improve the results. In order to capture the torsional properties of bulb sections, it is recommended to use a sufficient number of solid elements for modelling the bulb section.

### 3.3.7 Calculation of the geometric stress concentration

Two geometric stress concentration factors  $K_{ga}$  and  $K_{gb}$  are to be determined, for each load case mentioned in [3.3.3].

The geometric stress concentration factor is defined as the ratio of the hot spot stress derived from FE analysis on the nominal stress calculated according to analytical stress analysis for longitudinal stiffener connections.

The hot spot stress calculation is based on the procedure given in Sec 5, [3.3], Sec 5, [3.4] or Sec 5, [3.5].

The nominal stress is to be calculated according to analytical formulae based on unit load (i.e. the same loads than those used in the FEA).

- For the axial load case:

$$K_{ga} = \frac{\sigma_{HS\_AXIAL}}{\sigma_{nom\_AXIAL}}$$

where:

$\sigma_{HS\_AXIAL}$  : Hot spot stress determined by FE analysis at stiffener flange for the axial load

$\sigma_{nom\_AXIAL}$  : Nominal stress calculated at stiffener flange according to [2.2] for the same axial load applied in the FE analysis

- For the bending load case:

$$K_{gb} = \frac{\sigma_{HS\_Bending}}{\sigma_{nom\_Bending}}$$

where:

$\sigma_{HS\_Bending}$  : Hot spot stress determined by FE analysis at stiffener flange for the pressure load

$\sigma_{nom\_Bending}$  : Nominal stress calculated at stiffener flange according to [2.3] for the same pressure load applied in the FE analysis.

The  $K_{gb}$  value determined through this procedure includes the effect of the stiffener asymmetry, if any. Therefore, this value is generally to be associated with  $K_n = 1,0$ .

## 4 Hot spot stress

### 4.1 Hot spot stress range and mean value for rule based approach

#### 4.1.1 General

For the rule based approach, the hot spot stress is to be calculated separately from the load cases i1 and i2 of loading condition j as defined in Sec 11, [2.1].

Then the hot spot stress range is obtained as described in [4.1.2] and the associated hot spot mean stress is obtained as prescribed in [4.1.3].

#### 4.1.2 Hot spot stress range

The hot spot stress range due to still water plus wave induced loads, for load case (i) of loading condition (j), is obtained from the following formula:

$$\Delta\sigma_{HS,i(j)} = |(\sigma_{G,i1(j)} + \sigma_{\Omega,i1(j)} + \sigma_{L,i1(j)} + \sigma_{D,i1(j)}) - (\sigma_{G,i2(j)} + \sigma_{\Omega,i2(j)} + \sigma_{L,i2(j)} + \sigma_{D,i2(j)})|$$

where:

$\sigma_{G,i1(j)}$ ,  $\sigma_{G,i2(j)}$  : Global hull girder bending hot spot stress for load case i1 and i2 of loading condition j, calculated as prescribed in [2.2.1] using the still water plus wave induced bending moments

$\sigma_{\Omega,i1(j)}$ ,  $\sigma_{\Omega,i2(j)}$  : Global hull girder warping hot spot stress for load case i1 and i2 of loading condition j, calculated as prescribed in [2.2.2], if relevant, using the still water plus wave induced torsional moments

$\sigma_{L,i1(j)}$ ,  $\sigma_{L,i2(j)}$  : Local stiffener bending hot spot stress for load case i1 and i2 of loading condition j, calculated as prescribed in [2.3], using the still water plus wave induced pressures

$\sigma_{D,i1(j)}$ ,  $\sigma_{D,i2(j)}$  : Hot spot stress induced by the primary supporting members relative displacement, for load case i1 and i2 of loading condition j, calculated as prescribed in [2.4], using the still water plus wave induced loads.



### 4.1.3 Hot spot mean stress

The hot spot mean stress due to static plus wave induced loads, for load case (i) of loading condition (j), is obtained from the following formula:

$$\sigma_{\text{meanHS},i(j)} = \frac{1}{2} [(\sigma_{G,i1(j)} + \sigma_{\Omega,i1(j)} + \sigma_{L,i1(j)} + \sigma_{D,i1(j)}) + (\sigma_{G,i2(j)} + \sigma_{\Omega,i2(j)} + \sigma_{L,i2(j)} + \sigma_{D,i2(j)})]$$

where  $\sigma_{G,i1(j)}$ ,  $\sigma_{G,i2(j)}$ ,  $\sigma_{\Omega,i1(j)}$ ,  $\sigma_{\Omega,i2(j)}$ ,  $\sigma_{L,i1(j)}$ ,  $\sigma_{L,i2(j)}$ ,  $\sigma_{D,i1(j)}$ ,  $\sigma_{D,i2(j)}$  are defined in [4.1.2].

## 4.2 Hot spot stress for direct calculation approach

**4.2.1** For the direct calculation approach, the hot spot stresses are combined as follows, either in frequency domain or in time domain:

$$\sigma_{\text{HS}} = (\sigma_G + \sigma_{\Omega} + \sigma_L + \sigma_D)$$

where:

- $\sigma_G$  : Global hull girder bending hot spot stress calculated as prescribed in [2.2.1]
- $\sigma_{\Omega}$  : Global hull girder warping hot spot stress calculated as prescribed in [2.2.2], if relevant
- $\sigma_L$  : Local stiffener bending hot spot stress calculated as prescribed in [2.3.1]
- $\sigma_D$  : Hot spot stress induced by the relative displacement of the primary supporting members, calculated as prescribed in [2.4.5].

SECTION 4

HOT SPOT STRESS BASED ON ANALYTICAL  
APPROACH FOR TUBULAR JOINTS

1 General

1.1 Principles

**1.1.1** This Section deals with the determination of the hot spot stress in tubular node welded joints and tubular butt welded joints with an analytical approach. In this approach, the hot spot stress at the weld toe is derived from the nominal stress corrected by a geometric stress concentration factor  $K_g$ .

Partially penetrated tubular node joints and tubular butt joints are not permitted. Only fully penetrated tubular node joints and tubular butt joints are considered in this Section.

The nominal stress may be obtained from beam theory analytical calculations or from finite element models.

Geometric stress concentration factors may be already established (e.g. catalogue of details) or may be derived from FEA.

2 Tubular node welded joints

2.1 General

2.1.1 Scope

This Article deals with the fatigue of tubular node welded joints (i.e brace to chord connection) at weld toe (see Fig 1), based on hot spot stress obtained using the nominal stresses and the geometric stress concentration factor  $K_g$ .

$K_g$  is given by either parametric formulae (see [2.3.3]) or local FE analysis (see Sec 6, [2] for assessment methodology).

2.1.2 Nominal stress calculation

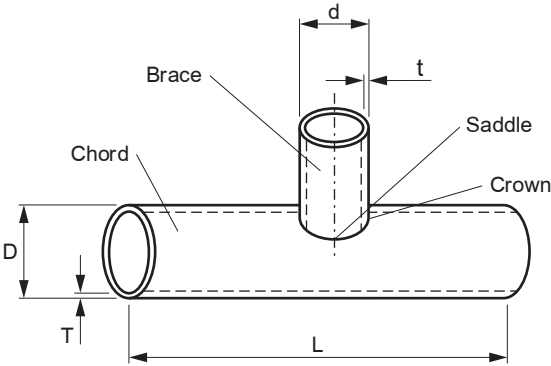
The nominal stresses are to be calculated by a space frame analysis, using a beam finite elements model. The calculations provide sectional forces and moments in the beam elements that represent the members of the structure. By definition, the corresponding stresses are nominal stresses.

The relevant nominal stresses to be considered for fatigue analysis are the following:

- axial stress
- in-plane bending stress
- out-of-plane bending stresses (see ISO 19902, par. 16.5).

The stress variations of these three nominal stress components shall be kept separate and shall not be combined. Shear stresses and torsional stresses may be neglected.

Figure 1 : Geometrical definitions for tubular joints



### 2.1.3 Hot spot stress calculation

For tubular joints, the geometric (hot-spot) stress ranges are to be determined at the connection, first by multiplying the brace nominal stress components by the associated geometric stress concentration factors ( $K_g$  associated to axial, in-plane bending, out-of-plane bending loading mode), and then by combining the geometric stress components.

The locations at which the geometric (hot spot) stress is to be assessed are given in [2.3.5].

## 2.2 Joint modelling

### 2.2.1 General

The modelling choices and the performance of the space frame analyses are not in the scope of the present Guidance Note. Guidance on the modelling of a joint structure is given in par. 12.3 of ISO 19902. However, the influence of joint modelling is mentioned due to its significant impact on the calculated nominal stresses.

### 2.2.2 Space frame model

The space frame model consists of members that are connected at nodes. The modelling of members is based on beam elements representing the axial, bending, shear and torsional stiffnesses of the structural members.

### 2.2.3 Simple node modelling

The simplest way of modelling tubular joints is to consider a node-to-node connection at the intersection of the centre lines of the brace and chord members, and to retrieve the nominal stresses at the intersection point.

### 2.2.4 Advanced node modelling

The node modelling can be refined by introducing joint flexibilities, which allows redistribution of the bending moments and retrieval of the nominal stresses at the actual weld position. Flexibilities modelling for fatigue analyses is accepted but shall be implemented with care for multi-braced joints due to cross terms contributions that may entail non-linear effects.

## 2.3 Simple tubular joints

### 2.3.1 Design hot spot stress

The design hot spot stress range  $\Delta\sigma_{HS}$  to be considered for fatigue analysis is the maximum value among the geometric stress ranges  $\Delta\sigma_G$  calculated at the specific locations around the tubular joint circumference defined in [2.3.5].

### 2.3.2 Joint classification

For the purpose of the evaluation of the geometric stress concentration factor  $K_g$ , tubular joints are usually classified into planar joints of T/Y, K, KT or X type (see typical examples in Fig 2).

Further details can be found in ISO 19902 (see section A.16.10.2.1.3).

The tubular joints classification is based on geometrical considerations (chord diameter, chord thickness, brace diameter, brace thickness), keeping in mind that the classification actually depends on the force flow in the framed structure and that the multi-planar effects are disregarded.

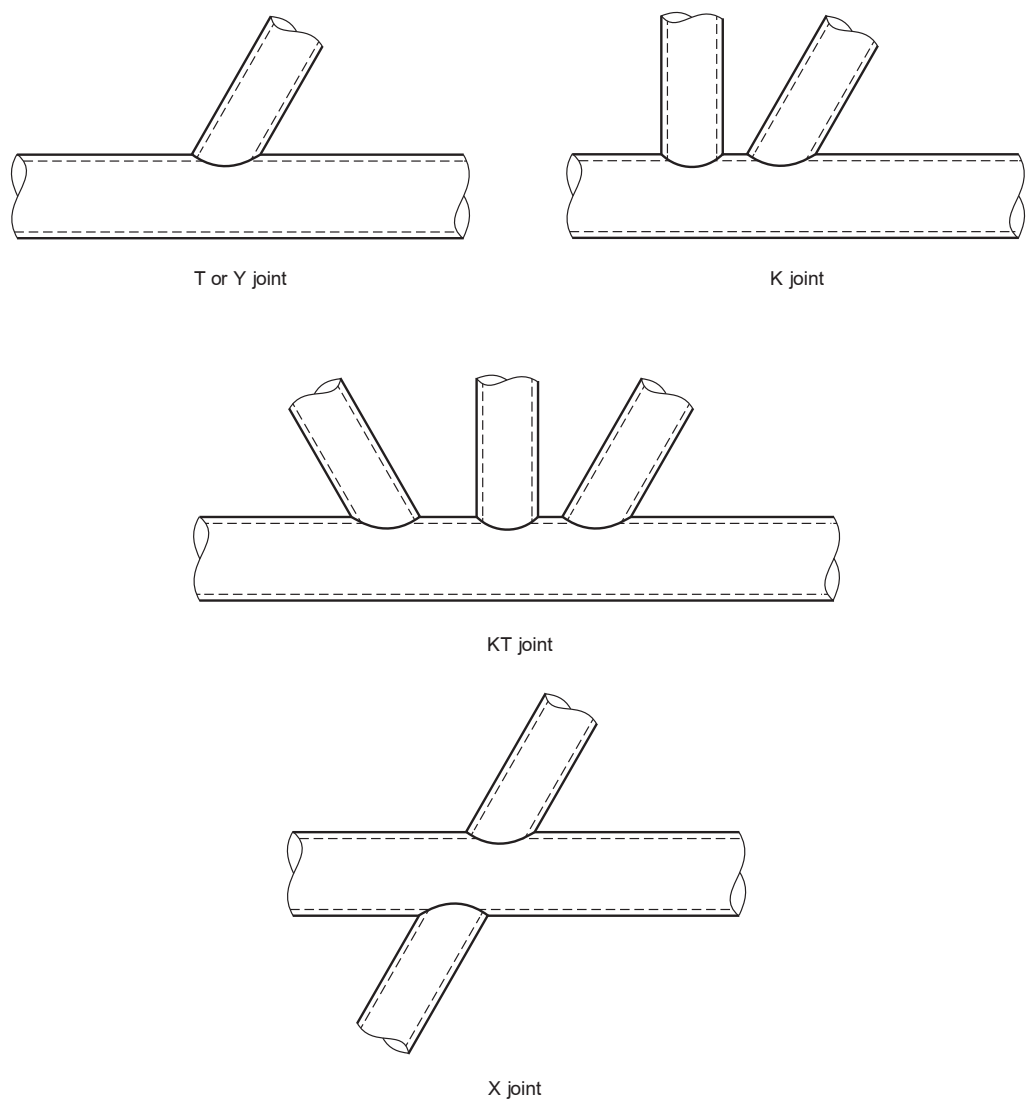
### 2.3.3 Geometric stress concentration factors

For simple planar joints (T/Y, K, KT, X) and simple loading mode (axial, in plane bending, out of plane bending), parametric  $K_g$  expressions have been developed. These equations are based on Efthymiou formulations and are detailed in ISO 19902, section A.16.10.2.2.2. These equations provide  $K_g$  for crown and saddle points of simple tubular joints at chord and brace side, as defined in Fig 1.

For crown and saddle locations, on both chord and brace sides,  $K_g$  is to be determined using Efthymiou equations and taking into account the chord length as prescribed in [2.3.4]. A minimum  $K_g$  value of 1,5 shall be considered (see ISO 19902, section 16.10.2.1).

Alternatively, or when the joint geometry does not allow the use of Efthymiou formulations, the geometric stress concentration factors  $K_g$  may be calculated at the locations defined in [2.3.5] by finite element analysis, as defined in Sec 6.

Figure 2 : Planar joint types



2.3.4 Influence of the chord length on the stress concentration factors

For fatigue assessment of the weld toe at chord side crown positions, the chord nominal bending stress should be considered and added to the hot spot stress due to the brace nominal loading. Actually, the chord bending stress is already included in the Efthymiou formulae via the parameter  $\alpha$ . The choice of this parameter is however not straight forward as it is linked to the chord length which has to be defined by the user.

As the chord nominal bending stress is already known from the space frame analysis, an alternative approach is to disregard the chord bending effect in Efthymiou formulae (i.e. by setting  $\alpha = 12$ ,  $C = 0,5$ ) and add the chord nominal bending stress obtained from the space frame analysis to the calculated hot spot stress.

In order to account for the presence of the welded brace, the chord bending stress to be added shall be multiplied by a  $K_g$  taken equal to 1,25 (see ISO 19902 A.16.10.2.1.5).

2.3.5 Combination of axial and bending stresses

The geometric stresses are to be calculated at eight locations around the circumference of the joint, at the chord side and at the brace side. Relevant locations shall include, as a minimum (see Fig 3):

- the chord sides at two crown positions
- the brace sides at two crown positions
- the chord sides at two saddle positions, and
- the brace sides at two saddle positions.

The geometric stresses at these points are derived by the combination of axial, in-plane bending and out-of-plane bending stresses.

When no  $K_g$  value is available at a given location, it can be estimated, considering:

- linear interpolation of the  $K_g$  values for axial loading, and
- sinusoidal interpolation of the  $K_g$  values for bending loading as detailed hereafter (see also Fig 3).

The geometric (hot spot) stress as a function of the circumferential location  $\phi$  can be expressed as follows:

$$\sigma_G(\phi) = K_{g_{AX}}(\phi) \sigma_{AX} + K_{g_{IPB}}(\phi) \sigma_{IPB} + K_{g_{OPB}}(\phi) \sigma_{OPB}$$

where:

$\phi$  : Angle around the chord to brace intersection, with  $\phi = 0$  at crown location (point 1 on Fig 3)

$\sigma_{AX}$ ,  $\sigma_{IPB}$ ,  $\sigma_{OPB}$  : Respectively the nominal maximum axial stress, in-plane bending stress and out-of-plane bending stress in the adjoining brace member

$K_{g_{AX}}(\phi)$ ,  $K_{g_{IPB}}(\phi)$ ,  $K_{g_{OPB}}(\phi)$  :  $\pi$ -periodic functions, defined as follows:

- for  $0 \leq \phi < \pi/2$ :

$$K_{g_{AX}}(\phi) = K_{g_{AX,crown}} + 2 (\phi/\pi) (K_{g_{AX,saddle}} - K_{g_{AX,crown}})$$

- for  $\pi/2 \leq \phi < \pi$ :

$$K_{g_{AX}}(\phi) = K_{g_{AX,saddle}} - K_{g_{AX,crown}} - 2 (\phi/\pi) (K_{g_{AX,saddle}} - K_{g_{AX,crown}})$$

$$K_{g_{IPB}}(\phi) = -K_{g_{IPB,crown}} \cos(\phi)$$

$$K_{g_{OPB}}(\phi) = K_{g_{OPB,saddle}} \sin(\phi)$$

with:

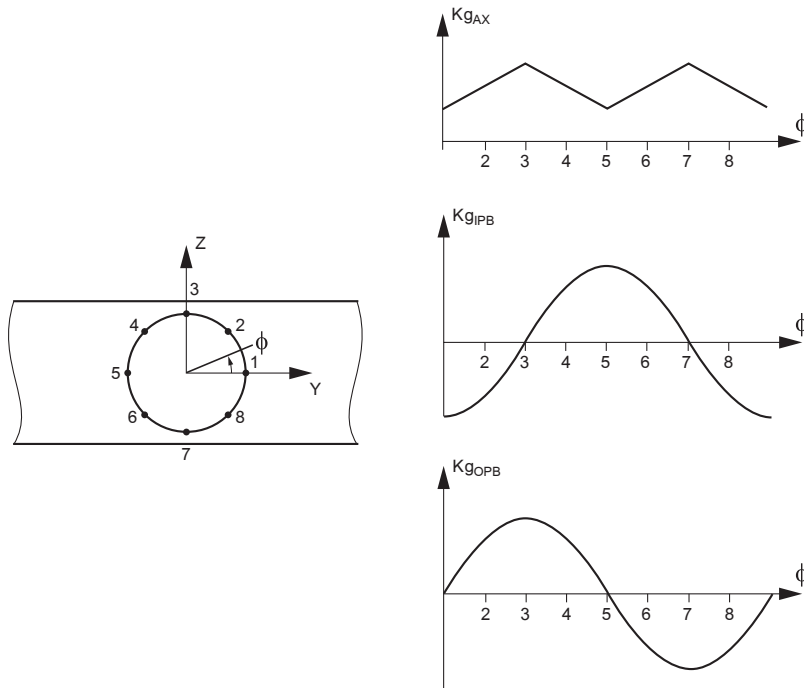
$K_{g_{AX,crown}}$ ,  $K_{g_{IPB,crown}}$  : Geometric stress concentration factors at crown, for axial stress and in plane bending

$K_{g_{AX,saddle}}$ ,  $K_{g_{OPB,saddle}}$  : Geometric stress concentration factors at saddle, for axial stress and out of plane bending.

These factors can be obtained according to Efthymiou equations or by finite element analysis (see [2.3.3]). In the later case, the finite element model may also provide directly  $K_{g_{AX}}(\phi)$ ,  $K_{g_{IPB}}(\phi)$  and  $K_{g_{OPB}}(\phi)$ .

The above procedure is to be applied independently for chord and brace sides.

**Figure 3 : Stress calculation locations and SCF ( $K_g$ ) periodic functions**



### 2.3.6 Alternative methods for geometric stress calculation

For more accurate calculations of geometric stresses, one of the following alternative methods can be adopted:

- to use the generalized concept of influence functions developed by Efthymiou
- to perform the global analyses integrating a detailed sub-model of the tubular joint according to Sec 6.

The influence function method is more accurate than the SCF approach because it can handle generalized forces and moments on the braces forming the joint, as opposed to the Kg approach which is based on individual planes and joint classification.

Moreover, the influence function method has several advantages:

- it avoids the need to classify joints and hence is more convenient to use than Kg method. It handles classification automatically on the basis of the actual load paths
- it allows to handle multiplanar joints for the important case of axial brace forces.

### 2.3.7 Geometric stress range

The geometric stress range  $\Delta\sigma_G$  is the range of  $\sigma_G$  calculated during a wave load cycle according to Sec 9, [2.2][2.3.5].

### 2.3.8 Applicable S-N curves

The tubular joints shall be checked versus toe cracking considering the 'T' curve as per ISO 19902.

The basic 'T' S-N curves to be used in air environment and in seawater with cathodic protection are given in Sec 9, [2.3]. These curves may need to be modified due to factors affecting the fatigue strength, as described in Sec 10.

## 2.4 Other tubular joints

### 2.4.1 Geometric stress concentration factors

For the following types of tubular joints, a detailed local FE analysis as per Sec 6 is required in order to determine the applicable Kg values:

- overlapping joints
- ring-stiffened joints
- cast joints.

A minimum Kg value of 2,0 shall be considered for these joints (see ISO 19902, section 16.10.2.1).

### 2.4.2 Applicable S-N curve

The casted joint shall be checked versus toe cracking considering the 'CJ' curve as per ISO 19902.

The 'CJ' S-N curve to be used in air environment is given in Sec 9, [2.3].

## 3 Tubular butt welded joints

### 3.1 General

#### 3.1.1 Local nominal stress

Tubular butt welded joints shall be designed based on the assessment of nominal stresses and the use of appropriate stress concentration factor due to eccentricity between welded members in order to obtain the local nominal stress given by:

$$\sigma_{\text{Loc Nom}} = K_m \sigma_{\text{nom}}$$

where:

- $K_m$  : Stress concentration factor due to eccentricity defined in Sec 10, [5.5]  
 $\sigma_{\text{nom}}$  : Cyclic nominal stresses defined in [2.1.2].

#### 3.1.2 Nominal stress

The relevant cyclic nominal stresses  $\sigma_{\text{nom}}$  to be considered for fatigue analysis are the ones produced by axial loads and bending moments, the stress components of which are normal to the weld toe.

The nominal stresses within the tubular members can be obtained by space frame finite element model where the members of the model are represented by beam elements and no eccentricities are modelled.

When the butt welded joint involves a thickness transition, the nominal stress to be considered is the stress calculated in the weakest member.

3.2 Classification of tubular butt welded joints

3.2.1 Tab 1 defines different tubular butt welded joint geometries and the potential hot spots at weld toe and weld root. Both single-sided joints and double-sided joints are considered, with or without thickness difference. Thickness transition between members may be located inside or outside the members.

The applicable formula of stress concentration due to eccentricity are given in Sec 10, [5.5] for each hot spot.

Each constructional detail incorporates local weld effects but not gross geometrical discontinuities which shall be considered using the appropriate geometric stress concentration factors.

For double-sided joints, hot spots are exclusively located at weld toe.

For single-sided joints, hot spots are located at both the weld toe and the weld root. In addition to the weld toe crack initiation checking, special consideration is to be given to the potential fatigue failure originated at the weld root which exhibits lower fatigue performances (see Sec 7, [2.2]).

3.3 Applicable S-N curves

3.3.1 Toe cracking

The applicable S-N curves for weld toe checking of tubular butt welded joints in air and in seawater with corrosion protection are given in Sec 9, [2.4].

3.3.2 Root cracking

The applicable S-N curves for weld root checking of tubular butt welded joints in air and in seawater with corrosion protection are given in Sec 9, [3.4].

Table 1 : Classification of tubular butt welded joints

Position of thickness transition	Type of weld	Hot spot 1	Hot spot 2	Illustration
Inside	single-sided	weld toe	weld root	
	double-sided	weld toe	weld toe	
Outside	single-sided	weld toe	weld root	
	double-sided	weld toe	weld toe	
Equal thickness	single-sided	weld toe	weld root	
	double-sided	weld toe	weld toe	

SECTION 5

FEA HOT SPOT STRESS FOR PLATED WELDED JOINTS AND FEA LOCAL NOMINAL STRESS FOR NON-WELDED DETAILS

1 General

1.1 Application

1.1.1 General

The aim of this Section is the determination of the hot spot stress for plated welded joints and of the local nominal stress for non-welded details such as cut plate edge from shell finite element models.

The stress at hot spot for welded joints is generally highly dependent on the finite element model used for the representation of the structure. Therefore the method for determination of hot spot stress is to be accurately specified.

The local nominal stress for non-welded area at cut plate edge requires a specific finite element model and a well specified method for the calculation.

Where other methods than those described in this Section are adopted for calculation of FEA based hot spot stress, these methods are to be submitted to the Society for review.

1.1.2 Rule based approach

When simplified rule based approach (see Sec 1, [5.2.1]) is used, according to the type of detail, the dedicated stress (hot spot or local nominal) analysis is to be carried out for each rule load case i1 and i2 associated to the loading condition (j) (see Sec 2, [1.2], Sec 2, [1.3], and Sec 11, [2.1.4]). Depending on the type of detail, the prescriptions in Articles [3], [4] or [6] are to be followed.

The procedure to obtain the dedicated stress range and associated mean stress is then given in Article [7].

1.1.3 Direct calculation approach

When a direct calculation approach is used according to the type of detail, the prescriptions given in [3], [4], [5] or [6] are to be used to derive the dedicated stress transfer functions or dedicated stress time series.

The prescriptions in Article [7] are not applicable to direct calculation approaches.

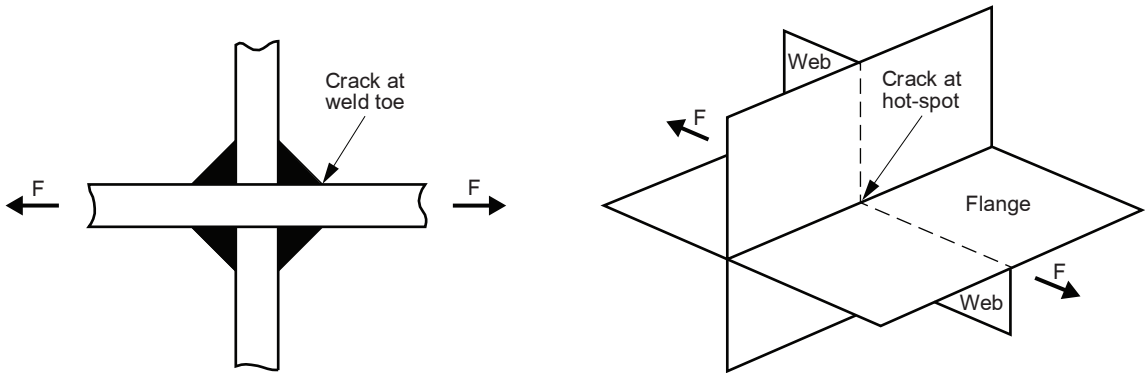
1.2 Type of details

1.2.1 Web-stiffened cruciform joints

A standard cruciform joint corresponds to the intersection of two plates (see Fig 1). A web-stiffened cruciform joint corresponds to a cruciform joint where the two plates are stiffened by another plate perpendicular to the first ones and acting as a web (see Fig 1).

The method for the calculation of the hot spot stress at the weld toes of web-stiffened cruciform joints is given in Article [4].

Figure 1 : Standard cruciform joint (left hand side) and web-stiffened cruciform joint (right hand side)





### 1.2.2 Bent hopper knuckle details

Prescriptions for the calculation of the hot spot stresses for bent hopper knuckles are given in Article [5].

### 1.2.3 Ordinary welded details

Ordinary welded details are commonly used welded details other than web-stiffened cruciform joints and bent hopper knuckle details such as simple butt welds, simple fillet welds of T joints and ordinary cruciform joints.

The method for calculation of hot spot stress for ordinary welded details is described in Article [3].

### 1.2.4 Non welded details

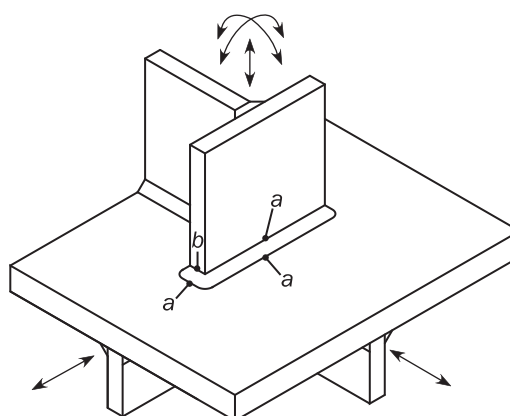
Prescriptions for the calculation of the local nominal stress for non-welded area such as cut plate edges, cut-outs for stiffeners connections at web frames, hatch corners, etc. are given in [6].

## 1.3 Types of hot spots for ordinary welded joints

**1.3.1** Two types of hot spots ('a' and 'b') at weld toe of ordinary welded joints are defined depending on their position on the plate, as follows (see Fig 2):

- Hot spot type 'a': weld toe on plate surface
- Hot spot type 'b': weld toe on plate edge.

**Figure 2 : Types of hot spots**



## 2 Finite element models

### 2.1 General

#### 2.1.1 General

The evaluation of the hot spot stresses for fatigue assessment requires the use of very fine mesh in way of high stress concentration areas.

These very fine mesh zones may be incorporated into the global FEM model as shown in Fig 3. Alternatively, the very fine mesh analysis may be carried out by means of separate local finite element models with very fine mesh zones to which boundary conditions obtained from a global model are applied. A typical local separate model of a hopper knuckle connection is shown in Fig 4.

#### 2.1.2 Corrosion

The FEM models used for fatigue assessment are based on the net scantling concept (see Sec 1, [3.3]).

### 2.2 Global FEM model

#### 2.2.1 General

The global FEM model is used to compute the structural response of the ship or offshore unit as a whole and at the scale of the primary supporting members. The typical element size is equal to the spacing between ordinary stiffeners.

The global FEM model may be either a full length FEM model or a partial FEM model. The type and the extent of the global FEM model is to be adapted to the considered ship or offshore unit, and to the considered fatigue detail, in such a way that the structural response is correctly captured.

Figure 3 : Very fine mesh zones included into the cargo hold model

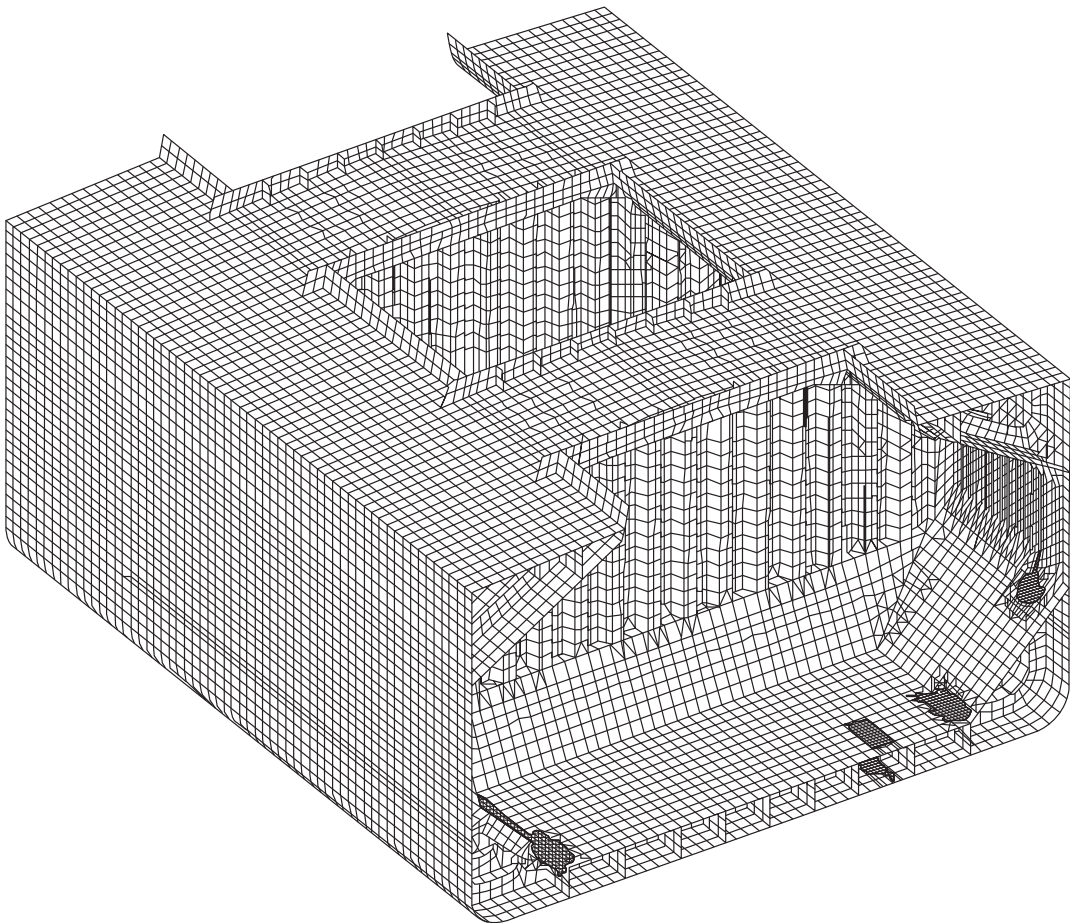
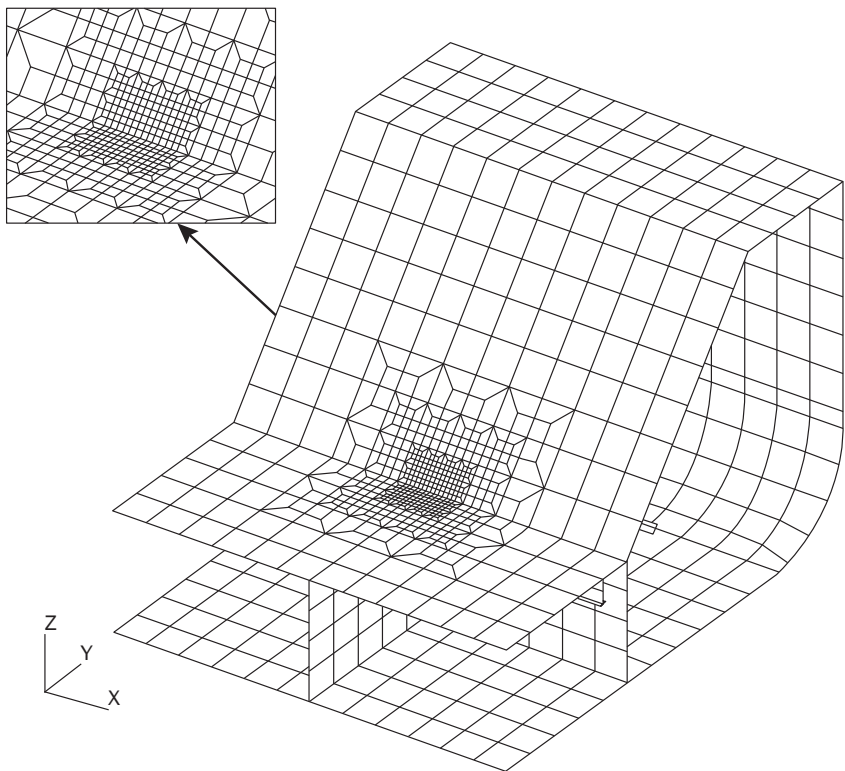


Figure 4 : Local separate FE model of hopper knuckle connection including very fine mesh zone



### 2.2.2 Full length FEM model

The structural model can be a “full length FEM model” where the entire structure of the vessel is included in the model. This type of model is suitable for any type of structure but is more demanding than partial models described in [2.2.3].

The modelling rules and boundary conditions are to be in accordance with the applicable requirements of the applicable rules.

Full length models need to be analysed through procedures that guarantee an accurate balance of the model under all wave induced loads, such as the direct calculation methods described in Sec 11, [3.2.5].

### 2.2.3 Partial FEM model

For some types of structures, a full length FEM model is not necessary for the correct evaluation of the structural response in the area of interest. In this case the extent of the FEM structural model can be reduced to a subpart of the structure.

The considered structural subpart has to be isostatic (i.e. statically determinate), thus limiting the applicability to slender structures. The structural response within the extent of the FEM model must not be significantly influenced by the distortion of the non-modelled parts, which excludes structures prone to warping or shear lag. This method is typically used for “three holds models” of ships and ship shaped units.

The modelling rules, model extent and boundary conditions are to be as prescribed in the applicable rules.

If a partial structural model is used, the forces and moments exerted by the structure parts not included in the FEM model need to be applied at the boundaries of the structural model.

## 2.3 Finite element modelling for hot spot stress calculation

### 2.3.1 Separate local FE model

Where a separate local finite element model is used, the extent of the local FE model is to be chosen so that the imposed boundary conditions and the applied loads are far enough from the very fine mesh zones in order not to affect the calculated stresses.

Boundaries of the fine mesh model are to be taken at adjacent primary supporting members such as girders, stringers and floors, as far as practicable. Transverse web frames, stringer plates and girders at the boundaries of the local model shall not be represented in the local model.

Other prescriptions that may be given in the applicable rules have to be applied.

### 2.3.2 Shell elements

In shell element models, the elements are arranged in the mid-plane of the structural components. For practical purposes, adjoining plates of different thickness may be assumed to be median line aligned, i.e. no staggering in way of thickness change is required. Workmanship misalignment is not required to be modelled.

### 2.3.3 Modelling of welds

The welds are usually not modelled except for cases where the results are affected by local bending, e. g. due to an offset between plates or due to a small free plate length between adjacent welds such as at collar plate. For those cases, hot spot stress calculation is to be performed according to suitable methods, to the satisfaction of the Society.

### 2.3.4 Mesh size

For type ‘a’ hot spots (see [1.3.1]), the very fine mesh density is to be based on shell element of mesh size  $t_n$  by  $t_n$ , where  $t_n$  is the net thickness of the plate in way of the considered hot spot.

For type ‘b’ hot spots (see [1.3.1]), the very fine mesh density is to be based on shell element of mesh size 10 by 10 mm.

The aforementioned mesh size is to be maintained within the very fine mesh zone, extending over at least ten elements in all directions from the fatigue hot spot position. The transition of element size between the fine mesh and the very fine mesh zone is to be done gradually and an acceptable mesh quality is to be maintained. An example of mesh transition in way of the side frame bracket toe is shown in Fig 5.

Figure 5 : Transition area between fine mesh and very fine mesh



**2.3.5 Element type**

Quadrilateral shell elements are to be used inside the very fine mesh zone. Shell elements with midside nodes are recommended particularly in case of steep stress gradients.

**2.3.6 Transition mesh**

Use of linear triangular elements is to be avoided as much as possible in close proximity to the very fine mesh zones. Quadrilateral elements are to have 90 degrees angles as much as possible or angles between 60 degrees and 120 degrees. The aspect ratio is to be close to 1. When the use of a linear triangular elements cannot be avoided, edges aspect ratio is to be as close as possible to unity.

**2.3.7 Beam elements for edge stress evaluation**

For type ‘b’ hot spots (see [1.3.1]) or for non-welded cut edge details, such as cut-outs for stiffeners connections at web frames, edge plating and hatch corners, stresses are to be evaluated on the plate edge. In such a case, the stress may be read out directly in beam elements put along the plate edge. In order to capture both the axial and bending stresses, such beam elements should have a rectangular section, with one side equal to the thickness of the plate along which they are fitted. The other section side is to be made very small in order to have a negligible beam element stiffness.

**3 Hot spot stress for ordinary welded details**

**3.1 General**

**3.1.1 Types of welded details**

The prescriptions in Article [3] apply to ordinary welded details: butt welds, fillet welds of T joints and ordinary cruciform joints.

They do not apply to web-stiffened cruciform joints and bent hopper knuckles.

**3.1.2 Types of FE mesh**

The prescriptions in Article [3] apply to FEM model based on shell elements, in which the welds are not explicitly modelled. For other types of meshes, other methods are to be used.

## 3.2 Hot spot stress calculation

### 3.2.1 Principle

The hot spot stress is to be evaluated at the structural intersection point (SIP). In shell element models, the SIP is located at the intersection of the shell elements mid-planes.

The hot spot stress is derived from the stress at particular points named “readout points”. The location of these readout points depends on the type of detail, as described in [3.2.2] and [3.2.3].

Two methods can be used to obtain the hot spot stress from the stress at the readout points:

- the hot spot stress is linearly extrapolated from two readout points to the structural intersection point or line as described in [3.2.4]
- the hot spot stress is taken as the stress from one readout point and multiplied by a coefficient as described in [3.2.5]. No stress extrapolation is performed.

### 3.2.2 Readout points for type ‘a’ hot spots

For type ‘a’ hot spots (see [1.3.1]), the two readout points are located on the surface of the plate, at a distance  $0,5 t_n$  and  $1,5 t_n$  from the SIP, where  $t_n$  is the plate thickness in way of the weld toe used for fatigue calculation.

The actual element size is not always exactly equal to  $t_n$  by  $t_n$  because hot spot can be located at intersection of plates having different thicknesses. Methods to obtain the stress at the readout points are given in the following three cases of shell element mesh sizes at the hot spot location:

- element size equal to  $t_n$  by  $t_n$  (see [3.3])
- element size smaller than  $t_n$  by  $t_n$  (see [3.4])
- element size larger than  $t_n$  by  $t_n$  (see [3.5]).

### 3.2.3 Readout points for type ‘b’ hot spots

For type ‘b’ hot spots (see [1.3.1]), the readout points are located on the edge of the plate surfaces, at 5 mm and 15 mm from the SIP. For type ‘b’ hot spots, the SIP is located at the intersection of the attachment plate edge and the mid-plane of the other plate.

The stress at the readout point may be read out directly in beam elements put along the plate edge as described in [2.3.7], provided that the mesh size along the edge is equal to 10 mm. Solutions to evaluate the stress at the readout points for meshes with a slightly different size may be acceptable. The element size should not be smaller than 5mm and not larger than 15mm.

The total stress including axial and bending stress is to be considered.

Alternative solutions based on the post-processing of the edge nodes displacements and rotations may be acceptable.

### 3.2.4 Hot spot stress by stress extrapolation

The recommended method is the linear stress extrapolation from the two readout points to the structural intersection point (SIP) considered as the hot spot in shell element models.

The hot spot stress is obtained by:

$$\sigma_{HS} = 1,5 \sigma_{RP\_C} - 0,5 \sigma_{RP\_F}$$

where:

- $\sigma_{RP\_C}$  : Stress at the readout point close to the SIP ( $0,5 t_n$  or 5 mm, depending on the hot spot type)
- $\sigma_{RP\_F}$  : Stress at the readout point further from the SIP ( $1,5 t_n$  or 15 mm, depending on the hot spot type).

For type ‘a’ hot spots, each component of the stress tensor is to be extrapolated individually. The principal stress at the hot spot is then calculated from the extrapolated component values.

### 3.2.5 Hot spot stress without stress extrapolation

As an alternative to the stress extrapolation, a simplified approach is proposed. The hot spot stress is taken as the stress from one readout point and multiplied by a fixed coefficient accounting for the possible stress gradient.

The hot spot stress is obtained by:

$$\sigma_{HS} = 1,12 \sigma_{RP\_C}$$

where:

- $\sigma_{RP\_C}$  : Stress as defined in [3.2.4].

This simplified method may be unconservative if the stress gradient at hot spot is too steep (i.e. when  $\sigma_{RP\_C} > 1,3 \sigma_{RP\_F}$ ).

3.2.6 Applicable S-N curves

The S-N curves to be used to check the weld toe of plate joints are the following ones:

- $P_{\perp}$  curve for the hot spot stress acting within sector 1 as defined in [7.2.2]
- $P_{//}$  curve for the hot spot stress acting within sector 2 as defined in [7.2.2].

If the weld toe angle is lower than or equal to 30°, the S-N curve to be used for all stress directions is  $P_{//}$ .

The way how to consider the stress direction is described in [7] for the rule based approach, in Sec 11, [3.3] for spectral analysis, and in Sec 11, [4.2] for time-domain analysis.

The  $P_{\perp}$  and  $P_{//}$  S-N curves to be used in air environment, in seawater without corrosion protection (i.e. under free corrosion) and in seawater with cathodic protection are given in Sec 9, [2.1].

3.3 Type ‘a’ stress readout for element with the prescribed size

3.3.1 General

If the shell elements in the vicinity of the hot spot have the exact prescribed  $t_n$  by  $t_n$  size, where  $t_n$  is the net thickness of the plate where the stress is measured, the procedures in [3.3.2] and [3.3.3] can be used to obtain the stress at the readout points.

3.3.2 4-node shell elements

The surface stress components at the centre points of the elements are considered. The stress tensor components at the two readout points are directly obtained by linear extrapolation of the element stress to the line A-A as shown in Fig 6.

The elements located on each side (side L, side R) of the line A-A need to be considered separately.

3.3.3 8-node shell elements

With a  $t_n$  by  $t_n$  element mesh size using a 8-node shell element, the element mid-side nodes are located on the line A-A at a distance  $0,5 t_n$  and  $1,5 t_n$  from the structural intersection. These nodes coincide with the stress readout points.

The element surface stress components at these mid-side nodes can be used directly without extrapolation as illustrated in Fig 7. The elements located on each side (side L, side R) of the line A-A need to be considered separately.

Figure 6 : Stress at readout points for 4-node shell elements (element size:  $t_n \times t_n$ )

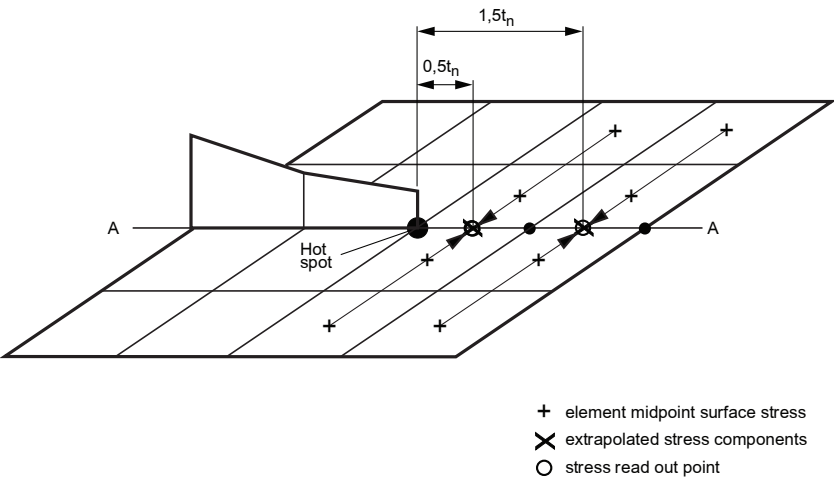
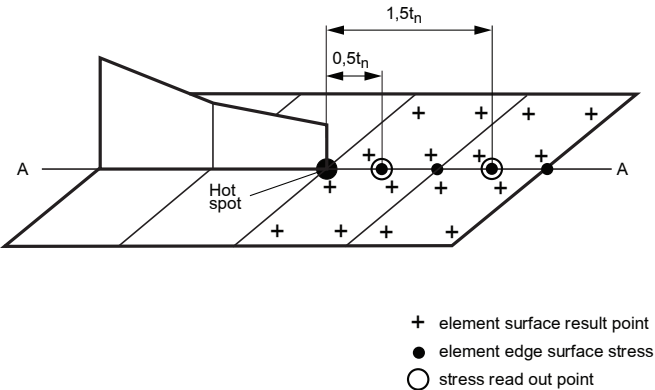


Figure 7 : Stress at readout points for 8-node shell elements (element size:  $t_n \times t_n$ )



3.4 Type ‘a’ stress readout for elements smaller than the prescribed size

3.4.1 General

If the shell elements in the vicinity of the hot spot are smaller than the prescribed  $t_n$  by  $t_n$  size, where  $t_n$  is the net thickness of the plate where the stress is calculated, the procedures in [3.4.2] and [3.4.3] can be used to obtain the stress at the readout points. These procedures are not applicable if the element size is smaller than  $0,5 t_n$ .

3.4.2 4-node shell elements

The element surface stress components at the element centre points are linearly extrapolated from to the line A-A as shown in Fig 8, to determine the extrapolated stress components. The stress components are then obtained at the readout points using a linear interpolation as shown in Fig 9.

The elements located on each side (side L, side R) of the line A-A need to be considered separately.

Figure 8 : Stress at readout points for 4-node shell elements ( $0,5 t_n \leq \text{element size} \leq t_n$ )

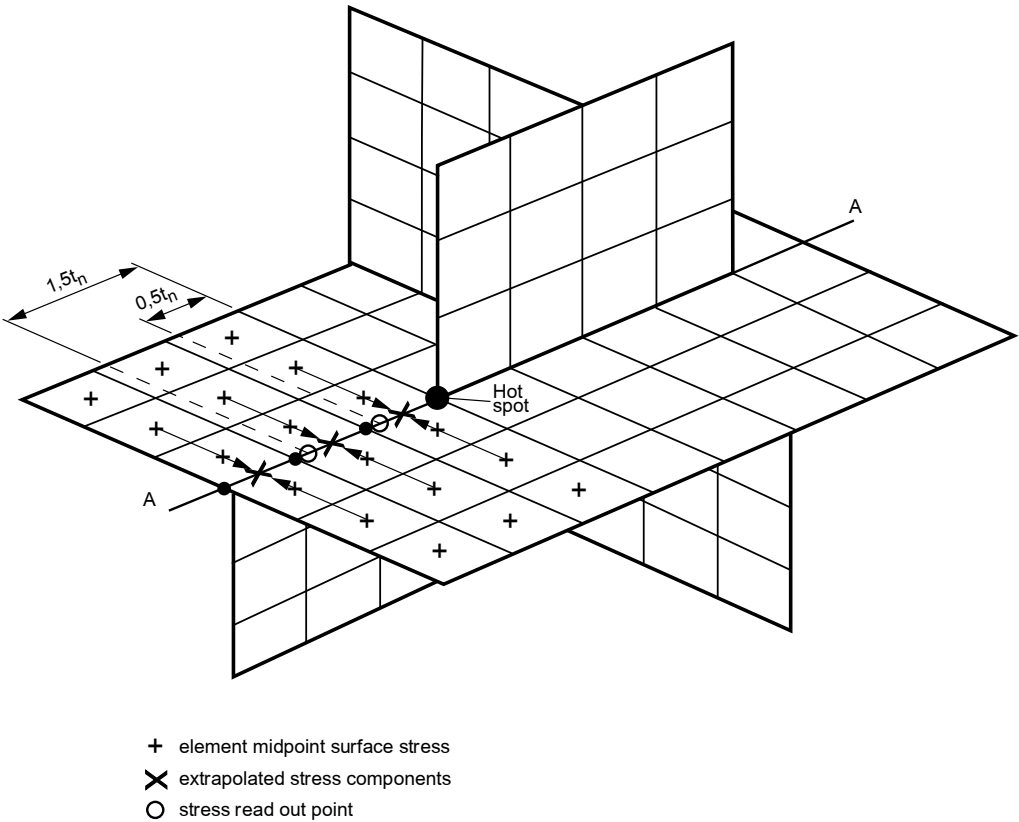
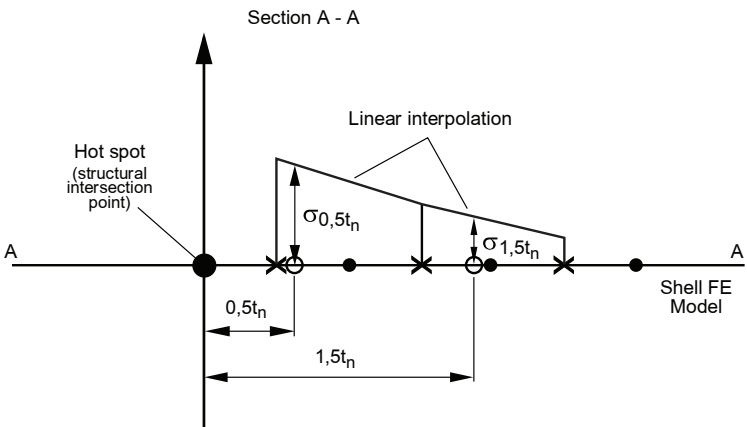


Figure 9 : Stress interpolation for 4-node shell elements ( $0,5 t_n \leq \text{element size} \leq t_n$ )



3.4.3 8-node shell elements

The element edge surface stress points to be considered are those located on line A-A close to the structural intersection point as shown in Fig 10. The stress components at  $0,5 t_n$  are obtained by linear interpolation of the element edge surface stresses inside the first element located on the side of line A-A. The stress components at  $1,5 t_n$  are obtained by linear interpolation of the element edge surface stresses inside the second element located on the line A-A (see Fig 11).

The elements located on each side (side L, side R) of the line A-A need to be considered separately.

Figure 10 : Stress at readout points for 8-node shell elements ( $0,5 t_n \leq \text{element size} \leq t_n$ )

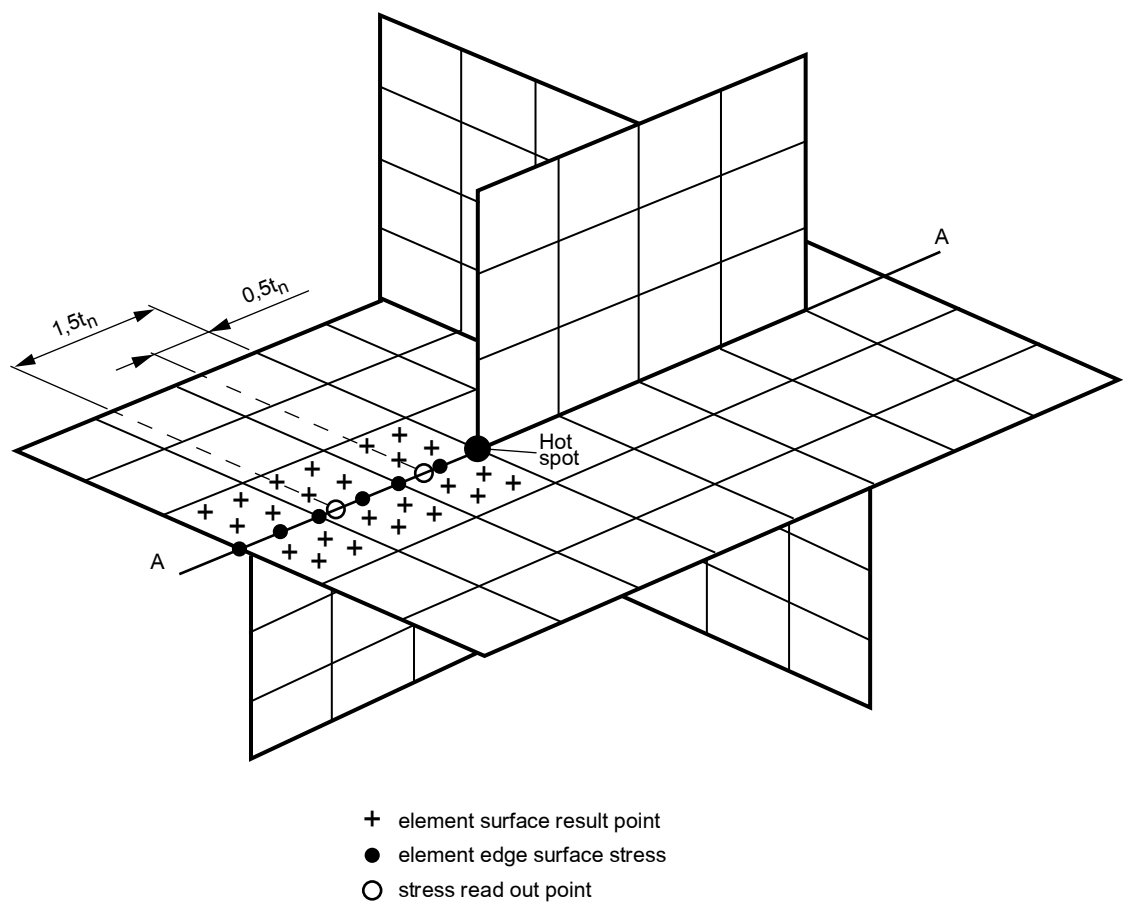
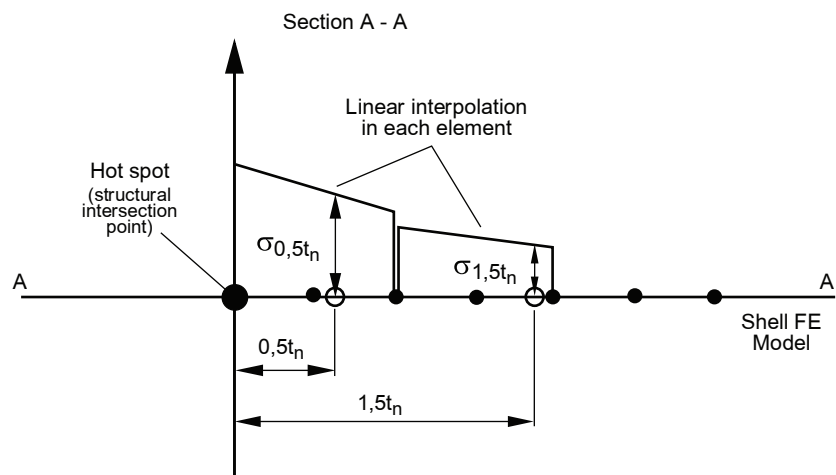


Figure 11 : Stress interpolation for 8-node shell elements ( $0,5 t_n \leq \text{element size} \leq t_n$ )





3.5 Type ‘a’ stress readout for elements larger than the prescribed size

3.5.1 General

If the shell elements in the vicinity of the hot spot are larger than the prescribed  $t_n$  by  $t_n$  size, where  $t_n$  is the net thickness of the plate where the stress is calculated, the procedures in [3.5.2] and [3.5.3] can be used to obtain the stress at the readout points. These procedures are not applicable if the elements size is larger than  $2 t_n$ .

3.5.2 4-node shell elements

The element surface stress components at the centre points are linearly extrapolated to the line A-A as shown in Fig 12 to determine the extrapolated stress components. Then, the stress components at the stress readout points may be derived as shown in Fig 13. It is recommended to fit a second order polynomial to the element stress components in the three first elements.

The elements located on each side (side L, side R) of the line A-A need to be considered separately.

Figure 12 : Stress at readout points for 4-node shell elements ( $t_n \leq \text{element size} \leq 2 t_n$ )

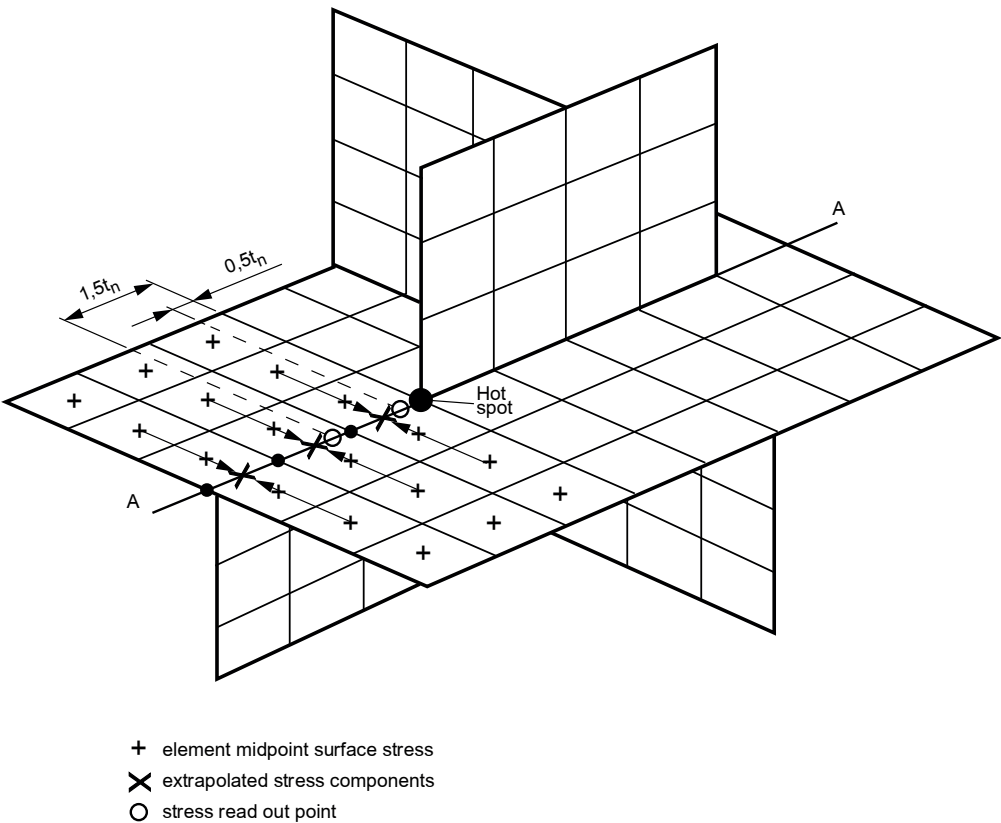
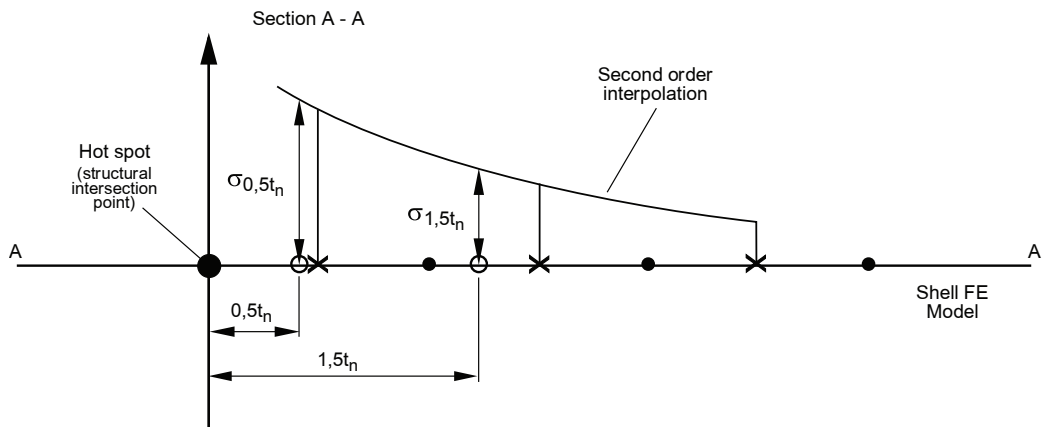


Figure 13 : Stress interpolation for 4-node shell elements ( $t_n \leq \text{element size} \leq 2 t_n$ )



3.5.3 8-node shell elements

The element edge surface stress points to be considered are located on line A-A close to the structural intersection point (see Fig 14).

The stress components at  $0,5 t_n$  are obtained by linear interpolation of the element edge surface stresses inside the first element located on the side of the line A-A. Stress components at  $1,5 t_n$  are obtained by linear interpolation of the element edge surface stresses inside the second element located on the side of the line A-A (see Fig 15).

The elements located on each side (side L, side R) of the line A-A need to be considered separately.

Figure 14 : Stress at readout points for 8-node shell elements ( $t_n \leq \text{element size} \leq 2 t_n$ )

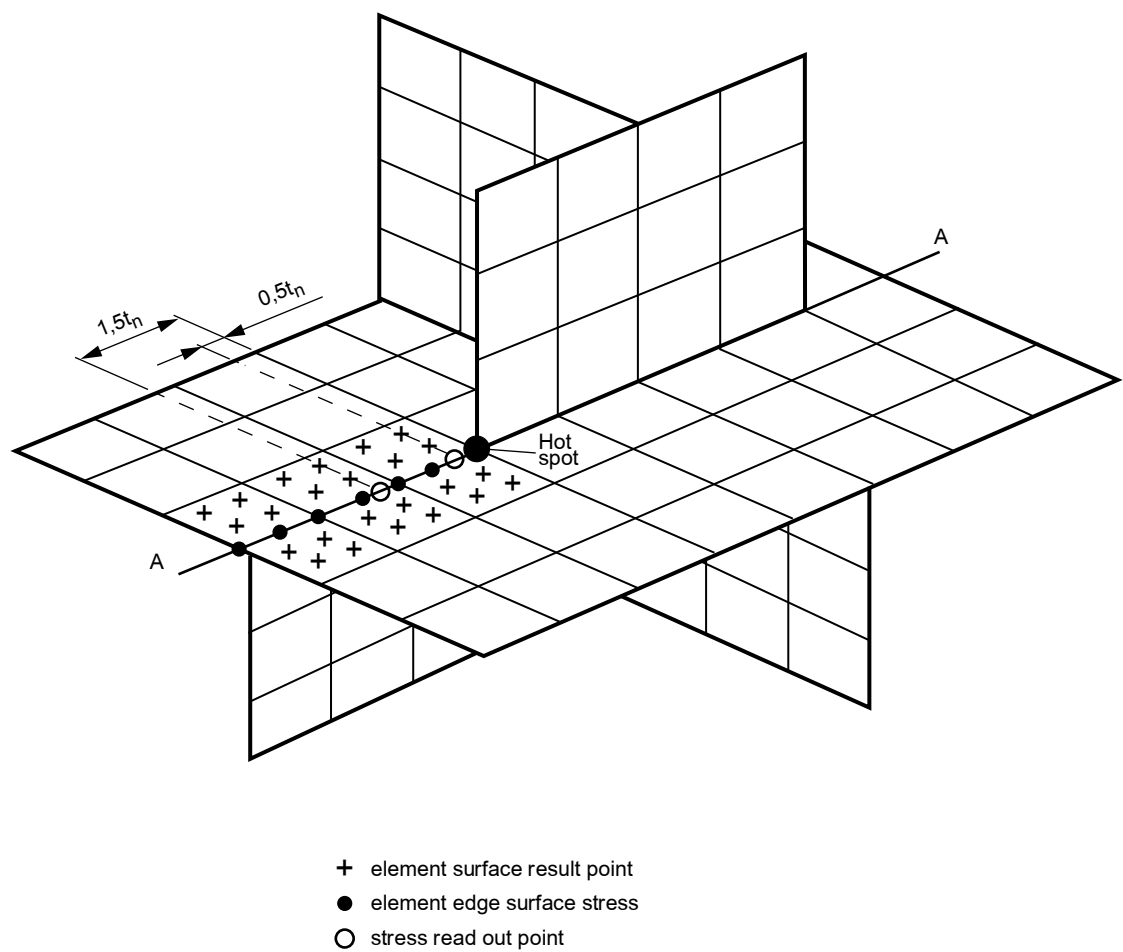
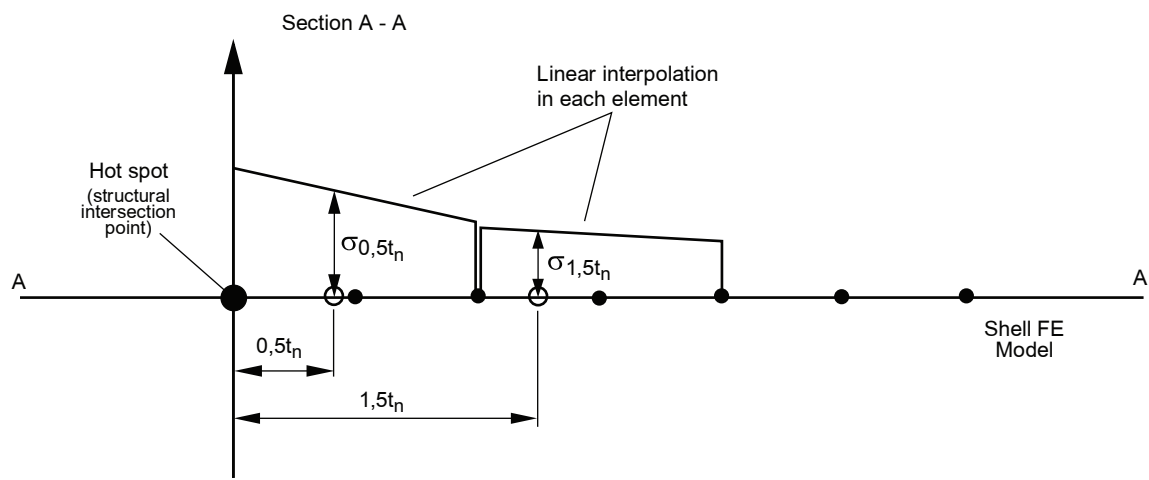


Figure 15 : Stress interpolation for 8-node shell elements ( $t_n \leq \text{element size} \leq 2 t_n$ )



## 4 Hot spot stress for web-stiffened cruciform joints

### 4.1 Application

#### 4.1.1 General

Concerning the web-stiffened cruciform joint, at the intersection of plates corresponding to the hot spot, there is a high local stress concentration with large gradients.

The following structural details are typically considered as a web-stiffened cruciform joint (see Fig 16 and Fig 17):

- a) welded hopper knuckle connection
- b) heel of horizontal stringer
- c) lower stool - inner bottom connection.

Two kinds of hot spots relative to the web-stiffened cruciform joints are to be assessed:

- hot spots at the flange of the web-stiffened cruciform joint
- hot spots in way of the web of the web-stiffened cruciform joint.

Three effects increase the calculated fatigue life of web-stiffened cruciform joints compared with the fatigue results given by the standard hot spot stress approach as defined in [3]:

- effect of stress gradient over the plate flange thickness (large bending stress versus membrane stress leading to longer propagation phase)
- effect of large stress gradient along weld line
- effect of structural support i.e. the web (stress redistribution).

So, an improved hot spot stress procedure for web-stiffened cruciform joint is derived to take into those effects by means of correction factors.

Figure 16 : Examples of web-stiffened cruciform joints (1)

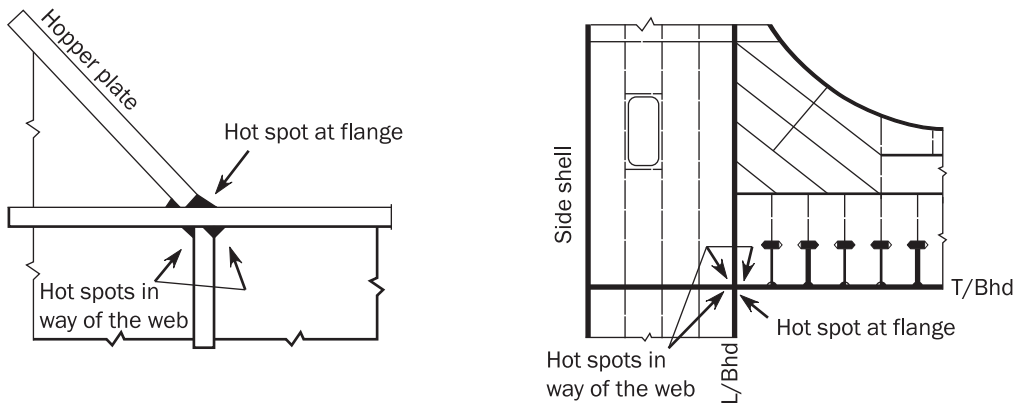
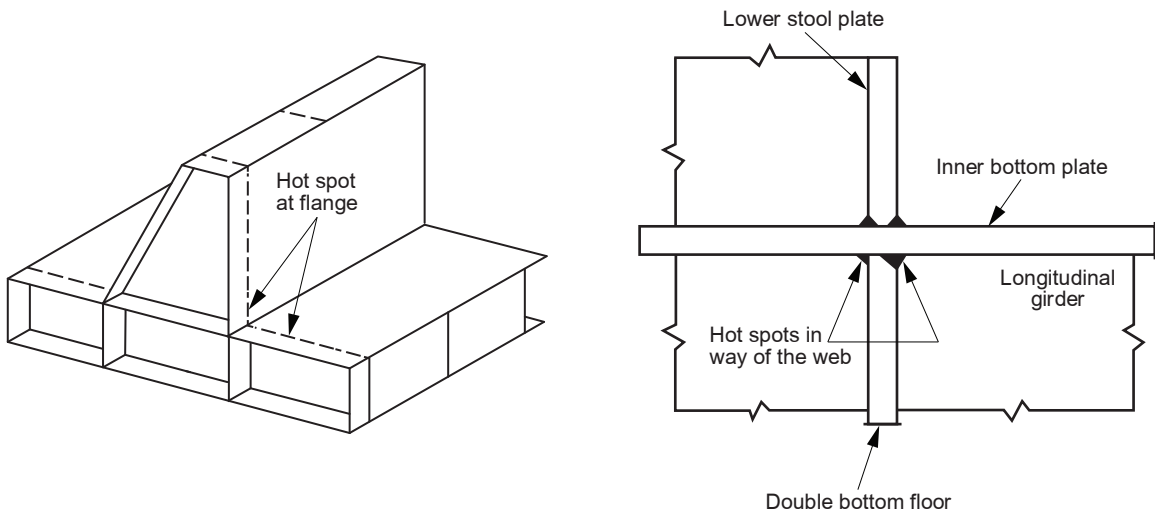


Figure 17 : Examples of web-stiffened cruciform joints (2)



#### 4.1.2 Hot spot stress at the flange

The method for calculating the hot spot stress at the flange of the web-stiffened cruciform joint is described in [4.2].

#### 4.1.3 Hot spot stress in the web

The method for calculating the hot spot stress in way of the web of the web-stiffened cruciform joint is described in [4.3].

### 4.2 Hot spot stress calculation at the flange

#### 4.2.1 Hot spot stress

The hot spot stress tensor at the flange of the web-stiffened cruciform joint is obtained from the surface stress (tensor  $\sigma_{\text{shift}}$ ) read out at a point shifted away from the intersection line to the position of the actual weld toe. The intersection line is taken at the mid-thickness of the cruciform joint assuming a median alignment.

The hot spot stress is to be obtained by:

$$\sigma_{\text{HS}} = 1,12 \sigma_{\text{shift}}$$

where:

$\sigma_{\text{shift}}$  : Surface stress at the shifted position  $x_{\text{shift}}$ .

The shifted position  $x_{\text{shift}}$  from the intersection line (see Fig 19) is obtained by:

$$x_{\text{shift}} = \frac{t_{1-n}}{2} + x_{\text{wt}}$$

where:

$t_{1-n}$  : Net plate thickness of the plate number 1 (i.e. the flange), as shown in Fig 18

$x_{\text{wt}}$  : Extended fillet weld leg length, as defined in Fig 18 and Fig 19, not taken larger than  $t_{1-n}$ .

#### 4.2.2 Stress at the shifted position

The stress at the shifted position is to be obtained by:

$$\sigma_{\text{shift}} = f_W \cdot f_S [\sigma_{\text{membrane}}(x_{\text{shift}}) + 0,6 \sigma_{\text{bending}}(x_{\text{shift}})] \beta$$

where:

$f_W$  : Correction factor for the effect of stress gradient along weld line, taken equal to:  $f_W = 0,96$

$f_S$  : Correction factor for the effect of supporting member, taken equal to:  $f_S = 0,95$

$\sigma_{\text{membrane}}(x_{\text{shift}})$  : Membrane stress tensor at position  $x_{\text{shift}}$

$\sigma_{\text{bending}}(x_{\text{shift}})$  : Bending stress tensor at position  $x_{\text{shift}}$

$\alpha$  : Angle between plate 2 and plate 1 (see Fig 18 and Fig 19)

$\beta$  : Hot spot stress correction factor depending on the  $\alpha$  parameter, taken equal to:

- for  $\alpha = 135^\circ$ :

$$\beta = 0,96 - 0,13 \left( \frac{x_{\text{wt}}}{t_{1-n}} \right) + 0,20 \left( \frac{x_{\text{wt}}}{t_{1-n}} \right)^2$$

- for  $\alpha = 120^\circ$ :

$$\beta = 0,97 - 0,14 \left( \frac{x_{\text{wt}}}{t_{1-n}} \right) + 0,32 \left( \frac{x_{\text{wt}}}{t_{1-n}} \right)^2$$

- for  $\alpha = 90^\circ$ :

$$\beta = 0,96 + 0,031 \left( \frac{x_{\text{wt}}}{t_{1-n}} \right) + 0,24 \left( \frac{x_{\text{wt}}}{t_{1-n}} \right)^2$$

For intermediate values of plate angle  $\alpha$ , correction factor  $\beta$  should be obtained by linear interpolation.

#### 4.2.3 Membrane and bending stresses at the shifted position

Element surface stress tensor components at the centre points of the elements adjacent to the line A-A (i.e. element on left hand side and on right hand side of the line A-A) are averaged (see Fig 20). They are then linearly interpolated along the line A-A in order to determine the shifted stress tensors  $\sigma_{\text{membrane}}$  and  $\sigma_{\text{bending}}$  at position  $x_{\text{shift}}$ .

Figure 18 : Geometrical parameters of web-stiffened cruciform connections

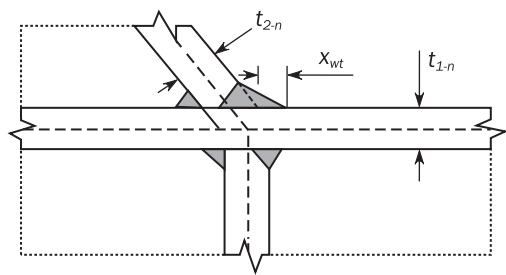


Figure 19 : Hot spot stress at flange of web-stiffened cruciform joint

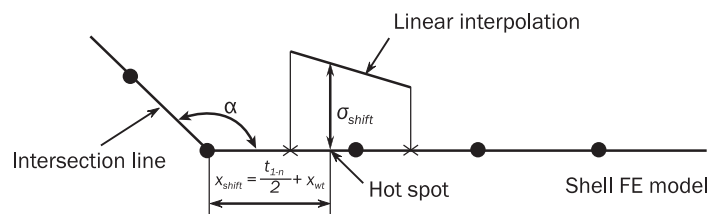
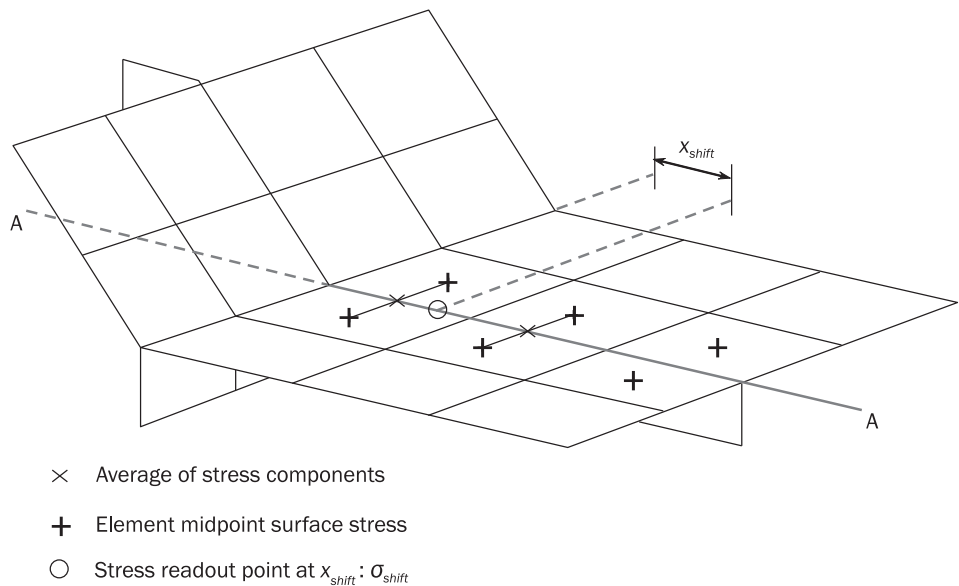


Figure 20 : Determination of stress  $\sigma_{shift}$  for the flange of web-stiffened cruciform joint



### 4.3 Hot spot stress calculation in the web

#### 4.3.1 Hot spot stress

Other hot spots located in way of the web are to be checked with the hot spot stress defined as the surface stress tensor at a distance equal to  $2^{0.5} \cdot x_{shift}$  from the crossing intersection lines (corresponding to the corner where vertical and horizontal weld lines meet) to the hot spot. See Fig 21.

The intersection line is taken at the mid-thickness of the cruciform joint assuming a median alignment.

The hot spot stress is to be obtained by:

$$\sigma_{HS} = \sigma_{shift}$$

where:

$\sigma_{shift}$  : Surface stress at a distance equal to  $2^{0.5} \cdot x_{shift}$  from the crossing element intersection lines

$x_{\text{shift}}$  : Distance from each element (horizontal and vertical) intersection line, obtained by:

$$x_{\text{shift}} = \frac{t_{3-n}}{2} + x_{\text{wt}}$$

with:

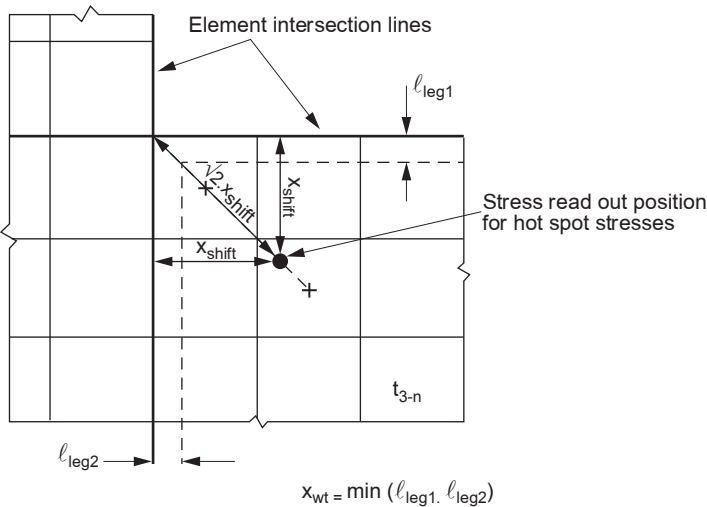
$t_{3-n}$  : Net plate thickness of the web, as shown in Fig 21

$x_{\text{wt}}$  : Extended fillet weld leg length, taken equal to:

$$x_{\text{wt}} = \text{Min} (\ell_{\text{leg1}} ; \ell_{\text{leg2}})$$

$\ell_{\text{leg1}}, \ell_{\text{leg2}}$  : Weld leg length of the vertical and horizontal weld beads, as shown in Fig 21.

**Figure 21 : Determination of the hot spot stress in way of web**



5 Hot spot stress for bent hopper knuckle details

5.1 Bent hopper knuckle details

5.1.1 Hot spots on inner bottom / hopper sloping plate

The hot spot stress at the inner bottom/hopper sloping plate of a bent hopper knuckle, in transverse and longitudinal directions, is to be taken as the surface principal stress read out from a point shifted away from the intersection line between the considered member and abutting member by the weld leg length.

The hot spot stress, in N/mm<sup>2</sup>, is obtained by the following formula:

$$\sigma_{\text{HS}} = \sigma_{\text{shift}}$$

where:

$\sigma_{\text{shift}}$  : Surface principal stress, in N/mm<sup>2</sup>, at the shifted readout position as defined in [4.2.1], taken equal to:

$$\sigma_{\text{shift}} = \sigma_{\text{membrane}} (x_{\text{shift}}) + \sigma_{\text{bending}} (x_{\text{shift}})$$

with:

$\sigma_{\text{membrane}} (x_{\text{shift}})$  : Membrane stress, in N/mm<sup>2</sup>, at position  $x_{\text{shift}}$

$\sigma_{\text{bending}} (x_{\text{shift}})$  : Bending stress, in N/mm<sup>2</sup>, at position  $x_{\text{shift}}$  .

The procedure for calculation of hot spot stress at the flange, such as inner bottom or hopper sloping plate, is the same as the one for web-stiffened cruciform joints as described in [4.2.1].

The procedure that applies for hot spots on the ballast tank side of the inner bottom / hopper plate in way of a bent hopper knuckle is in principle the same as the one applied on the cargo tank side of the inner bottom plate for welded knuckle in Fig 17 and Fig 18. The intersection line is taken at the mid-thickness of the joint assuming median alignment. The plate angle correction factor and the reduction of bending stress as applied for a web-stiffened cruciform joint in [4.2.2] are not to be applied for the bent hopper knuckle type.

5.1.2 Hot spots on transverse and longitudinal webs

The stress at hot spots located in way of the web (such as transverse web and side girder) of a bent hopper knuckle type is to be derived as described for web-stiffened cruciform joints in [4.3.1].

## 6 Local nominal stress for non-welded details

### 6.1 Plate cut edge details

#### 6.1.1 Plate cut edge stress calculation

The plate cut edge stress  $\sigma_{CE}$  to be considered for fatigue calculation is the local nominal stress at the cut plate edge. It may be read out directly in beam elements put along the plate edge as described in [2.3.7].

Alternative solutions based on the post-processing of the edge node displacements and rotations may be acceptable.

## 7 Stress range and mean stress for rule based approach

### 7.1 General

**7.1.1** This Article describes the procedure to derive from the stress tensor the principal hot spot stress range and the associated hot spot mean stress to be used for the rule based approach.

This Article is not applicable to the direct calculation approaches. For these approaches, specific requirements are given in Sec 11, [3.3] and Sec 11, [4.2].

### 7.2 Principal hot spot stress

#### 7.2.1 General

For type 'a' hot spots or for the web-stiffened cruciform joints, the hot spot stress is not a scalar, it is a plane stress tensor with three components.

#### 7.2.2 Hot spot axes and angular sectors

In this Article, a local XY rectangular coordinate system is associated to the considered hot spot. The origin of this system is located at the structural intersection point where the hot spot is located, and the two axes X and Y lie in the mid-plane of the considered plate where the stress is evaluated.

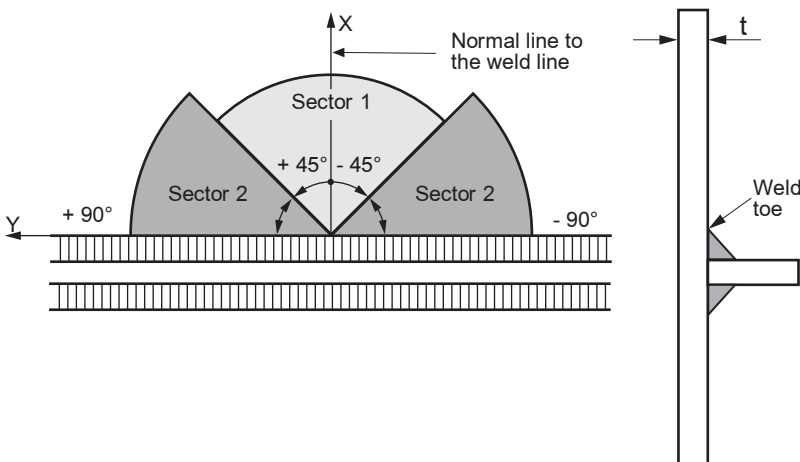
Y axis is tangent to the weld line at the hot spot (weld toe), and X axis is perpendicular to Y axis, i.e. is along the normal line to the weld line (see Fig 22).

Two angular sectors at the weld toe are identified (see Fig 22):

Sector 1 : Angular sector between  $[-45^\circ/+45^\circ]$  to the normal of the weld line

Sector 2 : Angular sector outside the sector 1, i.e. between  $[+45^\circ/+90^\circ]$  and  $[-90^\circ/-45^\circ]$  to the normal of the weld line.

**Figure 22 : Hot spot axes and angular sectors**



### 7.2.3 Hot spot stress range and hot spot mean stress definition

Two principal hot spot stress ranges are considered for the assessment of type 'a' hot spots and web-stiffened cruciform joints, for each load case (i) associated to the loading condition (j), as mentioned in [1.1.2].

They are determined as follows:

- the hot spot stress differences tensor is computed in the hot spot coordinate system using the prescriptions in [7.2.4]
- the principal directions of the stress range tensor and the associated principal stress range are computed using [7.2.5]
- the mean stress in the principal directions of the stress range tensor are computed using [7.2.6]
- the principal stress range located in sector 1 is denoted  $(\Delta\sigma_{HS1,i(j)})$  and its associated mean stress is denoted  $(\Delta\sigma_{meanHS1,i(j)})$
- the principal stress range located in sector 2 is denoted  $(\Delta\sigma_{HS2,i(j)})$  and its associated mean stress is denoted  $(\Delta\sigma_{meanHS2,i(j)})$ .

### 7.2.4 Hot spot stress differences in the hot spot coordinate system

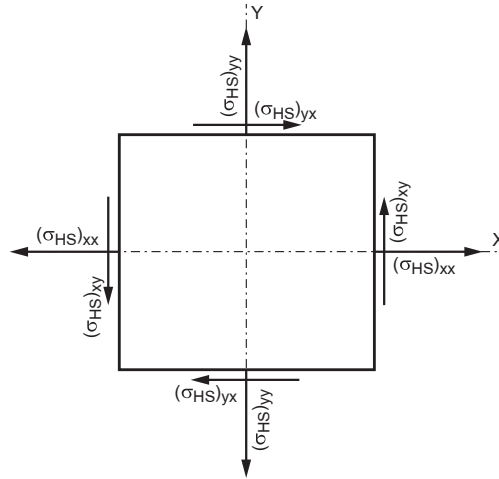
For each load case i, loading condition j, the corresponding hot spot stress component differences in the weld coordinate system are obtained by:

$$\begin{cases} (\Delta\sigma_{HS,i(j)})_{xx} = (\sigma_{HS,i1(j)})_{xx} - (\sigma_{HS,i2(j)})_{xx} \\ (\Delta\sigma_{HS,i(j)})_{yy} = (\sigma_{HS,i1(j)})_{yy} - (\sigma_{HS,i2(j)})_{yy} \\ (\Delta\sigma_{HS,i(j)})_{xy} = (\sigma_{HS,i1(j)})_{xy} - (\sigma_{HS,i2(j)})_{xy} \end{cases}$$

where:

$(\sigma_{HS,i1(j)})_{xx}$ ,  $(\sigma_{HS,i1(j)})_{yy}$ ,  $(\sigma_{HS,i1(j)})_{xy}$ , and  $(\sigma_{HS,i2(j)})_{xx}$ ,  $(\sigma_{HS,i2(j)})_{yy}$ ,  $(\sigma_{HS,i2(j)})_{xy}$  are the hot spot stress tensor components obtained for each load case 'i1' and 'i2' respectively, for loading condition j (see Fig 23). These hot spot stress tensor components are obtained according to [3.3], [3.4] or [3.5] for type 'a' hot spots, [4.2] for the flange of web-stiffened cruciform joints and [4.3] for the web of web-stiffened cruciform joints.

**Figure 23 : Hot spot stress components in the hot spot coordinate system (X, Y)**



### 7.2.5 Principal hot spot stress range calculation

For each load case i, each loading condition j and for each side (side L, side R) of the line A-A, two principal hot spot stress ranges are computed from the hot spot stress tensor component differences obtained in [7.2.4].

The principal direction of the hot spot stress range is given by:

$$\theta = 0,5 \operatorname{atan} \left[ \frac{2(\Delta\sigma_{HS,i(j)})_{xy}}{(\Delta\sigma_{HS,i(j)})_{xx} - (\Delta\sigma_{HS,i(j)})_{yy}} \right]$$

where:

$\theta$  : Angle between the hot spot axis X and the principal direction pX (see Fig 24).

The principal hot spot stress differences are given by the following matrix equation:

$$\begin{Bmatrix} (\Delta\sigma_{HS,i(j)})_{pXpX} \\ (\Delta\sigma_{HS,i(j)})_{pYpY} \end{Bmatrix} = [P] \cdot \begin{Bmatrix} (\Delta\sigma_{HS,i(j)})_{xx} \\ (\Delta\sigma_{HS,i(j)})_{yy} \\ (\Delta\sigma_{HS,i(j)})_{xy} \end{Bmatrix}$$

where:

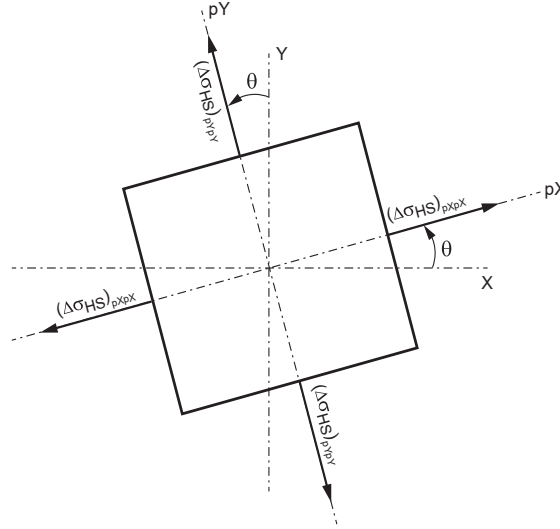


[P] : Matrix for the axis change, given by:

$$[P] = \begin{bmatrix} 0,5[1 + \cos(2\theta)] & 0,5[1 - \cos(2\theta)] & \sin(2\theta) \\ 0,5[1 + \cos(2\theta + \pi)] & 0,5[1 - \cos(2\theta + \pi)] & \sin(2\theta + \pi) \end{bmatrix}$$

$|(\Delta\sigma_{HS,i(j)})_{pXpX}|$  and  $|(\Delta\sigma_{HS,i(j)})_{pYpY}|$  correspond to the two principal hot spot stress ranges.

**Figure 24 : Hot spot stress range components in the principal directions coordinate system (pX, pY)**



### 7.2.6 Hot spot mean stress calculation

The hot spot mean stress corresponds to the average of the hot spot stress for load cases i1 and i2. In a first step, the average stress tensor components are determined in the weld axis using the following equation:

$$\begin{cases} (\sigma_{\text{meanHS},i(j)})_{xx} = 0,5[(\sigma_{HS,i1(j)})_{xx} + (\sigma_{HS,i2(j)})_{xx}] \\ (\sigma_{\text{meanHS},i(j)})_{yy} = 0,5[(\sigma_{HS,i1(j)})_{yy} + (\sigma_{HS,i2(j)})_{yy}] \\ (\sigma_{\text{meanHS},i(j)})_{xy} = 0,5[(\sigma_{HS,i1(j)})_{xy} + (\sigma_{HS,i2(j)})_{xy}] \end{cases}$$

The mean stress tensor is projected on the stress range principal directions (pX, pY) determined in [7.2.5]:

$$\begin{Bmatrix} (\sigma_{\text{meanHS},i(j)})_{pXpX} \\ (\sigma_{\text{meanHS},i(j)})_{pYpY} \end{Bmatrix} = [P] \begin{Bmatrix} (\sigma_{\text{meanHS},i(j)})_{xx} \\ (\sigma_{\text{meanHS},i(j)})_{yy} \\ (\sigma_{\text{meanHS},i(j)})_{xy} \end{Bmatrix}$$

where [P] is the same matrix as in [7.2.5].

## 7.3 Ordinary welded details

### 7.3.1 Type 'a' hot spot stress range and mean stress

The hot spot stress tensor is determined using the prescriptions in [3] for each dynamic load case i1 and i2 of each loading condition j, and for each side (side L, side R) of the line A-A.

The principal hot spot stress and the associated mean stress are then determined using [7.2].

In total, four principal hot spot stress ranges with their associated mean stress are computed and are to be considered for the fatigue strength checking:

- the first principal hot spot stress range  $(\Delta\sigma_{HS1,i(j)})_{\text{Side L}}$  at the left side of line A-A and its associated mean stress  $(\sigma_{\text{meanHS1},i(j)})_{\text{Side L}}$
- the second principal hot spot stress range  $(\Delta\sigma_{HS2,i(j)})_{\text{Side L}}$  at the left side of line A-A and its associated mean stress  $(\sigma_{\text{meanHS2},i(j)})_{\text{Side L}}$
- the first principal hot spot stress range  $(\Delta\sigma_{HS1,i(j)})_{\text{Side R}}$  at the right side of line A-A and its associated mean stress  $(\sigma_{\text{meanHS1},i(j)})_{\text{Side R}}$
- the second principal hot spot stress range  $(\Delta\sigma_{HS2,i(j)})_{\text{Side R}}$  at the right side of line A-A and its associated mean stress  $(\sigma_{\text{meanHS2},i(j)})_{\text{Side R}}$

### 7.3.2 Type 'b' hot spots stress range and mean stress

The hot spot stress is determined using the prescriptions in [3] for each dynamic load case i1 and i2 of each loading condition j.

The hot spot stress range is calculated for each dynamic load case (i) from the difference between hot spot stress from load case i1 and from load case i2:

$$\Delta\sigma_{HS,i(j)} = |\sigma_{HS,i1(j)} - \sigma_{HS,i2(j)}|$$

where:

$\sigma_{HS,i1(j)}$  : Hot spot stress induced by load case i1 for loading condition j

$\sigma_{HS,i2(j)}$  : Hot spot stress induced by load case i2 for loading condition j.

The hot spot mean stress for each dynamic load case (i) of each loading condition j is calculated by:

$$\sigma_{meanHS,i(j)} = \frac{\sigma_{HS,i1(j)} + \sigma_{HS,i2(j)}}{2}$$

## 7.4 Web-stiffened cruciform joint

### 7.4.1 Hot spot stress range and hot spot mean stress at the flange

The hot spot stress tensor is determined using the prescriptions in [4.2] for each load case i1, i2 of each loading condition j.

The principal hot spot stress and the associated mean stress are then determined using [7.2].

In total, two principal hot spot stress ranges with their associated mean stress are computed and are to be considered for the verification of the fatigue strength:

- the first principal hot spot stress range ( $\Delta\sigma_{HS1,i(j)}$ )<sub>Flange</sub> and its associated mean stress ( $\sigma_{meanHS1,i(j)}$ )<sub>Flange</sub>
- the second principal hot spot stress range ( $\Delta\sigma_{HS2,i(j)}$ )<sub>Flange</sub> and its associated mean stress ( $\sigma_{meanHS2,i(j)}$ )<sub>Flange</sub>.

### 7.4.2 Hot spot stress range and hot spot mean stress in way of the web

The hot spot stress tensor is determined using the prescriptions in [4.3] for each load case i1, i2, of each loading condition j.

The principal hot spot stress and the associated mean stress are then determined using [7.2].

In total, two principal hot spot stress ranges with their associated mean stress are computed and are to be considered for the verification of the fatigue strength:

- the first principal hot spot stress range  $\Delta\sigma_{HS1,i(j)}$  and its associated mean stress  $\sigma_{meanHS1,i(j)}$
- the second principal hot spot stress range  $\Delta\sigma_{HS2,i(j)}$  and its associated mean stress  $\sigma_{meanHS2,i(j)}$ .

## 7.5 Plate cut edge details

### 7.5.1 Stress range and mean stress calculation

The plate cut edge stress range is calculated for each beam element along the plate edge.

Cut plate edge stress range is calculated for each dynamic load case (i) from the difference between cut plate edge stress from load case i1 and from load case i2 of each loading condition j:

$$\Delta\sigma_{CE,i(j)} = |\sigma_{CE,i1(j)} - \sigma_{CE,i2(j)}|$$

where:

$\sigma_{CE,i1(j)}$  : Cut plate edge stress induced by load case i1 for loading condition j

$\sigma_{CE,i2(j)}$  : Cut plate edge stress induced by load case i2 for loading condition j.

The plate cut edge mean stress for each load case (i) corresponds to the average of the cut plate edge stress for load cases i1 and i2 of each loading condition j:

$$\sigma_{CE\_mean,i(j)} = \frac{\sigma_{CE,i1(j)} + \sigma_{CE,i2(j)}}{2}$$

## SECTION 6

## HOT SPOT STRESS BASED ON FEA FOR TUBULAR JOINTS

### 1 Global model

#### 1.1 Modelling recommendations

**1.1.1** Recommendations for global modelling of jackets and other framed structures can be found in the document (ISO 19902 clauses 16).

### 2 Hot spot stress for tubular joints

#### 2.1 General

##### 2.1.1 Element type

The hot spot stress within tubular joints can be determined using the finite element method with shell or solid elements.

##### 2.1.2 Separate finite element model

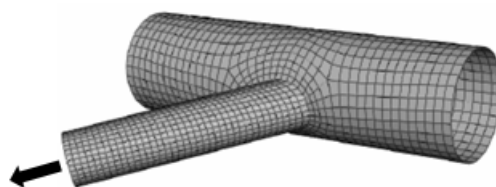
The tubular joint finite element model can be used separately from the global model, in order to define the applicable hot spot stress concentration factors (see Fig 1). In this case, the boundary conditions shall be defined with care, especially for multi-braced tubular joints.

##### 2.1.3 Integrated finite element model

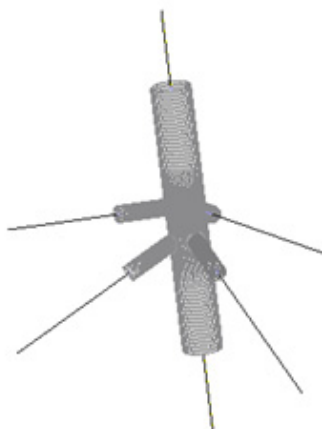
The tubular joint finite element model can be directly integrated within the global model (see Fig 2). In this case there is no ambiguity about the boundary conditions of the model. With appropriate modelling of the tubular joint, the hot spot stress can be directly extracted from the shell elements.

It is reminded that the hot spot stress approach is suitable for the assessment of fatigue cracks located at the weld toes. For fatigue cracks of tubular joints located at weld root, refer to Sec 7, [2.4].

**Figure 1 : Separate FE model**



**Figure 2 : FE tubular model integrated within the global model**



2.2 Finite element modelling

2.2.1 The finite element model shall be a three-dimensional representation of the tubular joint built using recognized finite element software.

2.2.2 When modelling the tubular joint, the length of the chord included in the model shall be defined with care in order to ensure that chord ovalisation is not restrained by the boundary conditions. It is recommended to consider a chord length equal to at least 6 times the chord diameter.

The model may be based on shell elements, where the plates's mid-surfaces are modelled and where the weld is not explicitly represented. Alternatively, the tubular joints may be modelled using solid elements for a more accurate assessment of the hot spot stress. In this case, the weld can be explicitly modelled.

2.2.3 For any of the above modelling choice, standard best practice of finite element modelling is to be adopted, avoiding elements with high length to width ratios, avoiding steep mesh sizes transition, avoiding triangular and tetrahedral elements and choosing relevant elements to avoid artificial strain energy modes (shear locking, hourglassing). The element size is to be chosen in such a way that the prescriptions for the readout points given in [2.3.4] can be satisfied.

2.3 Stress extrapolation

2.3.1 General

The hot spot stress at the tubular joint is obtained by linear extrapolation of the surface stress normal to the weld toe, at predefined read-out points located at distances  $a$  and  $b$  from the weld toe as indicated in Fig 3.

2.3.2 Shell element models

In case of shell elements model with no weld modelled, the weld toe corresponds to the brace/chord structural intersection. So, the distances  $a$  and  $b$  are measured from the brace/chord structural intersection and the stress extrapolation shall also be performed up to the brace/chord intersection. In addition, if the mid-surfaces of the plates are modelled, the stress at the plate top surface shall be retrieved from the finite element software.

2.3.3 Solid element model

When solid elements are employed together with explicit weld modelling, the distances  $a$  and  $b$  are measured from the weld toe position and the extrapolation procedure is straightforward.

2.3.4 Stress readout points

The finite element mesh is to be built to satisfy the position of the read-out points given in Tab 1. The read-out points can coincide with the Gauss points of the element (where the finite element stresses are determined) or with the nodes of the element (where in this case the averaged stress from adjoining elements is calculated). The procedure needs to be performed carefully since the position of the Gauss points varies with the type of element used.

Figure 3 : Read out points for derivation of hot spot stress in tubular joints

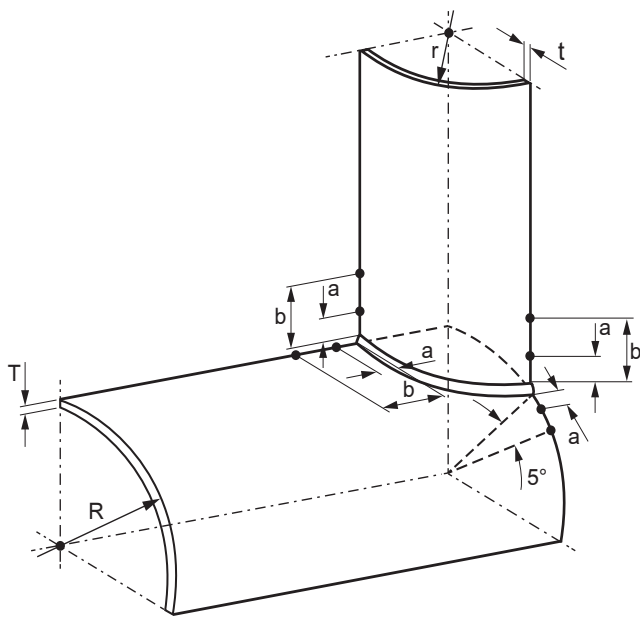


Table 1 : Distances for extrapolation to weld toes

Distance from weld toe	Brace side		Chord side	
	Crown	Saddle	Crown	Saddle
a (mm)	$\text{Max}(0,2 \sqrt{r \cdot t}; 4)$			
b (mm)	$0,65 \sqrt{r \cdot t}$		$0,44 \sqrt{r \cdot t \cdot R \cdot T}$	5° arc length

2.4 Applicable S-N curve

2.4.1 The tubular joints shall be checked versus toe cracking considering the ‘T’ curve as per ISO 19902.  
The ‘T’ S-N curves to be used in air environment and in seawater with corrosion protection are given in Sec 9, [2.3].

SECTION 7

WELD STRESS FOR ROOT CRACKING ANALYSIS

1 Scope of application

1.1 General

1.1.1 This Section applies to fatigue assessment of welded joints which may be sensitive to root cracking. In particular:

- tubular single sided butt welded joints
- plated single sided butt welded joints
- plated joints with partial penetration or fillet weld such as cruciform joints
- tubular joints welded from one side.

1.1.2 Weld root cracks are frequently considered to be more critical than weld toe cracks as their initiation can not be detected before they have grown through the whole weld thickness.

Indeed, it is difficult to detect weld root defects particularly for partial penetration and fillet welds by NDE (non-destructive examination) during inspection. Thus, the weld is to be designed so that the fatigue life at the root is greater than the fatigue life at weld toe.

A typical example for cruciform steel joints with partial penetration welds under axial loading is given in Fig 1 showing limit curves separating geometries leading to either fatigue fractures from the weld toe and root, respectively. An increased leg length ratio  $c/b$  avoids weld root failures.

1.1.3 Effect of post weld treatments

Attention should be paid to weld toe grinding impact. Weld toe grinding increases fatigue life at weld toe but doesn't increase the fatigue life at the root (see Sec 10, [7.4.2]).

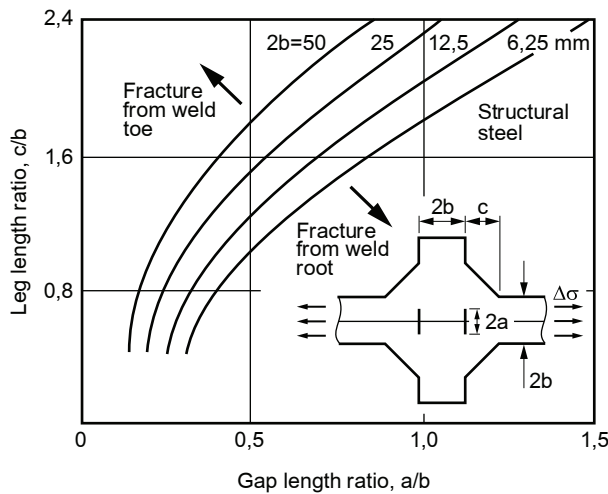
2 Weld stress calculation procedures

2.1 Definitions

2.1.1 Stress type

The weld stress may be defined either as a local nominal stress or a root structural stress. The root structural stress can be obtained either by geometric stress concentration factor ( $K_s$ ) or by finite element method (FEM).

Figure 1 : Limit curves separating weld toe failure from root failure (Maddox, 1974)



### 2.1.2 Local nominal weld stress

The local nominal stress corresponds to the nominal stress in the weld, including misalignment effects.

The nominal stress is often determined by formulas using load parameters such as the force and bending moment, as well as the weld section properties such as the section area and modulus. The local nominal stress is obtained by multiplying the nominal stress by the stress concentration factor due to misalignment  $K_m$ , as defined in Sec 10, [5].

$K_m$  considered here is due to the misalignment greater than the misalignment already included in the S-N curve  $\delta_0$  (see Sec 9, [1.1.2]).

For butt joints, the nominal weld stress can be calculated directly from the nominal stress in the adjacent plate taking into account the actual weld sectional area.

The procedure for the determination of the local nominal weld stress for tubular butt-welded joints is given in Sec 4, [3].

### 2.1.3 Weld root structural stress based on $K_g$

For tubular joints welded from one side, the weld root structural stress is obtained from the nominal stress multiplied by the internal  $K_g$  associated to the weld root, as described in [2.4].

If the misalignment is greater than the one included in the S-N curve (see Sec 9, [1.1.2]), the effect of misalignment is to be taken into account by means of a stress concentration factor given in Sec 10, [5].

### 2.1.4 Weld root structural stress based on FEM

The weld root structural stress can be obtained by the FEM method using a mesh where the weld bead is explicitly modelled. The FEM model can be based on solid elements or, in a more practical way based on shell elements representing both the plates and the weld, following the procedure given in [2.2.2].

The weld root structural stress should include all misalignment effects. If the misalignment is not included in the FEM model, the effect of misalignment may be taken into account by means of a stress concentration factor. This stress concentration factor is to be calculated using the prescriptions in Sec 10, [5] with  $\delta_0 = 0$  as the associated S-N curve does not include any misalignment effect.

## 2.2 Plated joints, weld root stress computed by FEA

### 2.2.1 General

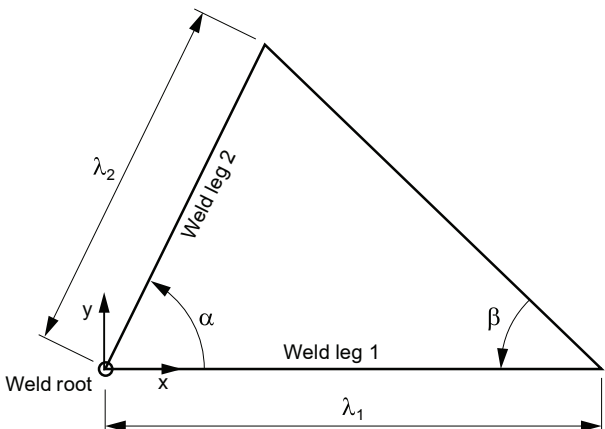
Weld root cracking may be checked for plated joints (e.g. cruciform joint, T joint, end of attachment) with partial penetration or fillet weld using a FEM model and a specific procedure for the determination of the root structural stress.

This procedure is based on a FEM model of the welded detail in which the weld itself is represented. This FEM model can be made of solid elements. It can also be made of shell elements, both for the plates and the weld, using the meshing procedure described in [2.2.2].

The weld root structural stress derives from the analysis of forces and moments internal to the weld. These forces and moments are determined for the FEM nodal forces and moments as described in [2.2.3].

The weld geometry is described by the parameters defined in Fig 2.

**Figure 2 : Weld geometry and local coordinate system**



2.2.2 FEA shell elements weld model

The weld is represented by shell elements which are defined and attached to the shell elements modelling the plates in such a way that the welded joint stiffness is correctly modelled.

The procedure for building the weld model is the following one:

The geometry of the welded joint is analysed in order to determine the location of the two weld legs connecting the weld bead to the attached plates. The attached plates are model ed with shell elements located at their mid-surfaces. The size of the shell elements in way of each weld leg is equal to the extend of the weld leg as shown on Fig 3.

The shell elements representing the weld bead connect the weld leg nodes (point A and point B of Fig 3), located at mid-width of each weld leg section. As shown in Fig 4, the thickness of the weld shell element is taken equal to the weld throat size. It results that the weld shell element has the same section area as the physical weld and thus similar transverse and longitudinal stiffness.

The connection of the weld leg nodes to the attached plates is performed with the FEA gluing technique that introduces no additional rigidity. As shown in Fig 3, it uses a rigid body element (RBE) connection from the weld leg node (point A or point B) to a projected node (respectively point A' and point B') on the mid-surface of the attached plates shell elements. It also uses a multi-point constraint (MPC) connecting the projected nodes (point A' and point B') to the corner nodes of the associated attached plate element (P1/P2 and P3/P4 respectively). The MPC equations are such that the projected node degrees of freedom are interpolated from those of the shell element corner nodes following the element shape functions.

2.2.3 Weld root structural stress calculation

The weld root structural stress  $\sigma_{WR}$  corresponds to the maximum value of the weld structural stress at the location of the root.

The weld structural stress is the distribution of the structural stress through one weld throat section. It corresponds to the combination of the membrane normal stress and the bending normal stress ( Fig 5).

Figure 3 : Weld shell element model based on gluing technique

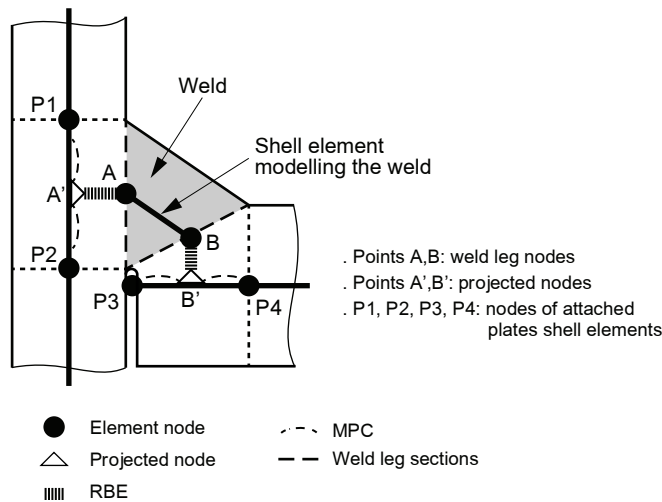
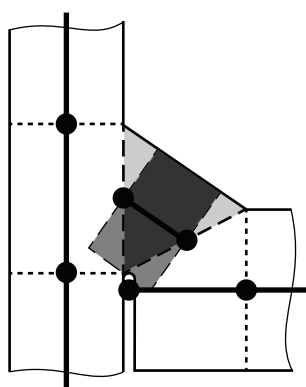
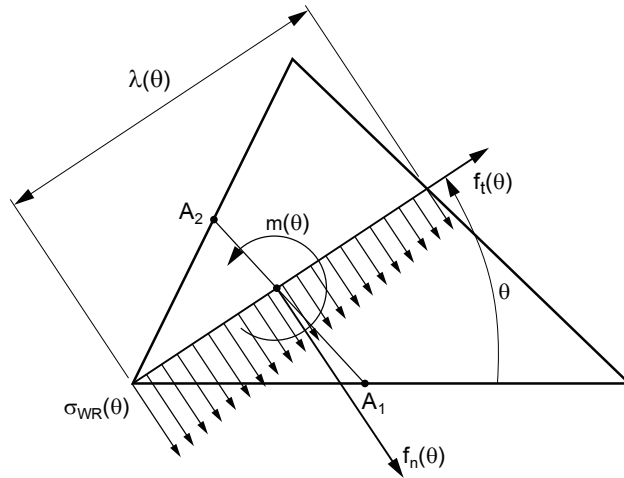


Figure 4 : Weld shell element equivalent section area





**Figure 5 : Weld throat section structural stress and weld root structural stress**



The weld root structural stress  $\sigma_{WR}$  thus corresponds to the maximum value of structural stress at the weld root calculated for various values of section angle  $\theta$ , using the following formula:

$$\sigma_{WR}(\theta) = \frac{f_n(\theta)}{\lambda(\theta)} + 6 \frac{m(\theta)}{\lambda(\theta)^2}$$

where:

$f_n(\theta)$ ,  $m(\theta)$ : Internal loads per unit length acting on the considered weld throat section, given by:

$$f_n(\theta) = f_{1x} \sin \theta - f_{1y} \cos \theta$$

$$m(\theta) = m_1 - \frac{1}{2} [\lambda_1 \cos \theta - \lambda(\theta)] \cdot f_n(\theta) + \frac{1}{2} \lambda_1 \cdot \sin(\theta) \cdot f_t(\theta)$$

$\lambda(\theta)$  : Weld throat section length given by:

$$\lambda(\theta) = \frac{\lambda_1}{\cos \theta + \frac{\sin \theta}{\tan \beta}}$$

with:

$f_{1x}$ ,  $f_{1y}$ ,  $m_1$ : Internal forces and moment per unit length acting on the weld at weld leg node  $A_1$  in Fig 6 in the weld local axes

$\theta$  : Angle of the section where the structural weld stress is calculated (see Fig 5)

$\lambda_1$ ,  $\lambda_2$  : Weld legs dimensions (see Fig 2)

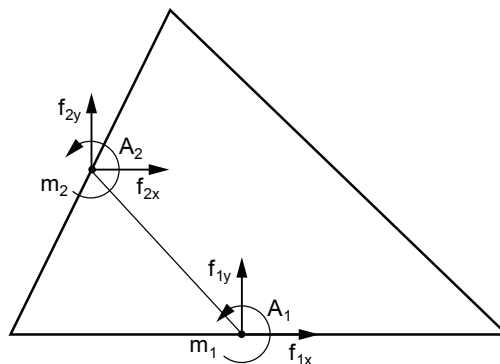
$$f_t(\theta) = f_{1x} \cos \theta + f_{1y} \sin \theta$$

$$\beta = \text{atan}\left(\frac{\lambda_2 \sin \alpha}{\lambda_1 - \lambda_2 \cos \alpha}\right)$$

$\alpha$  : Weld angle (see Fig 2).

The internal forces acting on the weld are determined by a procedure which depends on the type of FEM modelling of the weld.

**Figure 6 : Weld loads per unit length definition**



#### 2.2.4 Weld internal loads for shell elements weld model

When the shell element modelling described in [2.2.2] is used, the internal forces can be determined by:

- extraction of the nodal forces and moments acting on the weld shell element at the weld leg
- transformation of these nodal forces to the weld local axes
- derivation of the internal forces and moments per unit length ( $f_{1x}$ ,  $f_{1y}$ ,  $m_1$ ).

Alternatively, in case of shell element, the internal loads can be determined from the element internal loads provided by the FEM solver, if available. In such a case, attention should be given to the exact definition of the element loads results. In particular, the elemental bending moments at nodes does usually not include the term that balances the elemental out of plane shearing force.

For example, when the shell element force outputs are defined as shown on Fig 7, the weld loads can be determined by:

$$f_{1x} = f_m \cos(\beta) - f_s \sin(\beta)$$

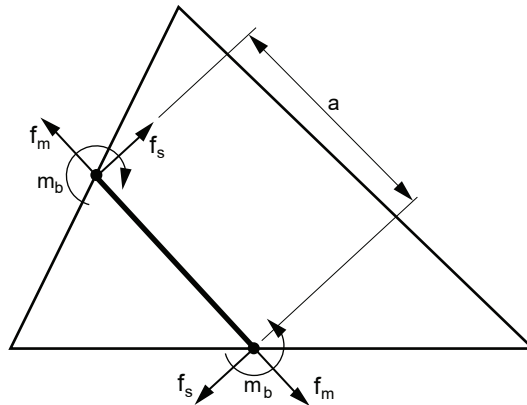
$$f_{1y} = -f_m \sin(\beta) - f_s \cos(\beta)$$

$$m_1 = m_b + 1/2 f_s a$$

where:

- $f_m$  : Elemental membrane force per unit length
- $f_s$  : Elemental out of plane shearing force per unit length
- $m_b$  : Elemental bending moment per unit length
- $a$  : Element length from one weld leg to the other.

**Figure 7 : Weld shell element internal loads**



#### 2.2.5 Weld internal loads for solid elements weld model

When the FEM analysis is based on solid elements modelling of the welded detail, the internal forces can be determined by:

- extraction of the nodal forces acting on a line of solid elements at the weld leg
- transformation of these nodal forces to the weld local axes
- integration of the nodal forces using the following equations:

$$f_{1x} = \frac{1}{b} \sum_i F_{xi}$$

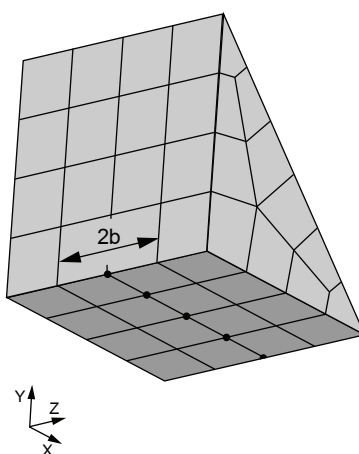
$$f_{1y} = \frac{1}{b} \sum_i F_{yi}$$

$$m_1 = \frac{1}{b} \sum_i \left[ F_{yi} \cdot \left( x_i - \frac{\lambda_1}{2} \right) \right]$$

where:

- $b$  : Length of weld bead associated with the processed line of FEM nodes, as illustrated on Fig 8
- $F_{xi}$ ,  $F_{yi}$  : Nodal forces acting on FEM node  $i$ , in the weld local axes
- $x_i$  : Local coordinate of FEM node  $i$ , in the weld local axes.

**Figure 8 : Example of weld solid mesh with post-processed nodes and weld length parameter  $b$  definition**



### 2.2.6 Applicable S-N Curve

The applicable S-N curves for weld root checking of plated joints are given in Sec 9, [3.1].

## 2.3 Plate butt-welded joints welded from one side

### 2.3.1 General

Weld root cracking is to be checked for single sided butt-welded joint.

### 2.3.2 Stress concentration factors

The stress to be considered is the local nominal weld stress, obtained as described in [2.1.2].

### 2.3.3 S-N curves

The S-N curves to be considered are given in Sec 9, [3.2].

## 2.4 Tubular butt-welded joints

### 2.4.1 General

Weld root cracking is to be checked for single sided welded joints (see Sec 4, Tab 1).

The tubular butt welded joints shall be designed based on the assessment of local nominal stresses at weld root (see Sec 4, [3.1.1]) and the use of appropriate stress concentration factor due to eccentricities (see Sec 10, [5.5]).

### 2.4.2 Classification of tubular butt welded joints for weld root checking

The classification of tubular butt welded joints sensitive to potential fatigue failure originated at the weld root is included in Sec 4, Tab 1.

### 2.4.3 Applicable S-N curves

The applicable S-N curves for weld root checking of tubular butt-welded joints are given in Sec 9, [3.4].

## 2.5 Tubular joints welded from one side

### 2.5.1 General

Historically, the fatigue assessment of the tubular joints has been focused on weld toe failures since tubular joints, even those welded from one side, were observed to fail at the weld toe. In addition, the laboratory tests considered to establish the S-N curve applicable for tubular joints at weld toe mainly included tubular joints with single sided welds.

However, even if the hot spot stress is lower at the weld root than at the weld toe, the weld root is also a more fatigue sensitive location due to the inherent presence of notch. Therefore, for fatigue sensitive tubular joints welded from one side, the potential fatigue failure at weld root shall be addressed considering the weld root structural stress based on  $K_g$  approach.

### 2.5.2 Weld root structural stress (internal $K_g$ )

For tubular joints welded from one side, the weld root structural stress is obtained by multiplying the nominal stress multiplied by the internal  $K_g$  (internal  $K_g$  is a geometric stress concentration factor derived for the weld root).

For a simplified approach, the internal stress concentration factor to be used for the weld root checking, both at brace and chord member location, is based on the largest external stress concentration factors derived for weld toe at the brace and chord, multiplied by a reduction stress concentration factor  $RK_g$ .

Note 1:  $RK_g$  formulae and their validity ranges can be found in Report OTO 1999 022, HSE Offshore Technology, Table 3.1 and Table 3.2, respectively.

The weld root checking is to be performed if  $RK_g$  is greater than 0,6.

### **2.5.3 Applicable S-N curves**

The applicable S-N curves for weld root checking of single sided tubular joints are given in Sec 9, [3.3].

## SECTION 8

## STRESS ANALYSIS OF BOLTED CONNECTIONS

### 1 General

#### 1.1 Bolt layout

**1.1.1** The bolt layout is to fulfil the following conditions (see Fig 1):

- $e_1 \geq 1,5 d$  and  $e_2 \geq 1,5 d$
- $p_1 \geq 2,5 d$  and  $p_2 \geq 2,5 d$

where  $d$  is the hole diameter.

Other layouts may be accepted if demonstrated as equivalent from the in-plate stress distribution point of view.

### 2 Bolted connection stress analysis procedures

#### 2.1 Bolted plate fatigue checking

##### 2.1.1 General

For bolted plate fatigue checking, nominal stresses are defined differently depending on whether the bolt is preloaded or not.

##### 2.1.2 Preloaded bolts

For double or simple overlap with preloaded bolts, the stress to be considered is the nominal stress in the gross plate cross-section.

##### 2.1.3 Non preloaded bolts

For double or simple overlap with calibrated, non preloaded bolts or normal holes, the stress to be considered is the nominal stress in the net plate cross-section.

##### 2.1.4 Applicable S-N curves

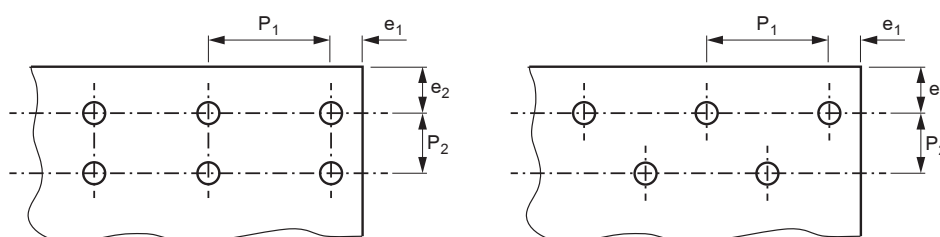
The S-N curves to be used for bolted plate fatigue checking are given in Sec 9, [7.2.1].

#### 2.2 Bolt fatigue checking

##### 2.2.1 General

When the bolts are loaded by variable tension and/or shear loads, they are to be checked as indicated in [2.2.2] and/or [2.2.3].

**Figure 1 : Bolt layout**



### **2.2.2 Tension load**

When the bolt is submitted to tension, the stress range to be associated to the S-N curve given in Sec 9, [7.2.2], is to be calculated with the bolt tensile stress area (see ISO 898).

For preloaded bolts, the stress range in the bolts depends on the level of preload and on the geometry of the connection. The prescriptions given in VDI 2230 "Systematic calculation of high duty bolted joints" standard should be applied.

The stress range for preloaded bolts to be associated to the S-N curve given in Sec 9, [7.2.2] takes into account the mean stress effect, including the preload.

### **2.2.3 Shear load**

When the bolt is submitted to shear load, the shear stress range to be associated to the S-N curve given in Sec 9, [7.2.2] is to be calculated with the shank area of the bolt (see ISO 898).

## SECTION 9

## BASIC DESIGN S-N CURVES FOR STEEL DETAILS

### 1 General

#### 1.1 Basic design S-N curves

##### 1.1.1 Probability of survival

Fatigue design is based on the use of S-N curves obtained from fatigue tests in laboratories. The basic design S-N curves represent two standard deviations below the mean S-N curves (corresponding to 50% of probability of survival) for relevant experimental data. Basic design S-N curves provided in this Section correspond to a survival probability equal to 97,7%. If another probability of survival is required, new design S-N curves are to be used (see [8.5.5]).

##### 1.1.2 Workmanship tolerances implicitly included in design S-N curves

Small specimens used for design S-N curves building include some fabrication misalignment. Values of misalignments ( $\delta_0$ ,  $\alpha_0$ ) are given in Sec 10, [5].

##### 1.1.3 Failure criterion for plated structures

The failure criterion associated to the S-N curves for plated structures correspond to the failure of small standard specimens tested in laboratories. Those specimens do not present any structural redundancy, so the crack propagation rate is very high. For small specimens, it means that the number of cycles corresponding to the initiation phase (N1, as defined in [8.2.4]) is close to the number of cycles corresponding to the through-thickness phase (N2, as defined in [8.2.4]) and close to the number of cycles corresponding to complete failure of the small specimen (N3 as defined in [8.2.4]).

Actual structures or large scale specimens often present a high number of structural redundancies. The increase of compliance due to the crack opening induces the redistribution of the stress in other components which may considerably slow down the crack propagation. As a consequence, the failure criterion relative to the S-N curves (N3 of small specimens) is close to the initiation criterion in the complex structures (N1 of complex structures).

The fatigue failure of actual plated structures determined by the S-N curve approach used in this Guidance Note corresponds to the initiation of a fatigue crack, not to the complete failure of the structure. The complete failure of complex plated structures N3 should not be used as a fatigue criterion at the design stage.

##### 1.1.4 Failure criterion for tubular joints

The failure criterion associated to the S-N curves for tubular joints corresponds to a failure of the welded joint associated to a through-thickness crack, so it includes the initiation phase and an important crack propagation phase along the brace/chord joint.

### 1.2 Scope of application

#### 1.2.1 Material

The basic design S-N curves given in this section are dedicated to steel details. For aluminium plated welded details, corresponding design S-N curves are given in App 2.

For welded details and for cut plate edge details in steel, S-N curves are valid for:

- ferritic/pearlitic or bainitic steel materials with specified minimum yield stress  $R_{eH}$  not greater than 960 MPa for details in air and not greater than 500 MPa for details in corrosive environment under free corrosion or with cathodic protection
- austenitic stainless steel materials with minimum yield strength  $R_{p0,2}$  not greater than 300 Mpa for details in air and corrosive environment (NR216, Sec 1, [9.6]).

### 1.2.2 Types of details

S-N curves in this Section are applicable to the following structural details:

- plated welded details
- cut plate edge details
- bolted connections
- tubular joints
- tubular cast joints
- tubular butt-welded joints.

### 1.2.3 Environment

S-N curves are provided for the three following types of environment:

- in air
- in seawater environment without protection
- in seawater environment with cathodic protection.

S-N curves in seawater environment are to be used for all types of corrosive environments.

S-N curves in air are to be used for details in non-corrosive environment and for details with protective coating located in a corrosive environment, provided that the protective coating is intact.

### 1.2.4 Welding process

The S-N curves provided from Articles [2] to [5] correspond to S-N curves for as-welded joints with welding conditions as defined in Sec 10, [7.3].

When automatic welding is applied, fatigue strength is increased thanks to the weld quality, weld profile and toe improvement. The improvement may be taken into account through improved S-N curves when duly justified in accordance with Article [5] and agreed by the Society.

### 1.2.5 Reference thickness

Basic design S-N curves derive from fatigue data of tested specimens fabricated with a plate thickness lower than a reference thickness  $t_{ref}$ . This reference thickness depends on the type of joint (plated welded joints, tubular joints, cast joint, etc).

Thus, basic design S-N curves provided in this Section are directly applicable for plates or members with a thickness lower than the reference thickness  $t_{ref}$ . For plate or member thicknesses greater than  $t_{ref}$ , the influence of thickness is to be taken into account in accordance with Sec 10, [3].

## 1.3 Basic design S-N curves formulae

### 1.3.1 Standard form

The standard form of the basic design S-N curves (see Fig 1) is:

$$N \Delta S^{m1} = K_1 \quad \text{for } \Delta S \geq \Delta S_q$$

$$N \Delta S^{m2} = K_2 \quad \text{for } \Delta S < \Delta S_q$$

where:

$$K_2 = K_1 (\Delta S_q)^{(m2 - m1)}$$

$N$  : Predicted number of cycles to failure at stress range  $\Delta S$

$m1$  : Inverse of first slope of the design S-N curve (for  $\Delta S \geq \Delta S_q$ )

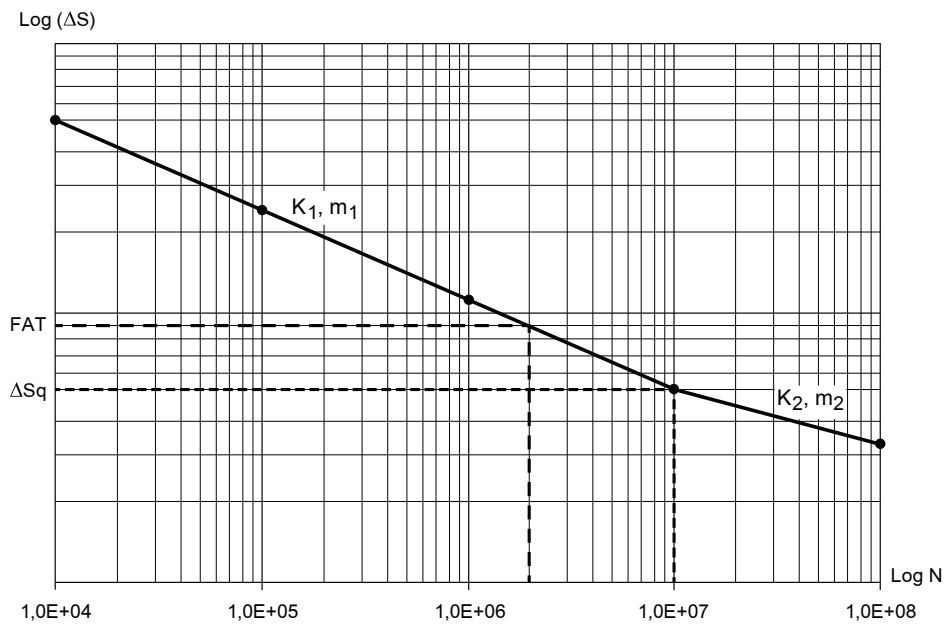
$\Delta S_q$  : Stress range at the number of cycles corresponding to the change of slope (slope intersection)

$m2$  : Inverse of second slope of the design S-N curve ( $\Delta S < \Delta S_q$ ).

The change of slopes usually corresponds to  $N=10^7$  cycles, except when otherwise specified.



Figure 1 : S-N curve



1.3.2 FAT definition

As an alternative to parameter  $K_1$ , design S-N curves can be designated by their FAT, which corresponds to the stress range associated with  $2 \cdot 10^6$  cycles.

The corresponding constant can be obtained by:

$$K_1 = 2 \cdot 10^6 \text{ FAT}^{m_1}$$

where:

FAT : Stress range at  $N = 2 \cdot 10^6$  cycles.

1.3.3 Log definition

In terms of  $\log_{10}$ , the S-N curves are written as follows:

$$\log_{10}(N) = \log_{10}(K_1) - m_1 \log_{10}(\Delta S) \quad \text{for } \Delta S \geq \Delta S_q \text{ cycles}$$

$$\log_{10}(N) = \log_{10}(K_2) - m_2 \log_{10}(\Delta S) \quad \text{for } \Delta S < \Delta S_q \text{ cycles}$$

where:

$\log_{10}(K_1)$  : Constant related to the design S-N curve, in  $\log_{10}$ , for the first slope of the design S-N curve

$\log_{10}(K_2)$  : Constant related to the design S-N curve, in  $\log_{10}$ , for the second slope of the design S-N curve.

2 As-welded joints, toe cracking

2.1 Plated joints, hot spot stress

2.1.1 Hot spot stress by FEA

Plated joints are assessed using two different S-N curves depending on the principal hot spot stress direction (see Fig 2). The hot spot stresses are calculated by finite element analysis (FEA) according to the procedure described in:

- Sec 5, [3] for ordinary welded details
- Sec 5, [4] for web-stiffened cruciform joints
- Sec 5, [5] for bent hopper knuckle details.

Two angular sectors at the weld toe are identified (see Fig 2):

Sector 1 : Angular sector between  $[-45^\circ/+45^\circ]$  to the normal of the weld line

Sector 2 : Angular sector outside the sector 1, i.e. between  $[+45^\circ/+90^\circ]$  and  $[-90^\circ/-45^\circ]$  to the normal of the weld line.

For the first principal hot spot stress range, the principal stress direction ( $\varphi$ ) of which is inside the sector 1 (see Fig 2), the  $P_\perp$  curve given in this Article is to be used.

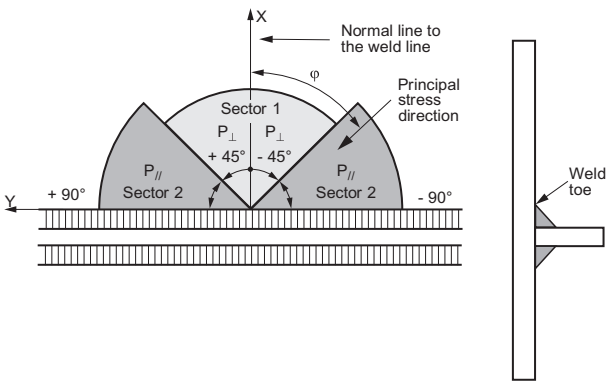
For the second principal hot spot stress range, the principal stress direction ( $\varphi$ ) of which is inside the sector2 (see Fig 2), the  $P_\parallel$  curve given in this Article is to be used.

If the weld toe angle is lower than or equal to 30°, the S-N curve to be used for all principal stress range directions is  $P_{//}$ .  
The corresponding  $P_{\perp}$  and  $P_{//}$  S-N curves are given from [2.1.3] to [2.1.5].

2.1.2 Hot spot stress by analytical stress analysis

For the assessment of longitudinal stiffener welded connections as defined in Sec 3, [2], the applicable S-N curve to be used is the  $P_{\perp}$  curve, since the calculated hot spot stress is taken perpendicular to the weld.  
If the weld toe angle is lower than or equal to 30°, the S-N curve to be used is  $P_{//}$ .

Figure 2 : S-N curves to be used with hot spot stress methodology



2.1.3 S-N curves in air

The  $P_{\perp}$  and  $P_{//}$  S-N curves in air environment are given in Tab 5.

2.1.4 S-N curves in seawater without corrosion protection

The S-N curves in seawater environment without corrosion protection have a single slope ( $m_1 = 3$ ). They correspond to S-N curves in air environment with a FAT divided by  $3^{1/3}$ .  
The  $P_{\perp}$  and  $P_{//}$  curves to be used for plated welded joints in seawater without corrosion protection are given in Tab 6.

2.1.5 S-N curves in seawater with cathodic protection

Design S-N curves in seawater environment with cathodic protection are derived from the S-N curves in air environment.  
The first slope (corresponding to high stress range level) of the design S-N curves in seawater with cathodic protection corresponds to the S-N curves in air with coefficient  $K_1$  divided by 2,5. The second slope corresponds to the second slope of the S-N curves in air.  
The  $P_{\perp}$  and  $P_{//}$  curves to be used for plated welded joints in seawater with cathodic protection are given in Tab 7.

2.2 Plated butt-welded joints, local nominal stress

2.2.1 Butt joint classification

The toe of plated butt-welded joints when using the local nominal stress may be designed according to the HSE 1995 classification (see Tab 1).  
The corresponding 'C', 'D' and 'E' S-N curves are given from [2.2.2] to [2.2.4].

Table 1 : Plated butt-welded joint classification for toe cracking according to HSE, 1995

Description of plated butt-welded joints	Applicable S-N curve
Weld cap ground flush with the surface and shown to be free from significant defect from NDE	C
Welding performed horizontally by a process other than submerged arc	D
Welding performed by submerged arc or not horizontally	E

2.2.2 S-N curves in air

The C, D and E S-N curves in air environment are given in Tab 5.

2.2.3 S-N curves in seawater without corrosion protection

The S-N curves in seawater environment without corrosion protection have a single slope ( $m_1 = 3$ ). They correspond to S-N curves in air environment with a FAT divided by  $3^{1/3}$ .

For plated butt-welded joint details located in seawater without corrosion protection, the C, D and E curves are given in Tab 6.

2.2.4 S-N curves in seawater with cathodic protection

The first slope (corresponding to high stress range level) of the design S-N curves in seawater with cathodic protection corresponds to the S-N curves in air with coefficient  $K_1$  divided by 2,5. The second slope corresponds to the second slope of the S-N curves in air.

For plated butt-welded joint details in seawater with cathodic protection, the C, D and E curves are given in Tab 7.

2.3 Tubular welded joints, hot spot stress

2.3.1 General

The weld toe of tubular joints when using the hot spot stress (see Sec 4, [2]) shall be designed considering the 'T' curve according to ISO 19902.

2.3.2 S-N curve in air

The 'T' S-N curve in air environment according to ISO 19902 is reminded in Tab 8.

2.3.3 S-N curve in seawater without corrosion protection

Tubular joint fatigue calculations in seawater environment without corrosion protection (under free corrosion) are not considered, given that the tubular joints located in seawater are always considered as designed with a corrosion protection system.

2.3.4 S-N curve in seawater with cathodic protection

The 'T' S-N curve in seawater environment with cathodic protection according to ISO 19902 is reminded in Tab 11.

2.4 Tubular butt-welded joints, local nominal stress

2.4.1 Butt joint classification

The toe of tubular butt-welded joints when using the local nominal stress (see Sec 4, [3]) shall be designed according to the ISO 19902 classification (see Tab 2).

The corresponding 'C', 'D' and 'E' S-N curves are given from [2.4.2] to [2.4.4].

Table 2 : Tubular butt-welded joint classification for toe cracking according to ISO 19902

Description of tubular butt-welded joints	Applicable S-N curve
Weld cap ground flush with the surface and shown to be free from significant defect from NDE	C
Welding performed horizontally by a process other than submerged arc	D
Welding performed by submerged arc or not horizontally	E

2.4.2 S-N curves in air

The applicable 'C', 'D' and 'E' S-N curves from ISO 19902 are reminded in Tab 9 for the in air condition.

2.4.3 S-N curves in seawater without corrosion protection

Tubular butt-welded joint fatigue calculations in seawater environment without corrosion protection (under free corrosion) are not considered because tubular butt-welded joints located in seawater are always designed with a corrosion protection system.

2.4.4 S-N curves in seawater with cathodic protection

The applicable 'C', 'D' and 'E' S-N curves from ISO 19902 are reminded in Tab 12 for seawater environment with cathodic protection.

2.5 Tubular cast joints, hot spot stress

2.5.1 General

The tubular cast joints shall be designed using hot spot stress (see Sec 4, [2.4.1]) and considering the 'CJ' S-N curve according to ISO 19902.

2.5.2 S-N curve in air

The ‘CJ’ S-N curve according to ISO 19902 is reminded in Tab 10 for the in air condition.

2.5.3 S-N curve in seawater with cathodic protection

The ‘CJ’ S-N curve according to ISO 19902 is reminded in Tab 13 for the seawater environment with cathodic protection.

3 Welded joints, root cracking

3.1 Plated joints, weld root stress computed by FEA

3.1.1 General

The weld root of plated joints (e.g. cruciform joint, T joint, end of attachment) when using weld root structural stress computed by FEM (refer to Sec 7, [2.1.4] and Sec 7, [2.2.3]) may be designed considering the ‘E’ S-N curve given from [3.1.2] to [3.1.4]. The ‘E’ S-N curve does not include any misalignment effect.

No thickness correction is to be considered for ‘E’ S-N curve when it is used for root cracking.

3.1.2 S-N curve in air

The weld root of plated joints in air environment is to be designed considering the ‘E’ S-N curve defined in Tab 5.

3.1.3 S-N curve in seawater without corrosion protection

The S-N curve in seawater environment without corrosion protection has a single slope ( $m_1 = 3$ ). It corresponds to S-N curve in air with a FAT divided by  $3^{1/3}$ .

The weld root of plated joints in seawater without corrosion protection is to be designed considering the E curve defined in Tab 6.

3.1.4 S-N curve in seawater with cathodic protection

The first slope (corresponding to high stress range level) of the design S-N curve in seawater with cathodic protection corresponds to the S-N curve in air with coefficient  $K_1$  divided by 2,5. The second slope corresponds to the second slope of the S-N curve in air.

The weld root of plated joints in seawater with cathodic protection is to be designed considering the E curve defined in Tab 7.

3.2 Plated butt-welded joints, local nominal stress

3.2.1 Butt joint classification

The root of plated butt-welded joints shall be designed according to the HSE/IIW classification (see Tab 3).

No thickness correction is to be considered for ‘E’, ‘F’ and ‘F2’ S-N curves when they are used for root cracking.

Table 3 : Plated butt-welded joint classification for root cracking (HSE/IIW)

Description of single-sided plated butt-welded joints	Applicable S-N curve
Full penetration single-sided weld made with temporary backing strip (no misalignment)	E
Full penetration single-sided weld made on permanent backing strip	F
Full penetration single-sided weld made without permanent backing strip	F2

3.2.2 S-N curves in air

The applicable E, F and F2 S-N curves in air environment are given in App 2, Tab 3.

3.2.3 S-N curves in seawater without corrosion protection

The S-N curves in seawater environment without corrosion protection have a single slope ( $m_1 = 3$ ) without change of slope. They correspond to S-N curves in air environment with a FAT divided by  $3^{1/3}$ .

The applicable E, F and F2 S-N curves in seawater environment without corrosion protection are given in Tab 6.

3.2.4 S-N curves in seawater with cathodic protection

The first slope (corresponding to high stress range level) of the design S-N curves in seawater with cathodic protection corresponds to the S-N curves in air with coefficient  $K_1$  divided by 2,5. The second slope corresponds to the second slope of the S-N curves in air.

The applicable E, F and F2 S-N curves in seawater environment with cathodic protection are given in Tab 7.

3.3 Single-sided tubular joints, weld root stress based on analytical approach

3.3.1 General

The weld root of single-sided tubular joints, when using weld root structural stress as defined in Sec 7, [2.5.2], may be designed according to the ‘F’ curve as per ISO 19902 given from [3.3.2] to [3.3.4].

3.3.2 S-N curves in air

The weld root of single-sided tubular joints in air environment may be designed according to the F curve as per ISO 19902 (see Tab 9).

3.3.3 S-N curves in seawater without corrosion protection

Single-sided tubular joint fatigue calculations in seawater environment under free corrosion are not considered because single-sided tubular joints located in seawater are always designed with a corrosion protection system.

3.3.4 S-N curves in seawater with cathodic protection

The weld root of single-sided tubular joints in seawater environment with cathodic protection may be designed according to the F curve as per ISO 19902 (see Tab 12).

3.4 Tubular butt-welded joints, local nominal stress

3.4.1 General

The weld root of tubular butt-welded joints when using local nominal stress (see Sec 4, [3.1.1]) may be designed according to the applicable curves as per ISO 19902, as given in [3.4.2].

3.4.2 Tubular butt-welded joint classification

The root of tubular butt-welded joints shall be designed according to the ISO 19902 classification (see Tab 4).

Table 4 : Tubular butt-welded joints classification for root cracking according to ISO 19902

Description of single-sided tubular butt-welded joints	Applicable S-N curve
Full penetration single-sided weld made on permanent backing strip (1)	F
Full penetration single-sided weld made without permanent backing strip	F2
(1) If the backing strip is welded from fillet or tack welding, this joint shall also be assessed according to ISO 19902 additional prescriptions (see Table A.16.10-9).	

3.4.3 S-N curves in air

The ISO 19902 is to be applied to the ‘F’ and ‘F2’ S-N curves in air environment (see Tab 9).

3.4.4 S-N curves in seawater without corrosion protection

Tubular butt-welded joint fatigue calculations in seawater environment without corrosion protection (i.e under free corrosion) are not considered because tubular butt-welded joints located in seawater are always designed with a corrosion protection system.

3.4.5 S-N curves in seawater with cathodic protection

The ISO 19902 is to be applied to the F and F2 S-N curves for seawater environment with cathodic protection (see Tab 12).

4 Tables of S-N curves

4.1 Tables of S-N curves for steel plated welded joints

4.1.1 S-N curves in air

S-N curves for steel plated welded joints in air environment are defined in Tab 5.

4.1.2 S-N curves in seawater without protection

S-N curves for steel plated welded joints in seawater environment without protection are defined in Tab 6.

4.1.3 S-N curves in seawater with cathodic protection

S-N curves for steel plated welded joints in seawater environment with cathodic protection are defined in Tab 7.

Table 5 : Basic design S-N curves for steel plated welded joints in air

Curve	FAT	First slope		Slope intersection		Second slope		Reference thickness $t_{ref}$ (mm)	Thickness exponent n
	$\Delta S$ (MPa)	m1	$\log_{10}(K_1)$	N cycles	$\Delta S_q$ (MPa)	m2	$\log_{10}(K_2)$		
C	123,84	3,5	13,6260	$10^7$	78,19	6	18,3589	25	see Sec 10, Tab 2
D	91,25	3,0	12,1818	$10^7$	53,36	5	15,6363		
E (1)	80,31	3,0	12,0153	$10^7$	46,96	5	15,3588		
F (1)	68,10	3,0	11,8004	$10^7$	39,82	5	15,0007		
F2 (1)	59,95	3,0	11,6345	$10^7$	35,06	5	14,7241		
$P_{\perp}$	91,25	3,0	12,1818	$10^7$	53,36	5	15,6363		
$P_{//}$	100,00	3,0	12,3010	$10^7$	58,48	5	15,8350		
(1) No thickness correction is to be considered when the S-N curve is used for root cracking in accordance with [3].									

Table 6 : Basic design S-N curves for steel plated welded joints in seawater without corrosion protection

Curve	FAT	Single slope		Reference thickness $t_{ref}$ (mm)	Thickness exponent n
	$\Delta S$ (MPa)	m1	$\log_{10}(K_I)$		
C	85,86	3	12,1025	25	see Sec 10, Tab 2
D	63,27	3	11,7046		
E (1)	55,68	3	11,5381		
F (1)	47,22	3	11,3233		
F2 (1)	41,57	3	11,1573		
P <sub>⊥</sub>	63,27	3	11,7046		
P <sub>∥</sub>	69,34	3	11,8239		
(1) No thickness correction is to be considered when the S-N curve is used for root cracking in accordance with [3].					

Table 7 : Basic design S-N curves for steel plated welded joints in seawater with cathodic protection

Curve	First slope		Slope intersection		Second slope		Reference thickness t <sub>ref</sub> (mm)	Thickness exponent n
	m1	log <sub>10</sub> (K <sub>1</sub> )	N cycles	ΔS <sub>q</sub> (MPa)	m2	log <sub>10</sub> (K <sub>2</sub> )		
C	3,5	13,2281	1,1·10 <sup>6</sup>	112,80	6	18,3589	25	see Sec 10, Tab 2
D	3,0	11,7838	10 <sup>6</sup>	84,38	5	15,6363		
E (1)	3,0	11,6173	10 <sup>6</sup>	74,25	5	15,3588		
F (1)	3,0	11,4025	10 <sup>6</sup>	62,97	5	15,0007		
F2 (1)	3,0	11,2365	10 <sup>6</sup>	55,44	5	14,7241		
P <sub>⊥</sub>	3,0	11,7838	10 <sup>6</sup>	84,38	5	15,6363		
P <sub>∥</sub>	3,0	11,9031	10 <sup>6</sup>	92,47	5	15,8350		
(1) No thickness correction is to be considered when the S-N curve is used for root cracking in accordance with [3].								

4.2 Tables of S-N curves from ISO 19902 for tubular welded joints, tubular butt-welded joints and tubular cast joints

4.2.1 S-N curves in air

S-N curve for steel tubular welded joints in air is defined in Tab 8.

S-N curves for steel tubular butt-welded joints in air are defined in Tab 9.

S-N curve for steel tubular cast joints in air is defined in Tab 10.

**Table 8 : T basic design S-N curve (ISO 19902) for steel tubular welded joints in air**

Curve	FAT	First slope		Slope intersection		Second slope		Reference thickness $t_{ref}$ (mm)	Thickness exponent n
	$\Delta S$ (MPa)	m1	$\log_{10}(K_1)$	N cycles	$\Delta S_q$ (MPa)	m2	$\log_{10}(K_2)$		
T	114,70	3	12,48	$10^7$	67,10	5	16,13	16	0,25

**Table 9 : Basic design S-N curves (ISO 19902) for steel tubular butt-welded joints in air**

Curve	FAT	First slope		Slope intersection		Second slope		Reference thickness $t_{ref}$ (mm)	Thickness exponent n
	$\Delta S$ (MPa)	m1	$\log_{10}(K_1)$	N cycles	$\Delta S_q$ (MPa)	m2	$\log_{10}(K_2)$		
C	124,20	3,5	13,63	$10^7$	78,40	5	16,47	16	0,25
D	91,10	3,0	12,18	$10^7$	53,30	5	15,63		
E	80,60	3,0	12,02	$10^7$	47,10	5	15,37		
F	68,10	3,0	11,80	$10^7$	39,80	5	15,00		
F2	59,70	3,0	11,63	$10^7$	34,90	5	14,71		

**Table 10 : CJ basic design S-N curve (ISO 19902) for steel tubular cast joints in air**

Curve	FAT	First slope		Slope intersection		Second slope		Reference thickness $t_{ref}$ (mm)	Thickness exponent n
	$\Delta S$ (MPa)	m1	$\log_{10}(K_1)$	N cycles	$\Delta S_q$ (MPa)	m2	$\log_{10}(K_2)$		
CJ	164,90	4	15,17	NR	NR	NR	NR	38	0,15

#### 4.2.2 S-N curves in seawater without corrosion protection

No S-N curves are proposed. It is considered that tubular joints located in seawater are always designed with a corrosion protection system.

#### 4.2.3 S-N curves in seawater with cathodic protection

S-N curve for steel tubular welded joints in seawater with cathodic protection is defined in Tab 11.

S-N curves for steel tubular butt-welded joints in seawater with cathodic protection are defined in Tab 12.

S-N curve for steel tubular cast joints in seawater with cathodic protection is defined in Tab 13.

**Table 11 : T basic design S-N curve (ISO 19902) for steel tubular welded joints in seawater with cathodic protection**

Curve	First slope		Slope intersection		Second slope		Reference thickness $t_{ref}$ (mm)	Thickness exponent n
	m1	$\log_{10}(K_1)$	N cycles	$\Delta S_q$ (MPa)	m2	$\log_{10}(K_2)$		
T	3	12,18	$1,8 \cdot 10^6$	94,40	5	16,13	16	0,25

**Table 12 : Basic design S-N curves (ISO 19902) for steel tubular butt-welded joints in seawater with cathodic protection**

Curve	First slope		Slope intersection		Second slope		Reference thickness $t_{ref}$ (mm)	Thickness exponent n
	m1	$\log_{10}(K_1)$	N cycles	$\Delta S_q$ (MPa)	m2	$\log_{10}(K_2)$		
C	3,5	13,23	$4,68 \cdot 10^5$	114,50	5	16,47	16	0,25
D	3,0	11,78	$10^6$	84,50	5	15,63		
E	3,0	11,62	$10^6$	74,70	5	15,37		
F	3,0	11,40	$10^6$	63,10	5	15,00		
F2	3,0	11,23	$10^6$	55,40	5	14,71		

**Table 13 : CJ basic design S-N curve (ISO 19902) for steel tubular cast joints in seawater with cathodic protection**

Curve	FAT	First slope		Slope intersection		Second slope		Reference thickness $t_{ref}$ (mm)	Thickness exponent n
	$\Delta S$ (MPa)	m1	$\log_{10}(K_1)$	N cycles	$\Delta S_q$ (MPa)	m2	$\log_{10}(K_2)$		
CJ	138,70	4	14,87	NR	NR	NR	NR	38	0,15

5 Post welding improved welded joints, toe cracking

5.1 Application

5.1.1 Type of welded joints

The post welding treatments can be applied on the types of welded joints given in Sec 10, [7.4.2].

5.1.2 Material yield strength

S-N curves for post welding improved details are valid only for plated welded details made in steel with  $R_{eH} < 960$  MPa. For steel of higher yield strength, the fatigue strength improvement is to be duly justified and agreed by the Society.

5.1.3 Protection against corrosion

The proposed fatigue strength improvements associated to grinding, TIG dressing or plasma dressing post-weld treatments are only valid for welded joints not submitted to corrosive environment.

This is the case for joints in air, or in seawater environment provided that a corrosion protection measure is applied after the post weld treatment and maintained during the design life time. Applicable corrosion protection methods are given in Sec 10, [6.1.2].

For welded joints in seawater without corrosion protection, no improvement due to any post-weld treatment is to be taken into account.

5.1.4 Design stage

Taking account of post-weld improvement treatment is normally not accepted at design stage, except for highly loaded limited areas with the agreement of the Society.

5.1.5 Fabrication stage

During fabrication stage, post welding improvement treatments may be allowed by the Society in case of damaged weld or weld defect repairs.

5.1.6 Post-weld treatment procedure

The selected post-weld treatment technique and post-weld treatment procedure are to be submitted to the Society for review (see Sec 10, [7.4]).

The improvement is greatly function of the quality of the improvement operation parameters, so the given improved S-N curves are valid only when the conditions of Sec 10, [7.4] are fulfilled.

5.2 S-N curves for post-weld improved plated joints

5.2.1 Types of post-weld treatments

The design S-N curves are given for the following post-weld treatments improving the weld toe geometry:

- grinding
- TIG dressing or plasma dressing.

Table 14 : Hot spot design S-N curve for improved plated joints by grinding, TIG dressing or plasma dressing ( $R_{eH} \leq 960$  MPa)

Curve	FAT	First slope		Slope intersection		Second slope		Reference thickness $t_{ref}$ (mm)	Thickness exponent n
	$\Delta S$ (MPa)	m1	$\log_{10}(K_1)$	N cycles	$\Delta S_q$ (MPa)	m2	$\log_{10}(K_2)$		
Grinding / TIG dressing	128,6	3,5	13,6831	$10^7$	81,18	6,0	18,4567	25	see Sec 10, Tab 2

5.2.2 S-N curves

Hot spot design S-N curves (both  $P_{\perp}$  and  $P_{//}$  curves) for improved weld toe details due to grinding, TIG dressing or plasma dressing are given in Tab 14.

5.3 Fatigue life improvement for post weld treated tubular joints

5.3.1 In case of tubular joint post-treated by weld toe grinding, the fatigue life after post weld treatment corresponds to the as-welded tubular joint fatigue life multiplied by a factor of 2. The as-welded tubular joint fatigue life is obtained considering the tubular joint environment (air or seawater with cathodic protection) using S-N curve in air or in seawater as applicable (see [2.3] and [2.4]).

In case of weld toe improvement, only the fatigue life at the weld toe is improved, so the weld root can become the fatigue critical location of the joint. The weld root is to be assessed using the methods given in Sec 7.



6 Cut edges

6.1 General

6.1.1 Classification

The cut edges are to be checked according to the classification defined in Tab 15, depending on:

- the edge cutting process (machine-cut or manually thermally cut)
- the edge treatment after the cutting process (edges chamfered or edges rounded and polished), if any
- the edge finish (mirror polished surface, smooth surface, edge and cut surface free of cracks and notches).

Table 15 : Applicable S-N curves for cut edge details

Edge cutting process	Edge treatment	Edge finish	Applicable S-N curve
Machine-cut (e.g. by a thermal process or sheared edge cut)	Edges rounding and polishing with a radius bevelling machine	3R edge (see Fig 5) Edge mirror polished	BP
	Edges chamfering or rounding with a grinder (flat disk tool)	1C (see Fig 3), 2C, 3C (see Fig 4) edges Smooth surface with grinding grooves paral- lel to the edge line	B
	No edge treatment	Edge and cut surface free of cracks and notches	C
Manually thermally cut (e.g. by flame cutting)	No edge treatment	Edge and cut surface free of cracks and notches	CED

6.1.2 Stress calculation

The stress on the plate edge is to be determined from a fine mesh FE analysis according to Sec 5, [6].

6.1.3 S-N curve selection

Tab 15 specifies the applicable S-N curves associated to each cut edge detail configuration.

‘C’ and ‘CED’ S-N curves are applicable to cut edge details without edge treatment, depending on the type of cutting process.

Higher edge finish quality may be taken into account, using ‘BP’ or ‘B’ S-N curves, provided that adequate protective measures are taken against wear, tear and corrosion.

‘B’ S-N curve may be applied if the edges are treated using chamfering techniques (1C, 2C or 3C, see Fig 3 and Fig 4).

‘BP’ S-N curve may be applied instead of ‘B’ S-N curve if (see Fig 5):

- the edges are rounded using 3R technique (as example with radius bevelling machine), and
- complete surface of detail, including the edges, is mirror polished.

Cut surface finish has to be a smooth surface free of cracks and notches, for all cut edge details.

Figure 3 : 1C corner chamfering

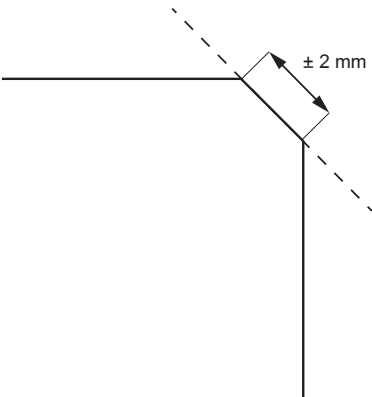


Figure 4 : 3C corner chamfering, 2C if only 2 chamfers

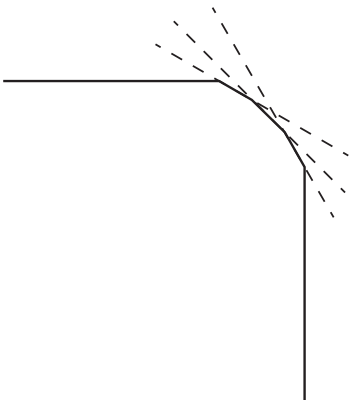
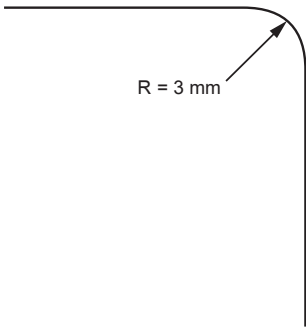


Figure 5 : 3R corner rounded + polishing



6.2 S-N curves for cut edge details

6.2.1 S-N curves in air

The design S-N curves, thickness exponents and reference thickness for cut edge details are given in Tab 16. These S-N curves are valid for steel material in air having a specified minimum yield stress  $R_{eH}$  equal to 235 MPa.

For higher strength steel having a specified minimum yield stress  $R_{eH}$  up to 960 MPa, the influence of the yield stress is to be taken into account in accordance with Sec 10, [2].

Table 16 : Design S-N curves for steel ( $R_{eH} = 235$  MPa) cut edges in air

Curve	FAT	First slope		Two slope intersection		Second slope		Reference thickness $t_{ref}$ (mm)	Thickness exponent n
	$\Delta S$ (MPa)	m1	$\log_{10}(K_1)$	N cycles	$\Delta S_q$ (MPa)	m2	$\log_{10}(K_2)$		
BP	160,00	5,0	17,3220	$10^7$	115,98	9	25,5796	25	0
B	150,00	4,0	15,0060	$10^7$	100,35	7	21,0105		0,1
C	123,80	3,5	13,6260	$10^7$	78,19	6	18,3589		0,1
CED	100,00	3,5	13,3000	$10^7$	63,10	6	17,8000		0,1

6.2.2 S-N curves in seawater without corrosion protection

The design S-N curves, thickness exponents and reference thickness for cut edge details in seawater without corrosion protection are given in Tab 17. These S-N curves are valid for steel material having a specified minimum yield stress  $R_{eH}$  equal to 235 MPa.

Table 17 : Design S-N curves for steel ( $R_{eH} = 235$  MPa) cut edges in seawater without corrosion protection

Curve	FAT	Single slope		Reference thickness $t_{ref}$ (mm)	Thickness exponent n
	$\Delta S$ (MPa)	m1	$\log_{10}(K_1)$		
BP	110,96	3	12,4365	25	0
B	104,04	3	12,3526		0,1
C	85,86	3	12,1025		0,1
CED	69,29	3	11,8230		0,1

The S-N curves in seawater correspond to the S-N curves in air with the FAT divided by 3<sup>1/3</sup>. The S-N curves in seawater environment have a single slope (m1 = 3).

For higher strength steel in seawater having a specified minimum yield stress R<sub>eH</sub> up to 500 Mpa, the influence of the yield stress is to be taken into account in accordance with Sec 10, [2].

6.2.3 S-N curves in seawater with cathodic protection

The design S-N curves, thickness exponents and reference thickness for cut edge details in seawater with cathodic protection are given in Tab 18. These S-N curves are valid for steel material having a specified minimum yield stress R<sub>eH</sub> equal to 235 MPa.

The first slope (corresponding to high stress range level) of the design S-N curves in seawater with cathodic protection corresponds to the S-N curves in air with coefficient K<sub>1</sub> divided by 2,5. The second slope corresponds to the second slope of the S-N curves in air.

For higher strength steel having a specified minimum yield stress R<sub>eH</sub> up to 960 Mpa, the influence of the yield stress is to be taken into account in accordance with Sec 10, [2].

Table 18 : Design S-N curves for steel (R<sub>eH</sub> = 235 MPa) cut edges in seawater with cathodic protection

Curve	First slope		Slope intersection		Second slope		Reference thickness t <sub>ref</sub> (mm)	Thickness exponent n
	m1	log <sub>10</sub> (K <sub>1</sub> )	N cycles	ΔS <sub>q</sub> (MPa)	m2	log <sub>10</sub> (K <sub>2</sub> )		
BP	5,0	16,9241	1,27 · 10 <sup>6</sup>	145,84	9	25,5796	25	0
B	4,0	14,6081	1,18 · 10 <sup>6</sup>	136,19	7	21,0105		0,1
C	3,5	13,2281	1,11 · 10 <sup>6</sup>	112,80	6	18,3589		0,1
CED	3,5	12,9021	1,11 · 10 <sup>6</sup>	91,03	6	17,8000		0,1

7 Bolted connections

7.1 General

7.1.1 Corrosion

S-N curves for bolted connections are only provided in air. Bolted connections are in principle to be protected against corrosion.

7.2 S-N curves for bolted connections

7.2.1 S-N curves for bolted plates

The bolted plates are to be checked versus fatigue using nominal S-N curves given in Tab 19. The stress range to be applied is defined in Sec 8.

7.2.2 S-N curves for bolts

The bolts loaded in tension and/or in shear are to be checked versus fatigue using the respective nominal S-N curves given in Tab 20.

Table 19 : Design S-N curves for bolted steel plates in air

Bolt / Hole	Joint type	FAT	First slope		Slope intersection		Second slope	
		ΔS (MPa)	m1	log <sub>10</sub> (K <sub>1</sub> )	N cycles	ΔS <sub>q</sub> (MPa)	m2	log <sub>10</sub> (K <sub>2</sub> )
Preloaded	double overlap	112	3	12,449	10 <sup>7</sup>	65,50	5	16,081
	single overlap	90	3	12,164	10 <sup>7</sup>	52,60	5	15,606
Calibrated	double overlap	90	3	12,164	10 <sup>7</sup>	52,60	5	15,606
	simple overlap	80	3	12,010	10 <sup>7</sup>	46,80	5	15,351
Normal	double or simple overlap	50	3	11,398	10 <sup>7</sup>	29,20	5	14,330

Table 20 : Design S-N curves for steel bolts in air submitted to tension and shear load

Load	FAT	First slope		Slope intersection		Second slope		Reference diameter d <sub>ref</sub> (mm)	Diameter Exponent n
	ΔS (MPa)	m1	log <sub>10</sub> (K <sub>1</sub> )	N cycles	ΔS <sub>q</sub> (MPa)	m2	log <sub>10</sub> (K <sub>2</sub> )		
Tension	50,00	3	11,398	10 <sup>7</sup>	29,24	5	14,330	30	0,25
Shear	100,00	5	16,301	—	—	—	—		

## 8 Design S-N curves obtained from fatigue testing

### 8.1 General

#### 8.1.1 Fatigue testing procedure

S-N curves may be determined by prototype or sample testing. The testing and fatigue data analysis procedures are to be in compliance with the recommendations in this Article and are to be submitted to the Society for agreement.

#### 8.1.2 Statistical analysis of test results

The derivation of design S-N curves requires data from fatigue testing and statistical analysis of fatigue data. Guidance for data statistical treatment may be found in the literature such as ISO 12107 'Metallic Materials - Fatigue testing - Statistical planning and analysis of data'.

### 8.2 Fatigue testing procedure

#### 8.2.1 Test specimens

The steel grade used for the test pieces is to be the same as the one provided for the actual structural detail under consideration. The specimen welding procedures are to be representative of the actual conditions of welding for the actual structure. The size of test specimens is to be such that the level of residual stresses is equivalent to the one of the actual structure.

#### 8.2.2 Loading

The fatigue assessment being based on the Miner sum, in spite of the randomness of the marine unit loads, the S-N curve is determined from constant amplitude tests.

The maximum nominal stress is to be lower than  $0,9 R_{eH}$ .

The stress ratio  $R$  is to remain constant during the experiments. When possible, the stress ratio  $R$  should be equal to 0,5. When larger stress ranges are applied,  $R$  may be lower than 0,5 but is always to be greater than 0.

An alternative method consists in testing with a maximum nominal stress equal to  $0,9 R_{eH}$  for all the stress ranges; it is to be performed with the agreement of the Society.

Testing in air may be performed at a higher frequency than the actual loads. However, under free corrosion, the testing frequency is to be of the same order of magnitude as the actual loads.

#### 8.2.3 Stress measurement

The measured stress range is to have the same definition as the stress range used for the design fatigue verification calculations, i.e. hot-spot or nominal stress.

Experimental hot spot stress analysis is usually performed on the basis of strain measurements at the surface of the component. Thus, only information about the stresses on the surface of the component or structure is available. No information of through-thickness stress distribution at the weld toe section is available.

In this context, the measured hot spot stress at the weld toe is determined from the strain distribution on the surface approaching the weld under consideration, usually on the basis of a particular method of strain extrapolation. Detailed prescriptions for the hot spot stress range measurement are given in [8.3] and [8.4].

#### 8.2.4 Failure

Four failure criteria are defined, as follows:

- N1 represents the point at which a crack is first noted by any method, or at which a 15% change in the strain output from a gauge located close to the point of crack initiation is detected
- N1' represents the first visual crack detection
- N2 represents the occurrence of a through-thickness crack
- N3 represents the end of the test due to specimen failure.

Both N1 and N1' criteria are based on the crack initiation concept but the number of cycles may be slightly different.

All fatigue testing specimens are to be tested until failure criteria N3 is reached.

For prototype testing (complex sample), the failure criterion is to be precisely defined.

### 8.3 Structural hot spot stress measurement for plated joints

#### 8.3.1 General

The recommended placement, number of strain gauges and method of stress extrapolation depend on the hot spot type (type 'a' or type 'b') for plated joints, according to the IIW recommendations (IIW-2259-15).

8.3.2 Type 'a' hot spots

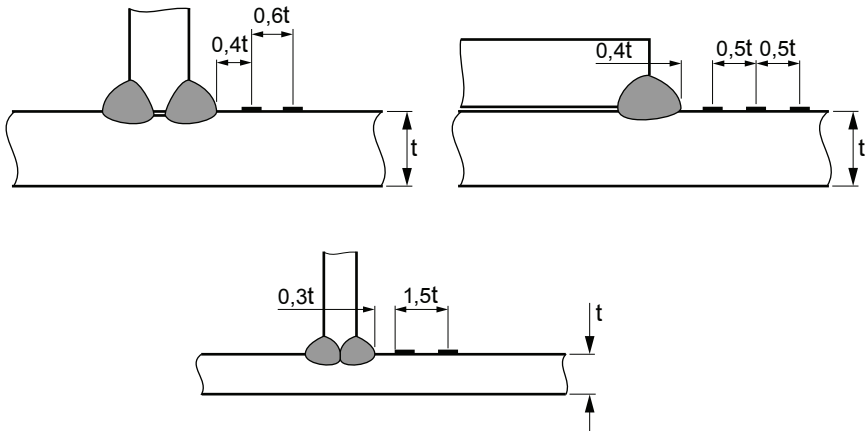
In type 'a' hot spots (see Sec 5, [1.3] and Sec 5, [3.3.2]) the stress distribution close to the weld toe depends on the plate thickness. Thus, the strain measurement points are to be established as a proportion of the plate thickness.

The recommended placement and number of strain gauges (see Fig 6) depend on both, the sharpness of the non-linear stress increase towards the weld toe and the plate thickness.

Extrapolation calculation procedures for hot spot strain determination are proposed in the recommendations (IIW-2259-15) for each strain gauge placement.

Hot spot stress is then obtained from hot spot strain results. If the stress state is close to uniaxial, the hot spot stress is obtained approximately by multiplying the hot spot strain with the Young's modulus. For biaxial stress states, the use of rosette strain gauges is recommended, and the hot spot stress is obtained from the longitudinal and transversal strains, Poisson's ratio and Young's modulus.

Figure 6 : Several strain gauge placements in plated structures for type 'a' hot spot



8.3.3 Type 'b' hot spots

In type 'b' hot spots (see Sec 5, [1.3]), in contrast to those of type 'a', the stress distribution close to the weld toe does not depend on the plate thickness. Thus, extrapolation points cannot be established as a proportion of the plate thickness. This entails the measurement of strains on the plate edge at three absolute distances from the weld toe.

Three strain gauges are to be attached to the plate edge at read-out points located 4, 8 and 12 mm away from the weld toe. The hot spot strain is determined by quadratic extrapolation to the weld toe.

It is to be noted that the procedure (read-out point location, extrapolation method) used for the determination of measured hot spot stress is the same as the one used in case of relatively fine FE models with mesh size less than 0,4 t.

8.4 Measurement of structural hot spot stress for tubular joints

8.4.1 General

The hot spot stress determination is obtained by linear extrapolation of the strain normal to the weld toe, at predefined strain gauges (read-out points) located at the surface of the chord/brace plate. The extrapolation procedure is shown in Fig 7.

8.4.2 Strain gauge locations

The strain gauges are to be located at distances 'a' and 'b' from the weld toe as defined in Fig 8 and Tab 21 (refer to ISO 19902 A.16.10).

Table 21 : Distances for extrapolation to weld toes

Distance from weld toe (mm)	Brace side		Chord side	
	Crown	Saddle	Crown	Saddle
a	Max ( $0,2\sqrt{r \cdot t}$ ; 4)			
b	$0,65\sqrt{r \cdot t}$		$0,4\sqrt[4]{r \cdot t \cdot R \cdot T}$	5° arc length

Figure 7 : Hot spot stress extrapolation

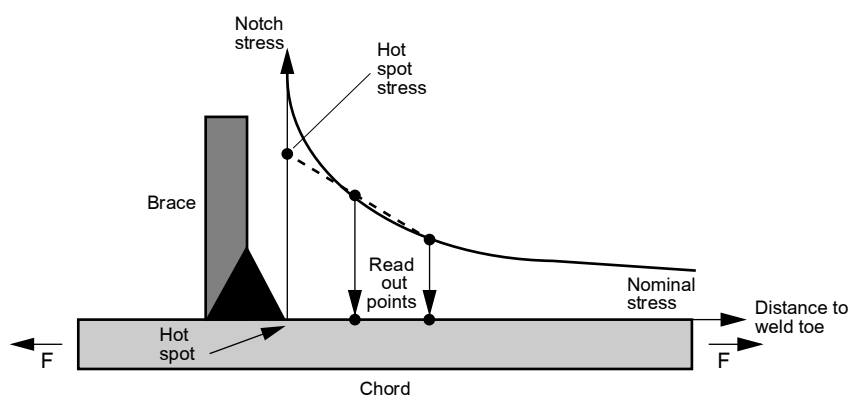
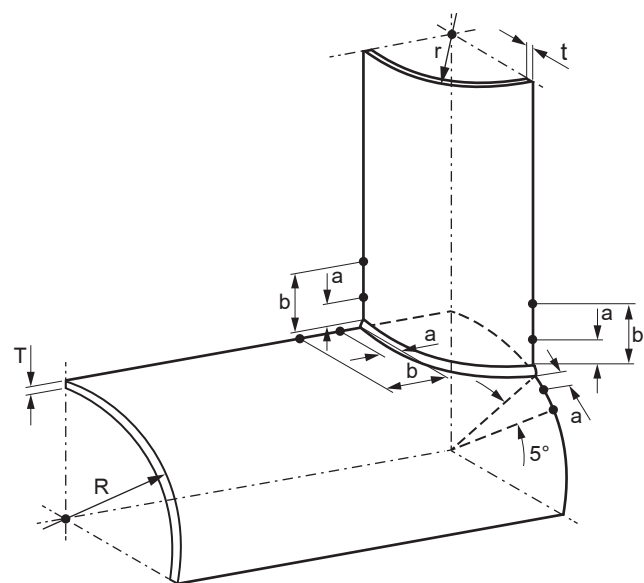


Figure 8 : Strain gauge placements for derivation of hot spot stress in tubular joints



8.5 Data statistical treatment

8.5.1 General

Test results are given as pairs  $(\Delta S_i, N_i)$ , where  $S_i$  is the applied stress range and  $N_i$  the number of cycles to failure. Only failed test specimens shall be considered to derive the S-N curve. The following paragraphs relative to data statistical treatment assume that the inverse slope of the S-N curve  $m$  is fixed.

8.5.2 Number of test samples

Due to the scattering of  $N$  for  $\Delta S$  fixed, either a large number of test samples (greater than 50) is required to determine precisely the S-N curve, or the uncertainty of statistical estimation of the S-N curve is to be taken into account thanks to the tolerance interval.

Where the coefficient  $m$  is known and standard-deviation is known, a priori due to previous tests or theoretical considerations (see IIW-2259-15), S-N curves may be determined accurately with 10 tests only, e.g.:

- 5 tests at the stress level corresponding to about  $N = 10^4$  cycles
- 5 tests at the stress level corresponding to about  $N = 5 \cdot 10^5$  cycles.

8.5.3 Mean S-N curves and standard deviation

On a log-log basis, the mean S-N curve is to be charted as a straight line fitted on the test results:

$$m \log_{10}(\Delta S) + \log_{10}(N) = \log_{10}(K_{50})$$

where:

N : Number of cycle to failure for stress range  $\Delta S$   
 $\Delta S$  : Stress range  
m : Inverse slope of the curve  
 $\log_{10}(K_{50})$ : Mean constant of the S-N curve in  $\log_{10}$ .

The parameters m and  $\log_{10}(K_{50})$  are obtained by statistical regression, using the least square method applied to all cracked specimens. The attention is drawn to the fact that the regression shall consider N as a function of  $\Delta S$ , when the standard representation of the S-N curve is  $\Delta S$  as a function of N.

$\log_{10}(K_{50})$  is the average value of  $\log_{10}(K)$  and  $\text{Stdv}(\log_{10}(K))$  is the standard deviation of  $\log_{10}(K)$ , which is equal to the standard deviation of  $\log_{10}(N)$  when the inverse slope of the S-N curve (m) is fixed.

See [3.7.2] in (IIW-XIII-2460-13) for more information.

8.5.4 Merging different fatigue data sets

If different sets of fatigue test data ( $\Delta S_i$ ,  $N_i$ ) of a same detail but coming from different test programs are available, they might be merged and considered together under certain conditions. It is to be demonstrated that they belong statistically to the same population.

This is to be achieved applying the Kruskal-Wallis H test on the  $N_i \cdot (\Delta S_i)^m$  parameter (which corresponds to the constant K).

8.5.5 Obtaining the design S-N curve

For a required survival probability p, the design S-N curve is defined as follows:

$$\log_{10}(K_0) = \log_{10}(K_{50}) - \lambda_p \text{Stdv}(\log_{10}(K))$$

where:

$\lambda_p$  : Coefficient, function of the survival probability p and the number n of test samples

$\text{Stdv}(\log_{10}(K))$  : Standard deviation of  $\log_{10}(K)$  estimated from test samples values.

Tab 22 provides values of coefficient  $\lambda_p$  (IIW-XIII-173-15, rev1) for a survival probability p equal to 97,7% with a two-sided confidence level on the design S-N curve equal to 75% for different numbers n of test samples. These  $\lambda_p$  values imply that coefficient m is a priori known (i.e. not determined from the test results). If it is not the case, another set of  $\lambda_p$  is to be used.

When a highest safety level is required, greater values of  $\lambda_p$  can be applied when duly justified.

When the number n of samples is not large enough to determine accurately the standard deviation  $\text{Stdv}(\log_{10}(K))$ , i.e.  $n < 10$ , it is recommended to consider  $\text{Stdv}(\log_{10}(K)) = 0,25$ .

Table 22 : Coefficient  $\lambda_p$

Number n of tests	$\lambda_p$
3	5,64
5	3,78
10	2,94
15	2,70
20	2,57
25	2,50
30	2,44
40	2,37
$\geq 60$	2,30

# SECTION 10 FACTORS AFFECTING FATIGUE STRENGTH OF STEEL DETAILS

## 1 General

### 1.1 General

#### 1.1.1 Correction of basic S-N curves

Basic design S-N curves for steel details (see Sec 9) have to be corrected to take into account the effects affecting the fatigue strength. Factors affecting the basic design S-N curves for aluminium plated welded details are given in App 2.

#### 1.1.2 Factors affecting the fatigue strength

The factors affecting the fatigue strength are:

- influence of yield stress for non welded details such as cut edge details, bolts
- influence of thickness
- influence of mean stress and residual stress relaxation
- influence of environment and corrosive protection
- influence of workmanship (misalignment)
- influence of post weld treatment.

#### 1.1.3 Effects taken into account by suitable basic S-N curves

The following effects are taken into account in Sec 9 by means of suitable basic S-N curves:

- influence of environment (in air, in seawater) and corrosive protection
- influence of post weld treatment.

#### 1.1.4 Effects taken into account by means of S-N curve constant modifications

The following effects are taken into account by shifting the S-N curves:

- influence of yield stress for non welded details such as cut edge details, plates
- influence of thickness
- influence of mean stress and residual stress relaxation.

These effects are taken into account by means of a correction factor  $f_{eff}$ , as defined in [1.1.5], affecting the constants ( $K_1$ ,  $K_2$ ) of the basic design S-N curves. The inverse slopes of the corrected S-N curves are the same as those of the basic design S-N curves (shifting of the basic design S-N curves).

The design S-N curve constants  $K_1'$  and  $K_2'$  are taken as:

$$K_1' = \left( \frac{1}{f_{eff}} \right)^{m_1} K_1$$

$$K_2' = \left( \frac{1}{f_{eff}} \right)^{m_2} K_2$$

with:

$m_1$  : Inverse slope of the first segment of the basic design S-N curve, for  $\Delta S \geq \Delta S_q$

$m_2$  : Inverse slope of the second segment of the basic design S-N curve, for  $\Delta S < \Delta S_q$ .

The stress range  $\Delta S_q'$  corresponding to the change of slope of the corrected S-N curves at  $\Delta S = \Delta S_q'$  is given by:

$$\Delta S_q' = \frac{\Delta S_q}{f_{eff}}$$

#### 1.1.5 Combination of effects

The effects of influence of yield stress for non welded details, thickness and mean stress and residual stress relaxation are combined by the multiplication of the correction factors. The combined correction factor  $f_{eff}$  is given by:

$$f_{eff} = f_{YS} f_{thick} f_{mean}$$

where:



- $f_{YS}$  : Correction factor for the yield stress effect, as defined in Article [2]  
 $f_{thick}$  : Correction factor for the effect of plate thickness, as defined in Article [3]  
 $f_{mean}$  : Correction factor for the effect of mean stress and residual stress relaxation, as defined in Article [4].

### 1.1.6 Equivalent stress correction

For practical reasons, instead of shifting the S-N curves the modification of the fatigue strength can be taken into account by defining an equivalent stress range  $\Delta\sigma_{EQ}$  taken equal to:

$$\Delta\sigma_{EQ} = \Delta\sigma_{RF} f_{eff}$$

where:

- $\Delta\sigma_{RF}$  : Reference fatigue stress range, defined in Sec 11, [2.2]  
 $f_{eff}$  : Correction factor, defined in [1.1.5].

## 2 Effect of yield strength

### 2.1 Correction factor

#### 2.1.1 Welded joints

For welded joints, the fatigue strength is independent on the steel yield strength. So, the correction factor for yield stress effect  $f_{YS}$  is taken equal to 1.

#### 2.1.2 Non welded details

For non welded details such as cut plate edges, the fatigue strength increases together with the yield stress of the base material. The correction factor for yield stress effect  $f_{YS}$  is taken as follows:

$$f_{YS} = \frac{1200}{965 + R_{eH}}$$

where  $R_{eH}$  is the specified minimum yield stress, to be taken not less than 235 MPa.

## 3 Thickness effect

### 3.1 General

#### 3.1.1 Principle

The fatigue strength of welded joints, cut edge details and bolted connections depends on the structural element typical size such as plate or tube thickness and bolt diameter. The fatigue strength decreases with the increasing thickness.

The member thickness primarily influences the fatigue strength at the weld toe of welded joints through the weld toe geometry in relation to the member thickness. The thickness effect also depends on the through-thickness stress distribution.

### 3.2 Plated welded joints

#### 3.2.1 Effective plate thickness

The effective plate thickness  $t_{eff}$  to be considered for the thickness effect correction depends on the type of detail.

For longitudinal stiffener connections (see Sec 3), for which the hot spots are located on the longitudinal stiffener flange, the plate thickness  $t_{eff}$  to be considered is the thickness of the flange for angle bars and T-bars. There is no thickness correction for flat bars and bulb profiles.

For 90° plated attachments, i.e. cruciform welded joints, T-joints and plates with attachment submitted to load transverse to the weld, the thickness effect is also dependent on the attachment width  $d$  (see Fig 1). Thus, the thickness  $t_{eff}$  to be used in the thickness correction equation given in [3.2.2] is obtained from the following formula:

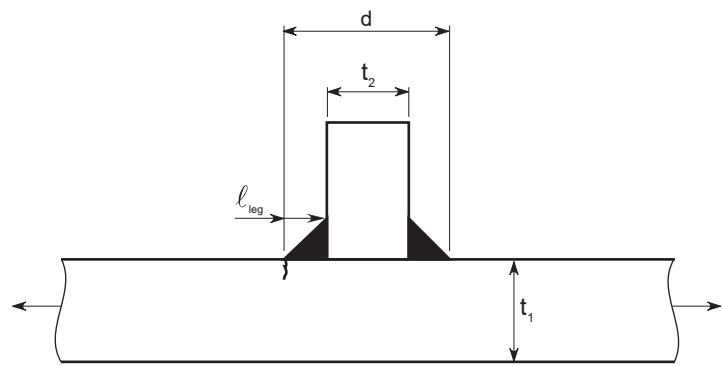
$$t_{eff} = \text{Min} (d/2 ; t_1)$$

where (see Fig 1):

- $t_1$  : Thickness of the continuous plate  
 $d$  : Attachment width, corresponding to the distance between the two weld bead toes:  
 $d = t_2 + 2 \ell_{leg}$   
 $t_2$  : Thickness of the transverse attached plate  
 $\ell_{leg}$  : Fillet weld leg length.

For other details,  $t_{eff}$  is taken as the net thickness of the considered member in way of the hot spot for welded detail or cut edge detail.

Figure 1 : Definition of attachment width d for a plate with transverse attachment submitted to load transverse to the weld



3.2.2 Thickness correction factor for plates and tubular joints

The correction factor for the thickness effect is taken as:

$f_{thick} = \left(\frac{t_{eff}}{t_{ref}}\right)^n$  for  $t_{eff} > t_{ref}$   
 $f_{thick} = 1,0$  for  $t_{eff} \leq t_{ref}$

where:

- t<sub>eff</sub> : Effective thickness as defined in [3.2.1]
- t<sub>ref</sub> : Reference thickness of the considered fatigue detail according to Tab 1
- n : Thickness exponent on fatigue strength according to Tab 1.

Table 1 : Reference thickness and thickness exponent for thickness correction

Type of detail	Reference thickness t <sub>ref</sub>	Thickness exponent n
Plated welded joints without post weld improvement	see Sec 9, [4.1]	see Tab 2
Welded tubular joints, tubular butt-welded joints and tubular cast joints	see Sec 9, [4.2]	
Post weld improved plated joints	see Sec 9, [5.2]	
Cut edge details	see Sec 9, [6.2]	

3.3 Bolted connections

3.3.1 Size correction for bolted plates and bolts

S-N curves for bolted plates and S-N curves for bolts are to be modified to take into account the influence of size effect (plate thickness for bolted plate, and bolt diameter for bolt).

3.3.2 Bolted plate

For the thickness effect correction, bolted plates are assimilated to cut plate edges. The thickness effect for bolted plates is described in [3.2.2].

3.3.3 Diameter correction factor for bolts

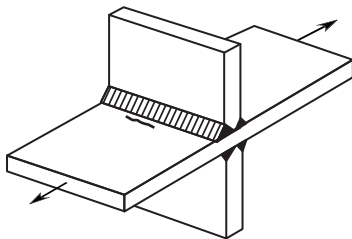
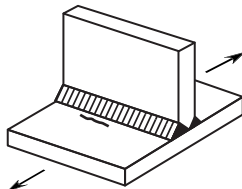
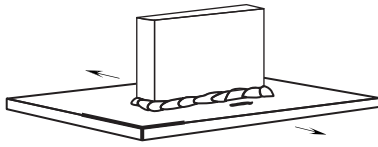

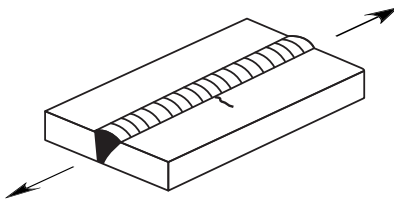
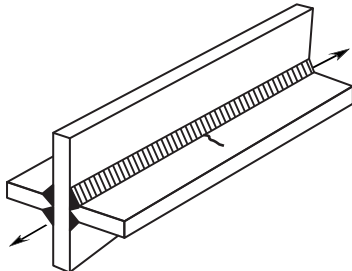
The correction factor for the bolt size effect is taken as:

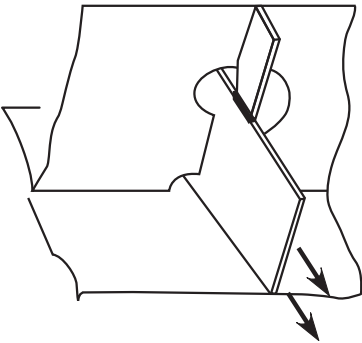
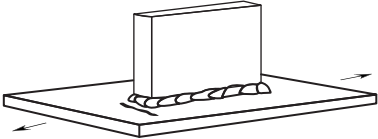
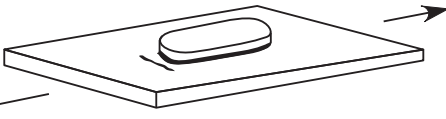
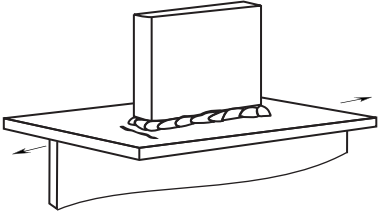
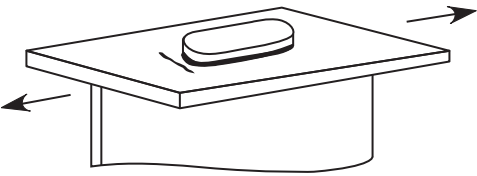
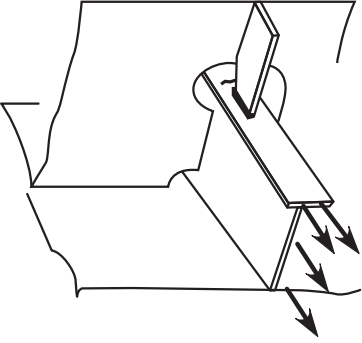
$f_{thick} = \left(\frac{d}{d_{ref}}\right)^n$  for  $d > d_{ref}$   
 $f_{thick} = 1,0$  for  $d \leq d_{ref}$

where:

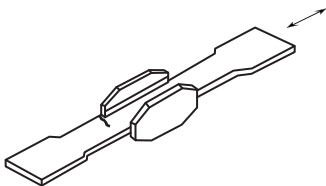
- d : Diameter of the bolt as defined in ISO 898
- d<sub>ref</sub> : Reference diameter of the bolt (see Sec 9, [7.2])
- n : Diameter exponent on fatigue strength (see Sec 9, [7.2]).

Table 2 : Thickness exponent n for welded plated joints

No.	Joint category description	Load direction	Geometry	Condition	n
1	Cruciform joint, T-joint, plate with attachment	Loading transverse to the weld	<p>Cruciform joint</p>  <p>T-joint</p>  <p>Plate with attachment</p> 	as-welded	0,25
				weld toe treated by PWT (1)	0,20
2	Butt weld	Loading transverse to the weld		as-welded	0,20
				Ground flush or weld toe treated by PWT (1)	0,10
3	Longitudinal welds: <ul style="list-style-type: none"><li>• butt weld</li><li>• cruciform joint</li></ul>	Loading parallel to the weld	<p>Butt weld</p>  <p>Cruciform joint</p> 	as-welded	0,10
				weld toe treated by PWT (1)	0,10
(1) PWT : Post weld toe improvement method.					

No.	Joint category description	Load direction	Geometry	Condition	n
4	Flat bar stiffener welded on flat bar or bulb profile longitudinal stiffener	Loading transverse to the weld around flat bar stiffener end		as-welded	0
				weld toe treated by PWT (1)	0
5	Attachment not supported longitudinally	Loading transverse to the weld around the attachment end	<p>Gusset</p>  <p>Doubling plate</p> 	as-welded	0,20
				weld toe treated by PWT (1)	0,10
6	Attachment supported longitudinally	Loading transverse to the weld around the attachment end	<p>Gusset above a longitudinal supporting member</p>  <p>Doubling plate above a longitudinal supporting member</p>  <p>Flat bar stiffener above a longitudinal stiffener</p> 	as-welded	0,10
				weld toe treated by PWT (1)	0

(1) PWT : Post weld toe improvement method.

No.	Joint category description	Load direction	Geometry	Condition	n
7	Attachment to plate edges	Loading transverse to the weld around the attachment end		as-welded	0,10
				weld toe treated by PWT (1)	0,10
(1) PWT : Post weld toe improvement method.					

4 Mean stress and residual stress relaxation

4.1 As-welded joints

4.1.1 General

For as-welded joints, in case of constant amplitude loading, the fatigue strength is considered to be independent of the loading mean stress. Due to the existence of high weld residual stress at weld toe, which is almost equal to the yield stress of the material, the maximum stress including the residual stress and the fluctuating stresses induced by external load can exceed the yield stress. The actual stress will hence fluctuate downward from the yield stress due to residual stress relaxation, irrespective of the applied stress ratio. This is the reason why the mean stress effect of welded joints submitted to constant amplitude loading may be neglected.

4.1.2 Ship and offshore structures

In ship and offshore structures where the stress range fluctuations are random and the mean stress varies due to several loading conditions during service life, the fatigue strength of the welded joints is considered to be dependent on the loading mean stress. In fact, due to fluctuations of wave stress ranges and static loading associated to the different loading conditions, the material yield stress can be exceeded.

This results in some relaxation of the residual stress. Therefore the damage due to the following cycles will be lower.

4.1.3 Tubular welded joints and tubular butt-welded joints

For tubular welded joints and tubular butt-welded joints, mean stresses and residual stress relaxation are not taken into account for the welded connections fatigue assessment. It is assumed that the residual stresses (already integrated in the S-N curves) impose high tensile stresses close to the material yield stress in the vicinity of the welded joint.

4.1.4 Rule-based correction for plated joints

The following formulae for mean stress correction are applicable for plated joints when the rule-based approach is used (see Sec 11, [2]). This correction assumes that shakedown of the mean stress occurs when the total stress including an initial welding residual stress exceeds the yield stress of the material  $R_{eEq}$ . Unless otherwise specified in the applicable rules, the initial welding residual stress  $\sigma_{res0}$  is to be taken equal to  $0.1R_{eEq}$  for a welded detail on sea-going steel ships.

The corrected mean stress  $\sigma_{mCor,i(j)}$ , for load case (i) of loading condition (j), is given by:

- for  $\sigma_{max} + \sigma_{res0} > R_{eEq}$  :  
 $\sigma_{mCor,i(j)} = \sigma_{meanHS,i(j)} + R_{eEq} - \sigma_{max}$
- for  $\sigma_{max} + \sigma_{res0} \leq R_{eEq}$  :  
 $\sigma_{mCor,i(j)} = \sigma_{meanHS,i(j)} + \sigma_{res0}$

where:

$R_{eEq}$  : Material shakedown yield stress equal to:

$$R_{eEq} = \text{Max} (315 ; R_{eH})$$

$\sigma_{max}$  : Maximum hot spot stress, associated with a probability level of exceedance of  $10^{-4}$ , equal to:

$$\sigma_{max} = \text{Max}_j \left[ \text{Max}_i \left( \frac{\gamma}{2} \Delta \sigma_{HS,i(j)} + \sigma_{meanHS,i(j)} \right) \right]$$

$\gamma$  : Coefficient to be taken equal to:

$$\gamma = \frac{\log(10^{-4})}{\log(p_R)}$$

$\Delta\sigma_{HS,i(j)}$  : Principal hot spot stress range, taken at the probability level of exceedance of  $p_R$  (see Sec 2, [1.3.1]), calculated according to:

- Sec 5, [7] for FE analysis, and
- Sec 3, [4.1.2] for analytical stress analysis of longitudinal stiffeners connections

$\sigma_{meanHS,i(j)}$  : Mean hot spot stress range, calculated according to:

- Sec 5, [7] for FE analysis, and
- Sec 3, [4.1.3] for analytical stress analysis of longitudinal stiffeners connections.

The mean stress correction factor  $f_{meanHS,i(j)}$  to be considered for each principal hot spot stress range of welded joint  $\Delta\sigma_{HS,i(j)}$  relative to load case (i) of loading condition (j) is then obtained as follows:

$$f_{meanHS,i(j)} = 0,7 + 0,3 \tanh\left(\kappa \cdot \frac{2}{\gamma} \cdot \frac{\sigma_{mCor,i(j)}}{\Delta\sigma_{HS,i(j)}}\right)$$

where:

$\kappa$  : Mean stress scale factor defined in Tab 3, accounting for the different S-N curve slope parameters used for plated joints.

Table 3 : Mean stress scale factor for plated joints and cut edges

Slope parameter m	Mean stress scale factor $\kappa$
3	3,125
3,5	2,750
4	2,475
5	2,050

4.1.5 Mean stress correction for plated joints for direct calculation

The following formulae for mean stress correction are applicable for plated joints when direct calculation is performed (see Sec 11, [3] Sec 11, [4]). This correction assumes that shakedown of the mean stress occurs when the total stress including an initial welding residual stress exceeds the yield stress of the material  $R_{eEq}$ . Unless otherwise specified in the applicable rules, the initial welding residual stress  $\sigma_{res0}$  is to be taken equal to  $0.1R_{eEq}$  for a welded detail on sea-going steel ships.

The corrected mean stress  $\sigma_{mCor,j}$ , for loading condition (j), is given by:

- for  $\sigma_{max} + \sigma_{res0} > R_{eEq}$  :  
$$\sigma_{mCor,j} = \sigma_{meanHS,j} + R_{eEq} - \sigma_{max}$$
- for  $\sigma_{max} + \sigma_{res0} \leq R_{eEq}$  :  
$$\sigma_{mCor,j} = \sigma_{meanHS,j} + \sigma_{res0}$$

where:

$R_{eEq}$  : Material shakedown yield stress as defined in [4.1.4]

$\sigma_{max}$  : Maximum hot spot stress, associated with a probability level of exceedance of  $10^{-4}$ , equal to:

$$\sigma_{max} = \max_j (\sigma_{meanHS,j} + \sigma_{waveHS,j})$$

$\sigma_{meanHS,j}$  : Hot spot mean stress for the loading condition (j). In case of spectral analysis, the hot spot mean stress is the still water hot spot stress, since the wave induced stress average value is equal to zero. In case of time-domain analysis, the hot spot mean stress is the mean value of the total hot spot stress (still water plus wave).

$\sigma_{waveHS,j}$  : Hot spot stress amplitude due to wave for the loading condition (j), associated with a probability level of exceedance of  $p_R = 10^{-4}$ .

The mean stress correction factor  $f_{meanHS,j}$  to be applied on each hot spot stress range value  $\Delta\sigma_{HS}$  of the long term stress distribution relative to a loading condition (j) is obtained as follows:

$$f_{meanHS,j} = 0,7 + 0,6 \frac{\sigma_{mCor,j}}{\Delta\sigma_{HS}}$$

with:

$$0,4 \leq f_{meanHS,j} \leq 1,0$$

## 4.2 Post weld treated joints

### 4.2.1 Plated joints

For post weld treated plated joints such as joints treated by grinding or TIG dressing, the load mean stress effect is considered as being the same as for as-welded plated joints, in a conservative way. Grinding and TIG dressing reduce the amount of maximum tensile welding residual stress. The formulae given in [4.1.4] are to be applied.

### 4.2.2 Tubular joints

For post weld treated tubular joints, mean stresses and residual stress relaxation are not taken into account as for the as-welded tubular joints fatigue assessment (see [4.1.3])

## 4.3 Cut edges

### 4.3.1 General

For base material cut edges, no initial residual stress is taken into account. In case of constant amplitude loading or random loading, the fatigue strength may be considered to be dependent on the loading mean stress.

Shakedown of the mean stress occurs when the maximum stress exceeds the yield stress of the material  $R_{eEq}$ , inducing new residual stress.

### 4.3.2 Rule based correction for cut edges

The following formulae for mean stress correction are applicable for cut edges when the rule based approach is used (see Sec 11, [2]). This correction assumes that shakedown of the mean stress occurs when the maximum stress exceeds the yield stress of the material  $R_{eEq}$ . This approach is similar to the one given in [4.1.4] for the welded joint, except that no initial welding residual stress is assumed for base material cut edges.

The corrected mean stress  $\sigma_{mCor,i(j)}$ , for load case (i) of loading condition (j), is given by:

- for  $\sigma_{max} > R_{eEq}$ :  

$$\sigma_{mCor,i(j)} = \sigma_{meanCE,i(j)} + R_{eEq} - \sigma_{max}$$
- for  $\sigma_{max} \leq R_{eEq}$ :  

$$\sigma_{mCor,i(j)} = \sigma_{meanCE,i(j)}$$

where:

$R_{eEq}$  : Material shakedown yield stress as defined in [4.1.4]

$\sigma_{max}$  : Maximum cut plate edge stress, associated to a probability level of exceedance of  $10^{-4}$ , equal to:

$$\sigma_{max} = \text{Max}_j \left[ \text{Max}_i \left( \frac{\gamma}{2} \Delta \sigma_{CE,i(j)} + \sigma_{meanCE,i(j)} \right) \right]$$

$\gamma$  : Coefficient to be taken equal to:

$$\gamma = \frac{\log(10^{-4})}{\log(p_R)}$$

$\Delta \sigma_{CE,i(j)}$  : Cut plate edge stress range, taken at the exceedance probability level of  $p_R$  (see Sec 2, [1.3.1]), calculated according to Sec 5, [7.5]

$\sigma_{meanCE,i(j)}$  : Mean cut edge stress, calculated according to Sec 5, [7.5].

The mean stress correction factor  $f_{meanCE,i(j)}$  to be considered for the cut plate edge stress range  $\Delta \sigma_{CE,i(j)}$  relative to load case (i) of loading condition (j) is then obtained as follows:

$$f_{meanCE,i(j)} = 0,7 + 0,3 \tanh \left( \kappa \cdot \frac{2}{\gamma} \cdot \frac{\sigma_{mCor,i(j)}}{\Delta \sigma_{CE,i(j)}} \right)$$

where:

$\kappa$  : Mean stress scale factor defined in Tab 3, accounting for the different S-N curve slope parameters used for cut edges.

### 4.3.3 Mean stress correction for cut edges for direct calculation

The following formulae for mean stress correction are applicable for cut edges when direct calculation is performed (see Sec 11, [3] Sec 11, [4]). This correction assumes that shakedown of the mean stress occurs when the maximum stress exceeds the yield stress of the material  $R_{eEq}$ . This approach is similar to the one given in [4.1.5] for the welded joint, except that no initial welding residual stress is assumed for base material cut edges.

The corrected mean stress  $\sigma_{mCor,j}$ , for loading condition (j), is given by:

- for  $\sigma_{\max} > R_{\text{eEq}}$  :  
$$\sigma_{\text{mCor},j} = \sigma_{\text{meanCE},j} + R_{\text{eEq}} - \sigma_{\max}$$
- for  $\sigma_{\max} \leq R_{\text{eEq}}$  :  
$$\sigma_{\text{mCor},j} = \sigma_{\text{meanCE},j}$$

where:

- $R_{\text{eEq}}$  : Material shakedown yield stress as defined in [4.1.4]  
 $\sigma_{\max}$  : Maximum cut edge stress, associated with a probability level of exceedance of  $10^{-4}$ , equal to:

$$\sigma_{\max} = \text{Max}_j (\sigma_{\text{meanCE},j} + \sigma_{\text{waveCE},j})$$

- $\sigma_{\text{meanCE},j}$  : Cut edge mean stress for the loading condition (j). In case of spectral analysis, the cut edge mean stress is the still water cut edge stress, since the wave induced stress average value is equal to zero. In case of time-domain analysis, the cut edge mean stress is the mean value of the total cut edge stress (still water plus wave).  
 $\sigma_{\text{waveCE},j}$  : Cut edge stress amplitude due to wave for the loading condition (j), associated with a probability level of exceedance of  $p_R = 10^{-4}$ .

The mean stress correction factor  $f_{\text{meanCE},j}$  to be applied on each cut plate edge stress range value  $\Delta\sigma_{\text{CE}}$  of the long term stress distribution relative to a loading condition (j) is obtained as follows:

$$f_{\text{meanCE},j} = 0,7 + 0,6 \frac{\sigma_{\text{mCor},j}}{\Delta\sigma_{\text{CE}}}$$

with:

$$0,4 \leq f_{\text{meanCE},j} \leq 1,0$$

4.4 Preloaded bolts

4.4.1 For preloaded bolts, the stress range to be associated to the S-N curves given in Sec 9, [7.2] is determined as prescribed in Sec 8, [2.2]. This stress range takes into account the mean stress effect, including the bolt preload.

5 Stress concentration factors due to misalignment

5.1 General

5.1.1 Misalignment origin and effects

Misalignment in axially loaded joints leads to an increase of stress in the welded joint due to the introduction of an additional local bending stress.

The misalignment between the plate mid-surfaces results from the thickness difference between members (eccentricity  $\delta_t$ , see Fig 2) and from fabrication misalignment (eccentricity  $\delta_m$ , see Fig 3).

Angular misalignment between flat plates is considered in [5.3].

Figure 2 : Butt weld with thickness transition

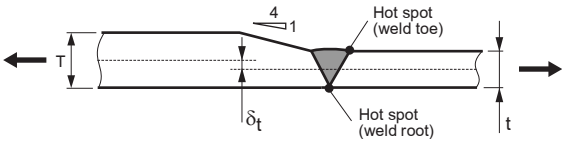
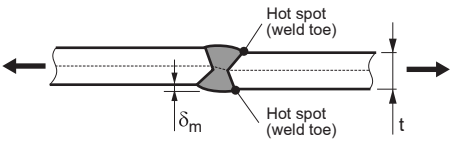


Figure 3 : Butt weld without thickness transition with fabrication misalignment





5.1.2 Stress concentration factors

The different stress concentration factors  $K_m$  due to misalignments are defined in [5.2] to [5.5] for plated joints and for tubular butt-welded joints.

As the actual fabrication misalignment direction versus the misalignment direction induced by the thickness difference between members is not known at the design stage, the calculation of  $K_m$  in this Article is based on the most severe combination between the fabrication misalignment and the misalignment due to the thickness difference.

The considered stress concentration factors  $K_m$  are due to the misalignment exceeding the eccentricity  $\delta_0$  or the angular misalignment  $\alpha_0$  already included in the S-N curves (see the formulae in [5.2] to [5.5]).

5.2 Plate butt weld - Axial misalignment

5.2.1 General

The stress concentration factor depends on the weld configuration, i.e.:

- the joint type: double-sided or single-sided
- for single-sided joints, the side of the misalignment with regard to the welded side.

5.2.2 Fabrication misalignment

The eccentricity  $\delta_m$  due to fabrication corresponds generally to the standard values given in the IACS Recommendation No.47 when workmanship complies with the normal shipbuilding practice (see [7.2]). It may correspond to the actual values specified by the designer.

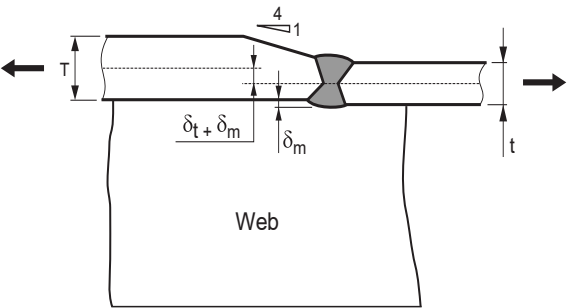
5.2.3 Plates supported by a web

When the butt weld is supported by a web perpendicular to the butt weld (see Fig 4), the effect of the misalignment is reduced in way of the web.

The stress concentration factor  $K_m$  is taken equal to 1,00 when the distance between the hot spot to be checked and the web is less than 2 T.

When this distance is greater,  $K_m$  is taken from the corresponding case where the plates are not supported by a web.

Figure 4 : Example of butt welds supported by a web



t : Thickness of the thinner plate

T : Thickness of the thicker plate.

5.2.4 Single-sided welds with thickness transition on the root side

Two hot spots are considered for this type of butt joint. The stress concentration factor  $K_m$  at each hot spot is given in Tab 4.

5.2.5 Single-sided welds with thickness transition on the toe side

Two hot spots are considered for this type of butt joint. The stress concentration factor  $K_m$  at each hot spot is given in Tab 5.

Table 4 : Stress concentration factor  $K_m$  for single-sided butt joint with thickness transition on the root side

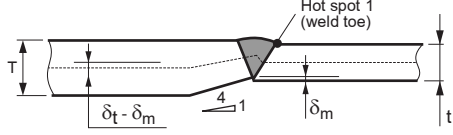
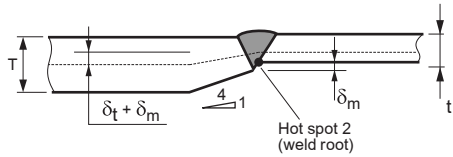
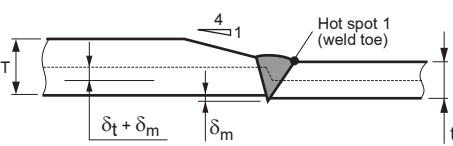
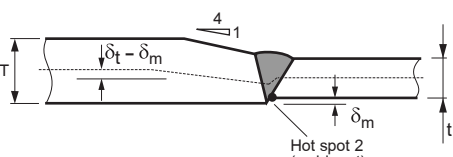
Hot spot 1: weld toe	Hot spot 2: weld root
$K_m = \text{Max} \left[ 1 - \frac{6(\delta_t - \delta_m)}{t} \cdot \frac{t^{1,5}}{t^{1,5} + T^{1,5}} ; 1,0 \right]$	$K_m = 1 + \frac{6(\delta_t + \delta_m - \delta_0)}{t} \cdot \frac{t^{1,5}}{t^{1,5} + T^{1,5}}$
	
<p><math>\delta_t</math> : Eccentricity due to thickness difference, equal to: <math>\delta_t = (T - t) / 2</math> <math>\delta_m</math> : Maximum eccentricity due to fabrication, specified by the designer. By default, <math>\delta_m = 0,15 t</math> <math>\delta_0</math> : Eccentricity included in the S-N curve for butt weld, equal to: <math>\delta_0 = 0,10 t</math> <math>t</math> : Thickness of the thinner plate <math>T</math> : Thickness of the thicker plate.</p>	

Table 5 : Stress concentration factor  $K_m$  for single-sided butt joint with thickness transition on the toe side

Hot spot 1: weld toe	Hot spot 2: weld root
$K_m = 1 + \frac{6(\delta_t + \delta_m - \delta_0)}{t} \cdot \frac{t^{1,5}}{t^{1,5} + T^{1,5}}$	$K_m = \text{Max} \left[ 1 - \frac{6(\delta_t - \delta_m)}{t} \cdot \frac{t^{1,5}}{t^{1,5} + T^{1,5}} ; 1,0 \right]$
	
For the definition of $\delta_t$ , $\delta_m$ , $\delta_0$ , $t$ and $T$ , see Tab 4.	

5.2.6 Double-sided welds with thickness transition

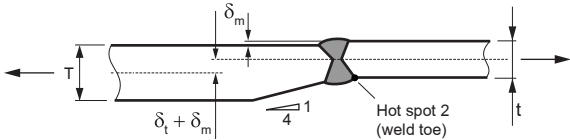
One hot spot is considered for this type of butt joint, located at the weld toe (see Fig 5).

The stress concentration factor  $K_m$  is equal to:

$$K_m = 1 + \frac{6(\delta_t + \delta_m - \delta_0)}{t} \cdot \frac{t^{1,5}}{t^{1,5} + T^{1,5}}$$

where the definitions of  $\delta_t$ ,  $\delta_m$ ,  $\delta_0$ ,  $t$  and  $T$  are given in Tab 4.

Figure 5 : Double-sided plated butt weld with thickness transition



5.2.7 Single-sided butt welds between plates with equal thickness

Two hot spots are considered for this type of butt joint (see Fig 6). The stress concentration factor  $K_m$  at each hot spot is given in Tab 6.

Figure 6 : Single-sided butt weld between plates with equal thickness

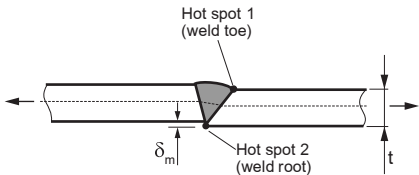


Table 6 : Stress concentration factor  $K_m$  for single-sided butt weld between plates of equal thickness

Hot spot 1: weld toe	Hot spot 2: weld root
$K_m = 1 + \frac{3(\delta_m - \delta_0)}{t}$	$K_m = 1,0$
For the definition of $\delta_m$ and $\delta_0$ , see Tab 4. t : Thickness of the two plates.	

5.2.8 Double-sided butt welds between plates with equal thickness

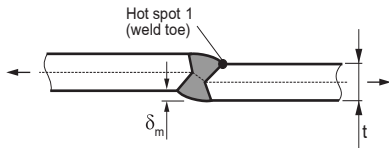
One hot spot is considered for this type of butt joint, located at the weld toe (see Fig 7).

The stress concentration factor  $K_m$  is equal to:

$$K_m = 1 + \frac{3(\delta_m - \delta_0)}{t}$$

where the definitions of  $\delta_m$ ,  $\delta_0$  and t are given in Tab 6.

Figure 7 : Double-sided butt weld between plates with equal thickness



5.3 Plate butt weld - Angular misalignment

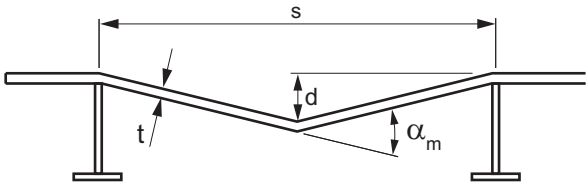
5.3.1 The stress concentration factor  $K_m$  due to angular misalignment between flat plates (see Fig 8) is given by:

$$K_m = 1 + \frac{\beta}{4} \cdot \frac{(\alpha_m - \alpha_0) \cdot s}{t}$$

where:

- $\beta$  : • for fixed ends:  $\beta = 3$   
• for pinned ends:  $\beta = 6$
- $\alpha_m$  : Maximum angular misalignment between flat plates, in rad, as specified by the designer.  
By default:  $\alpha_m = 4 d / s$  where d is the standard distortion from a flat plate defined in IACS Recommendation No.47.
- $\alpha_0$  : Angular misalignment between flat plates included in the S-N curve, equal to:  $\alpha_0 = 0,02$  rad
- s : Plate width between stiffeners
- t : Thickness of the plate.

Figure 8 : Angular misalignment between flat plates



5.4 Plate cruciform joint misalignment

5.4.1 Joints supported by a web

When the cruciform joint is supported by a web, the effect of the misalignment is reduced in way of the web.

The stress concentration factor  $K_m$  is taken equal to 1,00 when the distance between the hot spot to be checked and the web is less than 2 T.

When the distance is greater,  $K_m$  is taken as per [5.4.2].

5.4.2 Stress concentration factor

The stress concentration factor  $K_m$  due to eccentricity (e.g. fabrication misalignment) between plates is given by:

$$K_m = 1 + \frac{6t^2(\delta - \delta_0)}{\ell \cdot \left( \frac{t^3}{\ell} + \frac{T^3}{L} + \frac{t_1^3}{\ell_1} + \frac{t_2^3}{\ell_2} \right)}$$

where:

T, t, t<sub>1</sub>, t<sub>2</sub>: Plate thicknesses as shown on Fig 9, with t ≤ T

L, ℓ, ℓ<sub>1</sub>, ℓ<sub>2</sub>: Plate lengths as shown on Fig 9

δ : Total eccentricity between the plate mid-planes, as shown on Fig 10, equal to: δ = δ<sub>m</sub> + δ<sub>t</sub>

δ<sub>m</sub> : Maximum eccentricity due to fabrication, specified by the designer. By default, δ<sub>m</sub> = 0,3 t

δ<sub>t</sub> : Eccentricity due to thickness difference, equal to: δ<sub>t</sub> = (T – t) / 2

δ<sub>0</sub> : Eccentricity included in the S-N curve for cruciform joint, equal to: δ<sub>0</sub> = 0,15 t.

Figure 9 : Cruciform joint, plates dimensions

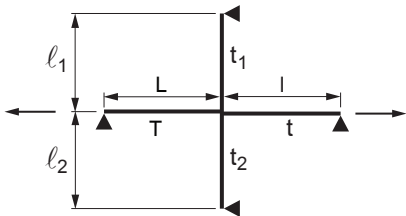
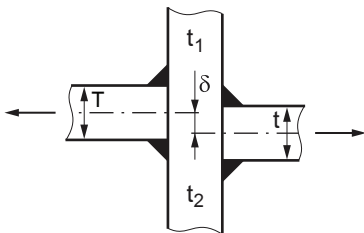


Figure 10 : Cruciform joint, eccentricity



5.5 Stress concentration factors due to eccentricities for tubular butt-welded joints

5.5.1 General

The applicable formulae of stress concentration factor K<sub>m</sub> due to misalignment are given for each hot spot of several tubular butt weld configurations: single-sided or double-sided butt welds, with the thickness transition between members located on the inside or on the outside, and for members with equal thickness.

Thickness transition with a slope exceeding 1/4 are not recommended and may be considered on a case-by-case basis.

5.5.2 Single-sided butt welds with thickness transition on the inside

Two hot spots are considered for this type of butt joint. The stress concentration factor K<sub>m</sub> at each hot spot is given in Tab 7.

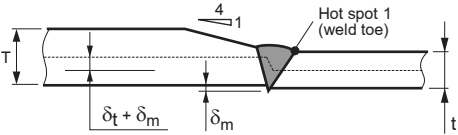
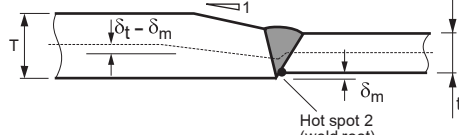
Table 7 : Stress concentration factor K<sub>m</sub> for single-sided butt weld with thickness transition on the inside

Hot spot 1: weld toe	Hot spot 2: weld root
$K_m = \text{Max} \left[ 1 - \frac{6(\delta_t - \delta_m)}{t} \cdot \frac{t^{1,5}}{t^{1,5} + T^{1,5}} ; 1,0 \right]$	$K_m = 1 + \frac{6(\delta_t + \delta_m - \delta_0)}{t} \cdot \frac{t^{1,5}}{t^{1,5} + T^{1,5}}$
<p>δ<sub>t</sub> : Eccentricity due to thickness difference, equal to: δ<sub>t</sub> = (T – t) / 2</p> <p>δ<sub>m</sub> : Maximum eccentricity due to fabrication, specified by the designer</p> <p>δ<sub>0</sub> : Eccentricity included in the S-N curve for butt weld, equal to: δ<sub>0</sub> = 0,10 t</p> <p>t : Thickness of the thinner member</p> <p>T : Thickness of the thicker member.</p>	

5.5.3 Single-sided butt welds with thickness transition on the outside

Two hot spots are considered for this type of butt joint. The stress concentration factor  $K_m$  at each hot spot is given in Tab 8.

Table 8 : Stress concentration factor  $K_m$  for single-sided butt weld with thickness transition on the outside

Hot spot 1: weld toe	Hot spot 2: weld root
$K_m = 1 + \frac{6(\delta_t + \delta_m - \delta_0)}{t} \cdot \frac{t^{1,5}}{t^{1,5} + T^{1,5}}$	$K_m = \text{Max} \left[ 1 - \frac{6(\delta_t - \delta_m)}{t} \cdot \frac{t^{1,5}}{t^{1,5} + T^{1,5}} ; 1,0 \right]$
	
For the definition of $\delta_t$ , $\delta_m$ , $\delta_0$ , $t$ and $T$ , see Tab 7.	

5.5.4 Double-sided butt welds with thickness transition

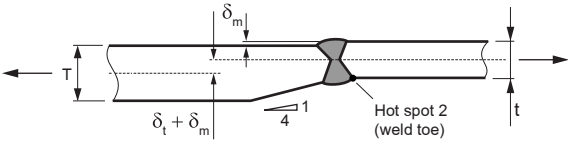
One hot spot is considered at the thickness transition for this type of butt joint (thickness transition at the inside or at the outside), located at the weld toe (see Fig 11).

The stress concentration factor  $K_m$  is equal to:

$$K_m = 1 + \frac{6(\delta_t + \delta_m - \delta_0)}{t} \cdot \frac{t^{1,5}}{t^{1,5} + T^{1,5}}$$

where the definitions of  $\delta_t$ ,  $\delta_m$ ,  $\delta_0$ ,  $t$  and  $T$  are given in Tab 7.

Figure 11 : Double-sided butt weld with thickness transition



5.5.5 Single-sided butt welds on members with equal thickness

Two hot spots are considered for this type of butt joint (see Fig 12). The stress concentration factor  $K_m$  at each hot spot is given in Tab 9.

Figure 12 : Single-sided butt weld on members with equal thickness

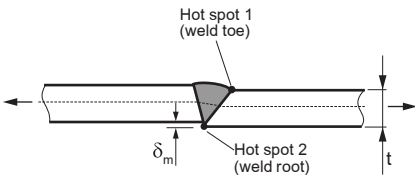


Table 9 : Stress concentration factor  $K_m$  for single-sided butt weld on members with equal thickness

Hot spot 1: weld toe	Hot spot 2: weld root
$K_m = 1 + \frac{3(\delta_m - \delta_0)}{t}$	$K_m = 1,0$
For the definition of $\delta_m$ and $\delta_0$ , see Tab 7. $t$ : Thickness of the two plates.	

5.5.6 Double-sided butt welds on members with equal thickness

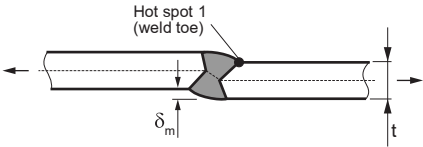
One hot spot is considered for this type of butt joint, located at the weld toe (see Fig 13).

The stress concentration factor  $K_m$  is equal to:

$$K_m = 1 + \frac{3(\delta_m - \delta_0)}{t}$$

where the definitions of  $\delta_m$ ,  $\delta_0$  and  $t$  are given in Tab 9.

Figure 13 : Double-sided butt weld on members with equal thickness



6 Corrosive environment

6.1 General

6.1.1 Influence of corrosion on fatigue strength

It is observed that the fatigue damage of steel parts is substantially increased by exposure to corrosive environment including sea water.

6.1.2 Protection against corrosion

Several corrosion protection methods may be used.

For sea-going ships and floating offshore units built with steel material, protective coating is considered as the single effective corrosion protection method in this Guidance Note.

For fixed offshore structures, such as jacket structures, made of a frame of welded tubular steel members, cathodic protection method is also applicable and is the most appropriate method of corrosion protection for underwater tubular joints.

The effects of corrosive environment and protection against corrosion is taken into account by means of the design S-N curves defined in Sec 9.

7 Workmanship

7.1 General

7.1.1 The fatigue life of welded joints depends on the workmanship quality in terms of building alignment and weld profile associated to the welding procedures.

Normal shipbuilding practices are in principle to comply with standard values of workmanship defined in IACS Recommendation No.47.

7.2 Building misalignment

7.2.1 The effect of misalignment on fatigue life is treated in [5].

The misalignment values to be considered for the fatigue design assessment correspond generally to the standard values given in the IACS Recommendation No.47 when the expected workmanship corresponds to the normal shipbuilding practice. The default values given in Tab 4 to Tab 9 correspond to those IACS standard values. They should be used in the absence of misalignment values specified by the designer.

7.3 Welding procedures

7.3.1 The welding procedures are to be in accordance with the applicable rules.

For multi-pass welds, the sequence can improve the fatigue strength. This improvement may be taken into account when duly justified and agreed by the Society.

7.4 Post weld treatments for welded joints

7.4.1 General

The post weld improvement methods covered in this Guidance Note are applied to the weld toe of welded joints. They may increase the fatigue strength, generally as a result of an improvement in the weld profile and in the residual stress conditions. They may be used to increase the fatigue strength of new structures, notably if a weld detail is found to be critical at fabrication stage, or in case of in-service repairs of an existing structure.

The benefit from post weld treatment can only be applied to welded joints in air, or in seawater environment provided that a corrosion protection measure is applied after the post weld treatment and maintained during the design life time. Applicable corrosion protection methods are given in [6.1.2].

The S-N curves for post weld treated plated joints are given in Sec 9, [5.2]. The fatigue life improvement for post weld treated tubular joints is given in Sec 9, [5.3].

The list and location on the unit of the details for which the post weld treatment has been applied are to be submitted to the Society for review.

#### **7.4.2 Weld types to be considered for post weld treatments**

Post weld treatment of the weld toe is intended generally for fully penetrated double-sided welds where fatigue failure is prone to start at the weld toe.

The fatigue resistance of fully penetrated double-sided welds can be improved by post welding treatment of the weld toe.

However, the possibility of a failure starting at other locations after post weld treatment is to be considered: for example, the weld toe at the transition between the grinded weld zone and the as-welded zone.

In addition, post weld treatment of the weld toe may be proposed for partially penetrated double-sided welds.

In the case of partially penetrated welds where fatigue failure is prone to start at both the weld toe and the weld root, the failure origin may be shifted from the weld toe to the weld root after post weld treatment. Consequently, there could be no significant improvement in the overall fatigue performance of the joint. In this case, root cracking assessment according to Sec 7 is to be carried out in addition to toe cracking assessment.

Any other procedure used to check fatigue root cracking is to be duly justified and reviewed to the satisfaction of the Society.

#### **7.4.3 Selected post weld treatment techniques**

Two post weld treatment methods are considered in this Guidance Note to improve fatigue strength at the weld toe. Both belong to the same group: the weld geometry improvement method, which allows to reduce the severity of the weld toe stress concentration.

They are:

- Grinding technique:

The aim of the grinding is to reduce the local stress concentration effect of the weld profile by increasing and smoothing the weld toe radius and, at the same time, by decreasing the weld surface angle versus plate surface. Grinding technique allows also to remove weld toe flaws from which fatigue cracks may propagate. Grinding is generally to be burr grinding. However other techniques may be considered by the Society on a case-by-case basis.

- TIG or plasma dressing:

The aim of the TIG or plasma dressing is to remove the weld toe flaws by re-melting the material at the weld toe. It aims also to reduce the local stress concentration effect of the local weld toe profile by providing a smooth transition between the plate and the weld face.

Other post weld improvement techniques are to be regarded as exceptional measures. The selected method and procedure are to be duly justified and reviewed to the satisfaction of the Society.

#### **7.4.4 Circumstances of use of post weld treatment techniques**

Post weld improvement treatment is normally not accepted at the design stage. Grinding of welds is to be regarded as an exceptional measure considered on the case-by-case basis by the Society and only when the design fatigue life cannot be achieved by alternative design measures such as improvement of cut-out shapes, softening of bracket toes, local increase in thickness or other changes in the structural detail geometry.

During the fabrication stage, post welding improvement treatments may be allowed by the Society in case of damaged weld or weld defect repairs.

In case of in-service repairs, post welding improvement treatments are recommended.

The selected method and the relevant procedure for grinding and TIG/plasma dressing are to be submitted and reviewed to the satisfaction of the Society.

7.4.5 Post weld treatment procedure

The post weld treatment procedure is to be submitted to the Society for review.

As an example, the grinding procedure is to specify the:

- weld preparation
- grinding tool used
- position of the tool over the weld toe
- location of the weld toe on which grinding is applied
- extent of grinding at the ends of attachments
- final weld profile
- final examination technique, including NDE.

7.4.6 Weld toe grinding application

- a) The weld may be machined using a burr grinding tool to produce a favourable shape to reduce stress concentrations and remove defects at the weld toe, see Fig 14. In order to eliminate the defects such as intrusions, undercuts and cold laps, the material in way of the weld toe is to be removed. The depth of grinding shall be at least 0.5 mm below the bottom of any visible undercut. The total depth of the burr grinding is to be not greater than the lesser of 2 mm and 7% of the local gross thickness of the machined plate  $t_{as\_built}$ . Any undercut not complying with this requirement is to be repaired by an approved method.
- b) To avoid introducing a detrimental notch effect due to small radius grooves, the burr diameter is to be scaled to the plate thickness at the weld toe being ground. The diameter is to be in the 10-25 mm range for application to welded joints with plate thickness from 10 to 50 mm. The resulting root radius of the groove is to be not less than  $0,25t_{as\_built}$ . The weld throat thickness and the leg length after burr grinding are to comply with the rule requirements or any increased weld sizes as indicated on the approved drawings.
- The inspection procedure is to include a check of the weld toe radius, the depth of burr grinding, and confirmation that the weld toe undercut was removed completely.
- c) The weld improvement is effective in improving the fatigue strength of structural details under high-cycle fatigue conditions. Therefore the fatigue improvement factors do not apply to low-cycle fatigue conditions, i.e. when  $N \leq 50\,000$ , where N is the number of life cycles to failure.
- d) Treatment of inter-bead toes is required for large multi-pass welds as shown in Fig 15.

Figure 14 : Details of ground weld toe geometry

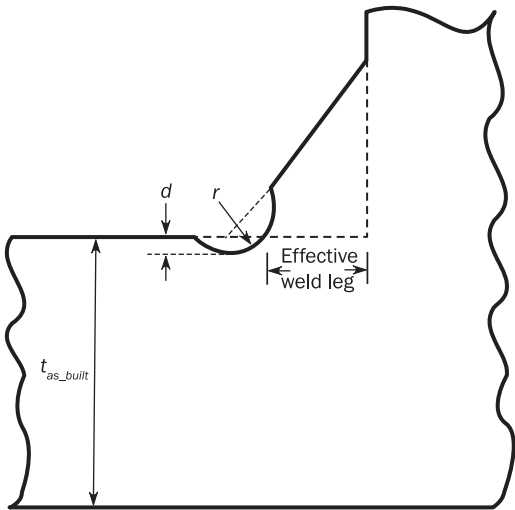
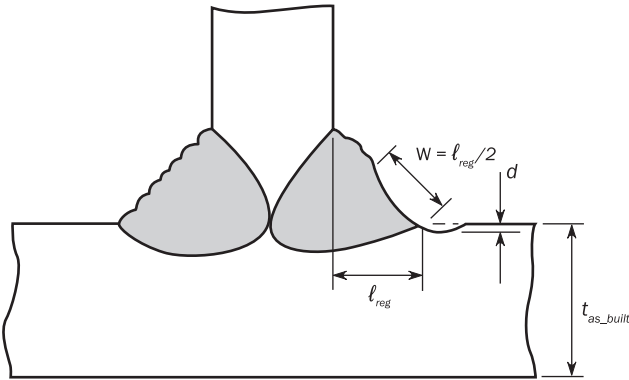




Figure 15 : Extent of weld toe burr grinding to remove inter-bead toes on weld face



# SECTION 11

## FATIGUE DAMAGE CALCULATION AND ACCEPTANCE CRITERIA

### Symbols

- $T_{DF}$  : Design fatigue life, in years, defined in the applicable Rules  
 $T_F$  : Calculated fatigue life, in years  
 $f_{c\_FEA}$  : Correction factor for the effect of corrosion, to be applied on the stress evaluated using FEM analysis.  $f_{c\_FEA}$  value is given in the applicable Rules in case the single structural model approach described in Sec 1, [3.3.3] has been selected. Otherwise  $f_{c\_FEA} = 1$   
 $\beta$  : Wave heading, relative to the ship or offshore unit axes, in degrees.  $\beta = 180^\circ$  for head seas  
 $\omega$  : Wave angular frequency (rad/s)  
 $\Delta S_q$  : Stress range, in N/mm<sup>2</sup>, at the change of slope of the S-N curve, as defined in Sec 9, [1.3]  
 $m_1, m_2$  : Characteristic inverse slope of the first and second segments of the S-N curve, as defined in Sec 9, [1.3]  
 $K_1, K_2$  : Characteristic constants of the S-N curve, as defined in Sec 9, [1.3]  
 $\gamma(1+X;S)$  : Lower incomplete gamma function, defined by:  

$$\gamma(1+X;S) = \int_0^S t^X e^{-t} dt$$
  
 $\Gamma(1+X;S)$  : Upper incomplete gamma function, defined by:  

$$\Gamma(1+X;S) = \int_S^\infty t^X e^{-t} dt$$
  
 $\Gamma(X)$  : Complete gamma function, defined by:  

$$\Gamma(1+X) = \int_0^\infty t^X e^{-t} dt$$

## 1 General

### 1.1 Principles

#### 1.1.1 Fatigue strength based on S-N curves

Fatigue damage is based on the application of linear cumulative damage (Miner's rule) resulting from the combination of stress response with the appropriate S-N curve associated to the kind of stress used.

#### 1.1.2 Methodologies for loads estimation

Several methodologies for fatigue assessment exist: simplified rule based approach, spectral analysis, time-domain approach.

#### 1.1.3 Fatigue assessment procedure

The assessment of the fatigue damage of structural members includes the following steps:

- determination of the long-term stress range cumulative distribution or histogram
- selection of the S-N curve which allows to determine the number of stress cycles to failure for each stress level
- determination of the fatigue damage from the stress distribution and the characteristics of the S-N curve by summing the partial damages due to each stress level, and
- verification that the cumulated fatigue damage and the corresponding fatigue life are consistent with the acceptance criteria.

### 1.2 Design fatigue life patterns

#### 1.2.1 Definition

For a given fatigue detail, the two models of design fatigue life patterns described in [1.2.2] and [1.2.3] are defined, corresponding to several combinations of corrosion exposure periods.

#### 1.2.2 Single period pattern

The design fatigue life is represented by a single period of exposure to corrosion. In this case, the fatigue damage rate is calculated for one environmental condition according to [1.3.2] and the total fatigue damage according to [1.3.3].

### 1.2.3 Two periods pattern

The design fatigue life is represented by one period of protection (by coating or by cathodic protection for example) and one period of no protection against corrosion.

In-air design S-N curves are to be used for details protected by coating. Design S-N curves in seawater under cathodic protection are to be used for details protected by cathodic system. The combined damage per year associated to the period of protection against corrosion is calculated according to [1.3.2].

For the second period, corresponding to corrosive environment, design S-N curves in seawater under free corrosion are to be used. The combined damage per year associated to the free corrosion period is calculated according to [1.3.2].

The total fatigue damage is then obtained according to [1.3.4].

## 1.3 Fatigue damage

### 1.3.1 General

The total fatigue damage on the entire design fatigue life is obtained by combination of the fatigue damage determined for each period constituting the design fatigue life pattern.

### 1.3.2 Combined fatigue damage per year

For a given period of the design fatigue life pattern, the combined fatigue damage per year  $D_{\text{Year}}$  is obtained by combining the damage per year of due to wave considering the different loading conditions, and the damage per year due to the loading and unloading loads when it is relevant:

$$D_{\text{Year}} = \sum_{j=1}^{n_{\text{Lcond}}} \alpha_j \cdot f_0 \cdot D_{\text{Wave},j} + D_{\text{L/U}}$$

where:

$n_{\text{Lcond}}$  : Number of applicable loading conditions in the considered period

$\alpha_j$  : Fraction of time spent in loading condition j, in the considered period, with

$$\sum_{j=1}^{n_{\text{Lcond}}} \alpha_j = 1$$

$f_0$  : Sailing factor, i.e. the fraction of time in sea-going operations, equal to 0,85 for sea going ships and 1,0 for fixed and floating offshore units, unless otherwise specified in the applicable rules

$D_{\text{Wave},j}$  : Wave induced fatigue damage per year for loading condition j, for the considered period

$D_{\text{L/U}}$  : Damage per year for the damage induced by loading and unloading cycles, for the considered period.

The damage rates  $D_{\text{Wave}(j)}$  and  $D_{\text{L/U}}$  are computed using one of the possible approaches: simplified rule based approach (see Article [2]), spectral analysis approach (see Article [3]) or time-domain approach (see Article [4]).

### 1.3.3 Single period design fatigue life pattern

If the design fatigue life corresponds to a single period of exposure to a given corrosion condition, the total fatigue damage  $D_{\text{Total}}$  is written as follows:

$$D_{\text{Total}} = D_{\text{Year}} \cdot T_{\text{DF}}$$

where:

$D_{\text{Year}}$  : Combined fatigue damage per year in the considered corrosion condition, obtained according to [1.3.2].

### 1.3.4 Two period design fatigue life pattern

The total fatigue damage  $D_{\text{Total}}$  associated to the two periods design fatigue life pattern defined in [1.2.3] is to be calculated as follows:

$$D_{\text{Total}} = D_{\text{Prot}} \cdot T_{\text{Prot}} + D_{\text{Corr}} \cdot (T_{\text{DF}} - T_{\text{Prot}})$$

where:

$D_{\text{Prot}}$  : Combined fatigue damage per year in protected condition, obtained according to [1.3.2]

$D_{\text{Corr}}$  : Combined fatigue damage per year in free corrosion condition, obtained according to [1.3.2]

$T_{\text{Prot}}$  : Duration of the initial period during which the protection against corrosion is effective, in years.

## 1.4 Fatigue life

### 1.4.1 Single period pattern

If a single period is considered, then the calculated fatigue life  $T_F$ , in years, is obtained from the total fatigue damage, as follows:

$$T_F = \frac{1}{D_{\text{Period}}}$$

where:

$D_{\text{Period}}$  : Combined fatigue per year for the considered period.

### 1.4.2 Two period pattern

If a two period design fatigue life pattern is considered, the fatigue life is obtained as follows:

- if  $\frac{1}{D_{\text{Prot}}} \leq T_{\text{Prot}}$  :

$$T_F = \frac{1}{D_{\text{Prot}}}$$

- otherwise:

$$T_F = T_{\text{Prot}} + \frac{1 - D_{\text{Prot}} \cdot T_{\text{Prot}}}{D_{\text{Corr}}}$$

where:

$D_{\text{Prot}}$  : Combined fatigue per year for the initial period with protection against corrosion

$D_{\text{Corr}}$  : Combined fatigue per year for the second period with free corrosion.

## 1.5 Acceptance criteria

### 1.5.1 Damage criteria

The fatigue failure is assumed to occur when the fatigue damage  $D_{\text{Total}}$  as defined in [1.3.3] and [1.3.4] is greater than the acceptable value given by the applicable Rules.

When no value is provided, the fatigue failure is assumed to occur when the fatigue damage  $D_{\text{Total}}$  as defined in [1.3.3] and [1.3.4] is greater than 1,0. Other fatigue damage criteria may be considered if duly justified and agreed by the Society.

### 1.5.2 Fatigue life criteria

The calculated fatigue life  $T_F$  as defined in [1.4.1] or in [1.4.2] is to be equal to or larger than the fatigue life required by the applicable Rules.

## 2 Simplified rule based approach

### 2.1 General

#### 2.1.1 Applicability

Simplified rule based approach is applied for ship hull and offshore unit hull structures for which rule loads are defined.

#### 2.1.2 Loads

In this approach, depending on structural detail and type of unit, the loads which are considered are:

- wave loads, and
- loads due to the loading/unloading process.

#### 2.1.3 Environmental corrosive exposure condition

The environmental corrosive exposure conditions (no exposure to corrosion, protection against corrosion i.e. coating or cathodic protection or exposure to corrosive environment), as well as the fraction of time over the life of the structure, are to be defined.

#### 2.1.4 Load cases

Rule load cases for fatigue assessment are defined by pairs. The two associated load cases in each pair define the two extremes leading to a rule stress range. In this Guidance Note, extremum 1 and extremum 2 related to the pair "i" of load cases are denoted with "i1" and "i2" subscripts.

#### 2.1.5 Fatigue damage

For rule calculation of fatigue damage, the reference fatigue stress range due to wave for each load case is given in [2.2] and wave induced fatigue damage is determined in [2.4].

### 2.1.6 Loading and unloading

For structural details of offshore unit exposed to loading/unloading process, [2.4.6] is intended to the determination of fatigue due to waves and loading/unloading sequences.

Real loading conditions representative of an entire loading and unloading sequence should be used in order to determine a realistic damage. If the loading/unloading sequence is not available, the damage due to loading/unloading cycles is obtained from the maximum still water stress range among combinations of rule loading conditions.

### 2.1.7 Angular sectors for hot spots type 'a'

For hot spots type 'a' as defined in Sec 5, [1.3.1], fatigue damage is to be calculated within each angular sector at the weld toe (see Sec 9, [2.1.1]), each one is associated to a specific S-N curve ( $P_{\perp}$  and  $P_{\parallel}$  S-N curve).

The fatigue damage is to be computed separately in each angular sector using [1.3]. The final total damage for the detail is the maximum damage between the two sectors.

## 2.2 Reference fatigue stress range for wave loads

### 2.2.1 General

The reference fatigue stress range at probability level ( $p_R$ ) for each load case (i) of each loading condition (j) is defined in [2.2.2] to [2.2.8] for several types of structural details: welded joints, cut edge details, bolted plates and bolts.

The reference fatigue stress range corresponds to the principal stress range used for the elementary wave induced fatigue damage calculation according to [2.4.3].

### 2.2.2 Welded joints: longitudinal stiffeners ends

The reference fatigue stress range for longitudinal stiffeners connections with transverse primary supporting members calculated by analytical method as described in Sec 3 is:

$$\Delta\sigma_{RF,i(j)} = \Delta\sigma_{HS,i(j)}$$

where:

$\Delta\sigma_{HS,i(j)}$  : Hot-spot stress range in load case (i) of loading condition (j), calculated according to Sec 3, [4.1].

### 2.2.3 Ordinary welded joints, web stiffened cruciform joints and bent hopper knuckles

For ordinary welded joints of type 'a' and type 'b' as defined in Sec 5, [1.3.1], and for web-stiffened cruciform joints, the reference fatigue stress range is calculated as follows from the principal hot spot stress range:

$$\Delta\sigma_{RF,i(j)} = f_{c-FEA} \cdot \Delta\sigma_{HS,i(j)}$$

where:

$\Delta\sigma_{HS,i(j)}$  : Hot-spot stress range in load case (i) of loading condition (j), calculated according to Sec 5, [7.3] for ordinary welded joints, and according to Sec 5, [7.4] for web stiffened cruciform joints and bent hopper knuckle details.

### 2.2.4 Welded joints, root cracking

For welded joints root cracking (see Sec 7), the reference fatigue stress range  $\Delta\sigma_{RF,i(j)}$  is taken as:

$$\Delta\sigma_{RF,i(j)} = f_{c-FEA} \cdot |\sigma_{WR,i1(j)} - \sigma_{WR,i2(j)}|$$

where:

$\sigma_{WR,i1(j)}$ ,  $\sigma_{WR,i2(j)}$  : Weld root structural stresses in load cases i1 and i2 of loading condition (j), calculated according to Sec 7, [2.2.3].

### 2.2.5 Cut edge details

The reference fatigue stress range at cut edge is taken as:

$$\Delta\sigma_{RF,i(j)} = f_{c-FEA} \cdot \Delta\sigma_{CE,i(j)}$$

where:

$\Delta\sigma_{CE,i(j)}$  : Local nominal stress range in load case (i) of loading condition (j) calculated according to Sec 5, [7.5].

### 2.2.6 Bolted plate

The reference fatigue stress range for a bolted plate is taken as:

$$\Delta\sigma_{RF,i(j)} = f_{c-FEA} \cdot |\sigma_{nom,i1(j)} - \sigma_{nom,i2(j)}|$$

where:

$\sigma_{nom,i1(j)}$ ,  $\sigma_{nom,i2(j)}$  : Nominal stresses in the bolted plate in load cases i1 and i2 of loading condition (j), calculated according to Sec 8, [2.1].

### 2.2.7 Bolts

The reference fatigue stress range for bolts is taken as:

$$\Delta\sigma_{RF, i(j)} = |\sigma_{Bolts, i1(j)} - \sigma_{Bolts, i2(j)}|$$

where:

$\sigma_{Bolts, i1(j)}$ ,  $\sigma_{Bolts, i2(j)}$  : Local nominal stresses in load cases i1 and i2 of loading condition (j), calculated according to Sec 8, [2.1].

### 2.2.8 Butt welded joints

The reference fatigue stress range for a butt welded joint is taken as:

$$\Delta\sigma_{RF, i(j)} = f_{c\_FEA} \cdot K_m \cdot |\sigma_{nom, i1(j)} - \sigma_{nom, i2(j)}|$$

where:

$\sigma_{nom, i1(j)}$ ,  $\sigma_{nom, i2(j)}$  : Nominal stresses in load cases i1 and i2 of loading condition (j)

$K_m$  : Stress concentration factor due to misalignment, as defined in:

- Sec 10, [5] for steel welded details
- App 2, [6] for aluminium plated welded details.

## 2.3 Design S-N curve

### 2.3.1 Principle

The fatigue assessment is based on a design S-N curve. This S-N curve is primarily defined by the basic S-N curve associated with the fatigue detail in consideration.

The basic S-N curves are given in:

- Sec 9 for steel details
- App 2, [2] to App 2, [4] for aluminium plated welded details.

The basic design S-N curves have to be corrected to take into account the factors affecting the fatigue strength given in:

- Sec 10 for steel details
- App 2, [5] for aluminium plated welded details.

They are:

- influence of the yield strength (applicable only for non-welded details such as cut edge details, plates, bolts)
- influence of thickness, and
- influence of mean stress and residual stress relaxation.

The procedure to apply these corrections are given in [2.3.2] to [2.3.4] according to the type of detail. These corrections are applied using the equivalent stress range approach described in:

- App 2, [5.1.5] for steel details
- App 2, [5.1.5] for aluminium plated welded details.

### 2.3.2 Welded joints

For welded joints, the following effects are to be considered:

- influence of thickness
- influence of mean stress and residual stress relaxation.

Those effects are taken into account by means of the equivalent hot spot stress range defined as follows:

$$\Delta\sigma_{EQ, i(j)} = f_{eff, i(j)} \cdot \Delta\sigma_{RF, i(j)}$$

where:

$\Delta\sigma_{RF, i(j)}$  : Reference stress range due to dynamic loads in load case (i) of loading condition (j) obtained in [2.2]

$f_{eff, i(j)}$  : Correction factor for effects affecting the fatigue strength, for load case (i) of loading condition (j)

$$f_{eff, i(j)} = f_{thick} \cdot f_{meanHS, i(j)}$$

where:

$f_{thick}$  : Correction factor for plate thickness effect, as defined in:

- Sec 10, [3] for steel details
- App 2, [5.2] for aluminium plated welded details.

$f_{meanHS, i(j)}$  : Correction factor for mean stress and residual stress relaxation effect applied to the hot spot fatigue stress range, as defined in:

- Sec 10, [4] for steel details
- App 2, [5.3] for aluminium plated welded details.

### 2.3.3 Cut edge details, bolted plates

For cut edge details and bolted plates, the following effects are to be considered:

- thickness effect
- mean stress effect
- yield stress effect.

Those effects are taken into account by means of the equivalent hot spot stress range defined as follows:

$$\Delta\sigma_{EQ, i(j)} = f_{eff, i(j)} \cdot \Delta\sigma_{RF, i(j)}$$

where:

$\Delta\sigma_{RF, i(j)}$  : Reference stress range due to dynamic loads in load case (i) of loading condition (j) obtained in [2.2.5] for cut edges and [2.2.6] for bolted plates

$f_{eff, i(j)}$  : Correction factor for effects affecting the fatigue strength, for load case (i) of loading condition (j):

$$f_{eff, i(j)} = f_{thick} \cdot f_{YS} \cdot f_{meanCE, i(j)}$$

with:

$f_{thick}$  : Correction factor for plate thickness effect (see Sec 10, [3])

$f_{YS}$  : Correction factor for yield stress effect (see Sec 10, [2])

$f_{meanCE, i(j)}$  : Correction factor for mean stress (see Sec 10, [4]) applied to the cut edge stress range.

### 2.3.4 Bolts

For bolts, the following effects are to be considered:

- thickness effect
- yield stress effect.

Those effects are taken into account by means of the equivalent hot spot stress range defined as follows:

$$\Delta\sigma_{EQ, i(j)} = f_{eff} \cdot \Delta\sigma_{RF, i(j)}$$

where:

$\Delta\sigma_{RF, i(j)}$  : Reference stress range in load case (i) of loading condition (j) obtained in [2.2.7]

$f_{eff}$  : Correction factor for effects affecting the fatigue strength, for load case (i) of loading condition (j):

$$f_{eff} = f_{thick} \cdot f_{YS}$$

where:

$f_{thick}$  : Correction factor for the bolt diameter (see Sec 10, [3.3])

$f_{YS}$  : Correction factor for yield stress effect (see Sec 10, [2]).

## 2.4 Fatigue damage calculation

### 2.4.1 General

The wave induced fatigue damage for the rule based approach is computed using the prescriptions in [2.4.2].

The fatigue damage due to waves and loading and unloading sequences is computed using the prescriptions in [2.4.6].

### 2.4.2 Wave induced fatigue damage

The wave induced fatigue damage per year  $D_{Wave, j}$  for a given loading condition j, in a specific corrosive environment condition, is obtained by computing the elementary wave induced fatigue damage per year for all the load cases prescribed by the applicable rules, and taking the maximum:

$$D_{Wave, j} = \max_i (D_{Wave, i(j)})$$

where:

$D_{Wave, i(j)}$  : Elementary wave induced fatigue damage rate for the load case i and the loading condition j, as defined in [2.4.3].

### 2.4.3 Elementary wave induced fatigue damage

The elementary wave induced fatigue damage per year at sea, for each load case (i) of loading condition (j) and a specific corrosive environmental condition is to be calculated as follows, assuming a Weibull distribution of stress ranges:

$$D_{Wave, i(j)} = \frac{N}{K_1} \cdot \frac{\Delta\sigma_{EQ, i(j)}^{m_1}}{(-\ln(p_R))^{m_1/\xi}} \cdot \mu_{i(j)} \cdot \Gamma\left(1 + \frac{m_1}{\xi}\right)$$

where:

- N : Total number of wave cycles experienced by the ship during one year
- $\Delta\sigma_{EQ, i(j)}$  : Equivalent fatigue stress range (in N/mm<sup>2</sup>) for load case (i) of loading condition (j) at the reference probability level of exceedance  $p_R$  (see [2.3.2] [2.3.3], [2.3.4])
- $p_R$  : Reference probability level of exceedance associated to the reference fatigue stress range (see Sec 2, [1.3.1])
- $\xi$  : Weibull shape parameter,  $\xi = 1$
- $\mu_{i(j)}$  : Coefficient taking into account the change of inverse slope of the S-N curve, determined as per [2.4.4] or [2.4.5].

The number N of stress cycles per year is defined in the applicable Rules, otherwise N is given by:

$$N = (365 \cdot 24 \cdot 3600)/T_s$$

where:

- $T_s$  : Rule stress average period, in seconds:  $T_s = 4 \log(L)$

with:

- L : Ship or offshore unit rule length, in m.

Another value can be considered if duly justified and agreed by the Society.

### 2.4.4 Effect of inverse slope change, free corrosion environment

For unprotected condition i.e. in seawater environment under free corrosion, no change of slopes considered in the S-N curves.

The coefficient to be used in [2.4.3] is:

$$\mu_{i(j)} = 1,0$$

### 2.4.5 Effect of inverse slope change, other corrosion environments

For protected condition, i.e. in air environment or in seawater environment under adequate protection:

$$\mu_{i(j)} = 1 - \frac{\left\{ \gamma\left(1 + \frac{m_1}{\xi}, v_{i(j)}\right) - v_{i(j)}^{(m_1 - m_2)/\xi} \cdot \gamma\left(1 + \frac{m_2}{\xi}, v_{i(j)}\right) \right\}}{\Gamma\left(1 + \frac{m_1}{\xi}\right)}$$

where:

$$v_{i(j)} = -\left(\frac{\Delta S_q}{\Delta\sigma_{EQ, i(j)}}\right)^\xi \cdot \ln(p_R)$$

- $p_R$  : Reference probability level of exceedance associated to the reference fatigue stress range (see Sec 2, [1.3.1])
- $\xi$  : Weibull shape parameter,  $\xi = 1$
- $\Delta\sigma_{EQ, i(j)}$  : Equivalent fatigue stress range, in N/mm<sup>2</sup>, for load case (i) of loading condition (j) at the reference probability level of exceedance  $p_R$ .

### 2.4.6 Fatigue damage due to waves and loading/unloading sequences

The alternate loading and unloading of the unit may induce low frequency stress cycles that will be superimposed on the wave induced cycles and induce additional fatigue damage if they are numerous and large enough (e.g. FPSO, dredger).

If the actual loading/unloading sequence is not known, the fatigue damage per year  $D_{L/U}$  due to loading/unloading cycles is given by the following formula:

$$D_{L/U} = n_{L/U} \frac{(\Delta\sigma_{L/U})^{m_1}}{K_1}$$

where:

- $n_{L/U}$  : Number of loading/unloading cycles per year, taking the fraction of time in sea-going operations (sailing factor) into account.



$\Delta\sigma_{L/U}$  : Loading/unloading stress cycle range defined between the highest stress and the lowest stress corresponding to the combined still water and wave induced stress, among all load cases and all loading conditions, and taken equal to:

$$\Delta\sigma_{L/U} = \Delta\sigma_{SW} + \Delta\sigma_W$$

with:

$\Delta\sigma_{SW}$  : Maximum still water stress range among combinations of rule loading conditions

$\Delta\sigma_W$  : Wave induced stress contribution to the loading/unloading stress range.

By default, unless otherwise specified in the applicable rules, a probability level of  $10^{-4}$  for the wave contribution to the loading/unloading stress may be considered. It corresponds to a duration of loading/unloading cycle of about one day.

3 Spectral analysis

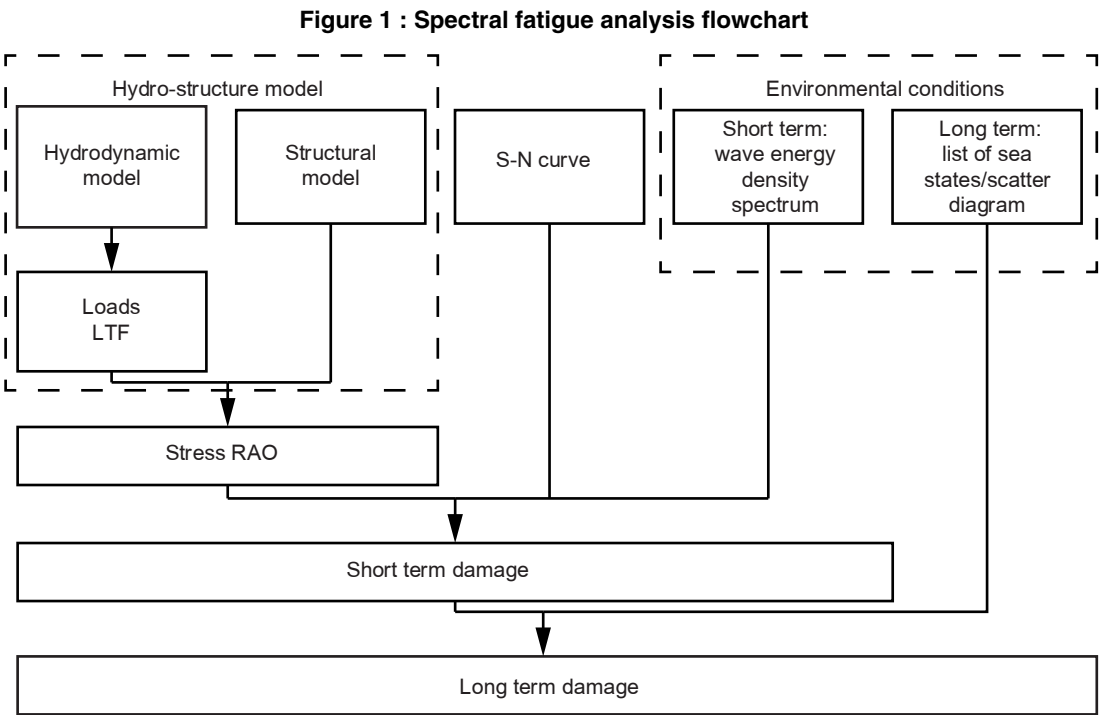
3.1 General

3.1.1 Definitions

FEM : Finite Element Method. In the context of this document, FEM refers to the numerical method for discretizing the structure and determining its response to loads

LTF : Linear Transfer Function, characterizing the response of a linear system in the frequency domain, both in terms of amplitude ratio and phase difference between the input and the output. In the context of this Guidance Note, the input is the wave elevation at a reference point

RAO : Response Amplitude Operator, the norm of the complete LTF.



3.1.2 Analysis principles

The aim of the spectral analysis is the determination of the long-term fatigue damage in the frequency domain that takes into account the different environmental conditions encountered by the structure.

The core of the analysis is the determination of a Response Amplitude Operator (RAO) between the waves and the stress, for each operating condition (loading condition, speed, wave heading). This RAO is obtained by the combination of a linear frequency domain hydrodynamic model with a linear structural model. Although different hydro-structure coupling schemes can be used, the most current one consists in transferring the wave loads from the hydrodynamic model on a three dimensional finite elements model for each wave heading and frequency.

Thanks to the stress RAO, a stress response spectrum is then determined for each wave energy density spectrum, providing short-term wave statistics and, considering the fatigue capacity given by the S-N curve, a short-term damage.

Finally the long-term fatigue damage is the summation of short-term damages taking the probability of occurrence of the sea states into account.

When the linearization of either the hydrodynamic loading or the structural response is not possible, then a time-domain approach as described in Article [4] is to be used instead of the spectral approach.

**3.1.3 Operational conditions**

The loading conditions to be considered for the spectral analysis, and the associated forward speed when relevant, are provided in Sec 2, [1.4].

A separate analysis is to be performed for each operational condition, with its own hydrodynamic and hydro-structure models. Therefore, the quantities defined in this Article are implicitly associated to a given operational condition j.

**3.1.4 Short-term wave conditions**

The short-term wave conditions are defined by means of sea energy density spectra. The wave elevation is supposed to be a stationary process over a short period (typically three hours). This process is described by a power spectral density function. Wave spectra are often given in the form of an analytical formula. Common wave spectrum formulae are given in App 1, [2.2].

**3.1.5 Long-term wave conditions**

The long-term wave conditions define the probability of encountering a given sea state during the expected service life of the unit. The two most common forms of long-term wave conditions are:

- the list of sea states, in which each sea state is described by its exact spectral parameter values. The list of sea states is generally used to describe a specific site or route, and
- the scatter diagram, in which the sea states are sorted in tables (typically according to the wave height and wave period spectral parameters), and the probability of occurrence of each cell is defined.

App 1, [2.1] provides two typical scatter diagrams that can be used for fatigue analysis of ships: IACS scatter diagram for North Atlantic, and worldwide sailing scatter diagram.

**3.1.6 Other environmental conditions**

In the spectral analysis described in this Section, environmental loads contributing to fatigue are limited to wave first order loads. However, in the case of single point moored units, the influence of other environmental loads such as current and wind on the relative wave direction can be taken into account. This influence is to be determined by a heading analysis preliminary to the spectral analysis itself. This heading analysis and the loads to be considered are described in NR493 Classification of Mooring Systems for Permanent Offshore Units, App 2.

Except for the influence on wave heading, the effects of other environmental loads on the structural response and on the fatigue damage have to be computed separately from the spectral analysis, using other models and simulations methods. The combination of the spectral analysis results with those of other environmental loads can be performed using the methods described in [3.7].

**3.2 Hydrodynamic and structural models**

**3.2.1 General**

The hydrodynamic and structural models are combined and used to produce transfer functions between the wave and the stress in the considered detail.

The transfer functions are to be computed for:

- wave directions covering a 360° range. For turret moored units, other discretization taking the heading analysis results into account can be adopted
- a wave direction discretization step not larger than 10° to 15°
- wave frequencies covering a range from 0,05 to 1,80 rad/s
- a wave frequency step between 0,040 and 0,075 rad/s. As a general rule, the frequency step should be not larger than:

$\Delta\omega = 0,3 (g/L)^{1/2}$ , where:

$g = 9,81 \text{ m/s}^2$

L : Length between perpendiculars of ships and ship-shaped offshore units, in m.

A particular attention is to be paid to mechanical or hydrodynamic resonant phenomena (e.g. roll resonant response) that may require a further reduction of the frequency stepping, at least in some parts of the frequency range.

### 3.2.2 Hydro-structure coupling

Several levels of assumptions can be chosen for the hydrodynamic model and the structural model, depending on which physical behaviour is expected to occur.

The ship structural response can be considered as:

- quasi-static, which means that the structural response is strictly proportional to the applied loads, or
- dynamic, if some dynamic amplification is likely to occur, for very soft structures with low natural frequencies.

In the first case, a rigid body hydrodynamic analysis is performed first, and the hydro-dynamic loads are transferred to the structural model. In the second case, a hydro-elastic coupling procedure is necessary, in which a dynamic structural analysis is done before the flexible body hydrodynamic analysis.

In any case, a particular attention is to be paid to the consistency between the structural and hydrodynamic models, regarding the definition of every type of external loads acting on the unit, including solid masses, liquids in tanks, sea pressure.

For more details about the hydro-structure coupling methods, refer to App 1, [3].

### 3.2.3 Hydrodynamic analysis

A hydrodynamic analysis is to be performed in order to evaluate the transfer functions between the waves and the hydrodynamic loads acting on the unit.

A validated numerical sea keeping code is to be used. The use of codes based on the three dimensional Boundary Element Method (BEM) is recommended. The mesh size is to be chosen so that the minimal wave length (defined on the basis of the encounter frequency) is covered by at least six panels. Alternatively, a special treatment of the high frequency calculations can be used in order to avoid the numerical inaccuracies inherent to the BEM method. In any case, the problem of irregular frequencies is to be properly solved.

The hydrodynamic problem is solved for every degree of freedom: the six rigid body motions, plus a certain number of the first natural elastic modes of the structure if a dynamic structural response is considered. The equation of motion is then solved in the frequency domain for all the generalized motions (rigid body modes and elastic modes). For ships, the effect of forward speed is to be taken into account, typically using the 'encounter frequency' approximation. Special attention is to be given to the possible singularities in the motion equation for some combinations of wave incidences and frequencies where the encounter frequency tends towards zero.

The results of the hydrodynamic model are the LTF of motions and hydrodynamic loads. The loads to be determined are governed by the type of structural model on which they will be applied, as explained in [3.2.4].

### 3.2.4 Structural analysis

Further to the hydrodynamic analysis, stress RAO have to be determined by applying the hydrodynamic loads on a structural model. The type and extent of the structural model is to be adapted to the considered unit and the considered structural element, in such a way that the structural response is correctly captured.

As a general rule, the stress RAO are obtained by coupling the hydrodynamic model with a three dimensional FEM structural model. To this purpose, the pressure and inertia loads have to be transferred to the structural model. In such a case, the procedure consists in computing the structural response to the real and imaginary parts of the complex loads for each wave frequency and each wave direction, to obtain the real and imaginary parts of the stress LTF.

### 3.2.5 Full length FEM model

The structural model can be a full length FEM model. The modelling requirements and boundary conditions prescribed in the applicable rules should be applied. Guidance may also be found in NR551 Structural Analysis of Offshore Surface Units through Full Length Finite Element Models.

The full length FEM model is to be perfectly balanced under the pressure and inertia loads. As a consequence, it is necessary to adopt some very accurate methods for the transfer of the loads between the hydrodynamic and structural models.

The model balance has to be verified thoroughly by checking the reaction forces at boundary conditions. In case some correction accelerations are used for finalizing the model balance (either explicitly or implicitly through solutions for free body analysis in FEM software), their level is to be carefully checked in order to verify the accuracy of the simulation.

### 3.2.6 Partial FEM model

For some types of structures a full length FEM model is not necessary for the correct evaluation of the structural response in the area of interest. The extent of the FEM structural model can be reduced to a subpart of the structure. The considered structural subpart is to be statically determinate, thus limiting the applicability to slender structures. The structural behaviour within the extent of the FEM model must not be significantly influenced by the distortion of the non-modelled parts, which excludes structures prone to warping or shear lag.

This method is typically used for ‘three holds models’ of ships and ship-shaped units. The modelling requirements, model extent and boundary conditions prescribed in the applicable rules should be applied.

If a partial structural model is used, the forces and moments exerted by the structure parts not included in the FEM model need to be determined in the hydrodynamic model and to be applied at the boundaries of the structural model, in addition to the pressures and inertia loads.

### 3.2.7 Simplified determination of the stress

In some specific cases, the stress RAO can be obtained by linear combination of the relevant hydrodynamic load transfer functions, without running a structural analysis for each wave frequency and heading. The combination factors describe the relationship between the load parameters (pressures, accelerations) and the stress in the detail. These factors can be obtained by strength of materials considerations or by FEM structural analyses under unitary load patterns.

In particular, a simplified spectral fatigue analysis of the connection of longitudinal stiffeners with the primary supporting members can be performed without using a FEM model by applying the analytical approach described in Sec 3. The hot spot stress RAO for the stiffener fatigue details can be obtained from the hull girder bending moments and the local pressure LTF using the prescription given in Sec 3, [4.2].

The stress RAO for the spectral fatigue analysis is the hot spot stress RAO. Unless the stress coefficients are obtained by FEM analysis, the prescriptions given in [3.3] do not apply to the simplified stress determination described in this paragraph.

## 3.3 Stress to be used for spectral analysis

### 3.3.1 Stress definition

For each type of detail, the stress RAO to be used for the spectral analysis is derived from the FEM stress, as follows:

- a) For ordinary plated joint details, type ‘a’ hot spots:

$$\sigma = f_{c\_FEA} f_{eff} \sigma_{HS}$$

where  $\sigma_{HS}$  is calculated according to Sec 5, [3] for each side (side L, side R) of the line A-A.

The fatigue damage in the most severe stress direction is then determined as described in [3.3.3], for each side of the line A-A.

The fatigue damage in the hot spot is the highest of the two fatigue damages for the two sides of the line A-A.

- b) For ordinary plated joint details, type ‘b’ hot spots:

$$\sigma = f_{c\_FEA} f_{eff} \sigma_{HS}$$

where  $\sigma_{HS}$  is calculated according to Sec 5, [3].

- c) For web stiffened cruciform joint details:

$$\sigma = f_{c\_FEA} f_{eff} \sigma_{HS}$$

where  $\sigma_{HS}$  is calculated according to Sec 5, [4].

The fatigue damage in the most severe stress direction is then determined as described in [3.3.3].

- d) For bent hopper knuckle details:

$$\sigma = f_{c\_FEA} f_{eff} \sigma_{HS}$$

where  $\sigma_{HS}$  is calculated according to Sec 5, [5].

The fatigue damage in the most severe stress direction is then determined as described in [3.3.3].

- e) For cut edge details:

$$\sigma = f_{c\_FEA} f_{eff} \sigma_{CE}$$

where  $\sigma_{CE}$  is calculated according to Sec 5, [6].

### 3.3.2 Hot spot axes and angular sectors

In this Sub Article, the same local XY rectangular coordinate system as in Sec 5, [7] is used. In addition, the same definition of angular sectors 1 and 2 as in Sec 5, [7] is used.

### 3.3.3 Most severe stress direction

In the context of spectral analysis, the prescriptions in Sec 5, [7.2] relative to the determination of the stress range principal directions and principal values cannot be applied.

For direct calculation, the fatigue damage computation is based on the following principles:

- the stress in a constant direction is used
- all possible stress directions have to be considered
- the stress direction with the highest fatigue damage is selected.

The procedures for determining the most severe stress direction are given in [3.3.6].  
The screening procedures given in [3.3.7] can be used in order to identify the hotspots for which a detailed analysis considering all stress directions is necessary.

3.3.4 Normal stress in a given direction

The normal stress  $\sigma_n$  in a direction at an angle  $\alpha$  from the x direction is given by:

$$\sigma_n(\alpha) = \frac{\sigma_{xx} + \sigma_{yy}}{2} + \frac{\sigma_{xx} - \sigma_{yy}}{2} \cos 2\alpha + \sigma_{xy} \sin 2\alpha$$

where:

$\sigma_{xx}$ ,  $\sigma_{yy}$ ,  $\sigma_{xy}$ : Stress tensor components linear transfer function, in the hot spot local axis.

3.3.5 Mean stress in spectral fatigue analysis

In spectral fatigue analysis, the mean stress is the still water stress since the wave induced stress average value is zero. Therefore, the mean stress in a given stress direction  $\alpha$  is determined from the components of the still water stress tensor using the formula in [3.3.4].

3.3.6 Fatigue analysis procedure

Different procedures can be used in order to determine the exact fatigue damage based on the most severe stress direction.

a) Discretization

The 180° range of possible stress directions is discretized with a fine angle step. The angle step should not be higher than two degrees.

For each stress direction, the normal stress is obtained as described in [3.3.4] and the fatigue damage is computed using the procedure given in [3.5].

The final fatigue damage for the considered hotspot is the maximum damage among all stress directions.

b) Using spline interpolation

The fatigue damage in the hotspot can be determined by spline interpolation between the fatigue damages obtained for a limited number of stress directions, using the following procedure:

- The fatigue damage is computed for the stress directions and S-N curves given in Tab 1.
- For each sector, the fatigue damages for the 7 directions are interpolated with a spline. The highest fatigue damage for each sector is obtained from the spline interpolation. Angle steps of not more than two degrees should be used for the interpolated values.
- The actual damage for the hotspot is the highest between the two sectors.

A linear interpolation is not accepted, as it would fail at finding the actual maximum damage (see Fig 2).

If the weld toe angle is lower than or equal to 30°, the same S-N curve  $P_{//}$  applies to all stress directions (see Sec 5, [3.2.6]). In this case, the fatigue damage is computed for the stress directions and S-N curve given in Tab 2 and a single spline interpolation is used.

Table 1 : Stress directions and S-N curves for fatigue damage interpolation

Sector	Angles	S-N curve
1	-45° , -30° , -15° , 0° , 15° , 30° , 45°	$P_{\perp}$
2	45° , 60° , 75° , 90° , 105° , 120° , 135°	$P_{//}$

Figure 2 : Spline interpolation of fatigue damage

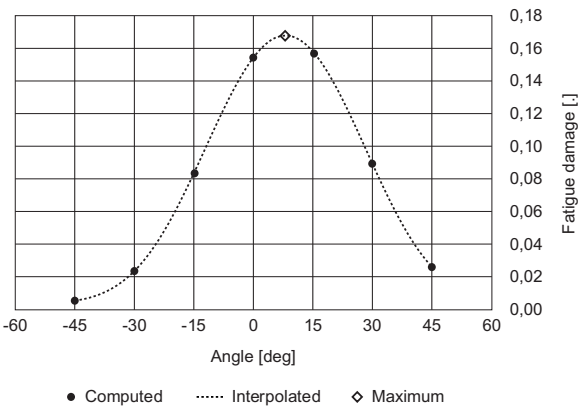


Table 2 : Stress directions and S-N curve for fatigue damage interpolation, one S-N curve

Angles	S-N curve
-90°, -75°, -60°, -45°, -30°, -15°, 0°, 15°, 30°, 45°, 60°, 75°, 90°	P <sub>//</sub>

3.3.7 Screening procedure for spectral analysis

In order to reduce the number of hotspots on which the detailed analysis described in [3.3.6] is performed, a screening procedure can be used. The screening procedure is designed in such a way that it always overestimates the fatigue damage. Therefore, all hot spots that pass the fatigue criteria using the screening procedure need not to be analyzed with the detailed procedure.

Instead of proceeding with several spectral analyses with the stress RAOs for different stress directions, a single stress RAO is used. This stress RAO is the envelope of all the RAOs for all stress directions. This envelope RAO is obtained by:

$$\sigma_{Env}(\omega,\beta) = \text{Max}_{\alpha} |\sigma_n(\omega, \beta, \alpha)|$$

where

$|\sigma_n(\omega,\beta,\alpha)|$ : Amplitude of the complex linear transfer function, as described in [3.3.4] from the linear transfer functions of the stress tensor components

When looking for the value of  $\alpha$  angle that maximizes the stress amplitude, angle steps of not more than two degrees should be used.

The S-N curve to be used in the screening procedure of the fatigue at the weld toe of plated joints is the P<sub>⊥</sub> curve.

However, if the weld toe angle is lower than or equal to 30°, the S-N curve to be used in the screening procedure is P<sub>//</sub>.

3.4 Short-term statistics

3.4.1 General

Using the spectral approach, short-term statistics can be obtained for the different results of the hydrodynamic and hydro-structure models, including -but not limited to- stress.

3.4.2 Response spectrum integration

The methodology for response spectrum integration is detailed in App 1, [4.1.2].

3.4.3 Short-term statistics

The methodology for short-term statistics is detailed in App 1, [4.1.3].

3.5 Short-term fatigue damage

3.5.1 General

The short-term fatigue damage can be computed, using the statistics of the stress response and the fatigue S-N curve for the considered detail.

The Miner sum of the damage for the short-term condition k is obtained by the following formula:

$$D_k^{ST} = \frac{T_{ST,k}}{T_{z-\sigma}} \left[ \frac{1}{K_1} \int_{\Delta S_q}^{\infty} (\Delta\sigma)^{m_1} p(\Delta\sigma) d\Delta\sigma + \frac{1}{K_2} \int_0^{\Delta S_q} (\Delta\sigma)^{m_2} p(\Delta\sigma) d\Delta\sigma \right]$$

where:

- T<sub>ST,k</sub> : Duration of the short-term condition k, in seconds
- T<sub>z-σ</sub> : Mean zero up-crossing period of the stress response, in seconds (see App 1, [4.1.3])
- p(Δσ) : Probability density function of the stress cycle ranges (see App 1, [4.1.3]).

3.5.2 Analytical integration of the stress distribution

Under the assumption that the stress cycle ranges follow a Rayleigh distribution, the damage can be computed analytically:

$$D_k^{ST} = \frac{T_{ST,k}}{T_{z-\sigma}} \left[ \frac{1}{K_1} (2\sqrt{2\lambda_0})^{m_1} \Gamma\left(1 + \frac{m_1}{2}; \frac{\Delta S_q^2}{8\lambda_0}\right) + \frac{1}{K_2} (2\sqrt{2\lambda_0})^{m_2} \gamma\left(1 + \frac{m_2}{2}; \frac{\Delta S_q^2}{8\lambda_0}\right) \right]$$

where:

- λ<sub>0</sub> : Moment of order 0 of the stress response spectrum as per App 1, [4.1.2], corresponding to the short-term condition k.

### 3.6 Long-term fatigue damage

#### 3.6.1 General

The long-term fatigue damage is defined as the sum of the damage accumulated in all the short-term conditions. It can be obtained either by computing the long-term distribution of stress ranges from the short-term statistics, or by summation of the short-term damages taking their probability of occurrence into account.

For spectral analysis, it is recommended to proceed by summation of the short-term fatigue damages. This solution provides some very valuable information about the most contributory conditions (sea states, wave directions), giving some insight about the validity and accuracy of the spectral approach. It also allows using different transfer functions for the different sea-states, introducing stochastic linearization of non-linear phenomena such as roll damping or intermittent wetting.

#### 3.6.2 Summation of short-term fatigue damages

The long-term fatigue damage on duration  $T_{LT}$  is given by:

$$D^{LT} = \sum_k D_k^{LT}$$

where:

$D_k^{LT}$  : Contribution of the short-term condition  $k$  to the long-term damage, given by:

$$D_k^{LT} = \frac{p_{LT,k} \cdot T_{LT}}{T_{ST,k}} D_k^{ST}$$

with:

$p_{LT,k}$  : Probability of occurrence of the short-term conditions  $k$  in the long-term statistics

$D_k^{ST}$  : Short-term damage for the computed short-term condition  $k$ , as defined in [3.5]

$T_{ST,k}$  : Duration of the short-term condition  $k$ , in seconds, as defined in [3.5]

$T_{LT}$  : Duration, in second, of the long-term period.

The long-term fatigue damage per year  $D_{wave,j}$  for a loading condition  $j$  is given by:

$$D_{wave,j} = D^{LT} \frac{365 \times 24 \times 3600}{T_{LT}}$$

### 3.7 Combination of low frequency and high frequency cycles

#### 3.7.1 General

The stress cycles at wave frequency considered in the spectral analysis might superimpose with some other stress cycles due to other loading processes, occurring at lower frequencies (eg. response of a soft mooring system) and at higher frequencies (eg. vortex induced vibrations).

The correct combination of the different loading processes in order to determine the total fatigue damage is not trivial and the method to be used depends on the particulars of the system and the loading processes.

#### 3.7.2 Coupled analysis

If the system responses to the different load processes are strongly coupled by mechanical effects or hydrodynamic effects, the only option is to determine the response in a single simulation encompassing all loads and physics, generally in time domain.

The methods for short-term and long-term fatigue damage computation in time domain are described in [4].

#### 3.7.3 Time-domain combination

When the responses to the different loading processes can be considered as weakly coupled, they can be computed by means of separate simulations. For example, the low frequency response of a soft mooring system can be solved independently from the wave frequency motions.

In this case, the response to wave frequency loads can be determined by a spectral approach as described in this section, provided that a linear model is satisfactory. The responses to other load contributions (LF and/or HF) can be determined with frequency domain or time-domain simulations.

The most accurate method for calculating the fatigue damage induced by the combination of different contributions is the time-domain summation of the different stress responses and the rainflow counting. Therefore when practicable, the results of frequency domain simulations should be turned into stress time series in order to be combined with other simulations results. The rainflow cycle counting is described in [4.3].

Although the different responses are weakly coupled they may be strongly correlated. Therefore it is recommended to use the exact same realization of the irregular wave in all simulations, and in the conversion of frequency domain results into time series.

### 3.7.4 Frequency domain combination

If the responses to two load contributions are determined in frequency domain, then these responses can be combined in frequency domain, by combining the response spectrums. This combination is not as accurate as time-domain combination but is much quicker.

The simplest and conservative approach consists in simply summing the different response spectra. The summation can be done before proceeding with the spectrum integration described in [3.4.2] or, alternatively, by summing the spectral moments as follows:

$$\lambda_{n(LF+HF)} = \lambda_{nLF} + \lambda_{nHF}$$

where:

$\lambda_{nLF}$  : Moment of order n of the lower frequency response spectrum (see App 1, [4.1.2])

$\lambda_{nHF}$  : Moment of order n of the higher frequency response spectrum (see App 1, [4.1.2]).

The fatigue damage is then computed applying [3.5.2] on the total spectrum.

In order to reduce the conservatism, a correction factor can be applied on the damage, considering the sum of two narrow banded processes instead of a single narrow band process. The short-term damage  $D_{DNB}^{ST}$  including the dual narrow band correction is defined as follows:

$$D_{DNB}^{ST} = \rho_{DNB} \cdot D_{LF+HF}^{ST}$$

where:

$D_{LF+HF}^{ST}$  : Short-term damage based on the total response spectrum

$\rho_{DNB}$  : Dual narrow band correction factor, determined as follows:

$$\rho_{DNB} = \frac{f_E}{f_C} \left[ \eta_{LF}^{\left(2 + \frac{m1}{2}\right)} \left(1 - \sqrt{\frac{\eta_{HF}}{\eta_{LF}}}\right) + \sqrt{\pi \cdot \eta_{LF} \cdot \eta_{HF}} \cdot \frac{m1 \Gamma\left(1 + \frac{m1-1}{2}\right)}{\Gamma\left(1 + \frac{m1}{2}\right)} \right] + \frac{f_{HF}}{f_C} \cdot \eta_{HF}^{\left(\frac{m1}{2}\right)}$$

with:

$$\eta_{LF} = \frac{\lambda_{0LF}}{\lambda_{0(LF+HF)}}$$

$$\eta_{HF} = \frac{\lambda_{0HF}}{\lambda_{0(LF+HF)}}$$

$m1$  : Inverse slope of the first segment of the S-N curve that was considered for computing  $D_{LF+HF}^{ST}$

$f_C$  : Mean up-crossing frequency of the combined response:

$$f_C = \sqrt{\frac{\lambda_{2(LF+HF)}}{\lambda_{0(LF+HF)}}}$$

$f_E$  : Mean up-crossing frequency of the envelope of the combined response:

$$f_E = \sqrt{(\eta_{LF}^2 \cdot f_{LF}^2) + (\eta_{LF} \cdot \eta_{HF} \cdot f_{HF}^2 \cdot \delta_{HF}^2)}$$

$f_{LF}$  : Mean up-crossing frequency of the lower frequency response:

$$f_{LF} = \sqrt{\frac{\lambda_{2LF}}{\lambda_{0LF}}}$$

$f_{HF}$  : Mean up-crossing frequency of the higher frequency response:

$$f_{HF} = \sqrt{\frac{\lambda_{2HF}}{\lambda_{0HF}}}$$

$\delta_{HF}$  : Bandwidth parameter of the higher frequency signal, taken equal to 0,1 or computed by:

$$\delta_{HF} = \sqrt{1 - \frac{\lambda_{2HF}^2}{\lambda_{0HF} \cdot \lambda_{4HF}}}$$

$\lambda_n$  : Moment of order n of the stress response spectrum, as per App 1, [4.1.2].

The correction factor  $\rho_{DNB}$  is applicable to fatigue damage based on a single slope S-N curve. For S-N curves with several slopes, the first slope parameter (i.e.  $m1$ ) is to be considered. If this simplification is considered as too conservative, then the combination of load components is to be done in time domain as in [3.7.3].



### 3.7.5 Damage combination

The simple summation of fatigue damages resulting from different processes should not be used.

As a first approach, the damages for two different responses at two different mean frequencies can be combined using the dual regular response approximation. The combined short-term damage  $D_{DRR}^{ST}$  based on the dual regular response approximation is defined as follows:

$$D_{DRR}^{ST} = \left(1 - \frac{f_{LF}}{f_{HF}}\right) D_{HF}^{ST} + f_{LF} \cdot \left[ \left(\frac{D_{LF}^{ST}}{f_{LF}}\right)^{1/m1} + \left(\frac{D_{HF}^{ST}}{f_{HF}}\right)^{1/m1} \right]$$

where:

- $f_{LF}$  : Mean frequency of the lower frequency component of the response
- $f_{HF}$  : Mean frequency of the higher frequency component of the response
- $D_{HF}^{ST}$  : Short-term damage for the higher frequency component of the response
- $D_{LF}^{ST}$  : Short-term damage for the lower frequency component of the response.

This approximation is applicable to fatigue damage based on a single slope S-N curve. For S-N curves with several slopes, the first slope parameter (i.e.  $m1$ ) is to be considered. If this simplification is considered as too conservative, then the combination is to be done in frequency domain as in [3.7.4] or in time domain as in [3.7.3].

## 3.8 Fatigue due to loading and unloading

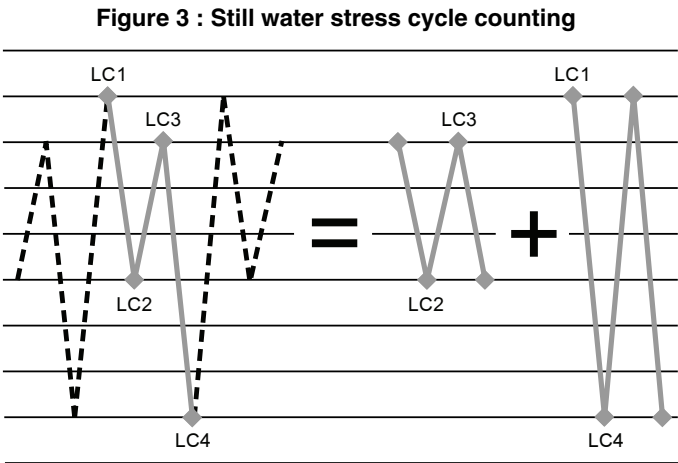
### 3.8.1 General

Spectral analysis is used to determine the distribution of wave induced stress cycles. The alternate loading and unloading of the unit may induce very low frequency stress cycles that will superimpose on the wave induced cycles and create additional damage if they are numerous and large enough (e.g. FPSO, dredger).

### 3.8.2 Range and number of still water stress cycles

A particular attention is to be given to the correct identification of the stress cycles due to the loading and unloading. The number of stress cycles and the loading conditions representative of the minimum and maximum still water stresses strongly depend on the considered structural detail and the type of dominant still water loads acting on this detail.

A sequence of still water loads conditions, representative of an entire loading and unloading cycle, should be described and analysed. The successive steps, assumed repeated indefinitely, will then form a periodical signal of the stress at any location of interest, from which stress ranges can be extracted by rainflow counting (see Fig 3).



Attention should be given that changes in the sequence can significantly alter the stress range amplitude and number. For example, the fact that two adjacent tanks are filled and emptied in reverse order or in the same order would change the count from two stress cycles to a single one with double amplitude.

When the loading and unloading sequence is not well defined, it is more appropriate to simply extract the maximum and minimum still water stresses among all the loading conditions.

### 3.8.3 Combination of still water stress cycles and wave induced stress cycles

The range of the low frequency stress cycles depends on the still water stress in the considered detail for each loading condition selected according to the recommendations in [3.8.2], and on the magnitude of the wave induced stress that occurs during the loading and unloading cycle (see Fig 4).

The loading/unloading stress range  $\Delta\sigma_{j1j2}$  between conditions  $j1$  and  $j2$  defining a still water stress cycle is:

$$\Delta\sigma_{j1j2} = |\sigma_{SW j1} - \sigma_{SW j2}| + \sigma_{wave j1} + \sigma_{wave j2}$$

where:

- $\sigma_{SW,j1}$  : Still water stress for loading condition j1
- $\sigma_{SW,j2}$  : Still water stress for loading condition j2
- $\sigma_{wave,j1}$  : Amplitude of the maximum wave induced stress cycle, for loading condition j1
- $\sigma_{wave,j2}$  : Amplitude of the maximum wave induced stress cycle, for loading condition j2.

If the loading/unloading sequence is not precisely known, the loading/unloading stress range  $\Delta\sigma_{LU}$  is defined by the highest and lowest combined still water and wave induced stress among all the loading conditions:

$$\Delta\sigma_{LU} = \max_j (\sigma_{SW,j} + \sigma_{Wave,j}) - \min_j (\sigma_{SW,j} - \sigma_{Wave,j})$$

Since the wave induced stress is a random process, the low frequency stress cycles are only statistically defined. The precise determination of their distribution is not trivial and would require some additional information or hypotheses regarding the sequencing of sea states, such as a storm model. For practical reasons, the maximum wave induced stress during a loading/unloading cycle can be taken as the maximum long-term wave induced stress on the duration of that cycle. This long-term value can be determined from the spectral analysis results using the definition of the long-term expected maximum value given in App 1, [5.1.3].

$\sigma_{Wave,j}$  is obtained by solving the following equation:

$$\sum_k \frac{p_{LT,k} \cdot T_{LU}}{T_{z,\sigma,k}} \cdot \bar{p}_k(\sigma_{Wave,k}) = 1$$

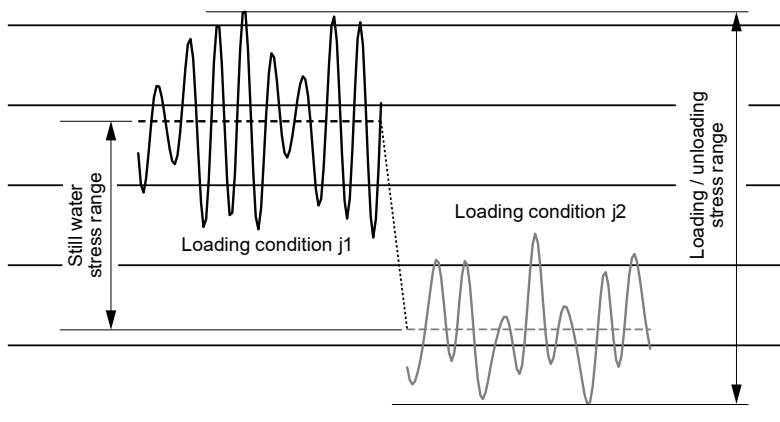
where:

- $p_{LT,k}$  : Long-term probability of the short-term condition k, defined in [3.5.2]
- $T_{LU}$  : Duration of the loading/unloading cycle, in s, selected as indicated in [3.8.2]
- $T_{z,\sigma,k}$  : Mean zero up-crossing period of the stress response, in s, for the short-term condition k, defined in App 1, [4.1.3]
- $\bar{p}_k(\sigma)$  : Complementary cumulative distribution function of stress amplitudes for the short-term condition k, defined in App 1, [4.1.3].

A further simplification consists in using a single predefined long-term probability level for the wave contribution  $\sigma_{Wave,j}$  to the loading and unloading stress. In this case, a probability of  $10^{-4}$  can be considered and  $\sigma_{Wave,j}$  is obtained by solving the following equation:

$$\sum_k \frac{p_{LT,k}}{T_{z,\sigma,k}} \cdot \bar{p}_k(\sigma_{Wave,k}) = 10^{-4} \cdot \sum_k \frac{p_{LT,k}}{T_{z,\sigma,k}}$$

**Figure 4 : Combination of still water and wave stress contributions**



### 3.8.4 Fatigue damage due to loading/unloading cycles

The damage due to the loading/unloading cycles is given by:

$$D_{LU} = n_{LU} \sum \left[ n_{j1j2} \frac{(\Delta\sigma_{j1j2})^{m1}}{K_1} \right]$$

where:

- $n_{LU}$  : Number of loading/unloading cycles per year, taking the fraction of time in sea-going operations (sailing factor) into account.
- $n_{j1j2}$  : Number of stress cycles of range equal to  $\Delta\sigma_{j1j2}$  per loading/unloading cycle
- $\Delta\sigma_{j1j2}$  : Stress cycle defined by still water conditions  $j1$  and  $j2$ , defined in [3.8.3].

If the loading/unloading sequence is not precisely known:

$$D_{LU} = n_{LU} \frac{(\Delta\sigma_{LU})^{m_1}}{K_1}$$

where:

$\Delta\sigma_{LU}$  : Loading/unloading stress range defined in [3.8.3].

The additional fatigue damage induced by the loading/unloading stress ranges is then simply added to the long-term wave induced fatigue damage.

### 3.9 Intermittent wetting

#### 3.9.1 General

The intermittent wetting effect induces a non-linear loading on the structure that is not accounted for in the linear model used for spectral fatigue analysis. This local non-linear effect can be taken into account with by means of the linearization method described in [3.9.2]. Other aspects of the intermittent wetting, such as non-linear hull girder loads, are not considered. Such effects can be addressed using Froude Krylov non-linear loads in time-domain simulations, as described in Article [4].

#### 3.9.2 Equivalent linearized local pressure

In a linear diffraction-radiation analysis, the hydrodynamic pressure is obtained over the wetted surface at rest, as a harmonic pressure variation at each point. Therefore, the pressure on the side shell between the surface at rest and a wave crest is not modelled, and in a wave trough below the surface at rest, an unrealistic negative pressure is generated.

The actual pressure history in the area affected by intermittent wetting is not a harmonic process, but for fatigue analysis, it can be approximated by an equivalent harmonic pressure having the same contribution to the fatigue damage. This equivalent harmonic pressure  $p_{equ}$  is obtained by adding a corrective pressure  $p_{corr}$  to the hydrodynamic pressure  $p_{hydro}$ :

$$p_{equ}(\omega, \beta, z) = p_{hydro}(\omega, \beta, z) + p_{corr}(\omega, \beta, z)$$

where:

$z$  : Elevation of the considered point above the still water free surface.

The corrective pressure itself is defined by a unitary pressure footprint  $\alpha_{corr}(z)$ , multiplied by the hydrodynamic pressure at the free surface  $p_0(\omega, \beta)$ :

$$p_{corr}(\omega, \beta, z) = \alpha_{corr}(z) p_0(\omega, \beta)$$

The corrective pressure can be either defined for each sea-state for a short-term approach in [3.9.3] or defined once for all sea-states for a long-term approach in [3.9.4].

#### 3.9.3 Corrective pressure footprint for a short-term approach

A different corrective pressure footprint is defined for each sea-state. The unitary pressure footprint is defined as follows (see Fig 5):

- for  $z < 0$ :

$$\alpha_{corr\_ST}(z) = -0,5 \exp\left(1, 2 \frac{z}{H_{ST}} - 1, 9 \left(\frac{z}{H_{ST}}\right)^2\right)$$

- for  $z > 0$ :

$$\alpha_{corr\_ST}(z) = 0,5 \exp\left(-\frac{z}{H_{ST}} - 0, 5 \left(\frac{z}{H_{ST}}\right)^2\right)$$

where:

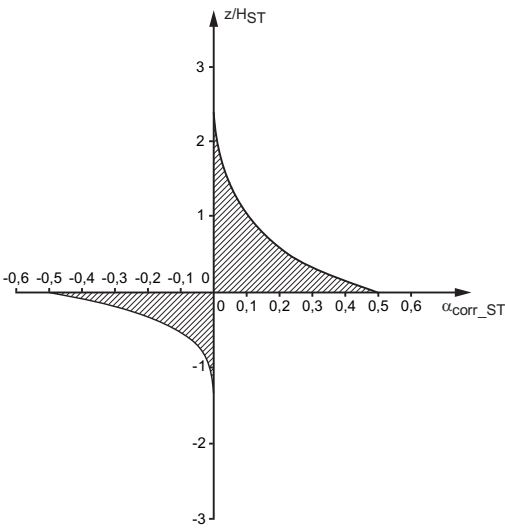
$H_{ST}$  : Height of the pressure footprint for intermittent wetting correction, taken equal to:

$$H_{ST} = \frac{(p_0)_{1/3}}{\rho g}$$

$(p_0)_{1/3}$  : Significant amplitude of the hydrodynamic pressure at the still water free surface, in way of the fatigue detail, for the considered sea-state.

$z$  : Elevation of the considered point above the still water free surface.

Figure 5 : Pressure footprint for intermittent wetting correction for a short-term approach



3.9.4 Corrective pressure footprint for a long-term approach

A single corrective pressure footprint is defined for all sea-states. The unitary pressure footprint is defined as follows (see Fig 6):

- for  $z < 0$ :

$$\alpha_{corr\_LT}(z) = -0,5 \exp\left(2,5 \frac{z}{H_{LT}} - 1, 1 \left(\frac{z}{H_{LT}}\right)^2\right)$$

- for  $z > 0$ :

$$\alpha_{corr\_LT}(z) = 0,5 \exp\left(-1,55 \frac{z}{H_{LT}}\right)$$

where:

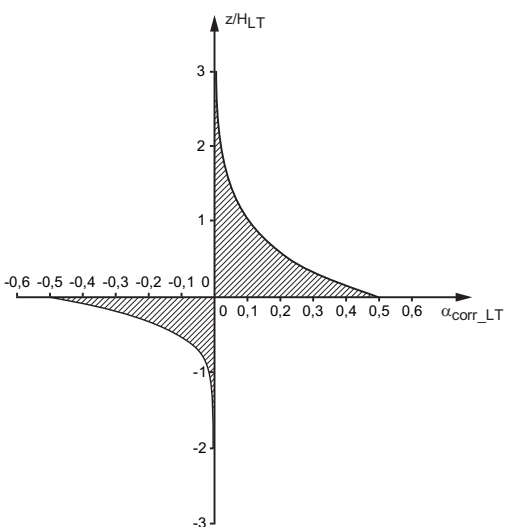
$H_{LT}$  : Height of the pressure footprint for intermittent wetting correction, taken equal to:

$$H_{LT} = \frac{p_0(10^{-2})}{\rho g}$$

$p_0(10^{-2})$  : Long-term value of the hydrodynamic pressure at the still water free surface in way of the fatigue detail, with an exceedance probability level equal to  $10^{-2}$ .

$z$  : Elevation of the considered point above the still water free surface.

Figure 6 : Pressure footprint for intermittent wetting correction for a long-term approach



### 3.9.5 Equivalent stress RAO

In a similar way as for the pressure, an equivalent linearized stress LTF  $\sigma_{\text{equ}}$  is defined, equal to the sum of the linear hydro-structure model stress and a corrective stress proportional to the hydrodynamic pressure at the free surface:

$$\sigma_{\text{equ}}(\omega, \beta, H) = \sigma_{\text{lin}}(\omega, \beta) + \sigma_{\text{corr}}(H) p_0(\omega, \beta)$$

where:

$\sigma_{\text{lin}}(\omega, \beta)$ : Linear hydro-structure model stress LTF

$\sigma_{\text{corr}}(H)$ : Correction stress for a unitary hydrodynamic pressure at the free surface that results from the application on the structural model of the correction pressure distribution defined in [3.9.3] for the short-term approach and defined in [3.9.4] for the long-term approach.

$p_0(\omega, \beta)$ : Hydrodynamic pressure at the free surface LTF.

When the structural model is a 3D FEM model, special attention is to be paid to the extent of the pressure distribution and the boundary conditions on the model, keeping in mind the assumption of a localized structural response governed by the local sea pressure.

### 3.9.6 Spectral analysis with intermittent wetting using short-term approach

The most accurate correction for the intermittent wetting effect can be obtained using a short-term approach.

The short-term fatigue damage for a short-term condition can be computed as follows:

- the significant amplitude of the hydrodynamic pressure at the free surface ( $p_0)_{1/3}$  is computed by spectral analysis for the considered short-term condition, in order to determine the correction pressure footprint height  $H_{\text{ST}}$  (see [3.9.3])
- the corrective stress  $\sigma_{\text{corr}}(H_{\text{ST}})$  for this footprint height is determined using the structural model
- the equivalent stress RAO for the detail  $\sigma_{\text{equ}}(\omega, \beta, H_{\text{ST}})$  is built (see [3.9.5])
- the fatigue damage for the considered sea state is computed from the equivalent stress RAO by spectral analysis.

The procedure can be simplified by pre-computing  $\sigma_{\text{equ}}(\omega, \beta, H_{\text{ST}})$  RAO for several pre-selected values of  $H_{\text{ST}}$  before doing the spectral analysis, and then interpolating the RAO in this database for the value of  $H_{\text{ST}}$  during the spectral analysis of each sea state. By doing this, the equivalent stress RAO construction and the spectral analysis can be dealt with one after the other, in separate dedicated tools.

### 3.9.7 Spectral analysis with intermittent wetting using long-term approach

As an alternative to the short-term approach, a correction based on a long-term approach can be used. The latter is simpler and quicker to apply, but less accurate.

The spectral analysis with long-term intermittent wetting correction is performed as follows:

- the long-term value  $p_0(10^{-2})$  of the hydrodynamic pressure at the free surface in way of the considered fatigue detail is computed by spectral analysis (see App 1, [5.1.3]), in order to determine the correction pressure footprint height  $H_{\text{LT}}$  (see [3.9.4])
- the corrective pressure is applied on the structural model to obtain  $\sigma_{\text{corr}}(H_{\text{LT}})$
- the equivalent stress RAO for the detail  $\sigma_{\text{equ}}(\omega, \beta, H_{\text{LT}})$  is built (see [3.9.5])
- the fatigue damage is computed by spectral analysis using the equivalent stress RAO. A single stress RAO is used for all the sea-states.

## 4 Time-domain fatigue analysis

### 4.1 Non-linear simulations

#### 4.1.1 Application domain

Time simulations are used when linear simulations are deemed as not capable of capturing the physics of the problem, either from a hydrodynamic point of view (large waves, large motions, or other non-linear effects), from a structural response point of view (large distortion, contact, friction, or other non-linear behaviours), or from a statistical point of view (bandwidth effect, ...).

Non-linear fatigue damage models or crack propagation analyses are not considered in this Section.

#### 4.1.2 Long-term analysis strategies

Different types of non-linear simulations can be performed, depending on the type of non-linear problem to be solved. As a general rule, non-linear simulations in time domain are very demanding in terms of computation cost and time, compared with frequency domain methods. With very few exceptions, the long-term fatigue analysis cannot be directly done by time-domain simulation of the entire life of the unit. As a consequence, time simulations need to be associated with long-term methodologies in order to determine the long-term fatigue damage.

Different types of time-domain simulations, and some approaches for long-term analysis using these simulations are given in App 2. They are briefly recalled here. These lists are not exhaustive, and many combinations and variants of the proposed methods can be adopted depending on the specific problem to be solved.

#### 4.1.3 Long duration time-domain simulations

When practically possible, the time-domain simulations are run on irregular waves having the energy density spectrum of a real sea state. The simulation duration is typically the duration of the sea state (3 hours) for the statistical convergence of the hourly fatigue damage.

In this case, the result of the analysis is a stress time series that can be analysed using the rainflow counting method described in [4.3.2]. The final result is a damage value for the considered short-term condition. In most cases this value then needs to be associated with other results by means of one long-term strategy (see [4.5]) in order to obtain the long-term fatigue damage.

#### 4.1.4 Short duration time-domain simulations

When the time-domain model computation time is too high for the entire sea state to be treated, time-domain simulations have to be run on shorter durations.

In this case, the hydrodynamic and structural response to specific equivalent design waves is simulated. The simulation duration is typically a few wave periods. The final result of the simulation is a single stress range determined by extracting the minimum and maximum stress from the time series.

This stress range obtained for a specific wave is then to be interpreted so that a damage can be determined, using one of the methodologies described in [4.4.2] or in [4.5.4].

### 4.2 Stress to be used for time-domain analysis

#### 4.2.1 Stress definition

For each type of detail, the stress to be used for the time-domain analysis is derived from the FEM stress as follows:

- a) For ordinary plated joint details, type 'a' hot spots:

$$\sigma = f_{c\_FEA} f_{eff} \sigma_{HS}$$

where  $\sigma_{HS}$  is calculated according to Sec 5, [3] for each side (side L, side R) of the line A-A.

The fatigue damage in the most severe stress direction is then determined as described in [4.2.3], for each side of the line A-A.

The fatigue damage in the hot spot is the highest of the two fatigue damages for the two sides of the line A-A.

- b) For ordinary plated joint details, type 'b' hot spots:

$$\sigma = f_{c\_FEA} f_{eff} \sigma_{HS}$$

where  $\sigma_{HS}$  is calculated according to Sec 5, [3].

- c) For web stiffened cruciform joint details:

$$\sigma = f_{c\_FEA} f_{eff} \sigma_{HS}$$

where  $\sigma_{HS}$  is calculated according to Sec 5, [4].

The fatigue damage in the most severe stress direction is then determined as described in [4.2.3].

- d) For bent hopper knuckle details:

$$\sigma = f_{c\_FEA} f_{eff} \sigma_{HS}$$

where  $\sigma_{HS}$  is calculated according to Sec 5, [5].

The fatigue damage in the most severe stress direction is then determined as described in [4.2.3].

- e) For cut edge details:

$$\sigma = f_{c\_FEA} f_{eff} \sigma_{CE}$$

where  $\sigma_{CE}$  is calculated according to Sec 5, [6].

#### 4.2.2 Hot spot axes and angular sectors

In this Sub Article, the same local XY rectangular coordinate system as in Sec 5, [7] is used. In addition, the same definition of angular sectors 1 and 2 as in Sec 5, [7] is used.

#### 4.2.3 Stress direction to be considered

In the context of time-domain analysis, the prescriptions in Sec 5, [7.2] relative to the determination of the stress range principal directions and principal values cannot be applied.

For direct calculation, the fatigue damage computation is based on the following principles:

- the stress in a fixed (i.e. constant) direction is used
- all possible stress directions have to be considered
- the stress direction with the highest fatigue damage is selected.

The procedures for determining the most severe stress direction are given in [4.2.6].

The screening procedures given in [4.2.7] can be used in order to identify the hotspots for which a detailed analysis considering all stress directions is necessary.

#### 4.2.4 Normal stress in a given direction

The normal stress  $\sigma_n$  in a direction at an angle  $\alpha$  from the x direction is given by:

$$\sigma_n(\alpha) = \frac{\sigma_{xx} + \sigma_{yy}}{2} + \frac{\sigma_{xx} - \sigma_{yy}}{2} \cos 2\alpha + \sigma_{xy} \sin 2\alpha$$

where:

$\sigma_{xx}$ ,  $\sigma_{yy}$ ,  $\sigma_{xy}$ : Stress tensor components time series in the hot spot local axis.

#### 4.2.5 Mean stress in time-domain analysis

In time-domain fatigue analysis, the mean stress is the mean value of the total stress time series, i.e. time series of still water stress plus wave induced stress. In case the total stress is not a direct output of the simulation, the summation of still water and wave induced stress is to be performed for the components of the stress tensor, before the formula in [4.2.4] is applied to obtain the stress in a given direction.

#### 4.2.6 Fatigue analysis procedure

Different procedures can be used in order to determine the exact fatigue damage based on the most severe stress direction.

##### a) Discretization

The 180° range of possible stress directions is discretized with a fine angle step. The angle step should not be higher than two degrees.

For each stress direction, the normal stress time series is obtained by [4.2.4] and the fatigue damage is computed using the procedure given in [4.4].

The final fatigue damage for the considered hotspot is the maximum damage among all stress directions.

##### b) Using spline interpolation

The fatigue damage in the hotspot can be determined by spline interpolation between the fatigue damages obtained for a limited number of stress directions, using the following procedure:

- The fatigue damage is computed for the stress directions and S-N curves given in Tab 1.
- For each sector, the fatigue damages for the 7 directions are interpolated with a spline. The highest fatigue damage for each sector is obtained from the spline interpolation. Angle steps of not more than two degrees should be used for the interpolated values.
- The actual damage for the hotspot is the highest between the two sectors.

A linear interpolation is not accepted, as it would fail at finding the actual maximum damage (see Fig 2).

If the weld toe angle is lower than or equal to 30° the same S-N curve  $P_{//}$  applies to all stress directions (see Sec 5, [3.2.6]). In this case, the fatigue damage is computed for the stress directions and S-N curve given in Tab 2 and a single spline interpolation is used.

#### 4.2.7 Screening procedure for time-domain analysis

In order to reduce the number of hotspots on which the detailed analysis is performed, a screening procedure can be used. The screening procedure is designed in such a way that it always overestimates the fatigue damage. Therefore, all hot spots that pass the fatigue criteria using the screening procedure need not to be analyzed with the detailed procedure.

Instead of proceeding with several time series of stress for different directions, two stress time series are used. These stress time series are obtained considering the principal stresses at each time step.

At each time step the principal directions  $\alpha_1(t)$  and  $\alpha_2(t)$  of the stress tensor are determined using the following formulae:

$$\begin{cases} \alpha_1(t) = \frac{1}{2} \text{atan} \left[ \frac{2\tau_{xy}(t)}{\sigma_{xx}(t) - \sigma_{yy}(t)} \right] \\ \alpha_2(t) = \alpha_1(t) + \frac{\pi}{2} \end{cases}$$

where:

$\alpha_i(t)$  : Angle between the x direction and the principal direction i.

The principal stress values  $\sigma_{p1}(t)$  and  $\sigma_{p2}(t)$  associated to these directions are determined as follows:

$$\sigma_{pi}(t) = \frac{1 + \cos(2\alpha_i(t))}{2} \sigma_{xx}(t) + \frac{1 - \cos(2\alpha_i(t))}{2} \sigma_{yy}(t) + \sin(2\alpha_i(t)) \tau_{xy}(t)$$

By comparison of  $|\alpha_1(t) - \alpha_{WT}|$  with  $|\alpha_2(t) - \alpha_{WT}|$  at each time step, the principal stress closest to the perpendicular to the weld toe is identified and is denoted  $\sigma_{p\perp}(t)$ . The other principal stress is denoted  $\sigma_{p//}(t)$ .

Then  $\sigma_{p\perp}(t)$  is analysed using  $P_{\perp}$  S-N curve and  $\sigma_{p//}(t)$  is analysed using  $P_{//}$  S-N curve.

However, if the weld toe angle is lower than or equal to 30°, the S-N curve to be used is  $P_{//}$  for both time series.

4.3 Analysis of long duration time-domain simulations

4.3.1 Realization of a short-term condition irregular wave

For the purpose of running a long duration time-domain simulation, it is necessary to define a particular realization of the irregular wave defined by the wave energy spectrum.

The irregular wave is modelled as the sum of a finite number of regular waves, using the random frequency and random phase method.

For long crested irregular waves without directional spreading, the number of wave components should be at least one hundred. For short crested irregular waves with directional spreading, wave directions every 5 to 10 degrees are recommended. The number of wave components in each wave direction can be reduced to 20. In both cases, the complete range of frequencies where significant wave energy is found is to be covered.

4.3.2 Rainflow cycle counting

When long duration time-domain simulations are run, the resulting stress time series have to be analysed using the rainflow cycle counting method, recognized as the most suitable for fatigue analysis.

The rainflow cycle counting algorithm is described ASTM E1049-1985 ‘Standard practice for Cycle counting in Fatigue Analysis’ and in ISO 12110-2 standard. It can be summarized as follows:

- the stress time series is characterized by the series of its local extremes values (maxima and minima) or ‘reversals points’. For practical reasons, the stress levels can be discretized, using at least 64 classes over the maximum range of the entire signal
- each pair of adjacent reversal point defines a range, taken as the absolute value of the difference between the stress at the two reversal points
- considering three adjacent ranges, if the middle one is smaller than (or equal to) both the previous one and the next one, then this range is counted as a complete stress cycle. The reversal points that define this range are removed from the list of reversal points, thus defining a new, and larger, range
- the analysis of the adjacent ranges is repeated until no complete cycle can be extracted.

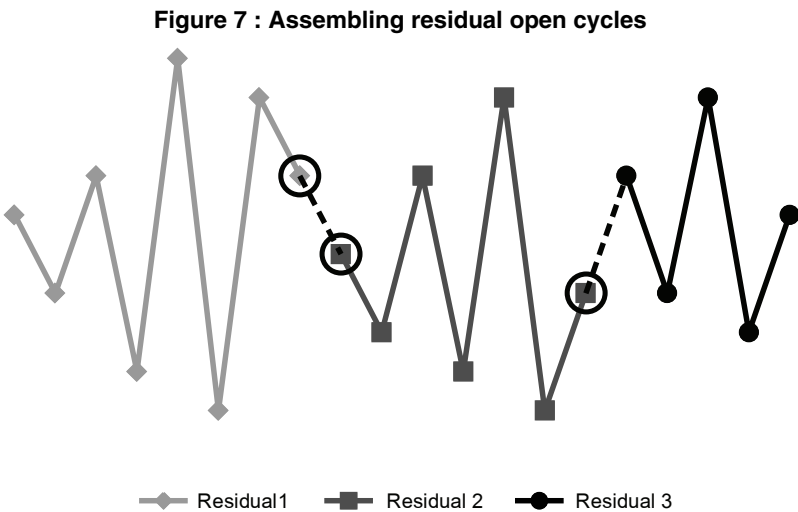
Once the entire signal has been processed as explained above, a number of reversal points remain, defining a number of ranges, or open stress cycles, of increasing then decreasing value. These residual reversal points need to be treated, either as described in [4.3.3] if several time series are considered, or as described in [4.3.4].

4.3.3 Assembling several time series

If several time series are analysed by rainflow counting and the total fatigue damage is to be considered, then the following procedure should be used:

- a) each time series is analysed by a rainflow counting as described in [4.3.2], yielding a list (or an histogram) of complete cycles and a list of residual half cycles
- b) the lists (or histograms) of complete cycles are assembled to build a global list (or histogram) of cycles
- c) the residual reversal points of the different time series are concatenated, and a new rainflow analysis is performed on the assembled list. The list (or histogram) of complete cycles thus obtained is added to the global list (or histogram). The residual reversal points are then treated as described in [4.3.4].

During the concatenation of the residual reversal points, it is necessary to verify that the points are still reversal points of the new concatenated list. The residual points, as drawn with circled points on the typical example in Fig 7, are to be removed. More details can be found in ISO 12110-2.





#### 4.3.4 Residual open stress cycles

After the rainflow counting described in [4.3.2] or the assembling of several time series in [4.3.3], the remaining open cycles need to be counted.

This is simply done by duplicating the residual reversal points and assembling them before performing a new rainflow counting on the duplicated signal. The same precautions have to be taken for the concatenation of the duplicated residue as described in [4.3.3] for the concatenation of different residues.

#### 4.3.5 Fatigue damage computation

The result of the rainflow counting is a list of cycles, or a list of cycle classes with a number of cycles for each of them.

The damage is obtained by summation of the contribution of each cycle or cycle class:

$$D = \sum_{\text{classes or cycles}} \frac{\Delta\sigma^{m_i}}{K_i} n(\Delta\sigma)$$

where:

$\Delta\sigma$  : Stress range value or representative stress range for the class

$K_i, m_i$  : S-N curve parameters for the stress range  $\Delta\sigma$

$n(\Delta\sigma)$  : Number of cycles in the class  $\Delta\sigma$ . When the cycles are stored individually,  $n(\Delta\sigma) = 1$ .

### 4.4 Short-term fatigue damage

#### 4.4.1 Long duration time simulation

The short-term fatigue damage can be directly obtained using a long duration time-domain simulation (see [4.1.3]). The simulation time necessary for a converged fatigue damage rate (damage per hour) depends on the statistics of the stress signal, in terms of period and variability. In general, for a response driven by wave loads the simulated time should be at least three hours. It is recommended to proceed with convergence analysis.

The beginning of the time series is usually to be disregarded until the response to the irregular wave is properly established, taking into account:

- the duration of the smooth transition from the initially still water to the irregular wave
- the duration of the wave radiation memory effects (typically 30 seconds) and the duration of the transient mechanical response of the system (e.g. mooring system).

The time series is then analysed by rainflow counting as described in [4.3]. The fatigue damage is computed for the duration of the simulation  $T$ , and then scaled to the actual duration  $T_{ST,k}$  of the short-term condition  $k$ .

The short-term fatigue damage  $D_k^{ST}$  for the short-term condition  $k$  is given by:

$$D_k^{ST} = D \frac{T_{ST,k}}{T}$$

where  $D$  is the fatigue damage as defined in [4.3.5].

#### 4.4.2 Short duration time simulation

If a long duration time-domain simulation is not practically feasible, the short-term fatigue damage can be obtained by means of short duration simulations, using the equivalent design wave technique (EDW). This technique is explained in details in App 2.

Several EDW have to be defined, corresponding to different probability levels, and analysed in time domain. An empirical short-term distribution of stress cycles is then obtained, that can be integrated to compute the short-term fatigue damage.

It should be noticed that if the final goal is a long-term fatigue damage, then the above procedure can be beneficially replaced with a similar one, directly driven by long-term values instead of short-term ones (see [4.5.4]).

### 4.5 Long-term fatigue damage

#### 4.5.1 Full duration time-domain simulation

If the direct simulation is fast enough, the entire life of the considered unit can be simulated in time domain.

Due to the statistical variability in the encountered conditions, the analysis actually consists in determining the damage for the different short-term conditions that the unit is supposed to encounter, and then combining the short-term damages according to the probability of occurrence of the short-term conditions.

The long-term fatigue damage  $D^{LT}$  on duration  $T_{LT}$  is given by:

$$D^{LT} = \sum_k D_k^{LT}$$

where:

$D_k^{LT}$  : Contribution of the short-term condition k to the long-term damage, given by:

$$D_k^{LT} = \frac{p_{LT,k} \cdot T_{LT}}{T_{ST,k}} D_k^{ST}$$

with:

$p_{LT,k}$  : Probability of occurrence of short-term conditions k in the long-term statistics

$T_{LT}$  : Duration, in second, of the long-term period

$D_k^{ST}$  : Short-term fatigue damage for the short-term condition k computed, as defined in [4.4.1]

$T_{ST,k}$  : Duration of short-term condition k, in seconds, as defined in [4.4.1].

The long-term fatigue damage per year  $D_{wave,j}$  for a loading condition j is given by:

$$D_{wave,j} = D^{LT} \frac{365 \times 24 \times 3600}{T_{LT}}$$

#### 4.5.2 Long duration time-domain simulations on selected sea states

If the cost of simulation is such that it is not practicable to do a full duration simulation, a design sea states approach can be selected, on the condition that long duration simulations are still feasible on all the sea states that contribute significantly to the long-term fatigue damage.

The sea states where a time-domain simulation is performed are chosen in a prediction-correction iterative procedure.

The long-term fatigue damage is obtained by summing the damages of the short-term conditions for which a simulation was run, neglecting the contribution of the other ones.

This analysis follows the 'multiple design sea states' approach described in App 1, [5.3].

The long-term fatigue damages  $D^{LT}$  and  $D_{wave,j}$  are obtained according to [4.5.1].

#### 4.5.3 Mixed spectral and time-domain simulation

Under certain conditions, it can be assumed that the non-linear response is just a correction of the linear response. In this case, it might be enough to compute the non-linear ship response for a single short-term condition and to use the results of this short-term condition to correct the linear result. The short-term condition used for time-domain simulation is to be chosen among those having the largest contribution to the total damage.

The long-term fatigue damage is then obtained by applying, to the long-term fatigue damage  $D^{LT}$  and the annual fatigue damage  $D_{wave,j}$  as defined in [3.6.2] (spectral approach), a correction factor based on the difference between spectral results and time-domain results for the selected short-term condition.

This analysis follows the 'single design sea state' approach described in App 1, [5.4].

#### 4.5.4 Short duration time simulations

The long-term fatigue damage can also be obtained by means of short duration simulations, using the equivalent design wave technique.

Several equivalent design waves have to be defined, and analysed in time domain. An empirical long-term distribution of stress cycles is then obtained by assembling the results of the different simulations.

The long-term fatigue damage  $D^{LT}$  is obtained from the long-term cumulative distribution as detailed in App 1, [5.5.5] or App 1, [5.5.6], as applicable.

This analysis is described with more details in App 1, [5.5].

## SECTION 12

## FATIGUE ASSESSMENT BASED ON CRACK PROPAGATION

### Symbols

B	: Section thickness, measured in the crack plane. The crack plane is defined as the plane which is normal to the stresses direction
E	: Material Young modulus
$S_u$	: Material ultimate stress
$S_y$	: Material yield stress
W	: Structural element width, measured in the crack plane
$\epsilon_u$	: Material ultimate strain.

### 1 General

#### 1.1 Scope

##### 1.1.1 General

The scope of this Section is to provide guidance for the remaining fatigue life assessment by means of crack propagation analysis. Fatigue cracks located at the following hot spot locations are considered: weld toe, weld root and plate cut edge.

##### 1.1.2 Remaining fatigue life of cracked structures

The application of crack propagation analysis in this section consists in assessing the remaining fatigue life of marine structure components when a fatigue crack has been discovered or is postulated. Due to constraints linked to inspection practices, cracks are generally rather large when detected. The goal of the analysis is to provide a deadline for the planning of repairs in the best conditions. Several types of repairs may be considered depending on environmental and economic criteria: repairs on site or repairs after sailing to the closest shipyard if possible.

#### 1.2 General considerations

##### 1.2.1 Fatigue process

As explained in Sec 1, [4], the fatigue process can be split into three main phases:

- a) The crack initiation phase at a hot spot location

During this stage, a damage accumulation exists. This phase ends when cracks can be detected by a non destructive testing (NDT) method (see [7]).

- b) The crack propagation or crack growth phase

Cracks propagate, increasing in size until failure.

- c) Failure phase

The propagation accelerates suddenly, without previous sign, leading to a sudden rupture by brittle or ductile failure, depending on the material strength characteristics.

This Section deals with phases b) and c).

##### 1.2.2 Fatigue approaches principles

Fatigue analysis based on S-N curves and on Miner's linear accumulation of damage makes the assumption that the fatigue phenomenon may be modeled as a local weakening of the material that increases in time.

Fatigue analysis based on crack propagation makes the assumption that the fatigue phenomenon may be modelled by the size increase of a flaw or a set of flaws. In the same way that the S-N curves present a fatigue limit below which no fatigue damage accumulation occurs, the crack propagation presents a threshold below which a crack does not propagate.

Both approaches are not contradictory since a local flaw may be considered as inducing a weakening of material strength characteristic, in a homogenized material approach. Alternatively a local weakening of material characteristics may be represented as an effect of voids, i.e. flaws, in the material.

Unfortunately the correspondence between these two approaches is not straightforward, and a choice is to be carried out. In this Guidance Note, the crack propagation approach is considered only for the remaining fatigue life assessment of in-service ships and offshore units.

### **1.2.3 Variable amplitude loading**

The wave induced loads on marine and offshore structures have a stochastic nature, both on the short term (typically three-hour sea states) and on the long term (sequence of sea states). The wave loading is only statistically defined, and the exact sequence of stress cycles is unknown.

Due to crack growth sensitivity to the order in which load cycles are encountered, the loads for crack propagation simulation are to be provided as a time history sequence. The analysis is recommended to be carried out with a representation of load cycles sequence as realistic as possible.

The load history is to be determined, taking into account the simulation duration. In the case of remaining life determination of cracked structures, the simulation period is the residual expected life. For typical simulation periods (in the range from a few weeks to a few years) the load history consists in sequences of waves encountered during a sequence of short-term conditions. A short-term condition corresponds to the combination of an operational condition (loading condition, speed, heading) with a wave condition (sea state, waves direction), on a short time period (typically three hours). In order to be fully representative, the sequence of short-term conditions can be organized in term of storms and calm sea periods. Generally the storm model is difficult to be established, and simplified approaches from long-term distributions may be applied. More detailed procedures are described in [5].

Unless the actual load history has been measured and recorded, the order of the stress cycles is not known but is estimated. In such case a sensitivity analysis on the order of the cycles is recommended. At least, increasing order and decreasing order of stress range magnitude are to be tested.

### **1.2.4 Interaction between cracks**

Several cracks or flaws may exist close to each other. These can be either initial detected cracks, or distant cracks becoming close during the propagation. The interaction between adjacent cracks has to be taken into account.

Rules referring to the merging of cracks and flaws are given in the British Standard BS 7910:2013 (Flaw dimensions and interaction) and in the International Institute of Welding document IIW-X-1637-08 Volume 2, Chapter B. Any other duly referenced document may be used with the agreement of the Society.

### **1.2.5 Residual stress**

The welding process creates residual stresses at the weld toe.

For as welded joints, a residual stress field remains within the plate thickness in the heat-affected zone (HAZ). The residual stress field is to be considered in addition to the load stress field when a crack propagates in depth from a weld toe. When no data are available, a value equal to the material yield stress is to be considered.

Residual stress distributions for ferritic and austenitic steels are proposed in the British Standard BS 7910:2013 Annex Q for the following as-welded joints:

- plate butt and pipe seam welds
- pipe butt welds
- T-butt welds (plate to plate)
- tubular T-butt welds.

Generally, marine structures are dealing with ferritic steels.

Residual distributions in as-welded joints can also be found in the International Institute of Welding document IIW-X-1637-08 (IIW FFS Recommendations for Fracture Assessment of Weld Flaws), Volume 2, Chapter F. Any other duly referenced document may be used with the agreement of the Society.

In case of post welding treatment, the welding residual stress field can be modified, so the value to be considered is to be duly justified by publications or measurements.

## 2 Crack propagation analysis

### 2.1 Procedure

#### 2.1.1 General

The fatigue analysis starts by postulating an initial crack size, obtained from a critical analysis of the inspection indications. The crack propagation under a loading history representative of the remaining life time is then simulated. At each step, the crack size is updated and the failure criteria are checked.

#### 2.1.2 Analysis preparation

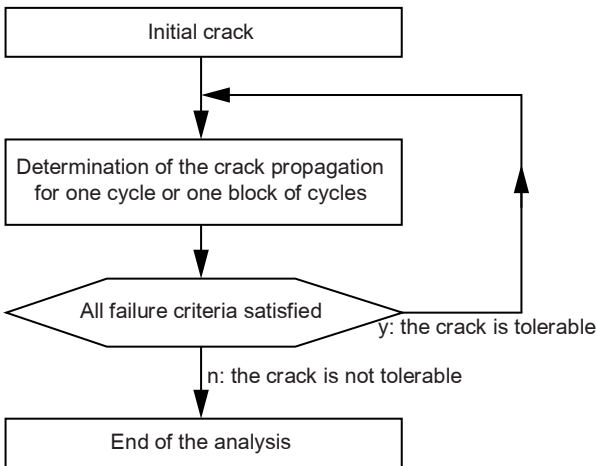
The analysis preparation steps are:

- choice of the crack model according to the type of fatigue crack, as described in [2.3]
- definition of the initial crack size (see [2.4])
- definition of the propagation law parameters (see [2.6])
- definition of the failure criteria to be considered (see [2.7] and [3])
- definition of the load history (see [5]).

#### 2.1.3 Crack propagation analysis

The analysis procedure described in Fig 1 is to be used so that the crack path and the critical crack size are updated as the crack propagates.

**Figure 1 : Crack propagation analysis procedure**



### 2.2 Crack models

#### 2.2.1 General

Three crack models are considered:

- surface cracks (see [2.2.2])
- through-thickness cracks (see [2.2.3])
- embedded cracks (see [2.2.4]).

#### 2.2.2 Surface crack

A surface crack is a crack with its opening limited to one plate surface, i.e. not reaching the other plate side. It is represented by a semi-elliptical crack of height  $a$  and length  $2c$  (see Fig 2).

When the surface crack is on the plate edge, it is to be represented by a corner crack of height  $a$  and length  $c$  (see Fig 3).

#### 2.2.3 Through-thickness crack

A through-thickness crack is a crack opened on the two plate surfaces. When the crack is not on the plate edge, it is represented by a rectangular through-thickness crack of length  $2a$  (see Fig 4).

When the through-thickness crack is on the plate edge, it is represented by a rectangular edge through-thickness crack of length  $a$  (see Fig 5).

2.2.4 Embedded crack

An embedded crack is a crack totally inside the plate thickness. It is represented by an elliptical crack of height  $2a$  and length  $2c$  (see Fig 6).

Figure 2 : Surface crack

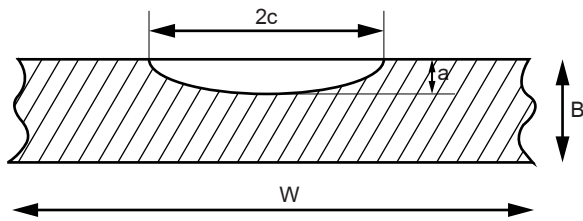


Figure 3 : Edge surface crack

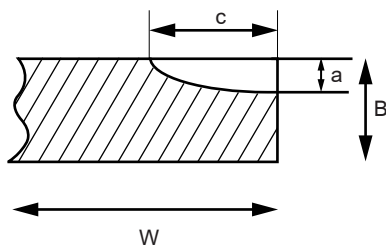


Figure 4 : Interior through-thickness crack

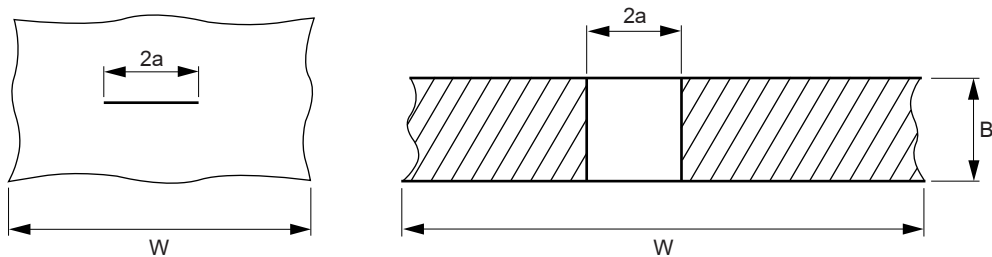


Figure 5 : Edge through-thickness crack

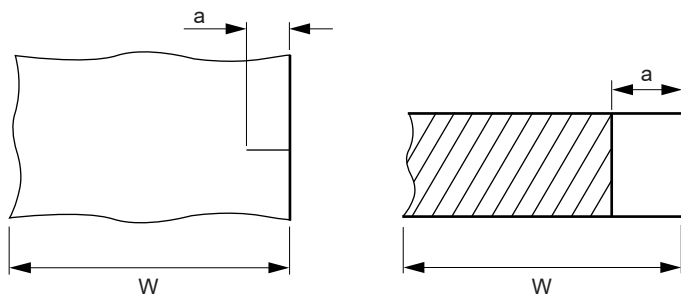
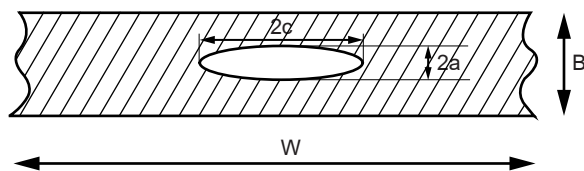


Figure 6 : Embedded crack



## 2.3 Fatigue cracks modeling

### 2.3.1 Crack locations

The fatigue cracks considered in this Section are those located at the weld toes, at the root of partially penetrated welds and at plate edges. The modeling of these different fatigue cracks with the crack models given in [2.2] is described in [2.3.2] to [2.3.4].

### 2.3.2 Weld toe crack

A welded joint presents cracks at the weld toes. Cracks are located at the plate surface, close to the weld toe (see Fig 7).

Cracks at weld toes are modelled by surface cracks (see [2.2.2]).

If the ligament between the surface crack and the other side of the plate fails, then the crack model is changed for a through-thickness crack (see [2.2.3]).

### 2.3.3 Partially penetrated weld root crack

Partially penetrated load carrying joints (see Fig 8) present an internal gap corresponding to an embedded crack of height  $2a$  (see [2.2.4]).

### 2.3.4 Cut edge plate crack

A fatigue crack may develop from a plate cut edge. Edge cracks are modelled using either an edge through-thickness crack (see [2.2.3]) or a semi-elliptical surface crack (see [2.2.2]).

Figure 7 : Examples of weld toe cracks

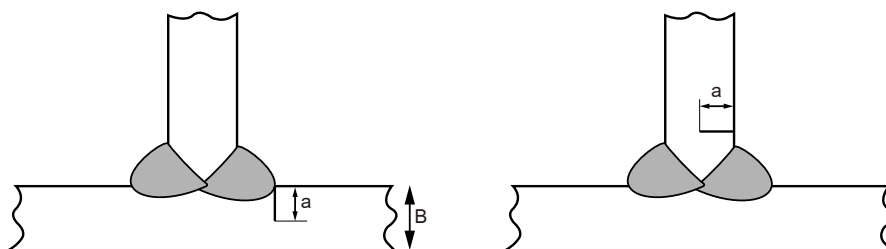
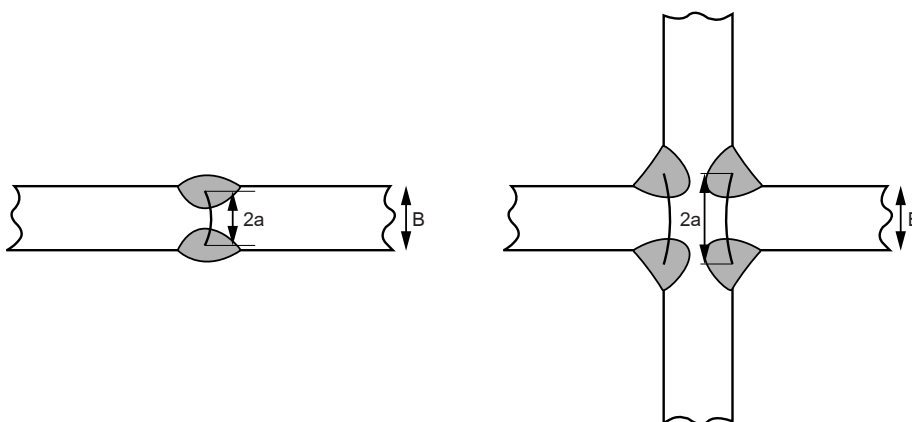


Figure 8 : Examples of weld root cracks



## 2.4 Initial crack size

### 2.4.1 General

Usually, the fatigue life calculated from crack propagation strongly depends on the initial crack size. Several analyses are therefore recommended to be carried out with different initial crack sizes, in order to assess the sensitivity to this parameter.

### 2.4.2 Measured crack size

When the initial crack size was measured during inspection, the uncertainty on the measured crack size depends on the inspection technique. Estimations of the sizing accuracy are given in [7.1.2].

2.4.3 Assumed crack size

If the existence of a crack is assumed, the choice of an initial crack size corresponding to the detectable crack size is recommended. Values of detectable crack sizes for different detection techniques are given in Article [7].

In any case, the initial crack height should be not less than 1 mm.

2.4.4 Depth of surface cracks

The depth of a surface crack found by means of visual inspection is unknown and is to be assumed. The following relationship between the initial crack length and the initial crack depth can be used:

$a_0 = 1/3 \ c_0$

Whenever it is possible, the determination of the initial crack depth by suitable detection techniques is strongly recommended, rather than using the above relationship.

2.4.5 Embedded crack at weld root

For an embedded crack at the root of a partially penetrated weld, the crack height  $2a_0$  corresponds to the estimated size of the non-fused part (see Fig 8). The initial crack length  $c_0$  may be taken as  $c_0 = 10 \ a_0$ .

2.5 Determination of the stresses and stress intensity factors

2.5.1 Stress intensity factor (SIF)

The main parameter for the crack propagation calculation (see [2.6]) and for the assessment against local brittle fracture (see [3.1.4]) is the stress intensity factor (SIF).

The displacements of the crack lips are conventionally decomposed on the three following modes:

- mode I (tension), see Fig 9
- mode II (shear), see Fig 10
- mode III (torsion), see Fig 11.

To each mode corresponds a stress intensity factor:

- $K_I$  (mode I)
- $K_{II}$  (mode II)
- $K_{III}$  (mode III).

For a plate structure, the first mode is generally considered as the most important one. It is why only  $K_I$  is considered in this Guidance Note.

Figure 9 : Displacements of crack lips - Mode I (tension)

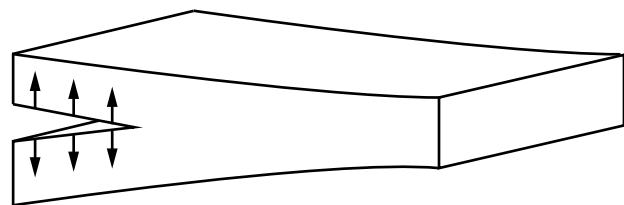


Figure 10 : Displacements of crack lips - Mode II (shear)

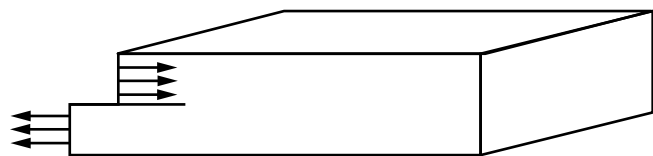


Figure 11 : Displacements of crack lips - Mode III (torsion)





### 2.5.2 Stress and stress intensity factor

The determination of the stress intensity factor  $K_I$  is detailed in Article [4].

When the stress intensity factor  $K_I$  is computed by means of a finite element analysis as per [4.3.3], it is directly obtained from the structural response. However, in many cases,  $K_I$  is computed from the stress in the intact structure, with the analytical formulations given in [4.2].

As a consequence, the word 'stress' is generally used in this Section to describe the structural response in the crack area (e.g. 'stress history', 'stress cycles', 'maximum stress'). If  $K_I$  is directly computed by means of a FEM, the words 'history', 'cycles' and 'maximum' refer to  $K_I$ .

### 2.5.3 Wave induced stress modelling

As mentioned in [1.2.3], the structural response to wave loads is only defined statistically. The different methods described in [5] can be used to derive a loads model suitable for the crack propagation analysis.

### 2.5.4 Maximum stress

For the verification of the failure criteria, the 'maximum stress' (i.e. the stress level that has a given probability of being exceeded) is to be determined using the long-term distribution as described in [5] and in App 2. The probability associated with this maximum stress is typically  $10^{-8}$ , but a different value may be specified in the applicable Rules.

### 2.5.5 Crack path determination

The crack path can be determined considering the direction of the principal stress in the structure. The stresses to be considered are those obtained for the load case leading to the maximum tensile stress. When the 'maximum stress' value is obtained by direct calculation, the equivalent design wave (EDW) technique can be used in order to define the 'maximum tensile stress load case' (see App 1, [5.5]).

The crack path is assumed to be perpendicular to the direction of the principal tensile stress.

## 2.6 Crack propagation

### 2.6.1 Crack propagation law

The crack propagation law used is the Paris's law, defined as follows:

- if  $\Delta K \geq \Delta K_{th}$  :

$$\frac{da}{dn} = C \cdot \Delta K^m$$

- if  $\Delta K < \Delta K_{th}$  :

$$\frac{da}{dn} = 0$$

where:

- $a$  : Crack size parameter
- $\Delta K$  : Applied range of the stress intensity factor  $K_I$
- $\Delta K_{th}$  : Threshold range of  $K_I$ , as given in [6.5]
- $C, m$  : Crack propagation law parameters, as given in [6.5].

The applied range of  $K_I$  is given by:

- when  $K_{max} \geq 0$  and  $K_{min} \geq 0$ :  
 $\Delta K = K_{max} - K_{min}$
- when  $K_{max} \geq 0$  and  $K_{min} < 0$ :  
 $\Delta K = K_{max}$
- when  $K_{max} < 0$  and  $K_{min} < 0$ :  
 $\Delta K = 0$

where:

- $K_{max}$  : Maximum stress intensity factor, corresponding to the maximum stress  $S_{max}$  of the cycle, including the residual stress
- $K_{min}$  : Minimum stress intensity factor, corresponding to the minimum stress  $S_{min}$  of the cycle, including the residual stress.

If the crack growth near the threshold is significant and if the residual stress is proved to be reduced (e.g. due to post weld treatment), then a less conservative crack propagation law can be considered (e.g. British standard BS7910:2013 [8.1.2]).

When the crack has two size parameters  $a$  and  $c$  (case of elliptic or semi-elliptic crack models, see [2.2.2] and [2.2.4]), the crack size increase is to be computed for each size parameter.

2.6.2 Overload effect on the stress intensity factors

The plastic zone at the crack tip plays a large role in the determination of the stress intensity factor range. When an overload occurs, it creates an area of permanent strain. A closure effect results from this plastic zone, reducing thus the stress intensity factor. The effective plastic zone decreases with the crack propagation until the effect of the overloading vanishes, i.e., when the plastic area due to current maximum stress intensity factor is greater than the remaining plastic area due to the overloading.

The crack propagation rate decrease due to overloads is a very complex phenomenon. It is generally not taken into account, which leads to safer results of the crack propagation analysis.

If the phenomenon is taken into account, an equivalent stress intensity factor is used. The principle of the equivalent stress intensity factor calculation consists in determining, at each time, the size of the plastic zone and updating this size as a function of the maximum stress intensity factor level within the cycle and the crack propagation during the cycle. For this purpose, formulae obtained from standards or handbooks can be applied, when duly documented and justified.

2.6.3 Cycle-by-cycle crack growth

The crack propagation law given in [2.6.1] can be used to determine the crack growth cycle by cycle. This procedure is slower than the integration method given in [2.6.4] but, in case the exact order of cycles is known, it is more precise and it allows to take the overload effect described in [2.6.2] into account.

2.6.4 Integration of the crack propagation law

As an alternative to a cycle-by-cycle crack growth, an approximate solution can be obtained by integration of the crack propagation law. This option is applicable to stress loads defined by histograms or distribution functions, and thus it is well adapted to the scope of this Guidance Note. It is quicker than the cycle-by-cycle procedure.

The integration may be performed with a numerical scheme, or analytically if the stress intensity factor formulation and the load history distribution allow it. The sensitivity of the analysis results to the chosen integration step (or cycle block size) is to be verified.

2.7 Crack propagation termination

2.7.1 General

The crack propagation analysis is terminated either when the total load sequence has been applied without failure or when one of the failure criteria is reached.

The applicable failure criteria are described in [3].

2.7.2 Crack interaction and coalescence

If several cracks are considered in the propagation analysis, the analysis is to be modified when these cracks become too close to each other. If two cracks coalesce, a new crack is defined, replacing the two separated cracks (see Fig 12).

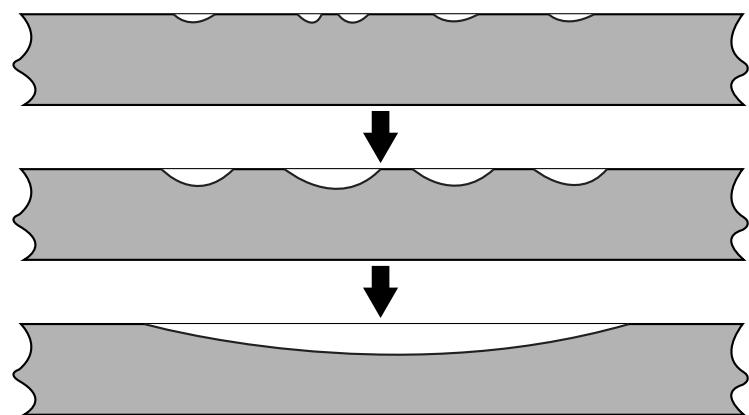
This new crack is then checked against the failure criteria. The crack propagation analysis may then resume with the new crack geometry. Criteria for crack interaction and rules for the definition of the coalesced crack are given in British Standard BS7910:2013 [7.1.2].

2.7.3 Crack breakthrough

The failure of the ligament between the plate surface and a surface crack (see [2.2.2]) or an embedded crack (see [2.2.4]) does not necessarily lead to the propagation termination, if leakage is not considered as a failure criteria.

In this case, the crack is re-characterized as a through-thickness crack and re-assessed. If the re-characterized crack does not fail, the crack propagation analysis may then resume with this new crack geometry (see [1.2.4]).

Figure 12 : Coalescence of multiple surface cracks



### 3 Failure criteria

#### 3.1 Failure modes

##### 3.1.1 General

One or several criteria, defining the end of the crack propagation phase, need to be chosen. Typical criteria are defined in [3.1.2] to [3.1.6].

##### 3.1.2 Specified maximum acceptable crack size

For this criterion, the maximum acceptable crack size is defined a priori. It is a contractual value recognized as safe for a given structure and material.

##### 3.1.3 Detectable leakage

Due to crack propagation, a surface crack may become a through-thickness crack, as described in [2.7.3].

Through-thickness cracks in pipes or in plates may lead to leakage before failure, which can be specified as non-acceptable. In this case, the re-characterization of a surface crack into a through-thickness crack becomes a failure criterion.

##### 3.1.4 Brittle local fracture and failure assessment diagram

This criterion corresponds to an applied stress intensity factor  $K_I$  exceeding the material critical stress intensity factor  $K_{mat}$ , or a point  $(K_r, L_r)$  out of the safe domain of the failure assessment diagram as defined in [3.2].

The value of  $K_{mat}$  can be obtained as described in [6.4].

##### 3.1.5 Local ductile failure

For non-brittle materials (e.g. aluminium alloys, stainless steel), a local ductile failure criterion can be used instead of the failure assessment diagram. The local ductile fracture can be considered as occurring when the stress or strain level in the remaining ligament (i.e. the non-failed material of the component in front of the crack tip) exceeds the material ultimate acceptable strength.

A conventional value for the ultimate acceptable strength is used and the failure occurs when:

$$S_{max} > S_{flow}$$

where:

$S_{max}$  : Maximum stress corresponding to the most severe load case, including the residual stress

$$S_{flow} = \text{Min}\left(\frac{S_y + S_u}{2} ; 1,2 S_y\right)$$

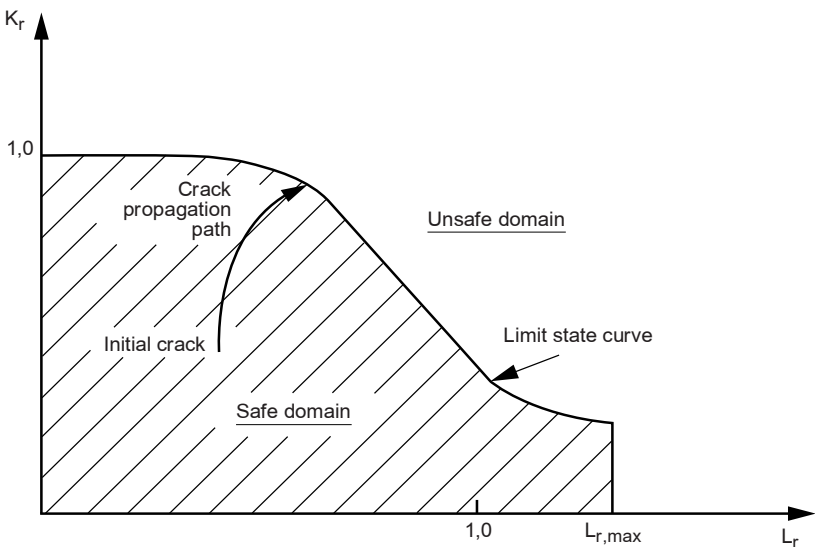
When the material stress-strain ( $S$ - $\epsilon$ ) curve is known, the following alternative criterion is recommended, for which the failure occurs when:

$$\epsilon_{max} > \epsilon_u$$

where:

$\epsilon_{max}$  : Maximum strain corresponding to  $S_{max}$ .

Figure 13 : Failure assessment diagram



### 3.1.6 Full collapse

The full collapse corresponds to the situation when the entire component is broken. It can occur in a redundant structure where the crack can develop throughout a component without brittle or ductile fracture.

## 3.2 Failure assessment diagram (FAD)

### 3.2.1 General

For materials presenting a possible brittle fracture, brittle fracture and ductile failure limit states interact so that checking the crack failure using the two associated criteria separately is not sufficient. The interaction between these two limit states is taken into account by the failure assessment diagram (FAD) criterion.

### 3.2.2 Principles

The FAD determines, in the space of the two parameters  $K_r$  and  $L_r$ , the limit state curve that separates the safe domain, where there is no risk of brittle or ductile fracture, from the unsafe domain (see Fig 13).

The vertical axis  $K_r$  of the FAD represents the ratio of the applied stress intensity factor to the material fracture toughness. The horizontal axis  $L_r$  represents the ratio of the applied load to the load required to cause ductile failure of the section. For a given crack and a given load,  $L_r$  and  $K_r$  are determined as described in [3.2.5] and [3.2.6], respectively.

The safe domain is bounded by:

- the limit state curve, and
- a maximum stress criterion.

The limit state curve  $K_r = f(L_r)$  describes the interaction between the ductile and fragile failure modes. The curve is obtained from the tensile properties of the material, using either [3.2.7] or [3.2.8] depending on the availability of the detailed material stress-strain relationship.

### 3.2.3 Primary and secondary stresses

For the assessment of the load ratio  $L_r$  and the fracture ratio  $K_r$  as defined in [3.2.4] and [3.2.5], a difference shall be made between the primary stresses and the secondary stresses. Indeed only the primary stresses are to be taken into account for the calculation of  $L_r$  while both primary and secondary stresses are to be considered for the calculation of  $K_r$ .

Primary stresses are stresses required to equilibrate external mechanical loads. These stresses arise from locally load-controlled conditions. These stresses are considered to be the only ones contributing to the plastic collapse.

Secondary stresses are self-equilibrating stresses satisfying the structure compatibility. These stresses arise from locally displacement-controlled conditions. Typically residual stresses would fall in this category in the general case.

When in doubt regarding the classification of stresses, the stresses should conservatively be treated as primary stresses.

For additional explanations regarding stress classification methodology, refer to BS7910:2016, §6.4, §7.1.6 and §7.1.9.

### 3.2.4 Load ratio $L_r$

The load ratio  $L_r$  is given by:

$$L_r = S_{\text{Max}} / S_Y$$

where:

$S_{\text{Max}}$  : Primary maximal stress in the cracked component for the most severe load case.

Alternatively, the load ratio can be defined from a limit load approach as follows:

$$L_r = \frac{P}{P_L(a, S_Y)}$$

where:

$P$  : Load for the most severe load case

$P_L(a, S_Y)$  : Limit load for flaw size  $a$  and yield strength  $S_Y$  obtained in elastic-perfectly plastic limit load analysis

$a$  : Flaw size including any ductile tearing

$S_Y$  : Yield strength

This definition is advantageously used when FEM is applied to determine  $L_r$ , as it does not require to classify the FEA stress into primary and secondary stresses. Additional explanations regarding  $L_r$  calculation methods can be found in BS7910:2016, Appendices P.2, P.3 and B5.5.

### 3.2.5 Fracture ratio $K_r$

The fracture ratio  $K_r$  is given by:

- if  $K_{I,s} \leq 0$

$$K_r = \frac{K_{l,p}}{K_{mat}}$$

- if  $K_{l,s} > 0$

$$K_r = \frac{K_{l,p} + V \cdot K_{l,s}}{K_{mat}}$$

where:

- $K_{l,s}$  : Stress intensity factor due to the secondary stress
- $K_{l,p}$  : Stress intensity factor due to the maximum tensile primary stress
- $K_{mat}$  : Material critical stress intensity factor
- $V$  : Correction factor for plasticity, determined as follows:

- for  $L_r \leq 1,05$ :

$$V = \text{Min} \left[ 1 + 0,2 L_r + 0,02 K_{l,s} \frac{L_r}{K_{l,p}} (1 + 2 L_r) ; 3,1 - 2 L_r \right]$$

- for  $L_r > 1,05$ :

$$V = 1,00$$

3.2.6 Stress criterion

The stress criterion is  $L_r < L_{r,max}$  with:

$$L_{r,max} = \left( \frac{S_Y + S_u}{2 S_Y} \right)$$

In any case:  $L_{r,max} < 1,2$

3.2.7 Limit state curve - Case 1

When the material yield stress and the tensile strength are known but the stress-strain relationship is not known, the definition of the limit state curve given in Tab 1 is used. This definition depends on whether the material stress-strain curve is continuous or has a discontinuous yielding (i.e. a Lüders plateau). Most of construction steels have a discontinuous yielding.

3.2.8 Limit state curve - Case 2

When the stress-strain relationship is known, a more precise limit state curve can be determined, as follows:

$$f(L_r) = \left( \frac{E \cdot \epsilon_r}{L_r \cdot S_Y} + \frac{L_r^3 \cdot S_Y}{2 E \cdot \epsilon_r} \right)^{-0,5}$$

where:

- $\epsilon_r$  : True strain, corresponding to the true stress  $S_r = L_r \cdot S_Y$  on the stress-strain curve.

This limit state curve is usually not applicable to the heat-affected zone in the vicinity of welds, where the prescriptions of [3.2.7] are to be applied.

Table 1 : Limit state curve - Case 1

Material	$L_r < 1,0$	$L_r = 1,0$	$1,0 < L_r \leq L_{r,max}$
• with a continuous stress-strain curve	$f(L_r) = \left(1 + \frac{1}{2}L_r^2\right)^{-0,5} [0,3 + 0,7 \exp(-\mu L_r^6)]$		$f(L_r) = f(L_r = 1) \cdot L_r^{\frac{N-1}{2N}}$
• with a discontinuous stress-strain curve	$f(L_r) = \left(1 + \frac{1}{2}L_r^2\right)^{-0,5}$	$f(L_r) = \left(\lambda + \frac{1}{2\lambda}\right)^{-0,5}$	
<b>Note 1:</b>  $\mu = \text{Min}\left[0,001 \frac{E}{S_Y} ; 0,6\right]$  $N = 0,3 \left(1 - \frac{S_Y}{S_u}\right)$  $\lambda = 1 + \frac{E \cdot \Delta \varepsilon}{R_{el}}$  $\Delta \varepsilon, R_{el}$ : Characteristics of the Lüders plateau in the stress-strain curve: $\Delta \varepsilon$ is the strain increase without stress increase, occurring at the lower yield stress $R_{el}$ If it is not known, $\Delta \varepsilon$ can be estimated by: $\Delta \varepsilon = 0,0375 (1 - 0,001 S_Y)$			

## 4 Determination of the stress intensity factors

### 4.1 General

**4.1.1** The stress intensity factor  $K_I$  may be calculated using either a closed-form expression for standard crack shapes or a finite element approach.

### 4.2 Stress intensity factors by closed-form expression

#### 4.2.1 General

Calculations of the fracture mechanics are based on the total stress at the crack tip location. This stress is determined assuming that no crack is present. Therefore, the stress to be considered as the input of the  $K_I$  formulation is the hot spot stress (or the local nominal stress for a plate edge crack) calculated according to the prescriptions in Sec 3, Sec 4, Sec 5 or Sec 6, depending on the type of structure and the structural analysis approach.

#### 4.2.2 Reference formulation

The reference formulation of  $K_I$  is given for an interior through-thickness crack in an infinite plate (see [2.2.3]):

$$K_I = \sigma \sqrt{\pi \cdot a}$$

where:

- $\sigma$  : Stress in the plate
- $a$  : Crack size parameter.

#### 4.2.3 Correction functions

The formulation of  $K_I$  for configurations different from the reference one are derived from the reference formulation in [4.2.2], applying different correction factors accounting for the crack geometry, the finite width effect, the presence of shell bending stress, of stress concentration effects.

The general form is:

$$K_I = (\sigma \cdot Y_u) \sqrt{\pi \cdot a}$$

where  $Y_u$  is a universal correction function.

The term  $(\sigma \cdot Y_u)$  is typically decomposed into different stress components and different corrections functions:

$$K_I = (\sigma_p \cdot Y_p + \sigma_s \cdot Y_s) \sqrt{\pi \cdot a}$$

where:

- $\sigma_p$  : Primary stress due to loads
- $Y_p$  : Geometrical factor for the primary stress, as defined in [4.2.4]
- $\sigma_s$  : Secondary stress due to displacement/strain controlled conditions, typically residual or thermal stresses
- $Y_s$  : Geometrical factor for the secondary stress, as defined in [4.2.5].

#### 4.2.4 Primary stress geometrical factor $Y_p$

The primary stress geometrical factor  $Y_p$  is the combination of correction functions accounting for:

- the finite width of the plate in which the crack propagates
- the crack geometry, and
- the local stress concentration due to the weld geometry.

In many  $K_I$  formulations, the primary and secondary stresses are decomposed into a membrane stress and a shell bending stress. Different geometrical correction factors are defined for the membrane and bending stresses.

The primary stress geometrical factor  $Y_p$  is given by:

$$\sigma_p \cdot Y_p = f_w (\sigma_{pm} \cdot Y_m \cdot M_{k,m} + \sigma_{pb} \cdot Y_b \cdot M_{k,b})$$

where:

- $f_w$  : Finite width correction factor
- $\sigma_{pm}, \sigma_{pb}$  : Primary stress membrane and bending components, respectively
- $Y_m, Y_b$  : Geometrical factors in standard configuration, for the membrane stress and the bending stress, respectively
- $M_{k,m}, M_{k,b}$  : Geometrical factors accounting for the weld local geometry, for the membrane stress and the bending stress, respectively.

The formulae to calculate these factors are given in the British Standard BS 7910:2013 Annex M (Stress intensity factor solutions) and in the International Institute of Welding document IIW-1823-07 (Recommendations for Fatigue Design of Welded Joints and Components). Their use is to be duly documented and justified.

Other standards or handbooks may be used with the agreement of the Society, when duly referenced.

#### 4.2.5 Secondary stress geometrical factor $Y_s$

The secondary stresses are self-equilibrating stresses, typically residual or thermal stresses. Secondary stresses need to be considered in the case of welded joints (see [1.2.5]).

The secondary stress geometrical factor accounts for the crack geometry. It is given by:

$$\sigma_s \cdot Y_s = \sigma_{sm} \cdot Y_m + \sigma_{sb} \cdot Y_b$$

where:

$\sigma_{sm}$ ,  $\sigma_{sb}$  : Secondary stress membrane and bending components, respectively

$Y_m$ ,  $Y_b$  : Geometrical factors in standard configuration, for the membrane stress and the bending stress, respectively.

The formulae to calculate these factors are given in the British Standard BS 7910:2013 Annex M (Stress intensity factor solutions) and in the International Institute of Welding document IIW-1823-07 (Recommendations for Fatigue Design of Welded Joints and Components).

$\sigma_{sm}$  and  $\sigma_{sb}$  may be found in Annex Q of BS 7910:2013 for some configurations.

Other standards or handbooks may be used with the agreement of the Society, when duly referenced.

### 4.3 Stress intensity factors by the finite element method (FEM)

#### 4.3.1 General

The stress intensity factor  $K_I$  can also be determined by finite element method calculations. Different solutions are available.

#### 4.3.2 Use of weight functions

The finite element method can be used to determine the stress distribution in the absence of the crack. The stress intensity factor  $K_I$  is then computed by integration of the stress multiplied by a weight function, over the extent of the crack.

The formulation of  $K_I$  is:

$$K_I = \int_{x=0}^{x=a} \sigma(x) \cdot h(x, a) \cdot dx$$

where:

$h(x,a)$  : Weight function depending on the crack type.

The formulae for the weight functions are given in fracture mechanics handbooks and in the International Institute of Welding document IIW-XIII-2259-15/XV-1440-13 (Recommendations for Fatigue Design of Welded Joints and Components) paragraph 6.2.4.2.

#### 4.3.3 Direct determination of $K_I$

This is the most accurate approach. The crack is explicitly introduced in the FEM model of the structure, and  $K_I$  is determined from the FEM results in the vicinity of the crack tip. A very fine mesh is required. Due to the singularity at this location, special element formulations are to be used at the crack tip. A common solution is the use of quadratic iso-parametric elements with mid-side nodes located at a fourth of the edge in the direction of the crack tip.

The finely meshed area may be directly embedded in the FEM model, or treated with a sub-modelling technique (crack box).

The FEM model needs to be updated as the crack propagates, to take into account the relocation of the crack tip and the stress redistribution. The crack propagation is modelled step by step, following a path that can be either pre-selected or determined during the propagation. A pre-selected path allows the usage of more computationally efficient techniques, such as line spring elements coupled with a crack box. Otherwise, re-meshing tools are necessary.

Alternatively, XFEM can be used in order to overcome the conventional FEM limitations such as the need for re-meshing or the pre-selection of the crack path.

## 5 Wave loads modelling

### 5.1 General

**5.1.1** The purpose of this Article is to provide a guidance for the determination of a loading scenario for the crack propagation analysis.

### 5.1.2 Stochastic loads

The wave induced loads on marine and offshore structures have a stochastic nature, both on the short term (typically three-hour sea states) and on the long term (sequence of sea states). The variability of the wave loading needs to be taken into account at these two time scales when the loading history for the crack growth analysis is created.

### 5.1.3 Influence of the cycle order

The values of the stress intensity factor depend on both the loads and the size of the existing crack. Considering a given distribution of stress cycles and a given initial crack, the crack propagation will be very different if the process starts with the highest cycles in decreasing order or starts from the lowest cycles in increasing order. Ideally the propagation calculation should be carried out following the exact stress range variation cycle by cycle, but this exact cycle order is generally not known.

This effect introduces an additional complexity in the treatment of wave loadings, compared with Miner sum approach for fatigue.

#### 5.1.4 Loading conditions

The different loading conditions encountered by the ship/offshore units during the simulation need to be taken into account:

- for the determination of the wave loading as described in Article [5]
- by additional load cycles created by the change in the still water loads during loading and unloading. These load cycles should be determined following the prescriptions given in Sec 11 [2.4.6] for the rule based approach, and in Sec 11, [3.8.2] for direct calculation approaches.

## 5.2 Short-term analysis

### 5.2.1 General

The typical duration of the fatigue analysis is much longer than the duration of a short-term condition. Therefore, the short-term analysis described in this sub-article is to be used in combination with long-term analysis procedures based on sea state sequences (see [5.3]).

### 5.2.2 Short-term variability

The stochastic process of the wave elevation during a sea state (typically three hours) is usually described by an energy density spectrum, characterized by its  $H_s$  (significant height) and  $T_z$  (mean zero up-crossing period) or  $T_p$  (mean peak period) (see App 2). The structural response to the wave induced loads can then be determined with a coupled hydro-dynamic and structural model, yielding either stress time series or statistical distributions of stress cycles.

### 5.2.3 Stress time series

When feasible, time series of the structural response should be produced using a hydro-structural model as described in App 1, [3].

For each short-term condition, a realization of the irregular wave is constructed as described in Sec 11, [4.3.1]. The time history of the structural response is then obtained either from a time-domain simulation, or by applying a stress transfer function (including amplitude and phase) previously determined by a hydro-structural model (see Fig 14).

The stress range sequence is determined from the stress time history by the ‘simple-range counting’ method. In this method, positive ranges are considered, i.e. ranges between a local minimum value and the following local maximum value, as illustrated in Fig 15.

In the stress time series, the cycles are randomly ordered, but this order will vary from one realization of the considered sea state to another one, leading to different crack growth speeds. Therefore, several simulations of the same sea state should be performed in order to estimate the mean short-term crack growth and its variability.

**Figure 14 : Stress time series (example)**

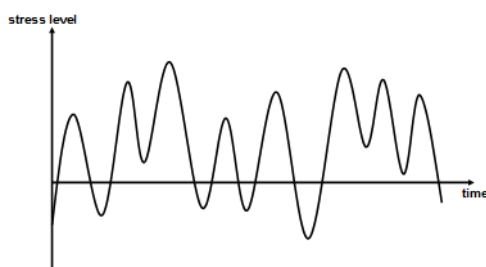
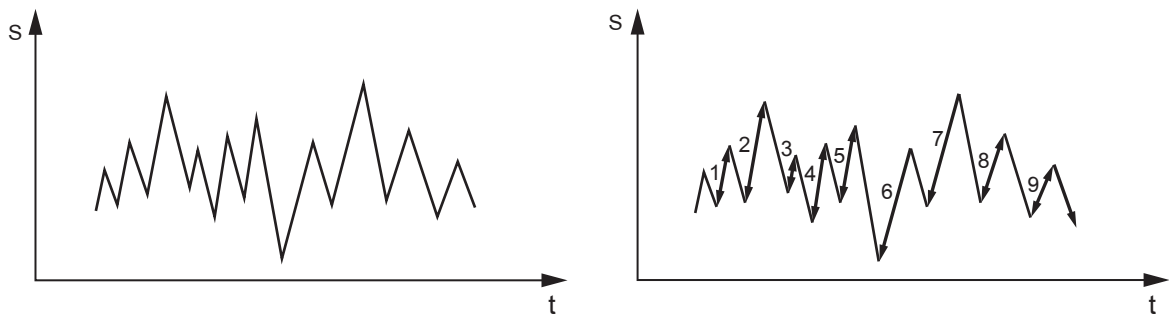




Figure 15 : Simple range counting method: stress time signal (on the left) and counting sequence (on the right)



5.2.4 Short-term statistical distributions

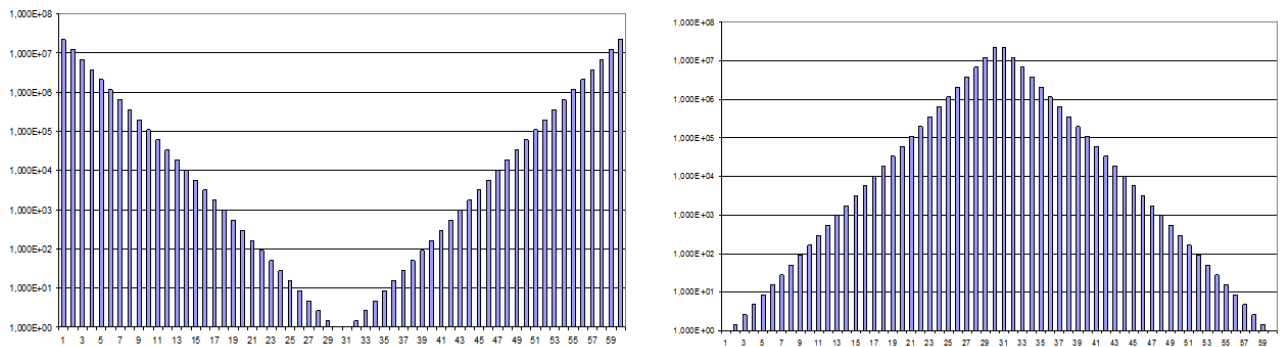
If a spectral approach is used for the hydro-structure analysis, then the wave induced stress is obtained in the form of a short-term statistical distribution. With a statistical distribution, the order of the cycles is unknown, and is to be assumed.

The crack propagation is calculated, considering:

- a) a decreasing then increasing sequence, starting from the maximum cycle, decreasing to the minimum cycle during the first half-time and then increasing to the maximum cycle during the second half-time (see Fig 16, left hand side)
- b) an increasing then decreasing sequence, starting from the minimum cycle, increasing to the maximum cycle during the first half-time and then decreasing to the minimum cycle during the second half-time (see Fig 16, right hand side).

Unless the failure occurs during the considered short-term analysis, the final crack sizes obtained with the two hypotheses are not too different and the final crack size at the end of the sea state is taken equal to the mean value of the two results.

Figure 16 : Short-term histograms of  $\Delta S$ , in decreasing-increasing order (on the left) and increasing-decreasing order (on the right)



5.3 Long-term analysis based on sea state sequences

5.3.1 Sea state sequence variability

The time period during which the crack propagation is to be performed (i.e. the residual expected life) can be anticipated to be in a range from a few weeks to a few years. During this time period, the number of encountered sea states is in the range from a few hundreds to a few thousands. These sea states need to be selected from the long-term wave statistics, and put in a certain order. Different modelling procedures for the sequence of sea states are given in [5.3.2].

In this process, the duration of the crack propagation, the seasons and the occurrence of storms and calm sea periods should ideally be taken into account. Therefore the best model to be accounted for the sea state sequence variability is the storm model, described in [5.3.4].

5.3.2 Sequence definition

When the total loading history is built from the concatenation of short-term conditions, these conditions are to be selected and ordered:

- from meteorological observations and recording if available: in such a case, the exact series of sea states can be used
- by Monte Carlo draws: in such a case, different series are to be considered as each series will provide different crack propagation results

- using simple sequences as described in [5.3.3]
- using storm models as described in [5.3.4].

The series of sea states to be considered are to be determined either from the scatter diagram of the ship route or the offshore unit location, as given in App 1, [2], or from meteorological observation statistics. The definition of the short-term conditions sequence must also take into account the different loading conditions of the ship or offshore unit, the fraction of time spent in each of them and the typical periodicity of the loading and unloading.

### 5.3.3 Simplified sequences of sea states

A simple approach consists in defining sea state sequences, sorting them according to their severity with respect to the ship or offshore unit structural response. This procedure can be improved by splitting the total simulation into repeated annual periods (or into seasonal periods in order to take into account the influence of seasons on the wave statistics).

For each considered period (total simulation, year or season period), the statistical distribution of sea states is taken from the long-term wave statistics (see App 2). The combination of the sea states with the operation conditions (forward speed, wave direction) defines a list of short-term conditions. These short-term conditions are taken one after the other, considering the following sequences:

- an increasing then decreasing sequence, starting from the less severe short-term condition and increasing to the most severe one during the first half-time and then decreasing to the less severe one during the second half-time
- a decreasing then increasing sequence, starting from the most severe short-term condition and decreasing to the less severe one during the first half-time and then increasing to the most severe one during the second half-time.

The severity of the short-term conditions with regard to the crack propagation is estimated from the short-term statistics of structural response, if possible, or from the short-term statistics of the load parameters that are relevant for the considered structural detail.

The crack propagation is calculated for each sequence of sea states as described in [5.3.5].

If the sequence is shorter than the total simulation time, then the sequence is repeated until the total simulation is done or until failure, whichever comes first (e.g. an annual sea state sequence is repeated N times, N being the target fatigue life in years).

The precision of this method for determining the fatigue life is equal to, or larger than, the sequence duration. If the failure occurs during one sequence, then the failure is considered to have occurred at the beginning of the sequence. The duration of each sequence should not be reduced further than what the underlying long-term wave statistics allow (typically not less than one year, unless seasonal wave statistics are used).

A single decreasing sequence over the entire simulation period, starting from the most severe short-term condition and reaching the less severe one can also be considered as a preliminary approach, this sequence being very conservative.

### 5.3.4 Sequences of sea states based on storm models

In order to be more representative of the actual wave environment, the sequence of short-term conditions can be organized in terms of storms and calm sea periods.

A storm is a sequence of several short terms conditions involving a growing phase and a decreasing phase. It is characterized by its duration, its maximum sea state significant height, and the position in time of the maximum sea state.

Calm sea periods, with randomly chosen moderate sea states, are inserted between the storms (see Fig 17).

The storms and the calm sea periods, with their operation conditions, are to be ordered:

- from meteorological observations and recording if available: in such a case, the exact series of storms can be used
- by Monte Carlo draws: in such a case, different series are to be considered, as each series will provide a different crack propagation result.

The crack propagation is calculated as described in [5.3.5].

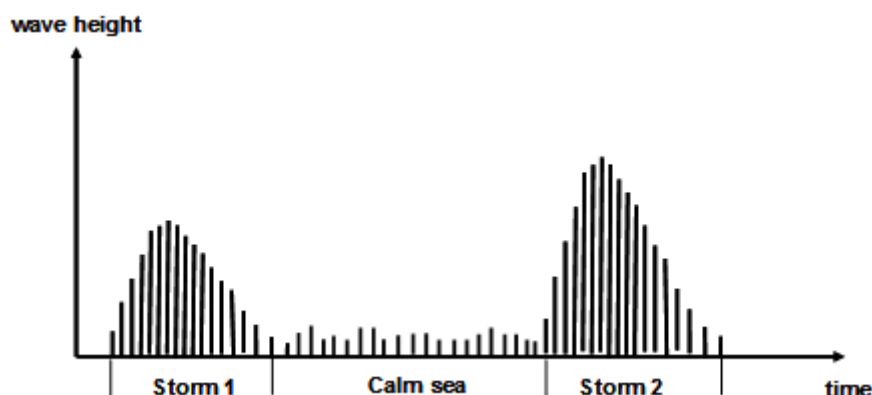
### 5.3.5 Combination of short-term analyses

Each sea state sequence is treated as follows:

- the initial crack size is defined
- the crack growth for the first sea state is determined, using one of the procedures described in [5.2]
- if the failure criterion is not reached during the short-term analysis, the next sea state is analyzed, starting from the updated crack size.

The procedure ends either with the failure or after all the sea states in the sequence have been analyzed.

Figure 17 : Storms and calm sea periods



## 5.4 Long-term analysis based on stress histogram

### 5.4.1 General

When building long-term structural response time history is practically not feasible, or when the structural response can be characterized by a single parameter (e.g., the tension in a mooring line), methods based on long-term distributions of cycles can be used.

For each loading condition, the long-term distribution of cycles can be obtained from a simplified rule based approach as described in [5.4.2] or from a direct calculation approach as described in App 1, [5].

The long-term distributions for the different loading conditions should then be combined, taking into account the fraction of time spent in each of them and the typical periodicity of the loading and unloading.

The order of occurrence of the cycles is unknown and thus is to be assumed. Two procedures for creating sequences of cycles for crack growth analysis are described in [5.4.3] and [5.4.4].

### 5.4.2 Stress long-term distribution obtained from rule based approach

The long-term distribution of stress ranges is taken as a Weibull function. Its complementary cumulative distribution function is given by:

$$\bar{P}(\Delta\sigma) = \exp\left(-\left(\frac{\Delta\sigma}{\lambda}\right)^\xi\right)$$

where:

$$\lambda = \frac{\Delta\sigma_{ref}}{(\ln(1/P_{ref}))^{1/\xi}}$$

with

$$\Delta\sigma_{ref} = \text{Max}_i(\Delta\sigma_{RF,i(j)})$$

and

$\Delta\sigma_{RF,i(j)}$  : Reference stress range in load case (i) of loading condition (j) obtained in Sec 11, [2.2]

$\xi$  : Weibull shape parameter,  $\xi = 1$ , except otherwise specified by the applicable rules

$P_{ref}$  : Reference probability level of exceedance associated to the reference fatigue stress range (see Sec 2, [1.3.1])

The total number of cycles per year can be determined as prescribed in Sec 11, [2.4.3].

### 5.4.3 Simplified sequences of cycles

A simple approach consists in defining cycle sequences, sorting them according to their stress range. This procedure can be improved by splitting the total simulation into repeated annual periods (or into seasonal periods, in order to take into account the influence of seasons on the wave statistics).

For each considered period (total simulation, annual or seasonal period), the long-term distribution of cycles is further split into two identical long-term distributions, i.e., for each class of cycles in the histogram, the number of cycles is divided by two. Then the following two sequences are considered:

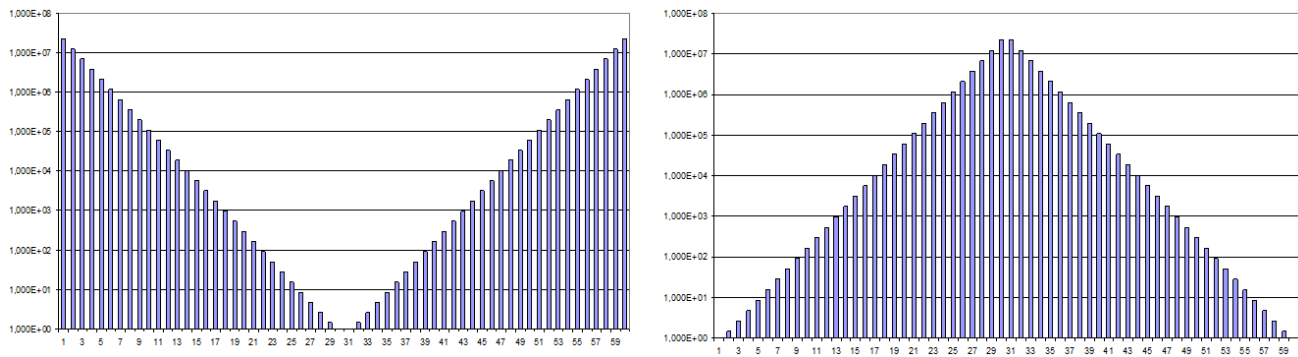
- a decreasing then increasing sequence, starting from the maximum cycle, decreasing to the minimum cycle during the first half-time and then increasing to the maximum cycle during the second half-time (see Fig 18, left hand side)
- an increasing then decreasing sequence, starting from the minimum cycle, increasing to the maximum cycle during the first half-time and then decreasing to the minimum cycle during the second half-time (see Fig 18, right hand side).

The crack propagation is calculated for each sequence. Unless the failure occurs during one of the sequences, the crack sizes obtained with the two hypotheses are not too different, and the final crack size is taken as the mean value of the two results.

If the sequence is shorter than the total simulation time, then the sequence is repeated until the total simulation is done or until failure, whichever comes first (e.g. an annual cycle sequence is repeated N times, N being the target fatigue life in years).

The precision of this method for determining the fatigue life is equal to, or larger than, the sequence duration. If the failure occurs during one sequence, then the failure is considered to have occurred at the beginning of the sequence. The duration of each sequence should not be reduced further than what the underlying long-term wave statistics allow (typically not less than one year, unless seasonal wave statistics are used).

**Figure 18 : Long-term histograms of  $\Delta S$ , in decreasing-increasing order (on the left) and increasing-decreasing order (on the right)**



**5.4.4 Sequences of cycles based on storm model**

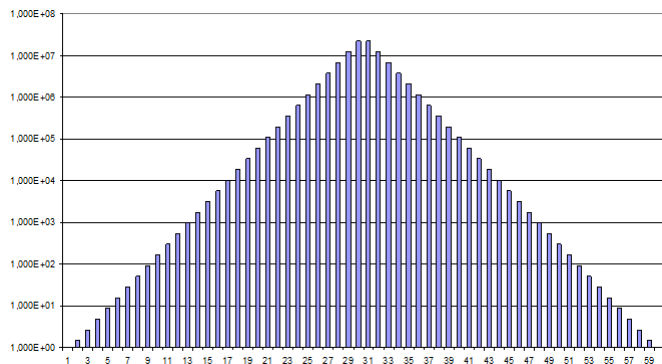
In a similar way as what is described in [5.3.4] for the sequences of sea states, a storm model can be adopted to define sequences of cycles in a more realistic way (see Fig 19).

The storms and the calm sea periods, with the associated operation conditions, are to be ordered:

- from meteorological observations and recording if available: in such a case, the exact series of storms can be used
- by Monte Carlo draws: in such a case, different series are to be considered, as each series will provide a different crack propagation result.

The crack propagation is calculated using the cycle sequence resulting from the sequence of storms and calm sea periods.

**Figure 19 : Histograms of  $\Delta S$  for a storm in increasing-decreasing order**



**6 Material characteristics**

**6.1 General**

**6.1.1** The material characteristics for ship and offshore structures are given in NR216 Rules on Materials and Welding for the Classification of Marine Units.

Other values may be used when duly documented and justified.

## 6.2 Young modulus

### 6.2.1 Default values

The following values are to be applied, unless actual values are available for the analyzed structure:

- for steel:  $E = 206000 \text{ MPa}$
- for aluminium alloys:  $E = 70000 \text{ MPa}$ .

## 6.3 Yield stress and tensile strength

### 6.3.1 Base metal

The minimum requirements of yield stress and tensile strength are given in:

- NR216, Ch 2, Sec 1 for steel and iron products, rolled steel plates, sections and bars
- NR216, Ch 2, Sec 2 for steel pipes, tubes and fittings
- NR216, Ch 2, Sec 3 for steel forging
- NR216, Ch 2, Sec 4 for steel casting
- NR216, Ch 2, Sec 5 for iron casting
- NR216, Ch 3, Sec 1 for copper and copper alloys
- NR216, Ch 3, Sec 2 for aluminium alloys
- NR216, Ch 4, Sec 2 for offshore mooring chain, cables and accessories.

The actual yield stress values are higher than the minimum values so, when analyzing an accident or a return of experience case, higher values may be applied when duly documented and justified.

### 6.3.2 Welded zone

In the heat-affected zone of a weld, the material characteristics vary between those of the base metal and those of the weld metal.

When determining the welding residual stress, the practice is to consider the minimum yield stress between the base metal and the weld metal. This may be taken into account when duly documented and justified.

## 6.4 Toughness

### 6.4.1 General

The material toughness can be given in different ways:

$C_V$  : Charpy V-notch impact energy, in J

$K_{mat}$  : Material critical stress intensity factor, in  $\text{MPa}\cdot\text{m}^{0.5}$ , taking into account the crack/plate geometry.

In the industry and the classification rules, the toughness is given in Charpy V-notch impact energy, while the material critical stress intensity factor  $K_{mat}$  is required for the verification of failure criteria during crack propagation. Correlations between these two characteristics are given in [6.4.6], [6.4.7] and [6.4.8], but these correlations are very conservative. It is why the direct measurement of  $K_{mat}$  at the service temperature is always preferable to the usage of correlations.

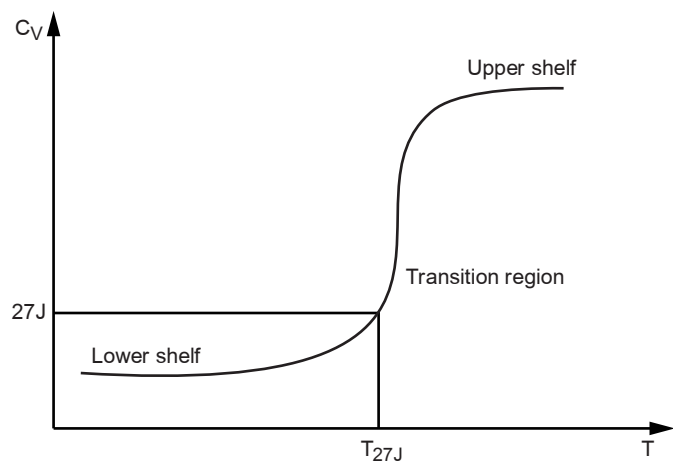
### 6.4.2 Influence of the temperature

The material toughness depends on the temperature. Three regions are considered in the toughness versus temperature curve: the lower shelf region, the transition region and the upper shelf region (see Fig 20).

In terms of Charpy V-notch impact energy, the transition region is conventionally characterized by the temperature  $T_{27J}$  at which the impact energy is equal to 27 J.

In terms of material critical stress intensity factor, the transition region is conventionally characterized by the temperature  $T_0$  at which  $K_{mat}$  is equal to  $100 \text{ MPa}\cdot\text{m}^{0.5}$  for a 25 mm thick specimen.

Figure 20 : Toughness versus temperature curve



6.4.3 Base metal Charpy V-notch impact energy

The minimum requirements of toughness are given in:

- NR216, Ch 2, Sec 1 for steel and iron products, rolled steel plates, sections and bars
- NR216, Ch 2, Sec 2 for steel pipes, tubes and fittings
- NR216, Ch 2, Sec 3 for steel forging
- NR216, Ch 2, Sec 4 for steel casting
- NR216, Ch 4, Sec 2 for offshore mooring chain, cables and accessories.

Actual Charpy V-notch impact energy values are generally higher, so, for the analysis of an accident or a return experience, higher values may be applied when duly documented and justified. When Charpy V-notch impact energy is determined by testing, the tests are to be performed in conformity with NR216, Ch 1, Sec 2, [4].

For a low temperature use, stainless steel and aluminium alloys are not brittle, at any temperature, so no toughness is specified.

6.4.4 Welded zone Charpy V-notch impact energy

When necessary, the toughness in the welded zone is to be determined by testing, as defined in NR216, Ch 1, Sec 2, [4].

6.4.5 Critical stress intensity factor at service temperature

The brittle failure criterion uses the critical stress intensity factor  $K_{mat}$ . For the assessment of the remaining fatigue life,  $K_{mat}$  needs to be taken at the actual service temperature.

Direct measurement of  $K_{mat}$  at the service temperature is always preferable. If this is not possible,  $K_{mat}$  can be estimated from the Charpy V-notch test results, using the correlations given in [6.4.6], [6.4.7] and [6.4.8], or in British Standard BS7910:2013.

6.4.6 Correlation between Charpy V-notch transition temperature and  $K_{mat}$

$K_{mat}$ , in  $MPa \cdot m^{0.5}$ , at the service temperature, can be estimated from the Charpy V-notch test results using the following correlation between  $K_{mat}$  and the transition temperature  $T_{27J}$ :

$$K_{mat} = 20 + [11 + 77 e^{0,019(T - T_0 - T_K)}] \left( \frac{25}{B} \right)^{0,25} [-\ln(1 - P_f)]^{0,25}$$

where:

- T : Service temperature, in deg
- $T_0$  : Temperature for a median toughness of  $100 MPa \cdot m^{0.5}$  in 25 mm thick specimens
- $T_K$  : Temperature term describing the uncertainty on the Charpy versus fracture toughness correlation
- B : Plate thickness, in mm
- $P_f$  : Probability of  $K_{mat}$  being less than the estimated value. The use of  $P_f = 0,05$  is recommended.

$T_0$  can be estimated from  $T_{27J}$ , using the following relationship:

$$T_0 = T_{27J} - T_{offset}$$

Except when more accurate information is available for the considered material, the following values should be considered:

- $T_K = +25^\circ C$
- $T_{offset} = +18^\circ C$

When  $T_{27J}$  is not known, a test temperature for which an impact energy higher than 27J has been measured is to be used instead.

#### 6.4.7 Correlation between Charpy V-notch energy and critical stress intensity factor in the lower shelf region

If the Charpy V-notch fracture energy at the service temperature is known, the following correlation can be used:

$$K_{mat} = 20 + (12 \sqrt{C_{VT}} - 20) \left( \frac{25}{B} \right)^{0,25}$$

where:

$C_{VT}$  : Charpy V-notch impact energy at the service temperature T.

If both the Charpy V-notch transition temperature and the impact energy at the service temperature are known, the correlation based on impact energy at service temperature may be considered as a lower bound for the  $K_{mat}$  obtained from the correlation on the transition temperature.

#### 6.4.8 Correlation between Charpy V-notch energy and critical stress intensity factor in the upper shelf region

In any case, the value of  $K_{mat}$ , in  $\text{MPa}\cdot\text{m}^{0,5}$ , obtained from the above correlations should not be taken greater than the value corresponding to the following correlation for the upper shelf region:

$$K_{mat} = \sqrt{\frac{E(0,53 C_{Vus}^{1,28})(0,2^{0,133} C_{Vus}^{0,256})}{1000(1 - \nu^2)}}$$

where:

E : Young's modulus, in MPa

$C_{Vus}$  : Upper shelf energy, in J

$\nu$  : Poisson's ratio.

When  $C_{Vus}$  is not known, the highest value of  $C_V$  in the transition zone is to be used as in the above correlation formula, giving a conservative estimation of  $K_{mat}$ .

#### 6.4.9 Parametric analysis

The correlations given in [6.4.6], [6.4.7] and [6.4.8] between the Charpy V-notch energy and the critical stress intensity factor  $K_{mat}$  provide a conservative value. It is generally beneficial to carry out a parametric analysis on a range of toughness values between  $40 \text{ MPa}\cdot\text{m}^{0,5}$  and  $160 \text{ MPa}\cdot\text{m}^{0,5}$  (for carbon steel), pointing out the sensitivity of the crack propagation result to the toughness. The outcome of the sensitivity analysis is then used to decide whether further investigation on the actual material toughness is necessary or not.

### 6.5 Crack propagation law parameters

#### 6.5.1 General

The crack propagation law parameters given in this sub-article correspond to dry air environment and marine environment with or without cathodic protection. Other values may be used when duly documented and justified.

The dry air environment condition is very unusual on marine structures. This condition can be considered for embedded cracks (see [2.2.4]) as long as there is no way for humidity to reach the cracked area. Protective coating can no longer be considered as a protection against corrosion when a crack has initiated.

For other materials, the values can be found in the literature or determined by testing. In such a case, they may be used when duly documented and justified.

#### 6.5.2 Dry air environment

In a dry air non-corrosive environment, the following parameters are generally to be applied in the crack propagation law (where  $da/dn$  is in  $\text{m}/\text{cycle}$  and  $\Delta K$  is in  $\text{MPa}\cdot\text{m}^{0,5}$ ):

- for steel:

$$C = 1,65 \cdot 10^{-11} \text{ m}/(\text{MPa}\cdot\text{m}^{0,5})^3$$

$$m = 3$$

$$\Delta K_{th} = 2,0 \text{ MPa}\cdot\text{m}^{0,5}$$

- for aluminium alloys:

$$C = 4,21 \cdot 10^{-10} \text{ m}/(\text{MPa}\cdot\text{m}^{0,5})^3$$

$$m = 3$$

$$\Delta K_{th} = 0,7 \text{ MPa}\cdot\text{m}^{0,5}$$

6.5.3 Marine environment with cathodic protection

In a marine corrosive environment with cathodic protection, the following parameters are generally to be applied in the crack propagation law (where da/dn is in m/cycle and ΔK is in MPa·m<sup>0.5</sup>):

- for steel:  
 $C = 7,27 \cdot 10^{-11} \text{ m}/(\text{MPa}\cdot\text{m}^{0,5})^3$   
 $m = 3$   
 $\Delta K_{th} = 2,0 \text{ MPa}\cdot\text{m}^{0,5}$

6.5.4 Marine environment without cathodic protection

In a marine corrosive environment without protection, the following parameters are generally to be applied in the crack propagation law (where da/dn is in m/cycle and ΔK is in MPa·m<sup>0.5</sup>):

- for steel:  
 $C = 7,27 \cdot 10^{-11} \text{ m}/(\text{MPa}\cdot\text{m}^{0,5})^3$   
 $m = 3$   
 $\Delta K_{th} = 0$

7 Initial crack size

7.1 General

7.1.1 Minimum crack size

When the size of the initial crack is not directly measured and is to be assumed, the values given in this Article may be applied. These values depend on the inspection technique which has been used. Other values may be considered when duly documented and justified.

7.1.2 Uncertainty on the measured crack size

The actual shape of a crack may be very complex, and its actual extent not fully known. Therefore, an uncertainty exists on a measured crack size.

The sizing accuracy given in Tab 2 may be considered.

7.2 Visual inspection

7.2.1 General

According to the Surveyor’s judgment on the criticality of the inspected area, his capability of detecting cracks by visual inspection may vary.

Moreover, it is obvious that only surface breaking cracks located in an accessible area, mainly at weld toe, can be detected.

7.2.2 Simple visual inspection

The values in Tab 3 correspond to a close visual inspection and should be considered carefully. The actual detection probability in current areas where there is no reason to consider a high criticality is likely lower, as they are not usually areas of focus for close-up inspections.

7.2.3 Visual inspection with dye penetrant testing

Dye penetrant testing method may be considered as a close visual inspection improving only the reliability of the detection. This means that the limitations concerning the location and size of the cracks are the same as for a simple visual inspection (see Tab 3).

Table 2 : Uncertainty on the measured crack size

Condition	Crack length accuracy (mm)
As welded	10,0
With local dressing	5,0
Ground	2,0

Table 3 : Detectable crack sizes for visual inspection

Condition	Surface crack length (mm)	Surface crack depth (mm)	Through-thickness crack length (mm)
As welded	20,0	NA	4,0
Ground	5,0	NA	1,0



7.3 Ultrasonic inspection

7.3.1 Conventional ultrasonic inspection

Ultrasonic testing efficiency is very sensitive to the operator’s experience and it is therefore difficult to provide information on the accuracy. However, the detectable sizes defined in Tab 4 may be assumed.

7.3.2 Phased array ultrasonic inspection

The detectable sizes defined in Tab 5 may be assumed.

Table 4 : Detectable crack size with conventional ultrasonic testing

Condition	Surface crack length (mm)	Surface crack depth (mm)	Through-thickness crack length (mm)
Accessible surface crack	15,0	3,0	3,0
Embedded crack	15,0	3,0	NA
Back surface crack	15,0	3,0	NA

Table 5 : Detectable crack size with phased array ultrasonic testing

Condition	Surface crack length (mm)	Surface crack depth (mm)	Through-thickness crack length (mm)
Accessible surface crack	10,0	1,5	3,0
Embedded crack	10,0	1,5	NA
Back surface crack	10,0	1,5	NA

7.4 Other inspection techniques

7.4.1 Magnetic particle inspection

The detectable sizes defined in Tab 6 may be assumed.

7.4.2 Alternative current field measurement

The detectable sizes defined in Tab 7 may be assumed.

7.4.3 Radiographic testing

The detectable sizes defined in Tab 8 may be assumed.

Table 6 : Detectable crack size with magnetic particle inspection

Condition	Surface crack length (mm)	Surface crack depth (mm)	Through-thickness crack length (mm)
As welded (poor profile)	20,0	4,0	4,0
As welded with local dressing	10,0	2,0	2,0
Ground	5,0	1,5	1,5

Table 7 : Detectable crack size with alternative current field measurement

Condition	Surface crack length (mm)	Surface crack depth (mm)	Through-thickness crack length (mm)
Accessible surface	15,0	2,0	4,0

Table 8 : Detectable crack size with radiographic testing

Condition	Surface crack length (mm)	Surface crack depth (mm)	Through-thickness crack length (mm)
Accessible surface	1,2	1,2	1,2
Sub-surface flaws	1,2	1,2	NA
Back surface flaws	1,2	1,2	NA

# APPENDIX 1

## METHODOLOGY FOR DIRECT HYDRO-STRUCTURE CALCULATION

### Symbols

- $H_s$  : Significant wave height, in m  
 $T_p$  : Peak period, in s  
 $T_z$  : Zero up-crossing period, in s  
 $\beta$  : Wave heading relative to the ship bow, in deg. For head seas:  $\beta = 180^\circ$   
 $\omega$  : Wave angular frequency, in rad/s  
 $N_T$  : Assumed total number of stress cycles over the total life of the unit  
 $\Delta S_q$  : Stress range, in N/mm<sup>2</sup>, at the change of slope of the S-N curve, as defined in Sec 9, [1.3]  
 $m_1, m_2$  : Characteristic inverse slope of, respectively, the first and second segments of the S-N curve, as defined in Sec 9, [1.3]  
 $K_1, K_2$  : Characteristic constants of the S-N curve, as defined in Sec 9, [1.3]  
 $\gamma(1+X;S)$ : Lower incomplete gamma function defined by:

$$\gamma(1+X;S) = \int_0^S t^X e^{-t} dt$$

$\Gamma(1+X;S)$ : Upper incomplete gamma function defined by:

$$\Gamma(1+X;S) = \int_S^\infty t^X e^{-t} dt$$

## 1 General

### 1.1 Introduction

**1.1.1** The present Appendix describes the various methods and tools to be used for the direct calculation of the hydro-structural response of ships and floating offshore units. These methods apply to cases where the first order wave loads are dominant, supplemented with limited non-linear effects. The simulation of responses to second order diffraction wave loads (either low or high frequency) or to other environmental loads is not covered.

## 2 Wave environment description

### 2.1 Wave scatter diagram

#### 2.1.1 General

A wave scatter diagram is a description of the joint probabilities of wave heights and wave periods. This description is made for a given geographical area. The scatter diagrams are usually based on visual observations and hindcast data, which are merged and extrapolated, using some analytical functions. The Global Wave Statistics atlas provides scatter diagrams for 104 areas in the world, including some seasonal and directional information (see Fig 1). The scatter diagrams generally used for the design of ships without any specific sailing area are those provided in [2.1.2] and [2.1.3].

#### 2.1.2 IACS scatter diagram

The IACS scatter diagram has been defined from the winter data of areas 8, 9, 15 and 16 (North Atlantic). This scatter diagram is the basis of many standard long-term analyses since the North Atlantic is considered as the worst area in the World (considering the wave heights).

The IACS scatter is given in Tab 1 and Tab 2, and defined according to the following probability density function:

$$P_{IACS}(H_s, T_z) = \frac{\beta}{\alpha} \left( \frac{H_s - \gamma}{\alpha} \right)^{\beta-1} \exp \left[ - \left( \frac{H_s - \gamma}{\alpha} \right)^\beta \right] \frac{1}{T_z \sigma \sqrt{2\pi}} \exp \left[ - \frac{(\ln(T_z) - \mu)^2}{2\sigma^2} \right]$$

where:

$$\alpha = 3,041$$

$$\beta = 1,484$$

$$\gamma = 0,66$$

$$\mu = 0,7 + 1,27 H_s^{0,131}$$

$$\sigma = 0,1334 + 0,0264 \exp(-0,1906 H_s)$$

The sea states are to be modelled by a Pierson-Moskowitz spectrum and a 'cos n' spreading function with  $n = 2$ , as defined in [2.2.2] and [2.2.5]. Equiprobability of the main wave direction is to be considered.

### 2.1.3 Worldwide scatter diagram

The worldwide scatter diagram is representative of wave conditions for worldwide trips. It is given in Tab 3 and Tab 4, and defined according to the following probability density function:

$$P_{ww}(H_s, T_z) = \frac{\beta}{\alpha} \left( \frac{H_s - \gamma}{\alpha} \right)^{\beta-1} \exp \left[ - \left( \frac{H_s - \gamma}{\alpha} \right)^{\beta} \right] \frac{1}{T_z \sigma \sqrt{2\pi}} \exp \left( - \frac{(\ln(T_z) - \mu)^2}{2\sigma^2} \right)$$

where:

$$\alpha = 1,807$$

$$\beta = 1,217$$

$$\gamma = 0,83$$

$$\mu = -0,1 + 2,847 H_s^{0,075}$$

$$\sigma = 0,161 + 0,146 \exp(-0,683 H_s)$$

The sea states are to be modelled by a Pierson-Moskowitz spectrum and a 'cos n' spreading function with  $n = 2$ , as defined in [2.2.2] and [2.2.5]. Equiprobability of the main wave direction is to be considered.

**Figure 1 : Areas of the global wave statistics**

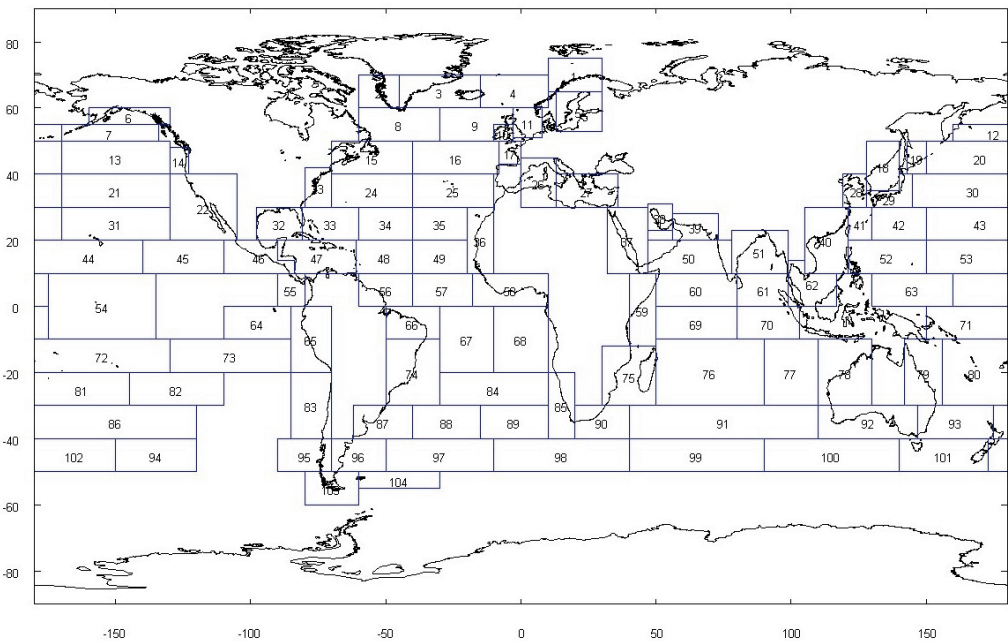


Table 1 : Wave scatter diagram for North Atlantic (IACS Recommendation 34)  
(continued in Tab 2)

Up-crossing period T <sub>z</sub> (s)												
	3,5	4,5	5,5	6,5	7,5	8,5	9,5	10,5	11,5	12,5		
Significant wave height (m)	21,5	0,000	0,000	0,000	0,000	0,000	0,000	0,000	0,000	0,000	0,001	0,001
	20,5	0,000	0,000	0,000	0,000	0,000	0,000	0,000	0,000	0,001	0,002	0,002
	19,5	0,000	0,000	0,000	0,000	0,000	0,000	0,001	0,003	0,006	0,008	0,008
	18,5	0,000	0,000	0,000	0,000	0,000	0,000	0,003	0,010	0,020	0,026	0,026
	17,5	0,000	0,000	0,000	0,000	0,000	0,001	0,010	0,034	0,066	0,082	0,082
	16,5	0,000	0,000	0,000	0,000	0,000	0,005	0,035	0,115	0,208	0,241	0,241
	15,5	0,000	0,000	0,000	0,000	0,001	0,019	0,125	0,374	0,628	0,677	0,677
	14,5	0,000	0,000	0,000	0,000	0,005	0,073	0,428	1,169	1,809	1,814	1,814
	13,5	0,000	0,000	0,000	0,000	0,019	0,270	1,407	3,488	4,955	4,599	4,599
	12,5	0,000	0,000	0,000	0,002	0,077	0,959	4,432	9,906	12,849	10,998	10,998
	11,5	0,000	0,000	0,000	0,007	0,304	3,271	13,311	26,648	31,381	24,657	24,657
	10,5	0,000	0,000	0,000	0,033	1,167	10,684	37,931	67,504	71,730	51,475	51,475
	9,5	0,000	0,000	0,001	0,152	4,321	33,245	101,894	159,849	152,221	99,212	99,212
8,5	0,000	0,000	0,005	0,682	15,367	97,874	255,920	350,546	296,856	174,620	174,620	
7,5	0,000	0,000	0,028	2,972	52,127	270,144	594,437	703,177	524,871	276,649	276,649	
6,5	0,000	0,000	0,167	12,567	167,023	690,240	1257,839	1268,549	825,936	386,772	386,772	
5,5	0,000	0,001	0,999	51,029	498,354	1602,922	2372,647	2008,287	1126,030	463,567	463,567	
4,5	0,000	0,015	5,953	196,120	1354,283	3288,418	3857,421	2685,481	1275,135	455,085	455,085	
3,5	0,000	0,174	34,939	695,509	3226,434	5674,915	5099,065	2837,967	1114,071	337,682	337,682	
2,5	0,001	2,156	197,452	2158,778	6229,957	7449,408	4860,305	2065,929	644,450	160,244	160,244	
1,5	0,032	29,310	986,006	4975,934	7737,889	5569,612	2375,647	703,447	160,720	30,476	30,476	
0,5	1,303	133,765	865,828	1186,377	634,434	186,350	36,904	5,609	0,713	0,080	0,080	
TOTAL	1,336	165,422	2091,378	9280,164	19921,761	24878,411	20869,761	12898,093	6244,657	2478,967	2478,967	

Table 2 : Wave scatter diagram for North Atlantic (IACS Recommendation 34)  
(continued from Tab 1)

		Up-crossing period T <sub>z</sub> (s)										TOTAL
		13,5	14,5	15,5	16,5	17,5	18,5	19,5	20,5	21,5		
Significant wave height (m)	21,5	0,001	0,001	0,000	0,000	0,000	0,000	0,000	0,000	0,000	0,003	
	20,5	0,003	0,002	0,001	0,001	0,000	0,000	0,000	0,000	0,000	0,011	
	19,5	0,008	0,006	0,003	0,002	0,001	0,000	0,000	0,000	0,000	0,037	
	18,5	0,024	0,017	0,009	0,004	0,002	0,001	0,000	0,000	0,000	0,115	
	17,5	0,070	0,046	0,024	0,010	0,004	0,001	0,000	0,000	0,000	0,348	
	16,5	0,196	0,120	0,059	0,024	0,009	0,003	0,001	0,000	0,000	1,016	
	15,5	0,517	0,300	0,140	0,055	0,019	0,006	0,002	0,000	0,000	2,865	
	14,5	1,296	0,709	0,314	0,117	0,038	0,011	0,003	0,001	0,000	7,786	
	13,5	3,067	1,576	0,659	0,233	0,072	0,020	0,005	0,001	0,000	20,373	
	12,5	6,819	3,282	1,292	0,433	0,128	0,034	0,008	0,002	0,000	51,221	
	11,5	14,162	6,363	2,354	0,746	0,209	0,053	0,012	0,003	0,001	123,482	
	10,5	27,274	11,399	3,950	1,179	0,313	0,075	0,017	0,004	0,001	284,736	
9,5	48,270	18,696	6,051	1,698	0,426	0,097	0,021	0,004	0,001	626,158		
8,5	77,615	27,741	8,356	2,199	0,520	0,113	0,023	0,004	0,001	1308,440		
7,5	111,676	36,659	10,238	2,518	0,560	0,115	0,022	0,004	0,001	2586,198		
6,5	140,814	42,213	10,879	2,491	0,520	0,101	0,018	0,003	0,001	4806,133		
5,5	150,896	41,013	9,696	2,057	0,401	0,073	0,013	0,002	0,000	8327,989		
4,5	130,895	31,937	6,868	1,340	0,243	0,042	0,007	0,001	0,000	13289,246		
3,5	84,320	18,188	3,511	0,623	0,104	0,016	0,003	0,000	0,000	19127,519		
2,5	33,689	6,251	1,057	0,167	0,025	0,004	0,001	0,000	0,000	23809,869		
1,5	5,050	0,759	0,106	0,014	0,002	0,000	0,000	0,000	0,000	22575,031		
0,5	0,008	0,001	0,000	0,000	0,000	0,000	0,000	0,000	0,000	3051,421		
TOTAL		836,671	247,279	65,569	15,912	3,593	0,765	0,155	0,030	0,006	100000,000	

Table 3 : Worldwide scatter diagram  
(continued in Tab 4)

		Up-crossing period T <sub>z</sub> (s)											
		2,5	3,5	4,5	5,5	6,5	7,5	8,5	9,5	10,5	11,5	12,5	
Significant wave height (m)	19	0,000	0,000	0,000	0,000	0,000	0,000	0,000	0,000	0,001	0,001	0,001	0,001
	18	0,000	0,000	0,000	0,000	0,000	0,000	0,000	0,001	0,003	0,004	0,004	0,004
	17	0,000	0,000	0,000	0,000	0,000	0,000	0,001	0,004	0,009	0,012	0,012	0,012
	16	0,000	0,000	0,000	0,000	0,000	0,001	0,004	0,015	0,028	0,036	0,034	0,034
	15	0,000	0,000	0,000	0,000	0,000	0,003	0,016	0,048	0,086	0,105	0,095	0,095
	14	0,000	0,000	0,000	0,000	0,001	0,010	0,056	0,157	0,262	0,299	0,255	0,255
	13	0,000	0,000	0,000	0,000	0,003	0,038	0,195	0,500	0,775	0,826	0,661	0,661
	12	0,000	0,000	0,000	0,000	0,012	0,144	0,662	1,553	2,223	2,203	1,651	1,651
	11	0,000	0,000	0,000	0,001	0,050	0,532	2,203	4,690	6,160	5,646	3,939	3,939
	10	0,000	0,000	0,000	0,006	0,209	1,944	7,148	13,706	16,387	13,794	8,904	8,904
	9	0,000	0,000	0,000	0,029	0,875	6,982	22,526	38,489	41,516	31,846	18,888	18,888
	8	0,000	0,000	0,001	0,146	3,650	24,567	68,468	102,915	99,068	68,612	37,095	37,095
	7	0,000	0,000	0,005	0,771	15,201	84,142	198,582	258,460	219,219	135,663	66,295	66,295
	6	0,000	0,000	0,042	4,242	63,057	277,308	540,215	597,239	439,962	240,687	105,474	105,474
	5	0,000	0,000	0,383	24,620	257,824	860,002	1339,259	1230,602	776,238	372,218	145,678	145,678
4	0,000	0,007	4,269	149,832	1007,271	2401,638	2882,476	2156,785	1154,775	485,360	170,784	170,784	
3	0,000	0,311	57,076	902,149	3473,100	5547,994	4972,291	3003,977	1376,350	517,480	168,604	168,604	
2	0,012	19,813	764,174	4453,034	8840,681	9044,627	6019,232	2999,974	1225,020	435,063	140,007	140,007	
1	2,443	310,529	2734,624	6403,577	7134,616	5072,812	2711,523	1201,987	470,151	169,019	57,413	57,413	
TOTAL		2,455	330,660	3560,574	11938,407	20796,550	23322,743	18764,858	11611,104	5828,231	2478,873	925,795	925,795

Table 4 : Worldwide scatter diagram  
(continued from Tab 3)

		Up-crossing period T <sub>z</sub> (s)									TOTAL
		13,5	14,5	15,5	16,5	17,5	18,5	19,5	20,5	21,5	
Significant wave height (m)	19	0,001	0,001	0,001	0,000	0,000	0,000	0,000	0,000	0,000	0,007
	18	0,003	0,002	0,001	0,001	0,000	0,000	0,000	0,000	0,000	0,021
	17	0,009x	0,006	0,003	0,002	0,001	0,000	0,000	0,000	0,000	0,061
	16	0,068	0,016	0,009	0,004	0,002	0,001	0,000	0,000	0,000	0,175
	15	0,068	0,041	0,021	0,010	0,004	0,002	0,001	0,000	0,000	0,499
	14	0,173	0,099	0,049	0,022	0,009	0,003	0,001	0,000	0,000	1,395
	13	0,425	0,229	0,108	0,046	0,018	0,006	0,002	0,001	0,000	3,833
	12	0,997	0,509	0,228	0,092	0,034	0,012	0,004	0,001	0,000	10,326
	11	2,227	1,069	0,451	0,172	0,061	0,020	0,006	0,002	0,001	27,230
	10	4,688	2,107	0,836	0,301	0,100	0,031	0,009	0,003	0,001	70,174
	9	9,200	3,848	1,429	0,483	0,152	0,045	0,013	0,003	0,001	176,326
	8	16,604	6,425	2,221	0,703	0,208	0,058	0,016	0,004	0,001	430,761
	7	27,078	9,639	3,086	0,910	0,252	0,066	0,017	0,004	0,001	1019,392
	6	39,093	12,754	3,773	1,036	0,268	0,067	0,016	0,004	0,001	2325,236
	5	48,965	14,671	4,029	1,035	0,253	0,060	0,014	0,003	0,001	5075,854
	4	52,673	14,724	3,825	0,941	0,222	0,051	0,011	0,003	0,001	10485,649
	3	49,485	13,456	3,461	0,855	0,205	0,048	0,011	0,003	0,001	20086,851
	2	42,023	12,011	3,320	0,897	0,239	0,063	0,017	0,004	0,001	34000,219
	1	18,786	6,003	1,891	0,592	0,185	0,058	0,018	0,006	0,002	26296,314
TOTAL		312,524	97,609	28,741	8,101	2,213	0,592	0,156	0,041	0,011	100010,000

## 2.2 Wave spectrum

### 2.2.1 General

A short-term sea state is described by a wave energy density spectrum, which is the power spectral density function of the vertical sea surface displacement. Wave spectra are often given in the form of an analytical formula.

Directional short-crested wave spectra  $S_{\eta}(\omega, \beta)$  may be expressed in terms of a unidirectional wave energy density spectrum  $S_{\eta}(\omega)$  multiplied by an angular spreading function  $G(\beta)$ :

$$S_{\eta}(\omega, \beta) = S_{\eta}(\omega) \cdot G(\beta)$$

For a two-peak spectrum expressed as a sum of a swell component and a wind-sea component, each component may have its own spreading function.

### 2.2.2 Pierson-Moskowitz spectrum

The Pierson-Moskowitz spectrum is frequently applied for wind seas. It was originally proposed for fully-developed sea. It describes the wind-sea conditions that often occur for the most severe sea states. The Pierson-Moskowitz spectrum is given by:

$$S_{\eta}(\omega) = \frac{5\omega_p^4 H_s^2}{16\omega^5} \cdot \exp\left[-1, 25\left(\frac{\omega_p}{\omega}\right)^4\right]$$

where:

$\omega_p$  : Peak angular frequency:

$$\omega_p = \frac{2\pi}{T_p} = \frac{2\pi}{1,408 T_z}$$

### 2.2.3 JONSWAP spectrum

The JONSWAP spectrum is formulated as a modification of the Pierson-Moskowitz spectrum for a developing sea state in a fetch limited situation. It includes a peak-enhancement factor, the effect of which is to increase the peak of the Pierson-Moskowitz spectrum. The JONSWAP spectrum is given by:

$$S_{\eta}(\omega) = A \cdot \frac{5\omega_p^4 H_s^2}{16\omega^5} \cdot \exp\left[-1, 25\left(\frac{\omega_p}{\omega}\right)^4\right] \cdot \gamma^{\left[\exp\left(\frac{-(\omega-\omega_p)^2}{2\sigma^2\omega_p^2}\right)\right]}$$

where:

$\gamma$  : Peak enhancement factor. For  $\gamma = 1$  the JONSWAP spectrum corresponds to a Pierson-Moskowitz spectrum

$\sigma$  : Relative measure of the peak width. In the most cases:

- for  $\omega < \omega_p$ :  $\sigma = 0,07$
- for  $\omega > \omega_p$ :  $\sigma = 0,09$

$$A = \frac{1}{5(0,065\gamma^{0,803} + 0,135)}$$

### 2.2.4 Ochi-Hubble spectrum

Combined wind-sea and swell may be described by a double peak frequency spectrum, i.e. where wind-sea and swell are assumed to be uncorrelated. The Ochi-Hubble spectrum is a general spectrum formulated to describe bimodal sea states.

The spectrum is a sum of two gamma distributions, each with 3 parameters for each wave system:

$$S_{\eta}(\omega) = \frac{1}{4} \sum_{i=1}^2 \left\{ \left[ \omega_{p,i}^4 \left( \lambda_i + \frac{1}{4} \right) \right]^{\lambda_i} \cdot \frac{H_{s,i}^2}{\Gamma(\lambda_i) \omega^{4\lambda_i+1}} \cdot \exp\left[-\left(\lambda_i + \frac{1}{4}\right) \left( \frac{\omega_{p,i}}{\omega} \right)^4\right] \right\}$$

where:

$\omega_{p,i}$  : Peak angular frequency, in rad/s, of component i

$H_{s,i}$  : Significant wave height, in m, of component i

$\lambda_i$  : Spectral shape parameter of component i.



### 2.2.5 Spreading function with 'cos n' formulation

The most commonly used directional spreading function is:

- when  $|\beta - \beta_0| \leq 90^\circ$ :

$$G(\beta) = \frac{\pi}{180} \cdot \frac{\Gamma(n/2 + 1)}{\sqrt{\pi} \Gamma(n/2 + 1/2)} \cdot \cos^n(\beta - \beta_0)$$

- when  $|\beta - \beta_0| > 90^\circ$ :

$$G(\beta) = 0$$

where:

$\beta_0$  : Main wave heading relative to the ship bow, in deg

$n$  : Spreading parameter specified according to the metocean data.

### 2.2.6 Spreading function with 'cos 2s' formulation

An alternative formulation for the directional spreading function is:

$$G(\beta) = \frac{\pi}{180} \cdot \frac{\Gamma(s + 1)}{2 \sqrt{\pi} \Gamma(s + 1/2)} \cdot \cos^{2s}\left(\frac{\beta - \beta_0}{2}\right)$$

where:

$\beta_0$  : Main wave heading relative to the ship bow, in deg

$s$  : Spreading parameter specified according to the metocean data.

## 3 Hydro-structural model

### 3.1 General

**3.1.1** A good evaluation of the structural response of a ship in waves needs a proper coupling between a hydrodynamic model, which describes the hydrodynamic interaction between the ship and the waves, and a structural model, which describes the structural response to the wave induced loads. Several levels of assumptions can be chosen for the hydrodynamic model and the structural model, depending on which physical behaviour is expected to be reproduced.

From the hydrodynamic analysis point of view, the loads can be considered as:

- linear (valid only for the smallest sea states), as described in [3.2.1]
- weakly non-linear (e.g. Froude-Krylov loads as described in [3.2.2], or Morison loads as described in [3.2.3])
- impulsive (e.g. slamming loads, as described in [3.2.4]).

From the structural analysis point of view, the response can be considered as:

- quasi-static, which means that the structural response is strictly proportional to the applied loads. This model is described in [3.4.1]
- dynamic, if a dynamic amplification or a resonant response occurs. This model is described in [3.4.2]
- non-linear (e.g. large deformation, contact, friction).

### 3.1.2 Linear hydro-structural model in frequency domain

When both the hydrodynamic loads and the structural response are considered linear, the whole analysis is performed in frequency domain, in a very time-efficient way.

The outputs of a linear hydro-structure computation are the transfer functions or Response Amplitude Operators (RAO). Ship motions RAOs and internal hull girder loads RAOs are directly computed by the sea-keeping software (the internal loads are calculated simply by integration of the external inertia and pressure loads between the ship end and the considered section). Stress RAOs are computed from the structural analysis.

### 3.1.3 Non-linear hydro-structural model in time domain

When non-linear or impulsive loads are considered, the analysis is to be performed in time domain.

The outputs of a weakly non-linear hydro-structure computation are time traces. Ship motions and internal hull girder loads are directly computed by the sea-keeping software (the internal loads are calculated simply as the sum of the inertial and pressure loads at each section). Time histories of stresses are computed by a structural analysis performed for each time step of the simulation. For each time step, a loading case is built and the corresponding structural response is calculated by 3D FEM analysis. For a ship, and for offshore units when the mooring system is not modelled, all extra forces needed in the time-domain simulation to ensure course keeping and to avoid low frequency motions should be properly included in the loading of the structural mesh.

If duly justified, a modal approach can also be used to reconstruct the stress history without performing a FE calculation at each time step.

## 3.2 Hydrodynamic loads

### 3.2.1 Linear loads

The linear part of the hydrodynamic loading is calculated by a validated numerical sea-keeping code. The use of codes based on the Boundary Element Method (BEM) is recommended. In the case of linear calculations, the mesh contains the mean under-water part only. The mesh size is to be chosen so that the minimal wave length (defined on the basis of encounter frequency) is covered by at least six panels. Alternatively, a special treatment of the high frequency calculations can be used in order to avoid the numerical inaccuracies inherent to the BEM method. In any case, the problem of irregular frequencies is to be properly solved.

### 3.2.2 Froude-Krylov non-linear loads

When non-linear hydrodynamic simulations are performed, the minimum non-linear loads that should be included are based on the so called Froude-Krylov approximation. The pressure of the undisturbed incoming wave is applied to the hull on every wet panel, and not only under the mean waterline as it is the case in the linear computation. The non-linear hydrostatic restoring forces are also included by taking into account the real position of the ship in the integration of the hydrostatic pressure. The mesh used to integrate the pressure loading is to include the part of the hull above the mean waterline.

### 3.2.3 Morison non-linear loads on slender elements

The Morison loads on slender structural elements, mainly of offshore units, can be introduced in non-linear hydrodynamic simulations. The general expression for these loads is:

$$dF_M = \frac{1}{2} \rho C_D D \left( v - \frac{dx}{dt} \right) \left| v - \frac{dx}{dt} \right| dl + \rho \frac{\pi D^2}{4} \left[ (1 + C_M) \frac{dv}{dt} - C_M \frac{d^2x}{dt^2} \right] dl$$

where:

$\rho$  : Fluid density, in kg/m<sup>3</sup>

$D$  : Diameter of the slender element, in m

$C_D, C_M$  : Drag and added mass coefficients, respectively

$v, dv/dt$  : Local fluid velocity and acceleration, respectively in m/s and m/s<sup>2</sup>, perpendicular to the slender element axis

$dx/dt, d^2x/dt^2$  : Local velocity and acceleration, respectively in m/s and m/s<sup>2</sup>, of the slender element due to the units motions.

### 3.2.4 Slamming

If slamming loads are considered in the simulation, the slamming pressures are to be computed using either a CFD code or a BEM code, provided that these codes are properly validated and coupled with the sea-keeping code. The slamming pressures are to be properly transferred to the FE model at each time step of the time-domain simulation.

## 3.3 Internal liquid loads

### 3.3.1 General

Different assumptions can be used for taking the liquids in tanks into account on the structural model (see Tab 5). The validity of the different models depends on the following criteria:

- the pressure exerted by the liquid in the tank has no direct influence on the response of the considered structure
- the liquid in the tank does not have a significant hydrostatic effect (significant free surface effect impacting the unit motions at sea)
- the liquid in the tank does not have a significant hydro-dynamic behaviour (sloshing in the sense of dynamic liquid motions, not mentioning impacts).

**Table 5 : Models for liquids in tanks**

	No direct pressure effect on the structural response	Direct pressure effect on the structural response
No liquid hydrostatic effect nor dynamic behaviour	liquid mass model	simplified pressure model
Liquid hydrostatic effect	simplified pressure model	simplified pressure model
Liquid dynamic behaviour	hydrodynamic pressure model	hydrodynamic pressure model

The risk of dynamic fluid behaviour depends on the dimensions of the tank and on the presence of structural elements inside the tank capable of preventing or strongly damping such motions (e.g. in a double hull of double bottom tank).

In any case, the choice of a model for the liquid in tank is to be carefully reflected in the structural model as well as in the hydrodynamic model, in order to keep the consistency between the two models for the sake of the structural model balance in the hydro-structure coupling procedure.

### 3.3.2 Tank mass

If the liquid in tank fulfils the criteria a) to c) of [3.3.1], then it can be simply represented as a mass matrix.

On a FEM model, the mass matrix element is to be attached to the tank boundaries by means of special elements which do not introduce any rigidity in the model (interpolation elements). Modelling the mass of the liquid with lumped masses directly located on the tank boundaries is not recommended as it creates some overestimated mass moments of inertia with very limited options to adjust them.

The mass, centre of gravity and mass moments of inertia resulting from the modelling of the liquid as a mass in the structural model are to be used in the hydrodynamic model.

### 3.3.3 Linear simplified tank pressure

A simplified pressure model can be used when the liquid in tank fulfils the criterion c) of [3.3.1]. In this case, the effect of the fluid is modelled as a pressure defined with the following analytical formulae:

- if  $z \leq z_F$  :  

$$p_{liq} = \rho [(x - x_F) \gamma_x + (y - y_F) \gamma_y + (z - z_F) \gamma_z]$$
- if  $z > z_F$  :  

$$p_{liq} = 0$$

where:

- $(x, y, z)$  : Location where the pressure is evaluated, in m
- $(x_F, y_F, z_F)$  : Location of the centre of the tank liquid free surface, in m
- $\rho$  : Liquid density, in  $\text{kg/m}^3$
- $(\gamma_x, \gamma_y, \gamma_z)$  : Local acceleration at the tank centre of gravity, in  $\text{m}\cdot\text{s}^{-2}$ .

The acceleration at the tank centre of gravity is deduced from the ship accelerations at the motion reference point, using the rigid body kinematic rule. The ship accelerations include the terms due to the influence of gravity when the unit pitches and rolls.

In case of a fully filled tank, the same pressure formulation can be used, setting the ‘centre of liquid free surface’ at the uppermost point of the tank, or at the centre of the liquid free surface for a ‘almost fully filled tank’. However,  $z_F$  is to be chosen so that  $z_F \geq z$  whatever  $z$ , in order that no free surface effect occurs.

The tank is to be introduced in the hydrodynamic model in a way fully consistent with the loads exerted on the structural model according to the above formulae. To this effect, the terms of the tank hydrostatic restoring matrix and mass matrix can be determined considering unitary motions, determining the liquid pressure resulting from the above formulae and integrating this pressure on the tank boundary.

### 3.3.4 Hydrodynamic tank pressure

If a significant fluid dynamic behaviour is expected, then the pressure exerted by the liquid is to be determined by means of a hydrodynamic computation and transferred to the structural model. As a general rule, the hydrodynamic model used for the external problem related to sea pressure is also to be used for solving the tank hydrodynamic problem.

### 3.4 Structural ship response

#### 3.4.1 Quasi-static ship response

Once the hydrodynamic sea-keeping problem is solved, the different loading cases for FE model analysis need to be constructed.

Each loading case is composed of the hydrodynamic pressure loading on the wet panels, the inertial and the gravity loading on each finite element and the additional damping loading. The perfect equilibrium of the overall loading needs to be ensured. In general, the hydrodynamic and structural meshes are different, and special care is to be given to the pressure transfer.

The structural problem is solved using FEA software for each loading case. The structural response is supposed to be static and linear.

#### 3.4.2 Dynamic ship response

If a dynamic ship response is anticipated, a coupled hydro-elastic model should be used.

The first step of the dynamic analysis is the modal FEM model analysis in dry condition (i.e. without liquid added mass effect), which is to be done with care. Local structural modes are to be removed. The first ten dry distortion modes are normally considered to be sufficient.

Once the dry modes are obtained, the modal displacements are to be transferred from the structural model to the hydrodynamic model and the corresponding hydrodynamic problems are to be defined. Once the hydrodynamic problems are solved, a fully coupled dynamic equation is solved, giving both the rigid body motions and the structural response in terms of modal amplitudes.

The modal reduction of the structural response is usually not fully satisfactory for strength or fatigue verification, since the number of modes in the base is not sufficient to capture the full distortion of the structure, in particular regarding the quasi-static response of the transverse structure. Therefore, the structural response needs to be evaluated by a quasi-static approach, in which the pressure and inertia loads arising from the hydro-elastic dynamic equation are applied in a static way on the FEM model. Alternatively, the motion equation results can be separated into a quasi-static part and a dynamic part. The quasi-static part of the response is then calculated using the quasi-static method explained in [3.4.1] while the dynamic part of the response is calculated by summing up the dynamic contribution of each mode.

### 3.5 General modelling considerations

#### 3.5.1 Mass properties

- mass
- radii of gyration
- longitudinal distribution
- location of the centre of gravity.

#### 3.5.2 Hydrostatic balance

For each loading condition, the computed values of the displacement, trim, and vertical still water bending moment are to be checked and compared to the values in the trim and stability booklet. The following tolerances are considered acceptable:

- displacement: 2%
- trim angle: 0,1°
- still water bending moment: 10%.

It is also worth checking the following hydrostatic properties:

- draught at the aft and forward perpendiculars
- location of the centre of buoyancy (LCB)
- transverse and longitudinal metacentric heights (GMt and GMI).

#### 3.5.3 Roll viscous damping

Additional damping forces are to be added to the motion equation, to take into account the viscous damping and the damping due to rudders, bilge keels and other existing appendages. This additional damping is to be added to the wave damping computed by the hydrodynamic program. It could be based on experimental data or empirical methods.

This damping is essentially non-linear and may be modelled by a linear and a quadratic damping coefficient. An equivalent linearized damping coefficient  $B_{eq}$  is used when the problem is solved in the frequency domain. This linearized damping should be determined for each short-term condition by stochastic linearization, using the following formula:

$$B_{eq} = B_{lin} + \sqrt{\frac{8}{\pi}} \sigma_{RV} B_{quad}$$

where:

$B_{lin}$ ,  $B_{quad}$ : Linear and quadratic damping coefficients, respectively, describing the non-linear viscous damping

$\sigma_{RV}$  : Standard deviation of the roll velocity, obtained as the second order spectral moment of the roll response, according to [4.1.2].

For ships and ship shaped offshore units, if no information is available, the quadratic damping may be neglected and a linear damping equal to 5% of the critical damping is to be applied, according to the following formula:

$$B_{lin} = 0,05 \frac{\Delta \cdot g \cdot GMt \cdot T_{roll}}{\pi}$$

where:

$$g = 9,81 \text{ m/s}^2$$

$\Delta$  : Mass of the ship, in kg

$GMt$  : Transverse metacentric height, in m

$T_{roll}$  : Roll natural period, in seconds.

The roll damping forces considered in the motion equation should be applied to the FE model as nodal forces to ensure a perfect equilibrium between the forces applied to the FE model and the acceleration solution of the motion equation.

### 3.5.4 Structural damping

If a hydro-elastic analysis is performed, some additional damping for the flexible modes is to be added to the wave damping computed by the hydrodynamic program, to take into account the other sources of damping (structural, cargo, viscous,...). The structural damping may vary between 1% and 3% of the critical damping and tends to increase for the higher vibration modes. The additional damping  $B_{ii}$  for the flexible mode  $i$  is given by:

$$B_{ii} = \eta_i \frac{K_{ii} T_i}{\pi}$$

where:

$\eta_i$  : Fraction of the critical damping for the flexible mode  $i$

$K_{ii}$  : Total stiffness (hydrostatic + structural) of the flexible mode  $i$

$T_i$  : Natural period of the mode  $i$ .

These damping forces should be applied to the FE model as nodal forces to ensure a perfect equilibrium between the forces applied to the FE model and the acceleration solution of the motion equation.

## 3.6 Types of hydro-structural simulations

### 3.6.1 General

The type of a hydro-structural simulations depends on which hydrodynamic loads and which structural model are used. The most common simulation types are listed in [3.6.2] to [3.6.7]. This list is non-exhaustive. For specific applications, some other hydro-structural simulation types can be defined, combining a hydrodynamic model with a structural model.

### 3.6.2 Linear sea-keeping

Rigid body linear sea-keeping response can be simulated using the quasi-static structural model (see [3.4.1]) with linear hydrodynamic loads (see [3.2.1]). This model is a frequency domain model (see [3.1.2]) and is used for linear fatigue assessment without springing effects.

### 3.6.3 Linear springing

Linear springing response can be simulated using the dynamic structural model (see [3.4.2]) with linear sea-keeping loads (see [3.2.1]). This model is a frequency domain model (see [3.1.2]) and is used for linear fatigue assessment including springing effects.

### 3.6.4 Non-linear sea-keeping

Non-linear hull girder loads, such as hogging and sagging bending moments, can be evaluated using Froude-Krylov non-linear wave loads (see [3.2.2]) with a quasi-static structural response (see [3.4.1]). This model is a time-domain model (see [3.1.3]) and can be used for intermediate results of the ultimate strength assessment.

### 3.6.5 Local slamming effect

Local structural deformations due to slamming pressures can be computed using impulsive slamming hydrodynamic loads (see [3.2.4]) with a local quasi-static structural model (see [3.4.1]).

### 3.6.6 Non-linear springing

As this model is taking into account non-linear wave loads and a structural dynamic response, it can simulate linear and non-linear springing. Non-linear wave loads (see [3.2.2]) are combined with a dynamic ship response model (see [3.4.2]). This model is a time-domain model (see [3.1.3]).

### 3.6.7 Non-linear springing and slamming induced whipping

This model is the most complex as it includes Froude-Krylov non-linear loads (see [3.2.2]) and slamming loads (see [3.2.4]), coupled with a structural dynamic response (see [3.4.2]). This model is a time-domain model (see [3.1.3]). It can simulate linear and non-linear springing as well as slamming-induced whipping. It is to be noted that it is not possible to separate the whipping response from the springing response. This model is used for ultimate strength assessment and non-linear fatigue assessment.

## 4 Statistical analysis of the response in an irregular sea state

### 4.1 Spectral analysis of frequency domain simulations

#### 4.1.1 General

Using the spectral approach, short-term statistics can be obtained for the different physical quantities given by the hydrodynamic and hydro-structure models.

#### 4.1.2 Response spectrum integration

For each sea state and each parameter  $x$ , the response spectrum is obtained from the wave energy density spectrum for this sea state, and the RAO of  $x$ :

$$S_x(\omega) = \int_{\beta=0}^{360} \text{RAO}_x^2(\omega, \beta) \cdot S_\eta(\omega, \beta) d\beta$$

where:

$S_\eta(\omega, \beta)$  : Wave energy density spectrum, as defined in [2.2.1].

The response spectrum can be characterized by its moments  $\lambda_n$ , as follows:

$$\lambda_n = \int_{\omega=0}^{\infty} \int_{\beta=0}^{360} \omega_e^n(\omega, \beta) \cdot \text{RAO}_x^2(\omega, \beta) \cdot S_\eta(\omega, \beta) d\beta d\omega$$

where:

$$\omega_e(\omega, \beta) = \omega - \frac{\omega^2 V \cos \beta}{g}$$

with:

$V$  : Ship forward speed, in m/s

$g$  : Gravity acceleration, in m/s<sup>2</sup>.

For accurate results in the response spectrum integration, it is recommended to discretize the wave spectrum and the stress RAO with steps of 0,005 rad/s for the wave frequency and 5° for the wave heading. The intermediate values for the RAO are obtained by interpolation between the values actually computed in the hydrodynamic and hydro-structure models, using a linear interpolation or a spline interpolation. Using a spline interpolation yields a higher accuracy but requires a careful check of the interpolated RAO since it is less robust than using a linear interpolation.

#### 4.1.3 Short-term statistics

The response is supposed to be a narrow banded process, so that the probability density of its extreme values follows a Rayleigh distribution:

$$p(x) = \frac{x}{\lambda_0} \exp\left(\frac{-x^2}{2\lambda_0}\right)$$

The cumulative distribution function of the cycle amplitudes  $P(X)$  is the probability of the amplitude  $x$  being lower than  $X$ . It is given by:

$$P(X) = 1 - \exp\left(\frac{-X^2}{2\lambda_0}\right)$$

The complementary cumulative distribution function (or exceedance)  $\bar{P}(X)$  is the probability of the amplitude  $x$  being higher than  $X$ . It is given by:

$$\bar{P}(X) = \exp\left(\frac{-X^2}{2\lambda_0}\right)$$

Similarly, the probability density, the cumulative distribution and the exceedance of response ranges (min to max) are respectively given by:

$$p(\Delta x) = \frac{\Delta x}{4\lambda_0} \exp\left(\frac{-\Delta x^2}{8\lambda_0}\right)$$

$$P(\Delta X) = 1 - \exp\left(\frac{-\Delta X^2}{8\lambda_0}\right)$$

$$\bar{P}(\Delta X) = \exp\left(\frac{-\Delta X^2}{8\lambda_0}\right)$$

The significant response amplitude is given by:

$$X_{1/3} = 2\sqrt{\lambda_0}$$

The significant response range is given by:

$$\Delta X_{1/3} = 4\sqrt{\lambda_0}$$

Within the narrow band assumption, the mean number of response ranges on duration T is:

$$N = T / T_x$$

where:

$T_x$  : Mean zero up-crossing period of the response x, given by:

$$T_x = 2\pi \sqrt{\frac{\lambda_0}{\lambda_2}}$$

## 4.2 Analysis of time-domain simulations

### 4.2.1 Up-crossing counting analysis of time-domain simulation

The up-crossing counting method consists in dividing the response into cycles (one cycle being defined between two consecutive mean level up-crossing), and to keep the maximum and the minimum of each cycle. The mean up-crossing period is defined as the mean period of all the cycles. The maxima and minima are sorted and used to define an empirical cumulative distribution function of the response. This distribution may be different from a Rayleigh distribution, because of the non-linearity of the simulation. The up-crossing counting method is used to define the extreme response on a sea state, or a set of sea states.

An analytical function (Weibull distribution, for instance) can be fitted to the empirical cumulative distribution function, in order to be able to extrapolate the results to a lower probability level. Special care should be taken to the fitting procedure and to the possible error introduced by an extrapolation.

If a linear result is available, it might be useful to compare the empirical distribution of the non-linear response with the empirical distribution of the linear response (which should converge to a Rayleigh distribution) and to fit a relationship between the non-linear response and the linear response having the same probability. Hence the cumulative distribution function of the non-linear response can be defined from the linear cumulative distribution function of the equivalent linear response.

### 4.2.2 Rainflow counting analysis of time-domain simulation

The rainflow counting method consists in dividing the responses into cycles, taking into account all the local maxima and minima. The mean period of all the cycles may be different from the mean up-crossing period. This counting method is used to compute fatigue damage.

The rainflow counting procedure is detailed in Sec 11, [4.3].

## 5 Long-term analysis

### 5.1 General

#### 5.1.1 Definition

A long-term analysis consists in simulating the ship or offshore unit behaviour over a very long period of time (several years), where the ship will encounter many different environmental conditions. The objective of the long-term analysis is to compute:

- the extreme response over that period of time (extreme stress, motion or load)
- the fatigue damage over that period of time.

These results are obtained from the combination of the short-term results for the different environmental conditions. A secondary output of the long-term analysis is the list of the short-term conditions (heading, sea state) having the highest contribution to the extreme response or to the fatigue damage.

### 5.1.2 Input data

A complete description of the environmental conditions is needed to do a long-term analysis. This description can come from some hindcast data or from a scatter diagram (see Article [2]).

To compute the hydro-structure ship response on every sea state of the environmental conditions, a proper model of the ship or offshore unit should be chosen (see [3]) and its operational profile should be given (see Sec 2).

If directionality information is available for both the operational profile (heading) and the environmental conditions (wave direction), this information is to be combined to obtain a relative wave direction for each short-term condition. For turret moored offshore units, this relative wave direction can be the outcome of a heading analysis. If either the ship heading or the wave direction information is missing, a probability distribution of relative wave direction is to be considered, thus increasing the number of short-term conditions to be considered. Equiprobability of the relative wave direction is considered in the absence of detailed information.

### 5.1.3 Long-term extreme response

For a long-term condition, defined as a list of short-term conditions (scatter diagram or list of sea states), the maximum long-term response  $X$ , corresponding to a return period  $T_r$ , exceeded with a risk  $\alpha$ , is defined by:

$$\alpha = 1 - \prod_k P_k(X)^{N_k}$$

where:

$P_k$  : Cumulative distribution function of the response in the short-term condition  $k$

$N_k$  : Number of response cycles in the return period, corresponding to the short-term condition  $k$ , given by:

$$N_k = \frac{p_k T_r}{T_{z,k}}$$

$p_k$  : Probability of the short-term condition  $k$  in the long-term wave statistics

$T_r$  : Return period, in seconds

$T_{z,k}$  : Zero up-crossing period of the response in the short-term condition  $k$  in seconds (See [4.1.3])

The usual definition of the long-term extreme response  $X$  without mentioning a risk of being exceeded is:

$$\sum_k N_k \cdot \bar{P}_k(X) = 1$$

where  $\bar{P}_k$  is the complementary cumulative distribution function (or exceedance) of the response in the short-term condition  $k$ , as defined in [4.1.3].

For a return period larger than a few days, the risk  $\alpha$  corresponding to this extreme response is 63%.

### 5.1.4 Long-term fatigue damage

For a long-term condition, defined as a list of short-term conditions (scatter diagram or list of sea states), the fatigue damage corresponding to a return period  $T_r$  is defined as the sum of the damage accumulated in all the short-term conditions. The procedure for long-term fatigue damage computation is described in Sec 11, [3.6] for spectral analysis and in Sec 11, [4.5] for time-domain analysis.

### 5.1.5 Analysis methods

Several methods can be employed to perform a long-term analysis. The most complex ones simulate all the life-time ship response, while the simplified methods, under given assumptions, focus on a limited number of simulation cases. All these methods are listed in [5.2] to [5.5].

## 5.2 Complete long-term analysis

### 5.2.1 General case

A complete long-term analysis consists in simulating the ship or offshore unit response in all the sea states of the environmental conditions. This analysis may be very time-consuming if the model chosen for calculating the ship hydro-structure response is not very time-efficient (a time-domain model including non-linearity, for example).

### 5.2.2 Linear long-term analysis

If the response is considered to be linear, the long-term analysis is done very easily. The ship behaviour is characterized by its linear RAOs defined in [3.1.2]. It can be a load RAO (vertical bending moment, torsion moment, acceleration, ...) or a stress RAO. A load RAO only needs the results of a sea-keeping computation, while a stress RAO needs, in addition, the results of a structural analysis.



The short-term response is determined using the spectral approach described in [4.1], for every short-term condition in the entire life of the ship or the unit. The long-term response is then obtained by combining the complete set of short-term results, as described in [5.1.3] regarding the extreme response and in Sec 11, [3.6] regarding the fatigue damage.

For both extreme response and fatigue damage, a very useful result of the linear long-term analysis is the identification of the short-term conditions, in terms of heading and sea state, that have the highest contribution to the long-term results. These most contributory conditions can then be studied in details, using non-linear models and the approaches described in [5.3] and [5.4].

### 5.2.3 Non-linear long-term analysis

If the selected non-linear simulation model is fast enough, the whole life of the unit can be simulated in time domain.

The non-linear model is applied to all short-term conditions encountered during the ship or unit life, and the long-term results are directly obtained by combining the short-term statistics as defined in [5.1.3] or the short-term fatigue damages as defined in Sec 11, [4.5.1].

## 5.3 Multiple Design Sea States approach

### 5.3.1 Principle

The principle of the multiple Design Sea States (DSS) approach is to focus the computation on a limited number of short-term conditions (sea states and heading). These conditions are the ones having the highest contribution to the extreme response or to the fatigue damage. This approach allows to use simulation models for which a complete non-linear approach as described in [5.2.3] is not possible due to too high computational time.

### 5.3.2 Choice of the design sea states based on a linear long-term analysis results

When the non-linear ship response is supposed to be partly governed by the linear ship response, it may be useful to choose the DSS among the short-term conditions having the highest contributions to the linear extreme response or to the total linear fatigue damage (see [5.2.2]).

### 5.3.3 Computation of extreme response and fatigue damage

The multiple DSS approach is an iterative process:

- a first set of sea states and headings is chosen and short-term computations are done on these conditions
- the long-term extreme response, or the long-term fatigue damage, is then computed using only these sea states, and neglecting the contribution of all the other conditions
- the contribution of each computed condition to the extreme response, or to the total fatigue damage, is determined. It is to be checked that the contribution of the less contributing conditions can be neglected. If it is not the case, new short-term conditions are added, and the process is started again.

## 5.4 Single Design Sea State approach

### 5.4.1 Principle

Under certain conditions, when it can be assumed that the non-linear ship response is just a correction of its linear response, it might be enough to compute the non-linear ship response for a single short-term condition and to use the results of this short-term condition to correct the linear long-term result.

If this condition is not fulfilled, the multiple DSS approach described in [5.3] is to be used instead of the single DSS approach.

### 5.4.2 Computation of the extreme response

The linear extreme response is computed first, using the linear long-term analysis method (see [5.2.2]). On the chosen single DSS, the risk of exceeding this linear extreme response is computed (see [4.2.1]). The short-term non-linear extreme response corresponding to the same risk is then derived from the non-linear simulation. To limit the duration of the non-linear simulation, a fitting function may be used.

This short-term extreme response is considered to be the long-term extreme response.

### 5.4.3 Computation of the fatigue damage

The linear fatigue damage is computed first, using the linear long-term analysis method (see [5.2.2]). On the chosen single DSS, the linear fatigue damage and the non-linear fatigue damage are computed (see [4.2.2]). A correction factor is defined as the ratio of the non-linear fatigue damage and the linear fatigue damage.

This correction factor is applied to the long-term linear fatigue damage to compute the long-term non-linear fatigue damage.

## 5.5 Equivalent Design Wave approach

### 5.5.1 Principle

An Equivalent Design Wave (EDW) is a wave or a group of waves (see [5.5.2], [5.5.3] and [5.5.4]) defined in order to create a given response, the probability level of which is known.

In a first step, one or several governing parameters, having a major influence on the stress in the considered structural detail, are identified, using experience or simplified analysis models. If several governing parameters are identified, then several EDWs are to be used, each of them being based on one parameter.

The governing parameters are to be quantities that can be evaluated by a linear model, so that their statistical distributions can be determined by spectral analysis. The EDW for one governing parameter and one probability level is then defined, in such a way that, when this EDW is applied on the linear model, the response for the EDW parameter is equal to its expected value at the defined probability level. All the EDWs are then simulated with the non-linear model in time domain, and the non-linear response at the considered probability level is the maximum non-linear response among all the EDWs.

In most cases, the governing parameters are the linearized hydrodynamic loads acting on the structure: pressure, accelerations, and global loads for slender units. The governing parameters can also be based on the structural response, such as the linearized stress in the structural detail.

### 5.5.2 Regular equivalent design wave

The EDW can be a regular wave, with a heading and a frequency to be determined from the governing parameter Linear Transfer Function (LTF) or from its response spectrum for the considered short-term condition. In case of long-term analysis, the response spectrum for the short-term condition with the highest contribution to the long-term value is used. The EDW amplitude is then obtained by dividing the target response by the amplitude of the LTF at the selected heading and frequency.

The regular EDW is characterized by the following four parameters:

$\beta_{EDW}$  : Regular EDW heading.  $\beta_{EDW}$  can be taken as:

- the main wave heading of the considered sea state, or
- the wave heading associated with the maximum of  $|LTF(\omega, \beta)|$

$\omega_{EDW}$  : Regular EDW frequency.  $\omega_{EDW}$  can be taken as:

- the frequency of the maximum of the response spectrum, or
- the frequency of the maximum of  $|LTF(\omega, \beta)|$

$A_{EDW}$  : Regular EDW amplitude, taken equal to:

$$A_{EDW} = \frac{X}{|LTF(\omega_{EDW}, \beta_{EDW})|}$$

$\varphi_{EDW}$  : Regular EDW phase, taken equal to:

$$\varphi_{EDW} = -\text{phase}(LTF(\omega_{EDW}, \beta_{EDW}))$$

where:

$X$  : Target response value

$LTF(\omega, \beta)$ : Linear transfer function of the governing parameter.

### 5.5.3 Irregular long-crested EDW

The EDW can be also a response conditioned wave (RCW), an irregular wave train that is completely defined by the response spectrum for the considered short-term condition. In case of long-term analysis, the response spectrum for the short-term condition with the highest contribution to the long-term value is used.

The irregular long-crested EDW is characterized by the following four parameters:

$\beta_{EDW}$  : EDW heading.  $\beta_{EDW}$  can be taken as the main wave heading of the considered sea state

$\omega_i$  : Frequency of the EDW component  $i$ . The values of  $\omega_i$  are chosen in order to discretize the wave frequency range, following the recommendations in Sec 11, [4.3.1]

$A_i$  : Amplitude of the EDW component  $i$ , taken equal to:

$$A_i = S_{\eta}(\omega_i) \cdot |LTF(\omega_i, \beta_{EDW})| \frac{X}{\lambda_0} \Delta\omega_i$$

$\varphi_i$  : Phase of the EDW component  $i$ , taken equal to:

$$\varphi_i = -\text{phase}(LTF(\omega_i, \beta_{EDW}))$$

where:

$X$  : Target response value

- $LTF(\omega, \beta)$ : Linear transfer function of the governing parameter  
 $S_\eta(\omega)$ : Wave energy density spectrum  
 $\lambda_0$ : Zero order moment of the governing parameter response spectrum (see [4.1.2])  
 $\Delta\omega_i$ : Frequency step associated with  $\omega_i$  in the frequency discretization.

#### 5.5.4 Irregular short-crested EDW

The EDW can also be a response conditioned wave that accounts for the wave energy spreading in the sea state.

The irregular short-crested EDW is characterized by the following four parameters:

- $\beta_j$ : Heading of the EDW component (i,j). The values of  $\beta_j$  are chosen in order to discretize the wave energy direction range, following the recommendations in Sec 11, [4.3.1]  
 $\omega_i$ : Frequency of the EDW component (i,j). The values of  $\omega_i$  are chosen in order to discretize the wave frequency range, following the recommendations in Sec 11, [4.3.1]  
 $A_{i,j}$ : Amplitude of the EDW component (i,j), taken equal to:

$$A_{i,j} = S_\eta(\omega_i, \beta_j) \cdot |LTF(\omega_i, \beta_j)| \frac{X}{\lambda_0} \Delta\omega_i \Delta\beta_j$$

- $\varphi_{i,j}$ : Phase of the EDW component (i,j), taken equal to:  
 $\varphi_{i,j} = -\text{phase}(LTF(\omega_i, \beta_j))$

where:

- $X, LTF(\omega, \beta)$ : As defined in [5.5.3]  
 $S_\eta(\omega, \beta)$ : Wave energy density spectrum including directional spreading  
 $\lambda_0, \Delta\omega_i$ : As defined in [5.5.3]  
 $\Delta\beta_j$ : Wave heading step associated with  $\beta_j$  in the heading discretization.

#### 5.5.5 Fatigue damage from EDWs at one probability level

If EDWs relative to a single level of probability are used to characterize the response, then an analytical long-term probability distribution function is to be chosen. In this context, it is essential to use EDWs associated with the long-term probability level expected to have the highest contribution to the fatigue damage, typically  $10^{-2}$ . The long-term distribution of stress ranges is then taken as a Weibull function having a shape parameter equal to 1. Its complementary cumulative distribution function is given by:

$$\bar{P}(\Delta\sigma) = \exp\left(-\frac{\Delta\sigma}{\lambda}\right)$$

where:

$$\lambda = \frac{\Delta\sigma_{ref}}{\ln(1/P_{ref})}$$

with:

- $\Delta\sigma_{ref}$ : Stress range determined by means of EDWs  
 $P_{ref}$ : Probability level that was considered for the construction of the EDWs.

The long-term fatigue damage is then obtained by analytical integration of the Weibull distribution. For a two-slope S-N curve:

$$D^{LT} = N_T \left[ \frac{\lambda^{m_1}}{K_1} \Gamma\left(1 + m_1; \frac{\Delta S_g}{\lambda}\right) + \frac{\lambda^{m_2}}{K_2} \gamma\left(1 + m_2; \frac{\Delta S_g}{\lambda}\right) \right]$$

#### 5.5.6 Fatigue damage from EDWs at several probability level

If EDWs relative to several levels of probability are used to characterize the response, then the long-term distribution can be either a Weibull distribution fitted on the EDW results or an empirical distribution defined by interpolation between EDW results.

- a) If a fitted Weibull distribution is chosen, its complementary cumulative distribution function is given by:

$$\bar{P}(\Delta\sigma) = \exp\left[-\left(\frac{\Delta\sigma}{\lambda}\right)^\xi\right]$$

where:

- $\lambda, \xi$ : Scale parameter and shape parameter, respectively, of the fitted Weibull function.

For a two-slope S-N curve, the long-term fatigue damage is then given by:

$$D^{LT} = N_T \left[ \frac{\lambda^{m_1}}{K_1} \Gamma\left(1 + \frac{m_1}{\xi}; \left(\frac{\Delta S_g}{\lambda}\right)^\xi\right) + \frac{\lambda^{m_2}}{K_2} \gamma\left(1 + \frac{m_2}{\xi}; \left(\frac{\Delta S_g}{\lambda}\right)^\xi\right) \right]$$

b) If interpolation between EDW results is chosen, the following procedure is recommended:

The results of the EDW analysis are sorted by decreasing exceedance probability values, corresponding to increasing levels of stress ranges:

$$\{(\bar{P}_0; \Delta\sigma_0); (\bar{P}_1; \Delta\sigma_1); \dots; (\bar{P}_i; \Delta\sigma_i); \dots; (\bar{P}_n; \Delta\sigma_n)\} \quad \text{with } (\bar{P}_0; \Delta\sigma_0) = (1; 0)$$

Between  $(\bar{P}_j; \Delta\sigma_j)$  and  $(\bar{P}_{j+1}; \Delta\sigma_{j+1})$ , the distribution is interpolated by:

$$\bar{P}(\Delta\sigma) = \exp\left(-\frac{\Delta\sigma}{\lambda} + \kappa\right)$$

with:

$$\lambda = \frac{\Delta\sigma_{j+1} - \Delta\sigma_j}{\ln \bar{P}_{j+1} - \ln \bar{P}_j}$$

$$\kappa = \ln \bar{P}_j + \frac{\Delta\sigma_j}{\lambda}$$

The damage is then obtained by:

$$D = \sum_{j=0}^{n-1} D_j$$

where:

$D_j$  : Damage for the part of the empirical distribution between  $(P_j; \Delta\sigma_j)$  and  $(P_{j+1}; \Delta\sigma_{j+1})$ , given, for a two-slope S-N curve, by:

- when  $\Delta S_q \leq \Delta\sigma_j$ :

$$D_j = N_T \cdot \exp(\kappa) \cdot \frac{\lambda^{m_1}}{K_1} \left[ \gamma\left(1 + m_1; \frac{\Delta\sigma_{j+1}}{\lambda}\right) - \gamma\left(1 + m_1; \frac{\Delta\sigma_j}{\lambda}\right) \right]$$

- when  $\Delta\sigma_j < \Delta S_q < \Delta\sigma_{j+1}$ :

$$D_j = N_T \cdot \exp(\kappa) \cdot \left\{ \frac{\lambda^{m_1}}{K_1} \left[ \gamma\left(1 + m_1; \frac{\Delta\sigma_{j+1}}{\lambda}\right) - \gamma\left(1 + m_1; \frac{\Delta S_q}{\lambda}\right) \right] + \frac{\lambda^{m_2}}{K_2} \left[ \gamma\left(1 + m_2; \frac{\Delta S_q}{\lambda}\right) - \gamma\left(1 + m_2; \frac{\Delta\sigma_j}{\lambda}\right) \right] \right\}$$

- when  $\Delta S_q \geq \Delta\sigma_{j+1}$ :

$$D_j = N_T \cdot \exp(\kappa) \cdot \frac{\lambda^{m_2}}{K_2} \left[ \gamma\left(1 + m_2; \frac{\Delta\sigma_{j+1}}{\lambda}\right) - \gamma\left(1 + m_2; \frac{\Delta\sigma_j}{\lambda}\right) \right]$$

# APPENDIX 2

## FATIGUE STRENGTH OF ALUMINIUM ALLOYS PLATED WELDED DETAILS

### 1 Basic design S-N curves for plated welded details in aluminium alloys

#### 1.1 General

##### 1.1.1 Probability of survival

Fatigue design is based on the use of S-N curves obtained from fatigue tests in laboratories. The basic design S-N curves represent two standard deviations below the mean S-N curves (corresponding to 50% of probability of survival) for relevant experimental data. Basic design S-N curves provided in this appendix correspond to a survival probability equal to 97,7%.

##### 1.1.2 Workmanship tolerances implicitly included in design S-N curves

Small specimens made in aluminium alloys used for design S-N curves building include some fabrication misalignment. Values of misalignments ( $\delta_0$ ,  $\alpha_0$ ) of aluminium welded specimens are given in Sec 10, [5]. Values of misalignments ( $\delta_0$ ,  $\alpha_0$ ) given in Sec 10, [5] are dedicated to both steel and aluminium welded joints.

##### 1.1.3 Failure criterion for aluminium plated welded structures

As for plated steel structures (see Sec 9, [1.1.3]), the fatigue failure of actual plated aluminium structures determined by the S-N curve approach used in this Guidance Note corresponds to the initiation of a fatigue crack, not to the complete failure of the structure. The complete failure of complex plated structures should not be used as a fatigue criterion at the design stage.

#### 1.2 Scope of application

##### 1.2.1 Types of details

S-N curves in this Appendix are applicable to plated welded details built in aluminium alloys (see [1.2.3]).

##### 1.2.2 Environment

S-N curves in this Appendix are provided for any environment.

##### 1.2.3 Material

S-N curves for welded details built in aluminium alloys are valid for details of series 5000 (aluminium-magnesium alloy) and series 6000 (aluminium-magnesium-silicon alloy) except the alloys grade 6005A and 6061 as defined in (NR216, Ch 3, Sec 2, [2.3]). The yield strength corresponding to 0,2% proof stress ( $R_{p0,2}$ ) of aluminium products are given in NR216, Ch 3, Sec 2, Tab 2 and Tab 3.

##### 1.2.4 Welding process

The S-N curves provided from Articles [2] to [4] correspond to S-N curves for as-welded joints with welding conditions as defined in [7.3].

##### 1.2.5 Reference thickness

Basic design S-N curves derive from fatigue data of tested specimens fabricated with a plate thickness lower than a reference thickness  $t_{ref}$ .

Thus, basic design S-N curves provided in this Appendix are directly applicable for plates or members with a thickness lower than the reference thickness  $t_{ref}$ . For plate or member thicknesses greater than  $t_{ref}$  the influence of thickness is to be taken into account in accordance with [5.2].

#### 1.3 Basic design S-N curve formulae

##### 1.3.1 Standard form

The standard form of the basic design S-N curves is defined in Sec 9, [1.3.1].

##### 1.3.2 FAT definition

The FAT of design curve is defined in Sec 9, [1.3.2].

##### 1.3.3 Log definition

S-N curves may be written also in terms of  $\log_{10}$  as defined in Sec 9, [1.3.3].

2 As-welded aluminium joints, toe cracking

2.1 Plated joints, hot spot stress

2.1.1 Hot spot stress by FEA

Plated joints built in aluminium alloys are assessed using hot spot stress calculated by FEA in the same way as plated joints built in steel (see Sec 9, [2.1.1]).

Two different S-N curves ( $P_{\perp}$  and  $P_{\parallel}$ ) are selected depending on the principal hot spot stress direction as defined in Sec 9, [2.1.1].

If the weld toe angle is lower than or equal to 30°, the S-N curve to be used for all principal stress range directions is  $P_{\parallel}$ .

The  $P_{\perp}$  and  $P_{\parallel}$  S-N curves for aluminium are given in Tab 3.

2.1.2 Hot spot stress by analytical stress analysis

For the assessment of longitudinal stiffener welded connections built in aluminium, the method is the same as for steel (see Sec 3, [2]). The applicable S-N curve to be used is the  $P_{\perp}$  curve since the calculated hot spot stress is taken perpendicular to the weld.

If the weld toe angle is lower than or equal to 30°, the S-N curve to be used is  $P_{\parallel}$ .

2.2 Plated butt-welded joints, local nominal stress

2.2.1 Butt joint classification

The toe of plated butt-welded joints when using the local nominal stress may be designed according to the classification given in Tab 1.

The corresponding 'C', 'D' and 'E' S-N curves are given in Tab 3.

Table 1 : Plated butt-welded joint classification for toe cracking

Description of plated butt-welded joints	Applicable S-N curve
Weld cap ground flush with the surface and shown to be free from significant defect from NDE	C
Welding performed horizontally by a process other than submerged arc	D
Welding performed by submerged arc or not horizontally	E

3 Welded aluminium joints, root cracking

3.1 Plated joints, weld root stress computed by FEA

3.1.1 General

The weld root of plated joints (e.g. cruciform joint, T joint, end of attachment) when using weld root structural stress computed by FEA (see Sec 7, [2.1.4] and Sec 7, [2.2.3]) may be designed considering the 'E' S-N curve given in Tab 3.

The 'E' S-N curve does not include any misalignment effect.

No thickness correction is to be considered for 'E' S-N curve when it is used for root cracking.

3.2 Plated butt-welded joints, local nominal stress

3.2.1 Butt joint classification

The root of plated butt-welded joints shall be designed according to the classification given in Tab 2.

No thickness correction is to be considered for 'E', 'F' and 'F2' S-N curves when they are used for root cracking.

Table 2 : Plated butt-welded joint classification for root cracking

Description of single-sided plated butt-welded joints	Applicable S-N curve
Full penetration single-sided weld made with temporary backing strip (no misalignment)	E
Full penetration single-sided weld made on permanent backing strip	F
Full penetration single-sided weld made without permanent backing strip	F2

## 4 Table of S-N curves for aluminium alloys plated welded details

### 4.1 General

4.1.1 S-N curves for aluminium alloys plated welded details are defined in Tab 3.

**Table 3 : Basic design S-N curves for aluminium alloys plated welded details**

Curve	FAT	First slope		Slope intersection		Second slope		Reference thickness $t_{\text{ref}}$ (mm)	Thickness exponent n
	$\Delta S$ (MPa)	m1	$\log_{10}(K_1)$	N cycles	$\Delta S_q$ (MPa)	m2	$\log_{10}(K_2)$		
C	40	3,5	11,9082	$10^7$	25,26	6	15,4141	25	see Sec 10, Tab 2
D	36	3,0	10,9699	$10^7$	21,05	5	13,6166		
E (1)	25	3,0	10,4949	$10^7$	14,62	5	12,8248		
F (1)	22	3,0	10,3283	$10^7$	12,87	5	12,5472		
F2 (1)	20	3,0	10,2041	$10^7$	11,70	5	12,3402		
$P_{\perp}$	36	3,0	10,9699	$10^7$	21,05	5	13,6166		
$P_{//}$	40	3,0	11,1072	$10^7$	23,39	5	13,8453		
(1) No thickness correction is to be considered when the S-N curve is used for root cracking in accordance with [3].									

## 5 Factors affecting fatigue strength of aluminium plated welded details

### 5.1 General

#### 5.1.1 Correction of basic S-N curves of aluminium plated welded details

Basic design S-N curves for aluminium alloys welded details (see [4]) have to be corrected to take into account the effects affecting the fatigue strength.

#### 5.1.2 Factors affecting the fatigue strength of aluminium plated welded details

The factors affecting the fatigue strength of aluminium plated welded details are:

- influence of thickness
- influence of mean stress and residual stress relaxation
- influence of workmanship (misalignment) (see Sec 11, [2.2.8] for application)

#### 5.1.3 Effects taken into account by means of S-N curve constant modifications

The following effects are taken into account by shifting the S-N curves:

- influence of thickness
- influence of mean stress and residual stress relaxation

These effects are taken into account by means of a correction factor  $f_{eff}$ , as defined in [5.1.4], affecting the constants ( $K_1$ ,  $K_2$ ) of the basic design S-N curves. The inverse slopes of the corrected S-N curves are the same as those of the basic design S-N curves (shifting of the basic design S-N curves).

The corrected design S-N curve constants  $K_1'$  and  $K_2'$  are taken as:

$$K_1' = \left( \frac{1}{f_{eff}} \right)^{m_1} K_1$$

$$K_2' = \left( \frac{1}{f_{eff}} \right)^{m_2} K_2$$

with:

$m_1$  : Inverse slope of the first segment of the basic design S-N curve, for  $\Delta S \geq \Delta S_q$

$m_2$  : Inverse slope of the second segment of the basic design S-N curve, for  $\Delta S < \Delta S_q$ .

The stress range  $\Delta S_q'$  corresponding to the change of slope of the corrected S-N curves at  $\Delta S = \Delta S_q'$  is given by:

$$\Delta S_q' = \frac{\Delta S_q}{f_{eff}}$$

#### 5.1.4 Combination of effects

The effects of thickness and mean stress and residual stress relaxation are combined by the multiplication of the correction factors. The combined correction factor  $f_{\text{eff}}$  is given by:

$$f_{\text{eff}} = f_{\text{thick}} f_{\text{mean}}$$

where:

$f_{\text{thick}}$  : Correction factor for the effect of plate thickness, as defined in [5.2]

$f_{\text{mean}}$  : Correction factor for the effect of mean stress and residual stress relaxation, as defined in [5.3].

#### 5.1.5 Equivalent stress correction

For practical reasons, instead of shifting the S-N curves, the modification of the fatigue strength can be taken into account by defining an equivalent stress range  $\Delta\sigma_{\text{EQ}}$  taken equal to:

$$\Delta\sigma_{\text{EQ}} = \Delta\sigma_{\text{RF}} f_{\text{eff}}$$

where:

$\Delta\sigma_{\text{RF}}$  : Reference fatigue stress range, defined in Sec 11, [2.2]

$f_{\text{eff}}$  : Correction factor, defined in [5.1.4]. For direct calculation,  $f_{\text{eff}}$  defined in [5.1.4] is to be applied in Sec 11, [3.3.1] and Sec 11, [4.2.1].

### 5.2 Thickness effect

**5.2.1** The thickness effect affecting the fatigue strength of welded joints built in aluminium alloys is assumed to be the same as for welded joints built in steel (see Sec 10, [3]).

### 5.3 Mean stress and residual stress relaxation

#### 5.3.1 General

The mean stress effect for welded aluminium joints submitted to constant amplitude loading may be neglected as for welded steel joints (see Sec 10, [4.1.1]).

#### 5.3.2 Ship and offshore structures

In ship and offshore structures where the stress range fluctuations are random and the mean stress varies due to several loading conditions during service life, the fatigue behaviour of welded aluminium joints is the same as for welded steel joints (see Sec 10, [4.1.2]) i.e. the fatigue strength is considered to be dependent on the loading mean stress. Due to fluctuations of wave stress ranges and static loading associated to the different loading conditions, the material yield stress can be exceeded. This results in some relaxation of the residual stress. Therefore the damage due to the following cycles will be lower.

#### 5.3.3 Rule-based correction for plated welded aluminium details

The mean stress rule correction used for plated welded steel joints (see Sec 10, [4.1.4]) is applied for plated welded aluminium joints.

The only difference concerns the material shakedown yield strength  $R_{\text{eEq}}$  to be taken equal to:

$$R_{\text{eEq}} = R_{\text{p0,2}}$$

where:

$R_{\text{p0,2}}$  : Proof stress (yield strength) of the material in delivery condition, as specified in NR216, Ch3, Sec2, Tab 2 and Tab 3.

#### 5.3.4 Mean stress correction for aluminium plated welded details for direct calculation

The mean stress correction for direct calculation used for plated welded steel joints (see Sec 10, [4.1.5]) is applied for plated welded aluminium joints.

The only difference concerns the material shakedown yield strength value  $R_{\text{eEq}}$  defined in [5.3.3].

## 6 Stress concentration factors due to misalignment

### 6.1 General

#### 6.1.1 Misalignment origin and effects

Misalignment origin and effects for plated welded joints built in aluminium are the same as those of plated welded steel joints (see Sec 10, [5.1.1]).

#### 6.1.2 Stress concentration factors

The different stress concentration factors  $K_m$  due to misalignment in plated welded aluminium joints are given in [6.2] to [6.4].



## 6.2 Plate butt weld - Axial misalignment

**6.2.1** The prescriptions given in Sec 10, [5.2] are applicable to plated butt welded aluminium joints axial misalignment. However, in the absence of a value provided by the designer, the default value for the eccentricity due to fabrication ( $\delta_m$ ) should be taken as the maximum allowable misalignment between plates of equal thickness in the applicable rules (NR561, Sec9, [3.4.7]). The maximum allowable misalignment between plates of equal thickness is equal to 10% of the plate thickness, without being greater than 3 mm.

## 6.3 Plate butt weld - Angular misalignment

**6.3.1** The prescriptions given in Sec 10, [5.3] are applicable to plated butt welded aluminium joints angular misalignment. However, the default value for the angular misalignment between flat plates due to fabrication ( $\alpha_m$ ) given in Sec 10, [5.3] should not be used, and the maximum angular misalignment specified by the designer is to be used.

## 6.4 Plate cruciform joint misalignment

**6.4.1** The prescriptions given in Sec 10, [5.4] are applicable to the plated cruciform aluminium joints misalignment. However, in the absence of a value provided by the designer, the eccentricity due to fabrication ( $\delta_m$ ) should be taken as the maximum allowable misalignment value given in the applicable rules (NR561, Sec 9, [3.4.8]). The maximum allowable misalignment value is equal to half of the maximum value of the two adjoining plate thicknesses.

# 7 Workmanship

## 7.1 General

**7.1.1** The fatigue life of welded joints depends on the workmanship quality in terms of building alignment and weld profile associated to the welding procedures. Current shipbuilding practices are in principle to comply with standard values of workmanship defined in dedicated rules (NR561, [3.4]).

## 7.2 Building misalignment

**7.2.1** The effect of misalignment on fatigue life is treated in [6]. The misalignment values to be considered for the fatigue design assessment correspond generally to the standard values given in the applicable rules (NR561, Sec 9, [3.4.7], [3.4.8]) when the expected workmanship corresponds to the current shipbuilding practice. The default values correspond to those Bureau Veritas standard values and should be used in the absence of misalignment values specified by the designer.

## 7.3 Welding procedures

**7.3.1** The welding procedures are to be in accordance with the applicable rules (NR561, Sec 9, [3.4]).



Shaping a World of Trust

Marine & Offshore  
Le Triangle de l'Arche - 8 Cours du Triangle - CS 50101  
92937 Paris La Defense Cedex - France  
Tel: + 33 (0)1 55 24 70 00  
<https://marine-offshore.bureauveritas.com/bv-rules>  
© 2020 Bureau Veritas – All rights reserved